

SNOWMELT RUNOFF MODELLING AND SEDIMENT STUDIES IN SATLUJ BASIN USING REMOTE SENSING AND GIS

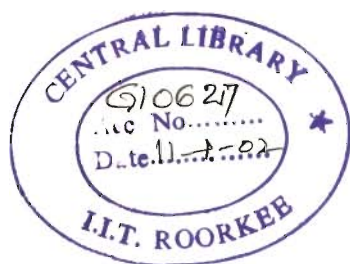
A THESIS

*Submitted in fulfilment of the
requirements for the award of the degree*

of
DOCTOR OF PHILOSOPHY
in
EARTH SCIENCES

By

SANJAY KUMAR JAIN



**DEPARTMENT OF EARTH SCIENCES
UNIVERSITY OF ROORKEE
ROORKEE-247 667 (INDIA)**

JUNE, 2001

CANDIDATE'S DECLARATION

I, hereby, certify that the work which is being presented in this thesis, entitled "Snowmelt runoff modelling and sediment studies in Satluj basin using remote sensing and GIS" in fulfilment for the award of the degree of **DOCTOR OF PHILOSOPHY** and submitted in the **Department of Earth Sciences** of the University of Roorkee, Roorkee, is an authentic record of my own work carried out during a period from April 1994 to June 2001 under the supervision of Dr. S.M.Seth, Dr. Pratap Singh and Dr. A.K.Saraf.

The matter embodied in this thesis has not been submitted by me for the award of any other degree of this or any other university.


(Sanjay K. Jain)

Date : 22.06.01


This is to certify that the above statement made by the candidate is correct to the best of my knowledge.


(Dr. S.M.Seth)

Principal

Poornima College of Engg.

Jaipur



(Dr. Pratap Singh)

Scientist 'E1'

National Institute of Hydrology

Roorkee



(Dr A.K.Saraf)

Asstt. Professor

Dept. of E.Sc., UOR

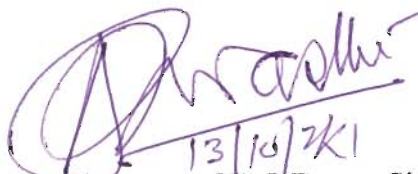
Roorkee

Date : 22.06.01

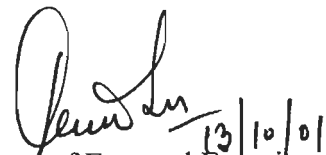
The Ph.D. viva-voce examination of **Mr. Sanjay Kumar Jain**, Research Scholar was held on 13/10/2001



Signature of supervisors


13/10/2001

Signature of H.O.D.


13/10/01

Signature of External Examiner

ABSTRACT

Most of the big rivers in the world originate from the mountainous areas and are considered important sources of water for the large population of the world. Himalayas provide one of the world's largest renewable supplies of fresh water. The chain of the Himalayan mountains act as an effective barrier to the summer monsoon and westerly winter disturbances. Due to this there is massive summer monsoon precipitation especially in the eastern and central parts of the Himalayas and snowfall at higher altitudes in the winters. The major river systems of India, the Indus, Ganges and Brahmaputra have their origin in the Himalayan mountain region and snow accumulated during winter becomes a major source of runoff for these rivers during summer. The spring and summer runoff of the Himalayan rivers is mostly from snowmelt is considered a dependable source of water for irrigation, hydroelectric power and drinking water supply. The availability of high runoff coupled with wide variations in elevations provides a large potential for hydroelectric power. India is endowed with enormous economically exploitable and viable hydropower potential mostly in Himalayan region. This is assessed to be about 84,000 MW at 60% load factor. However, only about 20% of the hydroelectric potential have been harnessed so far and 10% is under various stages of development.

Himalayan region is witnessing a large economic growth and demands for irrigation water, hydro-electricity are ever increasing. The provision of suitable flood control measure in the lowland areas is also an area of concern. These require proper understanding of the hydrological processes of the snowfed basins of the Himalayan region. Suitable hydrological models have to be developed to simulate these processes for generating the streamflow from such basins using observed flow records. Such studies are much needed for the planning, design, development and management of water resources

of the Himalayan region. At the same time, transportation of the high sediments from the Himalayan basins is also one of the serious problems for any water resources development project. The capacity of the reservoirs located in this region reduces at an alarming rate due to deposition of sediment, thus adversely affecting the optimal operation of the water resources schemes.

The present study is therefore focussed on snowmelt runoff modelling and sediment studies. An extensive literature survey has been made on snowmelt runoff processes and their modelling have been also reviewed. The relevant literature on sediment studies has also been reviewed. The remote sensing and GIS techniques have good potential for application in both these areas. The present study also includes a detailed review of such applications. The review of the studies in the Himalayan region shows that the modelling of streamflow for the snowfed basins and sediment studies are very limited. Therefore, it is planned to consider these important aspects for a Himalayan basin in the present study. Important snow covered basins in the western Himalayas are Satluj, Beas, Chenab, Ravi and Jhelum. Satluj basin has a significant contribution from snow/ice and has a reasonably good hydrometeorological network. The hydropower potential of Satluj basin is 8634 MW, which constitutes almost 50% potential of the state of Himachal Pradesh. The Bhakra Nangal project on the Satluj River is a major project producing large amounts of hydroelectric power besides irrigation of large areas in Northern India. The Bhakra dam on Satluj River is considered a boon for India. Some of the other prestigious projects such as Nathpa-Jhakri, Baspa, Kol dam and Karchham Wangtoo are under construction. Therefore, for ensuring representativeness and possible operational use, the study area chosen for this study is Satluj basin (Indian part) up to Bhakra dam.

The proper estimation of snow and glacier contribution in annual flow of a snowfed river is very important for planning and development of water resources. At present there is no systematic method available for this purpose for a snowfed basin in Himalayas having limited information on solid precipitation. In the present study, a methodology has been developed using a water balance approach for estimating snow and glacier contribution in the annual flows of a snowfed river. For this purpose, water budget analysis for the Satluj basin was made for a period of 10 years (Oct. 1986 - Sept. 1996). Precipitation data of 10 stations were used to compute total input to the basin over the water budget period. Total volume of flow for the same period was computed using discharge records at Bhakra dam. Evapotranspiration losses from the basin were estimated using a relationship developed between temperature and evapotranspiration. Snowcover and snow free areas needed in evapotranspiration computation was obtained using remote sensing data (Landsat-MSS, IRS-1A/1B-LISS-II) and image processing have been carried out on ERDAS IMAGINE software. It was found that generally a major part of the basin (65%) is covered with snow in the months of March/April, which reduces to about 20% in September/October. The average contribution of snow and glacier melt in the annual flow of Satluj River at Bhakra was found to be about 59% and remaining 41% was from the rain. It shows that snow and glaciers provide a substantial contribution to the flows of Satluj River. For all the sites upstream of Bhakra dam, the contribution of snow melt runoff in total runoff would be higher than 59% due to higher percentage of snow covered area in upper basins. These findings, of the present study are thus very relevant for all the projects planned/under execution in the upstream of Bhakra dam.

The Himalayan basins have runoff contribution for rainfall as well as snow and ice. In spite of significant contribution of snow and ice in the Himalayan rivers, no attempts have been made to develop a simple scientifically based snowmelt model for the

Himalayan basins. Therefore, development of a snowmelt runoff model, which caters for the sparse network, limited availability of data and rugged topography of the Himalayan basins and also handles rainfall, is of utmost importance. Therefore, simple conceptual snowmelt model (SNOWMOD) based on temperature index approach has been developed for the Satluj basin having range of elevation from 600 m to 6000 m. The basin was divided into suitable number of elevation bands. Daily precipitation and temperature are the basic inputs to the model beside some useful information derived from topographical maps and satellite data. The temperature was extrapolated to different elevation bands using temperature lapse rate. Snow covered area in the basin was determined using remote sensing data from Landsat-MSS, IRS-1A/1B-LISS II and IRS-WiFS. Contour and spot height data from Survey of India toposheets have been used to generate digital elevation model (DEM), which was used subsequently to prepare the area elevation curves. For this purpose, ILWIS GIS software has been used. Keeping in view, the physiographic features of the basin and elevation of meteorological stations, each elevation band was assigned to a representative meteorological station. The model structure is simple and involves use of relevant physical parameters. Only four parameters related with flow routing for snow covered and snow free areas need calibration. The model computes daily runoff from the snowcovered area and snow free area separately. The values of parameters representing degree day factor and runoff coefficients have been decided on the basis of literature review and have been varied from month to month to account for seasonal effect/behaviour of temperature and rainfall. The routing of surface and sub-surface flow is made using concept of linear cascade of reservoirs. The total outflow from the basin was computed by summing the different components of runoff. The model was calibrated using the dataset for a period of three years (1985-86 to 1987-88) and model parameters for structural routing were optimised. Because hydrological response of snow covered area

and snow free area is very much different, therefore separate parameters were considered for these parts of the basin. Using the optimised parameters, streamflow simulations were made for two data sets, each containing 3 years period (1987-88 to 1990-91) and (1996-97 to 1998-99). The accuracy of the streamflow simulation were also determined using different criteria such as shape of the outflow hydrograph, efficiency, difference in volume. In all the three cases (one for calibration and two for simulation), model successfully simulated the observed flow and efficiency of the model varied between 81-94%.

Increasing population and rapid development activities in the geologically fragile Himalayan region are causing major land use changes and hence increasing problems of soil erosion and sedimentation. In recent years, the ecology and hydrology of the Himalayan region has been greatly affected from intensive deforestation, large-scale road construction, mining and cultivation on steep slopes etc. The study of erosion-sedimentation processes and procedures for estimation of the sediment yield and sedimentation forms an important part of the present study.

For the assessment of sediment yield, two approaches have been used: (i) relationship between suspended sediment load and discharge, and (ii) empirical relationship consisting of rainfall and physiographical data of the basin. The first approach was used for Satluj basin at different locations such as at Suni (52,983 km²), at Kasol (53,768 km²) and also for the intermediate basin between Kasol and Suni (785 km²). A relationship between sediment and discharge was developed using data of a period of three years (1991-1993). It was applied for the data sets of two independent years, 1994 and 1996, for estimation of sediment yield. The second approach, which gives annual sediment yield, was used for a small intermediate basin because of the following two reasons: (a) this part is highly soil erosion prone area in the whole basin and; (b) the required

physiographical data was available only for this part of the basin. For estimation of the sediment yield using the empirical relationship, various physiographical parameters representing land use, slope, and drainage density were generated using ILWIS GIS system. The annual sediment yield for the intermediate basin was estimated for 3 years and compared with observed sediment yield. The difference between computed and observed sediment yield and its trend was found to be related to orography. The available empirical relationship was therefore, revised by incorporating an orographic factor in the equation. This orographic factor represented the spatial variation of the rainfall in the basin. Using the revised empirical relationship, the sediment yield was estimated for two independent years and a good correlation was found between computed and observed sediment yield.

The sediment generated from the Satluj basin is deposited in the Bhakra reservoir located in the foothills of the Himalayas. Reduction in the storage capacity of a reservoir beyond a permissible limit hampers the purpose of the reservoir for which it was designed. Thus, assessment of sediment deposition becomes very essential for the management and operation of such reservoirs. At present, some conventional methods such as hydrographic survey and inflow-outflow approaches are used for estimation of sediment deposition in a reservoir. But, these methods are cumbersome, data intensive, time consuming and expensive as well. There is a long felt need for developing a simple method, which requires less time and is also, cost effective. In the present study, a remote-sensing based approach has been developed for the assessment of sedimentation in a reservoir and applied for the Bhakra reservoir. Multi-date remote sensing data (IRS-1B-LISS II) was used to obtain the information on water spread area of the reservoir, which was used for computing the sedimentation rate. The revised capacity of the reservoir between maximum and minimum levels for the two periods, i.e., 1988-89 and 1996-97 was computed using the

trapezoidal formula. The loss in reservoir capacity due to deposition of sediments for a period of 24 years (1965-1989) was determined and it was found to be 491.315 M m³. For a period of 32 years (1965-1997) it is worked out to be 807.35 M m³. Assuming the uniform rate of sedimentation in the reservoir, the rate of sedimentation was found to be 20.47 M m³ per year and 25.23 M m³ per year over a period of 24 years and 32 years respectively. The corresponding value of average rate of sedimentation for this reservoir using hydrographic survey were 21.93 M m³ and 20.84 M m³ per year. The results obtained using remote sensing based approach reasonably agree with the results obtained from hydrographic survey.

The present study has resulted in (i) development and application of a simple and systematic approach for estimation of snow and ice melt contributions in the streamflow of Satluj basins (ii) development of simple conceptual model for daily streamflow simulation for Himalayan rivers having rain as well as snow/ice melt contributions, and its application in calibration as well as simulation model for Satluj basin (iii) simple approach for sediment yield estimation incorporating orographic factor, and (iv) remote sensing based approach for assessment of sedimentation in reservoirs. The application of these models and approaches for Satluj basin has been quite satisfactory.

Based on the present research work, the following recommendations are made for future studies and applications, particularly in Himalayan region. The water balance approach developed in this study can be applied for estimation of snow and ice contributions for the other Himalayan basins too. The snowmelt model (SNOWMOD) was developed and applied for Satluj basin for streamflow simulation. There is scope for extending such studies for the other Himalayan basins. SNOWMOD may be applied for streamflow forecasting in the Himalayan rivers, which would require an additional information on the meteorological parameters in advance.

Sediment yield and sedimentation studies in the other parts of the Himalayan region can also be estimated with the approaches developed and presented in this study. There is also much scope for application of the remote sensing based approach for assessment of sedimentation in reservoirs located in Himalayan region and elsewhere. Considering the time and cost involved the hydrographic surveys may be conducted at longer interval and the remote sensing based sedimentation surveys may be carried out at shorter intervals. Such practice will be very economical and quicker without any loss in the accuracy of results.

ACKNOWLEDGEMENTS

First and foremost, I would like to express my profound gratitude and sincere thanks to my supervisors Dr. S.M. Seth, Principal, Poornima College of Engineering, Jaipur, Dr. Pratap Singh, Scientist 'E1', National Institute of Hydrology, Roorkee, and Dr. A.K. Saraf, Assistant Professor, Department of Earth Sciences, University of Roorkee, Roorkee for their keen interest, valuable guidance and encouragement throughout the period of this research work. I am greatly obliged to them for their valuable advice, timely suggestions, and expert guidance along with vigilant supervision, which has been precious during the different stages of this work.

I am thankful to Dr. K.S. Ramashastri, Director, National Institute of Hydrology, Roorkee and Dr. S.M.Seth, former Director, National Institute of Hydrology, Roorkee for their encouragement and kind permission to carry out research at the University of Roorkee, Roorkee as a part-time scholar. I am also grateful to Dr. A.K.Awasthi, Professor & Head, Department of Earth Sciences, for his help and cooperation.

Heartful thanks are expressed to Mr. R.D. Singh and Dr. Sudhir Kumar, who have provided their full support from time to time. Their selfless and timely help inspite of their own research work activities and busy workload has led to the smooth completion of this work. I am thankful to Mr. M.K. Goel, Mr. D.S. Rathore and Mr. M.K. Jain, for having fruitful discussion on image processing and GIS.

For collection of relevant field data required for the work, I am grateful to the officials of the Bhakra-Beas Management Board, Nangal for their cooperation and help extended in providing the required data. Mr. Tanveer Ahmad, Mr. N.K.Bhatnagar and Mr. Naresh Kumar

provided their full support and necessary help in collection and compilation of the data. I extend my thanks to Mr. Vikas Vatsa, Mr. P.K. Agarwal, Ms. Anju Chaudhry, Mr. Rajesh Nema, Mr. Tejpal Singh and Mr. Mahipal Singh for their time to time help.

I am short of words to express my feelings for all my family members, who have stood besides me during the present work at various stages. My parents and in-laws were always source of inspiration for the completion of this work in time. I am really very thankful for their consistent encouragement and supportive gesture. I am deeply grateful to my wife, Rashmi and both the children, Ayushi and Akarsh, for their love, affection and patience.

Last but not the least, my sincere thanks to all who directly or indirectly helped me at various stages of this work.


(Sanjay Kumar Jain)

CONTENTS

ABSRTACT	i
ACKNOWLEDGEMENTS	ix
LIST OF FIGURES	xvi
LIST OF TABLES	xix
1.0 INTRODUCTION	
1.1 GENERAL	1
1.2 GENERAL CHARACTERISTICS OF HIMALAYAN REGION	3
1.2.1 Physiography and geology	3
1.2.2 Climate	4
1.2.3 Snow and ice	5
1.2.4 River systems	5
1.2.5 Water resources	6
1.2.6 Hydropower potential	8
1.3 HYDROLOGICAL PROBLEMS OF THE HIMALAYAN REGION	9
1.3.1 Estimation of snowmelt runoff	9
1.3.2 Floods	10
1.3.3 Soil erosion and sedimentation	11
1.3.4 Availability of hydrometeorological data	11
1.4 ROLE OF REMOTE SENSING AND GIS	13
1.5 OBJECTIVES AND SCOPE OF THE PRESENT STUDY	14
1.6 ARRANGEMENTS OF THE CHAPTERS	16
2.0 REVIEW OF LITERATURE	20
2.1 MODELLING OF SNOWMELT RUNOFF	20
2.2 SNOWMELT COMPUTATION	21
2.2.1 Energy balance approach	21
2.2.2 Degree-day approach or temperature index approach	23

2.3	CLASSIFICATION OF SNOWMELT MODELS	25
2.3.1	Statistical models	25
2.3.2	Simulation models	26
2.4	SATELLITE REMOTE SENSING OF SNOW COVER	29
2.5	SNOWMELT STUDIES FOR HIMALAYAN BASINS	34
2.5.1	Development of regression relationship	34
2.5.2	Application of empirical relationships	36
2.5.3	Application of snowmelt models	38
2.6	SOIL EROSION /SEDIMENT YIELD AND RESERVOIR SEDIMENTATION STUDIES	39
2.6.1	Soil erosion and sediment yield	39
2.6.2	Effects of sedimentation on reservoirs	42
2.6.3	Estimation of soil erosion	46
2.6.4	Relationships between suspended-sediment concentration and discharge	49
2.7	SEDIMENT YIELD STUDIES FOR HIMALAYAN BASINS AND SATLUJ BASIN	50
2.7.1	Himalayan basins	50
2.7.2	Satluj basin	53
2.8	CONCLUDING REMARK	57
3.	THE STUDY AREA AND DATA USED	59
3.1	THE STUDY AREA	59
3.3.1	The Satluj basin	59
3.3.2	Bhakra reservoir	63
3.2	CLIMATIC CONDITIONS AND SEASONAL VARIATIONS IN THE STUDY BASIN	64
3.3	PRECIPITATION DISTRIBUTION IN THE SATLUJ BASIN	67
3.4	STREAM FLOW CHARACTERISTICS OF SATLUJ RIVER AT BHAKRA DAM	70
3.5	DATA AVAILABILITY	70

3.5.1	Topographic data	71
3.5.2	Hydrometeorological network and observations	71
3.5.3	Sediment and reservoir level data	73
3.5.4	Remote sensing data	73
3.6	DATA PROCESSING	75
4.	CONTRIBUTION OF SNOW AND ICE AT BHAKRA IN ANNUAL STREAM FLOW	77
4.1	RAINFALL	78
4.2	STREAMFLOW	79
4.3	SNOWCOVERED AREA	83
4.3.1	Visual Classification	84
4.3.2	Digital Image Classification	85
4.3.2.1	Geometric correction and Registration	85
4.3.2.2	Shadows	86
4.3.2.3	Cloud cover	86
4.3.2.4	Classification	86
4.4	EVAPOTRANSPIRATION	88
4.5	SNOW AND GLACIER CONTRIBUTION	102
5.	MODELLING OF STREAMFLOW FOR A SNOWFED BASIN	104
5.1	DEVELOPMENT OF SNOWMELT MODEL (SNOWMOD)	105
5.2	MODEL STRUCTURE	106
5.3	MODEL VARIABLES AND PARAMETERS	108
5.3.1.	Basin Characteristics	108
5.3.1.1	Division of catchment into elevation bands	108
5.3.2	Meteorological characteristics	111
5.3.2.1	Precipitation data and distribution	111
5.3.2.2	Temperature data – Space and time distribution	114
5.3.2.3	Snow cover	116
5.3.2.4	Rain on snow	118

5.3.2.5	Degree-day days	122
5.3.3	Model Parameters	123
5.3.3.1	Degree day factor	123
5.3.3.2	Form of precipitation	124
5.3.3.3	Runoff coefficients	125
5.4	COMPUTATION OF DIFFERENT RUNOFF COMPUTATIONS	127
5.4.1	Surface runoff from snow covered area	127
5.4.2	Surface runoff from snow free area	129
5.4.3	Estimation of subsurface runoff	129
5.4.4	Total runoff	130
5.5	ROUTING OF DIFFERENT COMPONENTS OF RUNOFF	131
5.5.1	Routing of surface runoff	131
5.5.2	Routing of subsurface runoff	136
5.6	EFFICIENCY CRITERIA OF THE MODEL	140
5.7	CALIBRATION OF THE MODEL	141
5.7.1	Optimisation	141
5.7.2	Sensitivity analysis of optimised parameters	146
5.8	SIMULATION OF STREAMFLOW	150

6. ASSESSMENT OF SEDIMENT YIELD AND RESERVOIR

	SEDIMENTATION	155
6.1	SOIL EROSION AND SEDIMENT YIELD	156
6.1.1	Relationship between sediment yields and discharge	156
6.1.2	Estimation of annual sediment yield for intermittent basin using sediment yield equations (Second approach)	166
6.2	ASSESSMENT OF RESERVOIR SEDIMENTATION USING REMOTE SENSING	175
6.2.1.	Availability of Satellite Data	175
6.2.2.	Processing of remote sensing data	176
6.2.3.1	Import and Visualisation	177
6.2.3.2	Geometric registration	177

6.2.3.3	Identification of Water Pixels	178
6.2.4	Analysis and Results	179
6.2.4.1	Calculation of sediment deposition	179
6.2.4.2	Comparison of remote sensing results with hydrographic survey	188
7.	CONCLUSIONS	196
7.1	LIMITATIONS AND SCOPE FOR FURTHER WORKS	201
	BIBLIOGRAPHY	203

LIST OF FIGURES

S.No.	Title	Page No.
1.1	Indus river system flowing through western Himalayas (Indian part)	19
3.1	Map of the Satluj basin up to Bhakra dam	60
3.2	Drainage network map showing hydrometeorological stations	72
4.1	Cumulative Isohyetal map of the Satluj basin up to Bhakra dam for a period of 10 years (1986-96)	80
4.2	Monthly average discharge of Indian part of Satluj river at Bhakra dam	81
4.3	Snow cover distribution in the Satluj basin for 7.3.1988	89
4.4	Snow cover distribution in the Satluj basin for 30.09.1988	89
4.5	Snow cover distribution in the Satluj basin for 03.03.1989	90
4.6	Snow cover distribution in the Satluj basin for 08.05.1989	90
4.7	Snow cover distribution in the Satluj basin for 09.09.1989	91
4.8	Snow cover distribution in the Satluj basin for 12.03.1990	91
4.9	Snow cover distribution in the Satluj basin for 22.07.1990	92
4.10	Snow cover distribution in the Satluj basin for 26.09.1990	92
4.11	Snow cover distribution in the Satluj basin for 04.05.1991	93
4.12	Snow cover distribution in the Satluj basin for 27.10.1991	93
4.13	Relationship between mean monthly temperature and monthly pan evaporation at Bhakra	96
4.14	Digital elevation model of the Satluj basin up to Bhakra dam	98
4.15	Monthly evapotranspiration distribution in the Satluj basin for March, 1989	100
4.16	Potential evapotranspiration distribution in the Satluj basin for Oct., 1989	100
5.1	Structure of the snowmelt model (SNOWMOD)	107
5.2	Area elevation curve for Satluj basin up to Bhakra	110

5.3	Plot of daily rainfall data for some stations in Satluj basin for the year 1985-86	113
5.4	Daily temperature distribution for some stations in Satluj basin for the year 1985-86	117
5.5	Snowcover depletion curves for Satluj basin for the years (1986-93)	119
5.6	Snowcover depletion curves for Satluj basin for the years (1996-99)	119
5.7	Fraction of snow cover area in different elevation bands of Satluj for the water year 1985-86	120
5.8	Time distribution of effective snow cover, snow free area and total snow cover area for the water year 1985-86	135
5.9	Storage coefficient (K_b) for subsurface flow for different years	139
5.10	Comparison between observed and simulated runoff hydrographs for calibration period of 3 water years (1985-86 to 1987-88) for Satluj basin upto Bhakra	145
5.11	Variation in objective function with variation in the different model parameters	149
5.12	Comparison between observed and simulated daily runoff for Two data sets of validation period (a) 3 water years (1996-97 to 1998-99) (b) 3 water years (1988-89 to 1990-91)	151
5.13	Comparison between observed and simulated runoff hydrographs for validation period of 3 water years (1988-89 to 1990-91 for Satluj basin upto Bhakra	152
5.14	Comparison between observed and simulated runoff hydrographs for validation period of 3 water years (1996-97 to 1998-99) for Satluj basin upto Bhakra	153
6.1	Location of intermediate basin and Bhakra reservoir	157

6.2	Relationship between log values of discharge and sediment yield at Suni, Kasol and for intermediate sub-basin	163
6.3	Comparison between observed and estimated sediment yield at Suni, Kasol for intermediate sub-basin (1994)	164
6.4	Comparison between observed and estimated sediment yield at Suni, Kasol for intermediate sub-basin (1996)	165
6.5	Drainage network map of the Intermediate sub-basin	169
6.6	Digital Elevation Model of the Intermediate sub-basin	170
6.7	Drainage network map showing different order streams of the intermediate basin	171
6.8	FCC of IRS 1 A LISS II data of 1 October, 1988 and water spread area of the Bhakra reservoir	182
6.9	FCC of IRS 1 A LISS II data of 17 April, 1989 and water spread area of the Bhakra reservoir	183
6.10	FCC of IRS 1 B LISS II data of 16 October, 1996 and water spread area of the Bhakra reservoir	184
6.11	FCC of IRS 1 B LISS II data of 15 June, 1997 and water spread area of the Bhakra reservoir	185
6.12	Elevation capacity curves for Bhakra reservoir, India (1988-89)	191
6.13	Elevation capacity curves for Bhakra reservoir, India (1996-97)	192
6.14	A comparison of the results obtained through remote sensing technique and hydrographic survey	193

LIST OF TABLES

S.No.	Title	Page No.
1.1	Major river systems of the Himalayan region and their catchment areas falling in the Himalayas	7
1.2	Potential and utilisable water resources of major river systems Himalayan region	8
1.3	Minimum density of precipitation network	12
2.1	Reservoir sedimentation rates in India	45
2.2	Average sediment yields in the Chenab basin at different locations alongwith their composition during the monsoon period	52
2.3	Correlation of mean basin monsoon rainfall with sediment yield	53
2.4	Composition of suspended sediment in the Satluj system	56
2.5	Comparison of sediment yield observed for different Himalayan catchments	57
3.1	The salient topographical and hydrometeorological features of the Satluj catchment	62
3.2	Seasonal distribution of average rainfall in different ranges of Himalayas in the Satluj basin	69
3.3	Average annual rainy days, rainfall intensities for different ranges of Himalayas in the Satluj basin	69
3.4	Details of Landsat and IRS LISS I data used in the study	74
4.1	Computed rainfall, runoff and evapotranspiration for different years for Satluj river basin	82
4.2	Quarterly distribution of the annual flows of Satluj river at Bhakra dam	82
4.3	Snow covered area and permanent snow covered area in the Indian part of Satluj basin up to Bhakra reservoir	88

4.4	Monthly evapotranspiration computed for different years for the Indian part of the Satluj basin	101
4.5	Snow and glacier melt for Satluj river at Bhakra using 10 years (1986/87-1995/96) data	102
5.1	Satluj basin area covered in different elevation band	111
5.2	Raingauge and temperature stations used for different bands	114
5.3	Parameter values used in calibration of the model	126
5.4	Storage coefficients for subsurface flow for different years	138
5.5	Model efficiency during calibration period for three years	154
5.6	Percentage change in objective function due to percentage change in parameter values	148
5.7	Model efficiency for the two sets of simulation period of three years	154
6.1	Statistics of daily discharge at Suni, Kasol and Intermediate basin	159
6.2	Statistics of daily sediment yield at Suni, Kasol and Intermediate basin	160
6.3	Observed and estimated annual total of sediment yield for different years	162
6.4	Number of different order streams and their lengths	168
6.5	Annual values of sediment yield for different years	172
6.6	Observed and estimated values of sediment yield for different years	174
6.7	Sediment yields using developed regression equation and using revised equation	174
6.8	Original elevation area capacity table for Bhakra reservoir	180
6.9	Reservoir elevation and estimated area on the date of satellite pass	181
6.10	Calculation of sediment deposition in Bhakra reservoir using remote sensing for the year 1988-89	187
6.11	Calculation of sediment deposition in Bhakra reservoir using remote sensing for the year (1996-97)	188

6.12	Revised elevation capacity information for Bhakra reservoir using results of hydrographic survey of 1988-89	189
6.13	Comparison of results of hydrographic survey with remote sensing	190
6.14	Results of hydrographic survey (1996-1997)	194

CHAPTER 1

INTRODUCTION

1.1 GENERAL

Water is essential for our livelihood, from basic drinking water to food production and health, from energy production to industrial development, from sustainable management of natural resources to conservation of the environment. Growing populations, intensifying agriculture, industrial development and increasing urbanization are leading to higher demands of water. Fresh water plays a major role in satisfying these growing demands. More than half of the humanity relies on the fresh water that accumulates in mountains- for drinking, domestic use, irrigation, hydropower, industry and transportation. Rapid and increasing changes in mountain landscapes, and increasing demands on mountain resources, have many impacts on fresh water availability. Fresh water has already become a scarce resource in many parts of the world. Mountains are expected to satisfy the greater part of this growing demand of fresh water. In general, mountains are treated as a resource of water because all the important rivers of the world originate from mountains. Mountain areas constitute a relatively small proportion of river basins, yet they provide significant part of the river flows downstream. There has been very limited monitoring of hydrological data in mountainous areas. An inadequate knowledge of the hydrology of mountainous areas and poor management of water resources can result in serious degradation of water quantity and quality. There is a great need of proper assessment of mountain water resources and their proper utilization.

The mountains cover a large portion of the earth surface. As the mean altitude of the land area of the earth is 875 m above sea level, and therefore over 28% of the land

areas are above 1,000 m. In these high mountains, it is estimated that 10 to 20% of the total surface area is covered by glaciers while an additional area ranging from 30 to 40% has seasonal snow cover. Out of the total mountain glaciers, central Asian Mountains contain about 50% of the glaciers, a large portion of which drain into the landmass of Indian sub-continent. There are of course variations in depths of snow and ice from place to place depending on the location. Snow and glaciers are the reservoirs with vast storage of fresh water. Snow forms a natural reservoir, storing water for weeks, months or season. If it is properly harnessed it can be used for water supply, agriculture, industry and energy production.

With increasing pressure of human and livestock population, mountain areas are constantly being over-exploited by mankind. The exploitation activities include large-scale construction of mountain roads, mining activity, overgrazing, deforestation etc. leading to land degradation. Soil loss/degradation occurs at an accelerated rate throughout the mountainous and sub -mountainous regions, which are generally more susceptible to erosion as compared to the plains, due to topography of the land, intensity of rains and the nature of soils. These degraded land surfaces have also become one of the sources of pollution of the natural water. Deposition of soil eroded from upland areas causes aggradation in the downstream reaches of rivers. This has resulted in rising of bed levels and increase in the flood plain areas of the rivers, reduction of the clearance below bridges and culverts and sedimentation of the reservoirs. The rivers emerging out from the mountain region flow at high velocities and transport the sediment at a very high rate. The natural factors that lead to high levels of sediment transport from the region are the steepness of the terrain, the tectonic instability of the area, the relatively young age of the mountains, the large and active glaciers, the high intensity monsoon rainfall and natural weathering processes. Steep topographic gradient and poor structural characteristics of

soils available on these slopes and in the valleys become an important factor for high rate of sediment erosion. In the high mountain regions, glaciers also scour the mountain slopes and transport rock and boulders to the lower valleys.

1.2 GENERAL CHARACTERISTICS OF HIMALAYAN REGION

The word Himalaya is a compound of Sanskrit words, "hima" for snow and "alaya" for abode, referring to the lofty range between the Indo-Gangetic plain and the Tibetan plateau. It extends nearly 2,400 km in a vast southerly arc between the bend of the Indus marked by Nanga Parbat (8,125 m) on the west to the Brahmaputra bend around Namcha Barwa (7,755 m) in the east. The Himalayan range is the loftiest mountain complex on earth with 31 peaks exceeding 7,600 m in height. The extreme elevation and rugged relief are the result of rapid mountain-building forces and vigorous erosion processes. In places, they are traversed by extremely deep river gorges resulting in great vertical contrasts over very short horizontal distances (Mountain Forum Newsletter, 1999).

1.2.1 Physiography and geology

The Himalayas is the highest and youngest mountain system of the world, on the northern edge of the Indian subcontinent. The width of this mountain system is variable, being broadest in Kashmir (about 400 km.) and narrowest in Sikkim (about 160 km.). Based on its geological and geomorphological history, the system is divisible into three well-recognized transverse zones separated by distinct escarpments or fault lines. From west to east, these zones are further divisible into three sectors. These are referred to as Western Himalayas between the Indus and the Sutlej rivers, comprising the States of Jammu and Kashmir and Himachal Pradesh; Central Himalayas, between the Satluj river and Singalila range (dividing range between Nepal and Sikkim) formed of Uttranchal and

Eastern Himalayas formed of Sikkim, Bhutan and Arunachal Pradesh. The Indian Himalayan region, which is more than 2,800 km in length and 220 to 300 km wide, is spread over the states of Jammu & Kashmir, Himachal Pradesh, Sikkim, Arunachal Pradesh, Nagaland, Manipur, Mizoram, Tripura, Meghalaya, and a part of Assam, along with eight districts of Uttranchal and one district of West Bengal.

The landscape of Himalayas is founded on an immature geology and on unconsolidated rock-systems. The Siwaliks are the youngest part of the mountain system. The Siwaliks are composed of tertiary sand stones and shales. The thick Upper Siwaliks are made of conglomerates and the Lower Siwaliks beds are formed of soft and hard stones. North of the Siwaliks rise the formidable ranges of the Outer Lesser Himalayas. These extremely rugged ranges looking down on the Siwaliks are thickly forested. The rocks in Lesser and Central Himalayan zone are mainly sedimentary low grade metamorphosed and of igneous origin. The Himalayas have a wide range of parent material and the soils thus have also developed varying characteristics (Kawosa, 1988).

1.2.2 Climate

The Himalayan region has large variations in the topography, elevation and location resulting in great contrasting climates from region to region. In general the entire western Himalayan region tends to be semi-arid and/or subhumid. Only the windward slopes of the southern edge are wet, especially between 900 and 2000 m. Here the Middle Himalayas and the Siwaliks have a mean rainfall between 500 and 1000 mm. In the Siwaliks and Middle Himalayas precipitation occurs largely during summer and monsoon months whereas the greater amount of precipitation occurs in the form of snow in the Great Himalayas in the winter months. There is a great variation of temperatures between summer and winter in this region. In July the maximum temperature ranges from 26°C to

29°C in the Siwaliks, in the Middle Himalayas it is between 21°C and 26.5°C and in the Great Himalayas the mean temperature is less than 21°C. In January the western Himalayan region registers a mean temperature of less than 4°C. The higher regions experiences snow largely in winter.

1.2.3 Snow and ice

Snow cover is an important component of the hydrologic cycle. A significant part of the earth is covered by snow for at least a portion of the year, producing a substantial change in surface characteristics from those exhibited when snow is absent. About 10% of the earth's surface, $15 \times 10^6 \text{ km}^2$, is covered by polar ice caps and glaciers (Singh and Singh, 2001). The Himalayas contains over 50% of permanent snow and ice fields outside the Polar Regions. This region covers an area of 4.6 million km^2 above 1500 m, 0.56 million km^2 above 5400m and 3.2 million km^2 above 3000 m (Upadhyay, 1995). The upper catchment of the Himalayan basins is covered by seasonal snow during winters. For example average snow and glacier contribution in the annual flows of Chenab river at Akhnoor was estimated to be 50% and that for Ganga at Devprayag was about 30% (Singh et al., 1997). The accumulated snow in the Himalayan basin becomes an important source of streamflow during the summer time.

1.2.4 River systems

The Himalayas are the source of a large number of rivers, which ensure all the year round availability of water, i.e., they are perennial in nature. Since, agriculture in India is main source of livelihood, therefore, water resources generated in the Himalayas are considered as a boon to the country. Broadly rivers originating from the Himalayan region can be grouped in three main river systems; the Indus, the Ganga and the Brahmaputra. The

rivers that originate and drain through Himalayas are given in Table 1.1. The most important river system of the Himalayan region, which is also the most important system of the country, is the Indus system. It flows from the Tibetan plateau, through India and Pakistan to the Arabian Sea (Indian Ocean). Rivers Shyok, Shigar and Gilgit join it in Jammu and Kashmir. The important tributaries, including the Jhelum, Chenab, Ravi, Beas and Satluj join it after entering Pakistan. The different basins of Indus covered within the Indian territory is shown in Figure 1.1. About 90% of the mean annual flow into the Indus basin originate in the front ranges and high mountains of the Hindu Kush, Karakorum and western Himalayas. The contributions of the main rivers measured at the foot of the mountains are 13% from the Kabul, 37 % from the Indus, 14 % from the Jhelum, 15 % from the Chenab, 4 % from the Ravi, 7 % from the Beas and 10 % from the Satluj. Less than 10 % of the average runoff is the result of rainfall over the Indus plains. The runoff reflects the seasonal rainfall and snowmelt regimes of the mountain watersheds. The foothills and front ranges are predominantly exposed to seasonal monsoon rains, leading to runoff peaks from June to September, which produce some 70 % of the total annual runoff of the Indus. (Mountains of the World, 1998)

1.2.5 Water resources

There is very limited scientific information available for Himalayan water resources. This is due to very difficult terrain and hence insufficient network of observations for both precipitation and streamflow measurements. However, the available estimates show that the water yield from high Himalayan catchments is roughly two times as compared to the catchment located in peninsular India. It is believed that this is mainly due to additional inputs from snow and ice melt contributions for the Himalayan rivers. Various investigators have estimated the water resources of the Himalayan region.

Table 1.1: Major river systems of the Himalayan region and their catchment areas falling in the Himalayas (Bahadur, 1992 ; Singh and Singh, 2001)

S. No.	River	Catchment area in Himalayas (km ²)
A. Indus System		
1.	Indus	268,842
2.	Jhelum	33,670
3.	Chenab	27,195
4.	Ravi	8,029
5.	Beas	14,504
6.	Satluj	56,500
B. Ganga System		
7.	Ganga	23,501
8.	Yamuna	11,655
9.	Ramganga	6,734
10.	Kali	16,317
11.	Karnali	53,354
12.	Gandak	37,814
13.	Kosi	61,901
C. Brahmaputra System		
14.	Brahmaputra	256,928
15.	Teesta	12,432
16.	Raidak	26,418
17.	Manas	31,080
18.	Subansiri	18,130
19.	Luhit	20720

Murthy (1978) estimated that the Himalayan water resources are 245 km³/yr. Bahadur and Dutta (1996) reported that a very conservative estimates gives at least 500 km³/yr from snow and ice melt water contributions to Himalayan streams. Alford (1992) reported that the specific runoff in the Himalayas is at a maximum in an altitude belt of

considerable human activity - 1500 to 3500m and this is about 515 km³/yr from the upper mountains. Bahadur (1999a) re-evaluated that 400-800 km³/yr. flows down as meltwater contributions from the snow and glacier fields in the high mountain region as against earlier conservative estimates of 200 - 500 km³/yr. The potential and utilisable water resources of the Himalayan river systems as assessed recently is also shown in the Table 1.2.

Table 1.2: Potential and utilisable water resources of major river systems in the Himalayan region (Bahadur, 1999b)

S.No.	Item	Indus	Ganga	Brahma putra	Meghna
1.	Water resource potential (km ³)	73.3	525	537.2	48.4
2.	Utilisable surface water (km ³)	46.0	250	24.0	
3.	Groundwater potential (km ³)	25.5	171.7	27.9	1.8
4.	Per capita annual availability of water (m ³)	1757	1473	18417	7646
5.	Per hectare of culturable area annual availability (m ³)	7600	8727	44232	43447

1.2.6 Hydropower potential

Because of water availability in abundance due to melting of snow/ice and topographical setting, the Himalayan region is bestowed with a tremendous hydropower potential in its river basins. In Himalayan region, the potential of hydropower generation has not been exploited to the maximum. As per the assessment made by Central Electricity Authority during the period 1978-87, India is endowed with economically exploitable hydropower potential to the tune of 84044 MW at 60 % load factor (Prasad, 1999). Hydropower potential of the Himalayan river systems is about 78 % of the total Indian hydropower potential. The hydropower potential of Indus, Ganga and Brahmaputra river basins is assessed to be about 20000, 11000 and 35000 MW at 60% load factor respectively (Naidu, 1995). The hydropower potential of three states of J&K, Himachal

Pradesh and Uttaranchal located in western/central Himalayan region, is 7487, 11647 and 9744 MW respectively at 60 % load factor. The corresponding potential exploited so far in these states is only 480, 2007 and 1127 MW (Prasad, 1999). Several major hydroelectric projects like Nathpa Jhakri, Tehri, Chamera-II, Uri, Dulhasti, Baspa and several others are under construction in these states. A number of new additional projects are contemplated on the Himalayan rivers.

1.3 HYDROLOGICAL PROBLMES OF THE HIMALAYAN REGION

The Himalayan regions are very young, highly fragile and unstable. The hydrological problems of the western Himalayan region are different than the plain areas due to variation in topography, climate, landuse and soil characteristics. Rapid population growth and industrialization are leading to major changes in landuse and water utilisation of the region. The need for food, fiber, shelter and energy has caused many watersheds to undergo rapid landuse changes, deforestation and urbanisation. This is affecting hydrological characteristics of the Himalayan basins. Various hydrological problems of the Himalayan region are discussed in detail in the following sections.

1.3.1 Estimation of snowmelt runoff

The majority of rivers originating from the Himalayas have their upper catchment in the snow covered areas. The solid precipitation results in temporary storage and the melt water reaches the river in the melt season. The snow accumulation in Himalayas is generally from November to March, while snowmelt is from April to June. During April to June, snowmelt is the predominant source of runoff and during July to September it forms a significant constituent of melt. The snowmelt runoff modelling is of vital importance in forecasting water yield. Snow and glacier melt runoff is very important

particularly in the lean season and it plays a vital role in making perennial nearly all the rivers originating in Himalayas perennial. The contribution of the snow and glacier melt in annual flows of Himalayan rivers at potential project site is not available. Further, the extent of snow cover and its distribution with time is not available for the Himalayan region. Such information is necessary to solve the hydrologic problems of this region. There is great need to develop simple and systematic hydrological models considering rain and snowmelt inputs based on the limited data availability for this region.

1.3.2. Floods

Mountainous regions are also highly susceptible to water-related disasters. They are particularly flood-prone owing to the enhanced orographic precipitation, steep slopes covered with a thin soil over the impervious bedrock, a high runoff coefficient, and limited valley storage. Flood may be caused due to cloudbursts, rock-faults and landslides, snowmelt and glacial melt, soil erosion, and earthquake.

The floods disrupt the ecological balance and bring in its wake economic instability. The roads are damaged, rivers take diversions, buildings collapse and normal life is disrupted. The events of extremely high precipitation and other adverse hydro-meteorological conditions or cloudburst are one of the major natural hazards in the Himalayas. The water, which gushes down with cloudbursts, uproots even high trees and carries small and big boulders with it. In recent years, various severe flash floods observed in the Himalayas have been caused by cloudburst occurring during the monsoon period. There was a case of cloudbursts in the Satluj basin in the August 2000 while there was a similar incident in the upper Ganga basin in June 2000. Due to this flood, a number of bridges on Satluj River were completely destroyed. The Nathpa-Jhakri hydroelectric project, which is coming up on the Satluj River in Rampur district, was worse effected.

The floods in the mountainous areas have somewhat unique characteristics and therefore, the understanding of hydrology of mountainous areas has an important bearing on our capability and preparedness for flood management.

1.3.3 Soil erosion and sedimentation

The Himalayan regions have greatly deteriorated from intensive deforestation, large-scale road construction, mining, and cultivation on steep slopes. A large number of reservoirs have been constructed in Himalayas for hydroelectric power generation, domestic water supply, irrigation, flood mitigation etc. Excessive siltation in the reservoirs due to accelerated erosion in the Himalayan basins is reducing the capacity of reservoirs which in turn is threatening the useful life of these projects. This has considerable economic significance since the reduced soil depth leads to loss of nutrients, decline in crop productivity and downstream transport of eroded sediment leads to raising of riverbeds and decrease in reservoir capacities. The significant difference in the river dynamics, topography, geology, and size of material of the mountainous areas to those in the plains has a major effect on the characteristics of the sediments. In India a total of 1,750,000 km² out of the total land area of 3,280,000 km² is prone to soil erosion. Thus about 53 % of the total land area of India is prone to erosion. The mean annual erosion rate varies from 350 t km⁻² to 2500 t km⁻². The soil erosion in most part of the Himalayan region is high and is a serious problem. Suitable methodologies need to be evolved for an integrated approach in watershed resources development and management.

1.3.4 Availability of hydrometeorological data

WMO (1981) has suggested certain minimum density of the precipitation network for different regions as given in the Table 1.3. According to this, the minimum density for

mountainous region of mediterranean and tropical zones, should be 100-250 km² per station.

Table 1.3: Minimum density of precipitation network

	Type of the region	Range of norms for minimum network , Area (km ²) per station	Range of provisional norms tolerated in difficult conditions *
1.	Flat regions of temperate, mediterranean and tropical zones	600-900	900-3000
2(a)	Mountainous region of mediterranean and tropical zones	100-250	250-100 ⁺
(b)	Small mountainous islands with very irregular precipitation, very dense hydrographic network	25	
3.	Arid and polar zones ⁺⁺	1500-10000 ^{**}	

* Last figure of the range should be tolerated only under exceptionally difficult conditions

⁺ Under very difficult conditions this may be extended to 2000 km.

⁺⁺ Great deserts are not included ^{**} Depending on the feasibility

The hydrometeorological/hydrological network in the Himalayan regions is not as per the norms suggested by WMO. There are various reasons for such poor network in the region. In case of the Himalayas, difficult terrain/rugged topography, and harsh weather conditions restrict the installation and operation of the instruments in the high altitude regions. It has resulted in the sparse network in the headwaters of the basin, while it is reasonably good in the lower part of some of the basins, where rainfall is experienced. Thus for most of the river basins in Himalayan region, the database for hydrological and climatological studies is not sufficient. However, there are few basins like Satluj, Beas and Chenab in the western Himalayas, which have generally good network both in the lower altitude and high altitude regions. Keeping in view the requirement of data for various hydrological studies, there is an urgent need to strengthen the network of the Himalayan region. There is much scope for using the automatic weather stations for such type of terrain.

1.4 ROLE OF REMOTE SENSING AND GIS

The problems due to harsh climate, difficult accessibility and poor communication facilities could be overcome to some extent by using remote sensing data. Remote sensing and GIS are being used increasingly as tools to assist in resource inventory and the integration of data and as a mechanism for analysis, modelling, prediction and forecasting to support decision making processes.

Potential application areas of remote sensing and GIS in mountain environment include snow cover analysis, terrain analysis, mountain hazard mapping, watershed management and accessibility analysis. With the advent of modern earth resources/monitoring satellites, considerable data on the Himalayan region's natural resources are now available. Advances in satellite image processing and computer analysis have made it possible to evolve a realistic, accurate and uniform database for hydrological studies. Integration of biophysical and socio-economic data can be made in the GIS environment and can be used to develop a good database for the difficult terrain. Contrary to the conventional approach, these tools enable the combination of multi-spectral spatial data and their presentation in a reasonable understandable map format.

Measurements of snow cover in the mountainous basins are very difficult. Conventional methods have limitations in the monitoring of snow covered area in the Himalayan basins because of inaccessibility. Because of the difficulty of making field measurements in snow covered mountainous regions, remote sensing is perhaps the only means of measuring snow cover extent and properties. Fresh snow has a very high reflectivity in the visible wavelengths, however, it decreases as the snow ages. The reflectivity of snow is dependent on many snow characteristics like shape and size of snow crystals, liquid water content (especially of the near surface layers), impurities in the

snow, depth of snow, surface roughness etc. In addition, the solar elevation and azimuth also influences the spectral reflectance to a large extent (Hall and Martinec, 1985).

Since, very little information on snow is collected regularly in the Himalayas, remote sensing remains the only practical way of obtaining some relevant information of the snow cover in the large number of basins in the Himalayas. At present the visible, near IR and thermal IR data from various satellite (Landsat, IRS, NOAA) are being used operationally for mapping the areal extent of snow cover in the Himalayan basins. Visible and near infrared wavelengths, because they do not penetrate far into the snowpack, mainly provide information about the surface of the snowpack. Chang et al. (1976) showed that microwave wavelengths can penetrate the snowpack. Microwave remote sensing is promising because of its ability to penetrate the dry snow-pack, and its capability to acquire data in cloudy or nighttime conditions (Carsey, 1992).

1.5 OBJECTIVES AND SCOPE OF THE PRESENT STUDY

As mentioned above, the snowmelt is a vital component of the streamflow for the Himalayan river system. The spring and summer runoff, comprising mostly snowmelt, is the main source of water for irrigation, hydroelectric power and drinking water supply. Therefore, estimation of snowmelt runoff is very essential for regulating the flow from the reservoirs, estimating design flood for the hydraulic structure and other water resources development activities in the Himalayan region. The development of suitable modelling approach of this valuable source of water supply is, therefore, of utmost important for management and utilization of water resources in the Himalayan region. In spite of the importance of snowmelt runoff in the Himalayan water resources, very limited efforts have been made for modelling of snowmelt runoff. Therefore, one of the main objectives of the present research work is to develop a suitable conceptual snowmelt runoff model for

a Himalayan basin keeping in view the availability of data in this region. Also the contribution from snow and glacier in annual flows of a snowfed river is very significant and requires a simple approach for its estimation. The development of a water balance approach for this purpose is also included. High sediment yield from Himalayan basins partially offset the enormous hydroelectric potential of its rivers by sedimentation of the reservoirs located at downstream. Consequently, studies of sediment yield and reservoir sedimentation are equally important. There is a need for simple scientific approach to estimate sediment yield from the Himalayan basins using a simple scientific approach. Therefore, in the present work, in addition to snowmelt modelling, sediment yield estimation and reservoir sedimentation have also been included as important observations.

The study area chosen for present study is Satluj basin (Indian part) up to Bhakra dam in western Himalayas. The Satluj basin has a significant contribution from snow/ice and feed the Bhakra reservoir located in the foothills of the Himalayas. The hydrometeorological network in this basin is reasonably good and therefore reasonable adequate data is available for such hydrological studies. At present Bhakra project is operational on this river and some more large projects are under construction. The outcome of the present study is of immediate use for the concerned agencies and projects.

For carrying out this research work, all the hydrometeorological data (rainfall, discharge, temperature, snow and evaporation etc.) has been collected from BBMB, Nangal. The remote sensing data for the study basin for the estimation of snow-cover area and water spread etc. was obtained from National Remote Sensing Agency, Hyderabad. For creation of digital elevation model which is used for extraction of topographical information and creation of elevation bands etc., the Survey of India toposheets have been used. Beside the collection of the data required and processing of the data for extraction of

useful information required in the study, the total work has been divided into following four main objectives; defining the scope of the study:

1. Development of suitable method for estimation of snow and glacier contribution in the annual flows of Satluj river
2. Development of snowmelt runoff model structure for the estimation of runoff and testing of snowmelt model for simulation of streamflow for the Satluj basin
3. Development of relationship between sediment yield and discharge and estimation of sediment yield for the study basin
4. Estimation of sediment deposition in Bhakra reservoir using remote sensing approach

1.6 ARRANGEMENT OF THE CHAPTERS

This thesis comprises of seven chapters in total, including Chapter 1 on introduction. In this chapter, brief description about the Himalayan region including drainage systems, water resources and hydropower potential have been covered. The hydrological problems such as estimation of snowmelt runoff, floods, sedimentation of the Himalayan region in general have been provided. The scope and objectives of the present study have been described.

Chapter 2 covers the review of the relevant literature available. On all the concerned topics associated with present work like, hydrological modeling of snow melt runoff, soil erosion/sediment yield and reservoir sedimentation using remote sensing. The use of remote sensing in snow cover estimation has also been reviewed. The snowmelt and sediment yield studies made in Himalayan region and in Satluj basin in particular have also been reviewed and discussed.

Chapter 3 gives the description of the study area and the data used for the present work. The importance of the study basin has also been presented. The climatic conditions and seasonal variations in the study basin have been dealt with. The distribution of temperature and precipitation with elevation has also been covered. The availability of the hydrometeorological and sediment data has been discussed. The remote sensing data used in the study have been presented in the form of tables.

Chapter 4 deals with the development of water balance approach for the estimation of contribution of snow and ice in the annual flow of Satluj River at Bhakra site. The streamflow characteristics of the study basin have been described. Snow cover area obtained from remote sensing data has been covered. The methodologies for estimation of evapotranspiration using two different approaches, which were used in the present study, have been described.

Chapter 5 describes relevant physical processes for the snowmelt runoff modeling and the structure of the model developed. The requirement of the input data for the model has been discussed. The data preparation from field data, Survey of India toposheets and from satellite data for the study basin has been described. The computation of streamflow and its routing from snow cover area and snow free area has been dealt separately. The different parameters taken for the optimization purpose including their sensitivity analysis have been discussed. The results of calibration and simulation have been discussed. The efficiency criteria for testing of the results obtained for this study has been discussed.

Chapter 6 covers the estimation of sediment yield as well as the assessment of reservoir sedimentation using remote sensing approach. Statistical analysis of the sediment and

discharge data is also presented. The different approaches adopted for sediment yield estimation have been discussed. The generation of some of the parameters required for the study using GIS approach has been explained. The results obtained from remote sensing approach have been compared with the results of hydrographic survey.

Chapter 7 presents the conclusions of the present research work along with some recommendations. Some suggestions have been made to extend the present study for other Himalayan basins.

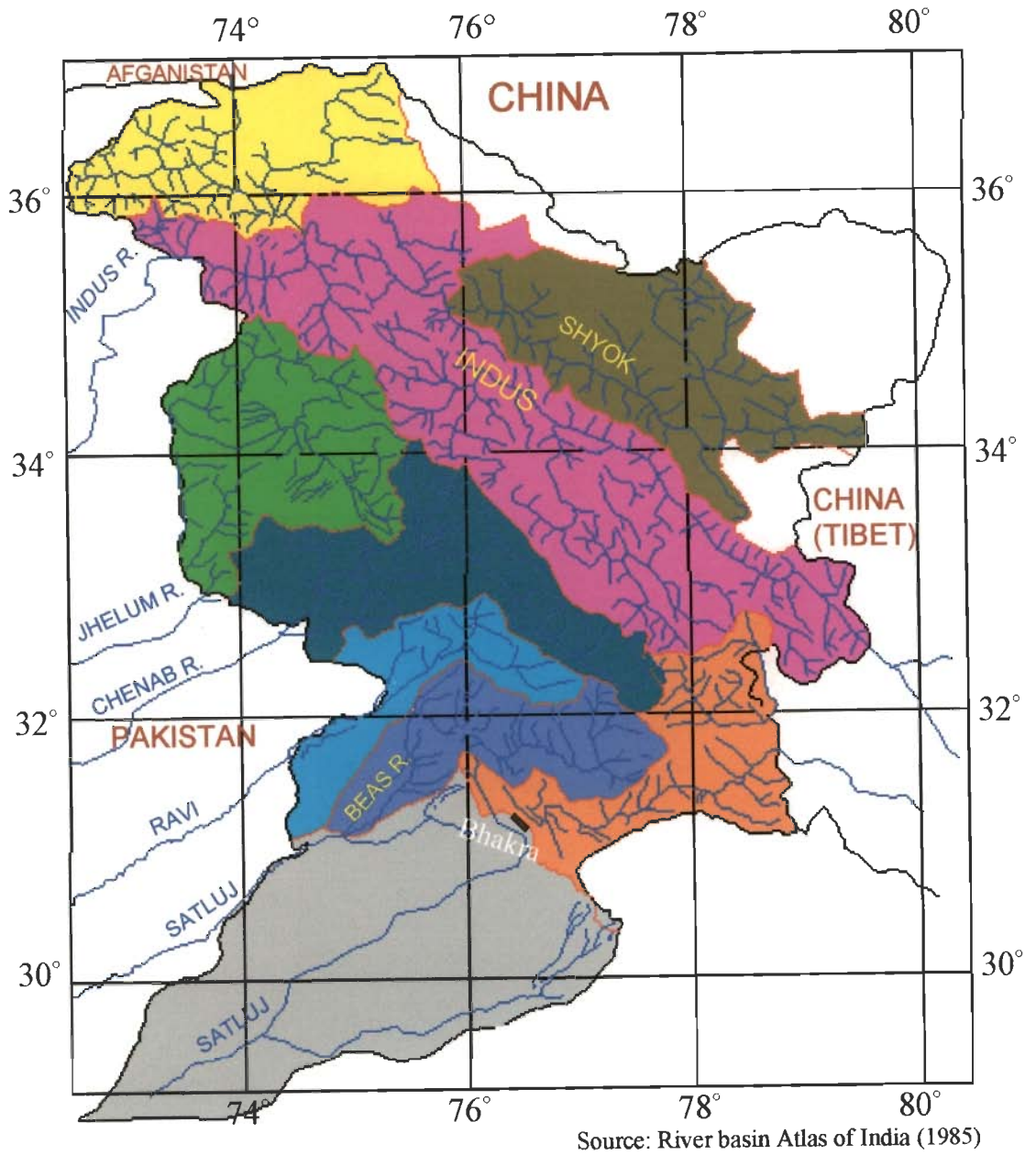


Figure 1.1 Indus river system flowing through western Himalayas (Indian part)

CHAPTER 2

REVIEW OF LITERATURE

The main objective of the present work is to develop a snowmelt runoff model for a Himalayan basin. The problems of soil erosion and reservoir sedimentation studies are also closely associated with streamflow and therefore these studies have also been included in this work. This chapter presents a review of relevant literature for snowmelt/rainfall modelling and sediment yield/ reservoir sedimentation studies. A section is also devoted to the application of remote sensing in snow studies. Snowmelt and sediment studies carried out for the Himalayan basins have been reviewed and presented.

2.1 MODELLING OF SNOWMELT RUNOFF

Hydrologic simulation models that include snow are generally divided into three basic components namely the snow cover, a precipitation-runoff relationship and a runoff distribution and routing procedure. Snowmelt runoff simulation models generally consist of a snowmelt model and a transformation model (WMO, 1996). The snowmelt model generates liquid water from the snowpack that is available for runoff. The transformation model is an algorithm that converts the liquid output at the ground surface to runoff at the basin outlet. The snowmelt and transformation models can be lumped or distributed in nature. Lumped models consider whole catchment as a single unit and use one set of parameter values to define the physical and hydrological characteristics. Distributed models attempt to account for the spatial variability by dividing the basin or catchment into sub-areas and computing snowmelt runoff for each sub area independently with a set of parameters corresponding to each of the sub-areas. Generally distributed models use

one of the following general approaches to sub-divide a basin: (i) Elevation zone or band (ii) basin characteristics such as slope, aspect, soil, vegetation etc. and (iii) a fixed or variable length, two or three-dimensional grid. Lumped and distributed models are classified further by their use of energy balance approach or temperature index approach to simulate the snowmelt process.

2.2 SNOWMELT COMPUTATION

The snowmelt component of snowmelt runoff simulation models generally takes the form of an energy balance or a temperature index to simulate the process of melting. The first approach is known as energy budget or the energy balance approach and the second is the temperature index or degree-day approach. These approaches are discussed below:

2.2.1 Energy balance approach

The energy balance or heat budget of a snowpack governs the production of meltwater. This method involves accounting of the incoming energy, outgoing energy, and the change in energy storage for a snowpack for a given period of time. The net energy is then expressed as equivalent of snowmelt. The energy balance equation can be written in the form (Anderson, 1973).

$$\Delta Q = Q_n + Q_e + Q_h + Q_g + Q_m \quad (2.1)$$

where:

Q_n = net radiation (long and short wave)

Q_e = latent heat transfer

Q_h = sensible heat transfer

Q_g = ground snow interface heat transfer

Q_m = heat transfer by mass changes (advected heat)

ΔQ = change in heat storage

In the above energy balance equation, different components of energy are considered in the form of energy flux, which is defined as the amount of energy received on a horizontal snow surface of unit area over unit time. The positive value of Q_m will result in the melting of snow.

The relative importance of the various heat transfer processes involved in melting of a snowpack depends on time and local conditions. For example radiation melting dominates the weather conditions when wind is calm. Melting due to sensible heat flux dominates under warm weather conditions. When all the components of energy balance equation are known, the melt rate due to energy flux can be expressed as,

$$M = Q_m / [\rho_w \cdot L \cdot \beta] \quad (2.2)$$

where,

M = depth of meltwater (m/day)

L = latent heat of fusion (333.5 kJ/kg)

ρ_w = density of water (1000 kg/m³)

β = thermal quality of snow

The thermal quality of snow depends on the amount of free water content (generally 3 – 5 %) and temperature of the snowpack. For a snow that is thermally ripened for melting and contains about 3% of free water content, the value of β is 0.97. For such cases equation (2.2) reduces to,

$$M = Q_m / [1000 \cdot 333.5 \cdot 0.97] \quad (2.3)$$

which leads to a simple relationship,

$$M = 0.0031 * Q_m \quad (\text{mm/day}) \quad (2.4)$$

Data required to evaluate Equation (2.1) are measurements of air temperature, albedo, wind speed, vapour pressure and incoming solar radiation (Anderson, 1973). These data are difficult to obtain on a basin scale and extrapolation to areal values from point data is another problem, especially the spatial detail is required for distributed models. This becomes further difficult when such data is required for a highly rugged terrain, such as Himalayan terrain. As such application of the energy balance equation is usually limited to small, well-instrumented or experimental watersheds.

2.2.2 Degree-day approach or Temperature index approach

The specific type of data required for the energy budget method is rarely available for carrying out the snowmelt studies. This is particularly true for the Himalayan basins where the network for data collection is poor. The commonly available data in the Himalayan basins are daily maximum and minimum temperatures, humidity measurements and surface wind speed. This is why the temperature indices are widely used in the snowmelt estimation. It is generally considered to be the best index of the heat transfer processes associated with the snowmelt. Air temperature expressed in degree-days is used in snowmelt computations as an index of the complex energy balance tending to snowmelt. A 'degree-day' in a broad sense is a unit expressing the amount of heat in terms of persistence of a temperature for 24-hour period of one-degree centigrade departure from a reference temperature. The simplest and the most common expression relating daily snowmelt to the temperature index is,

$$M = D (T_i - T_b) \quad (2.5)$$

where,

M = melt produced in mm of water in a unit time

D = degree-day factor ($\text{mm } ^\circ\text{C}^{-1}\text{day}^{-1}$)

T_i = index air temperature ($^\circ\text{C}$)

T_b = base temperature (usually $0\text{ }^\circ\text{C}$)

Daily mean temperature is the most commonly used index temperature for snowmelt. The mean temperature is computed by,

$$T_i = T_{\text{mean}} = (T_{\text{max}} + T_{\text{min}}) / 2 \quad (2.6)$$

There are several methods of dealing with the index temperatures used in calculating the degree-day value. When using the maximum-minimum approach, the most common way is to use the temperature as they are recorded and calculate the average daily temperature. Garstka et al., (1958), reported that sometimes the degree-days from the daily mean temperature are found to be misleading. In many parts of the Western U.S. mountainous areas, the drop in minimum temperature is so much that the daily mean temperature comes to below $0\text{ }^\circ\text{C}$, thereby indicating no possible degree-days, whereas snowmelt conditions have prevailed during a part of the day when air temperatures were much above the freezing point. The inclusion of minimum temperature at an equal weight with the maximum temperature gives undue emphasis to this effect. On the other hand the use of maximum temperature only excludes this effect entirely. In order to counteract such problems, alternatives have been suggested in which unequal weight to the maximum and minimum temperature are given. U.S. Army Corps of Engineers (1956), used the following index temperatures,

$$T_i = (2T_{\text{max}} + T_{\text{min}}) / 3 \quad (2.7)$$

Another approach is given by,

$$T_i = T_{\text{max}} + (T_{\text{min}} - T_{\text{max}}) / b \quad (2.8)$$

where, b is a coefficient less than 2.

When the basin is subdivided based on elevation zones, the degree-days are extrapolated to an elevation zone by using a suitable lapse rate i.e.,

$$T_{ij} = \delta (h_{st} - h) \quad (2.9)$$

where,

T_{ij} = degree-day of the elevation zone

δ = temperature lapse rate in °C per 100 m

h = zonal hypsometric mean elevation in m.

h_{st} = altitude of the temperature station in m.

In a basin with little seasonal variation, a lapse rate of 0.65 °C /100 m has been found to be suitable. A study carried out by Singh (1991) indicates that a lapse rate of 0.65 °C /100 m. is suitable for Satluj basin in Himalayas.

2.3 CLASSIFICATION OF SNOWMELT MODELS

The snowmelt models are categorized based on two basic approaches namely (i) Statistical (ii) Simulation models. These are briefly discussed below:

2.3.1 Statistical models

The statistical correlation models are generally used for seasonal yield forecasting. The basic method uses the correlation analysis to relate the current snow cover or the past precipitation, or combinations thereof, to the observed seasonal runoff (U.S. Army Corps of Engineers, 1956). Other variables have been added to the analysis in an attempt to improve results. These include base flow, soil moisture, wind, high elevation and low elevation water equivalent or precipitation ratios and aerial extent of snow cover (Anderson, 1972). Long-term forecasts are made using statistically developed equations relating the volume of runoff to snow pack and antecedent conditions. The long-term

forecasts are generally concerned with seasonal volumes or, some times, seasonal maximums using current snow cover conditions plus probable future climatic patterns. In such forecasts the detailed time distribution of runoff is not concerned although monthly distribution may be attempted. Statistical methods are widely used and yet they are limited in accuracy by the theoretical constraints on the data as well as by their inability to represent the complex physical interaction of the snowmelt runoff processes.

2.3.2 Simulation models

Both conceptual and physical approaches of simulation have been employed in snowmelt-runoff modelling. Conceptual models use a mathematical relationship between snowmelt and measured quantities; thus melt can be calculated without treating in detail all the physical processes and parameters that affect snowmelt. Conceptual models have the benefit of requiring less informational input, but suffer from the uncertainty about the degree of applicability of parameters estimated under one set of model conditions to other conditions.

One of the main obstacles to physically based modeling is the observation/collection and compilation of the necessary meteorological and snow-cover data to run, calibrate, and validate such models. For example, basin discharge has frequently been used as the sole physical criterion of model calibration and performance assessment for conceptual snowmelt models. But as it is an integrated response to melt and runoff, basin discharge is not sufficient to discriminate between the effects of the multiplicity of data inputs driving physical models and that distributed snow cover data are required to assess model performance (Bloschl et al., 1991 a; Bloschl, 1991 b). A comparison of a detailed research-oriented point-snowmelt model and a simpler operational model revealed that in the absence of detailed measurements of snowpack

variables, a detailed physical model of the snowpack is needed to reduce the need for parameter calibration (Bloschl and Kirnbauer, 1991). Several simplifying assumptions are necessarily made in order to solve physically based point models, thus limiting their validity in many field situations (Illangasekare et al., 1990). Nevertheless, wherever sufficient data is available physically based models are being tested and applied such as in alpine catchments (Ranzi and Rosso, 1991).

Several simulation models to account snow accumulation and melting processes have been developed. These models attempt to mathematically represent each component of the total process. The basic difference between the various models is the mathematical relationships, which they use for each component. The simulation models are relatively recent innovations and offer a great potential both as a forecasting tool and as a means to improve the understanding of snowmelt processes.

Anderson (1978), dealt in detail the various aspects of the model structure, including snow accumulation, surface energy exchange, water retention and movements, snow cover properties, snow cover distribution, snow-soil interaction etc. Seasonal variation in melt factor has been considered essential primarily because of the variation in net available solar energy. The air temperature, in general, has been found as adequate index of snow cover energy exchange where the meteorological factors such as dew point, wind etc. do not deviate significantly from normal. The effects of transmission melt water through snow, resulting in lag and attenuation has also been mentioned. Thus, it is obvious that improvement in seasonal yield forecasting may come through the use of simulation models, and incorporation of more advanced statistical methods, such as stochastic processes, which allow more accurate statements as to the probability of future runoff volume and its distribution.

Other typical scheme for watershed discretization is the grouped response unit (GRU) presented by Kouwen et al. (1993). A GRU is a region in a watershed that can be grouped in a manner that is convenient for modelling of the basin. This can be on the basis of zones of uniform meteorology (ZUM's) (Schroeter, 1988) which is convenient for interpolating gauged meteorological data, or on the basis of grid cells that are convenient for integrating with map coordinates and remotely sensed data (Kouwen et al., 1993). In the GRU approach, regions with hydrologically similar response within each unit are grouped together, regardless of location, and treated separately for runoff calculations. The sum of the runoff from each type of region within a GRU becomes the total runoff from the GRU that is available for streamflow routing. For watershed modelling, the importance of considering the unique contribution of each land cover type to the hydrological response of the watershed is well recognized (Duchon et al., 1992; Tao and Kouwen, 1989). Groups within each GRU are usually assembled by vegetation type. This is an extension of the urban runoff modelling practice of summing runoff contributions from distinctly different areas (pervious and impervious) within a watershed prior to routing (Viessman et al., 1977). In practice, the method has significantly reduced the calibration and validation errors in the modelling of rainfall-runoff events in southern Ontario (Tao and Kouwen, 1989) and the concept has subsequently been used in other studies (Kite and Kouwen, 1992; Duchon et al., 1992).

Williams et al. (1999) developed a model based on the physically justifiable method that uses elevation and radiation indices together with some measurements to distribute melt over a watershed. This model separates the energy that causes snowmelt into three components: a spatially uniform component, a component that uses elevation, and one that is proportional to solar illumination. Measurements of snowmelt at several topographically unique points in a watershed are related to elevation and solar illumination

through regression in order to factor the melt energy into three separate components at each time step. The model is driven using inputs from snowmelt measurements at the index locations used to calibrate the regression at each time step. Then the spatial pattern of solar illumination is used to predict the spatial distribution of melt over the whole watershed.

The energy balance is mostly used for studies at a point or on small plots (Leavesley 1989). For the basin scale the Institute of Hydrology Model, IHDM (Morris, 1980) and the Systeme Hydrologique Europeen, SHE (Jonch-Clausen,, 1979) were developed and tested. Simplified versions of the energy balance equation are used in the Precipitation Runoff Modelling System, PRMS (Leavesley et al., 1983) and the Snowmelt Model, MELTMOD (Leaf and Brink, 1973). The HBV model (Bergstrom, 1976), the Snowmelt Runoff Model, SRM (Martinec et al., 1983), the UBC-model (Quick and Pipes, 1977), the Cequeau-model (Charbonneau et al., 1977), the National Weather Service River Forecast System, MWSRFS (Anderson, 1973) and the Streamflow Synthesis and Reservoir Regulation Model, SSARR (US Army, 1975) use the degree-day-model. An intercomparison of some models is given by the WMO (1986).

2.4 SATELLITE REMOTE SENSING OF SNOW COVER

Distributed hydrological models, which can account for the spatial variability of basin physiography and meteorological inputs, have the potential to exploit detailed snow cover data, including distributed SCA. Conventional snow cover data, such as snow surveys, provide detailed information on such snow pack properties but their site specific nature and infrequent occurrence limit their potential for use in distributed models. In order to provide distributed information characterizing the snow cover of a watershed, snow survey measurements must be extended to regions where no snow survey data are

available. Remote sensing offers a significant potential for collecting this data in cost effective manner. Because of difficult access and expensive operation of hydrological stations, radar or satellite data are particularly appropriate. However, ground truth data are indispensable in the calibration and verification of remotely sensed data. Aerial and satellite surveys are useful in mapping snow lines. The wealth of observational material obtained by remote sensing can be integrated into models, such as snowmelt runoff models, considerably improving the forecast accuracy. Snow was first observed by satellite in eastern Canada from the TIROS-1 satellite in April 1960 (Barnes and Smallwood, 1975). Since then, the potential for operational satellite based snow cover mapping has been improved by the development of higher temporal frequency satellites such as GOES (Geostationary Operational Environmental Satellite), Landsat, SPOT and IRS series, and NOAA-AVHRR, NIMBUS-SMMR and DMSP SSM/I satellites.

Snow has a high albedo in the visible region of the electromagnetic spectrum compared to most natural surface cover. For this reason snow covered area maps were one of the first satellite remote sensing applications (Tarble, 1963; Martinec, 1972). The technology has developed to the point where image processing systems are widely available (Baumgartner and Rango, 1991) and percent SCA estimates on a watershed basis can be obtained in near real-time for most of North America (Carroll, 1990; NOAA, 1992).

The net radiation balance is usually the most important factor in the snow pack energy budget (Wiscombe and Warren, 1980; Dozier, 1987) and snow covered area (SCA) estimates can provide a means to estimate the net radiation flux over a discontinuous snow pack. However, few hydrological models make use of SCA, partly because data are difficult to obtain. Exceptions are the U.S. National Weather Service River Forecast Simulation (NWSRFS) model (Anderson, 1973) and the Snowmelt Runoff Model (SRM)

(Rango and Martinec, 1979). In the NWSRFS model SDC's are used to relate basin water equivalent to basin SCA in order to apportion the energy balance and melt. The SDC's are basin dependent and are generally developed as part of calibrating the model to a particular watershed. In the SRM, the SCA is used directly in the regression-based degree-day melt equation, incorporating a procedure to update the SCA using Landsat imagery. Elevation bands are used in addition to snow cover depletion curves to account for the SCA. Both the NWSRFS and SRM models have worked particularly well in alpine watersheds, which typically have long ablation periods and snow cover depletion patterns that are similar from year to year.

The network of geostationary meteorological satellites allows mapping of both snow and ice from several high mountainous regions of the world, and allows a comparison to be made of large-scale seasonal changes. However, the spatial and spectral resolution of the sensors on board these satellites is too coarse for snow cover mapping. The high-resolution satellites, such as Landsat, SPOT, IRS and JERS and the medium resolution satellites such as NOAA are widely used for mapping snow cover (Rango and Martinec, 1981; Baumgartner et al., 1986, Swamy and Brivio, 1996, 1997). However, the repeat cover period for high resolution satellites such as Landsat is 16 days, which is not adequate for mapping shallow snow cover that can completely melt between consecutive overpass. Also, clouds often obscure visible imagery of the earth's surface and thus estimates of watershed state parameters using visible imagery are not a reliable source of data. However, mapping of shallow snow cover would be useful if provided at the daily repeat coverage intervals of meteorological sensors such as GOES or NOAA. GOES and NOAA imagery have an approximate spatial resolution of 1 km. (Hord, 1986).

Another possible source for snow cover information is microwave satellite imagery. The regular and frequent mapping of snow cover is possible using a sensor

independent of time and weather. Depending on wavelength, microwave radiation will penetrate clouds and most precipitation, thus providing an all-weather observational capability, which is very significant in snow regions where clouds frequently obscure the surface (Schanda et al. 1983). There are two types of microwave sensors: active and passive. Passive radiometers include NIMBUS-7 Scanning Multi-channel Microwave Radiometer (SMMR) and the DMSP SS/I (Hord, 1986) satellites and measure surface brightness temperatures. Active satellite sensors contain synthetic aperture radar (SAR) and emit microwave radiation at a specific frequency and polarization and measure the return backscatter in the form of the backscatter coefficient.

Microwaves have unique capabilities for snow cover modelling:

1. They can penetrate cloud cover (Chang, 1986), providing reliable data;
2. They can penetrate through various snow depths depending on wavelength therefore potentially capable of determining internal snowpack properties such as snow depth and water equivalent (Rott, 1986);

Microwave sensors have been studied as potential sources for snowcover information (Rott, 1986; Goodison et al., 1990; Bernier, 1987; Rango, 1986, Leconte & Pultz, 1990, Saraf et al., 1999). Of interest in the studies is measurement of the snow cover areal extent, depth and water equivalent.

Active microwave sensor was there on the First European Remote Sensing Satellite (ERS-1) and Canadian RADARSAT offer the possibility to observe seasonal snow cover characteristics in detail over the entire snow-cover season (Way et al., 1993). In one simulation of RADARSAT data, snow-cover classification accuracy was 80%, comparable to aircraft Synthetic Aperture Radar (SAR) (Donald et al., 1993). Comparing a classification of snow-covered area based on SAR with that done using TM suggests that a SAR-based classification is sufficiently accurate to substitute for visible-and-near-IR

based estimates when such data are not available, for example due to cloudiness (Shi and Dozier, 1993).

Passive microwave signals are also sensitive to the liquid-water content of snow, thus offering the potential to develop snow wetness estimates. The sensitivity of passive microwave signals to snow wetness aids in determining the onset of spring melt and the occurrence of multiple melt events during the winter (Goodison and Walker, 1993). In passive mode, microwave emission is strongly dependent on the condition of the snow in terms of humidity, metamorphism and water equivalence. Microwave penetration depth of dry snow is much larger and dry snow cover less than 2.5 cm depth is transparent to the microwaves and ignored even though it is thick enough to reflect incoming short-wave radiation (Carsey 1992). The interaction of microwaves with snow strongly depends on the snow wetness, size and structure of snow grains. The dielectric constants of water and snow are so drastically different that even a little melting will cause a strong microwave response (Rango 1986). Wang et al. (1992) found good agreement between aircraft and microwave depth estimates for an Alaskan snowpack; but they also noted that the radiometric correction for the effect of atmospheric absorption is important at all wavelengths used for a reliable estimation of snow depth. Experimental snow mapping with satellite derived passive microwave radiometer data show the high potential of mapping for dry snow (Kunzi et al. 1982). However, the poor spatial resolution of the satellite microwave sensors, typically of the order of 25km, has restricted the use of snow cover values estimated from passive remote sensing for snowmelt run-off determination in high mountainous catchments (Chang et al., 1991).

Several researchers have reported on efforts to incorporate remote-sensing data into snowmelt-runoff modeling. Rango (1993) reviewed the progress that has been made for incorporating remote-sensing data into regional hydrologic models of snowmelt runoff.

The National Oceanic and Atmospheric Administration's (NOAA) Advanced Very High-Resolution Radiometer (AVHRR) sensor provides daily views over large areas (1000-km swath) and snow-cover maps are produced operationally. In large basins ($>10^3$ km²) AVHRR or other medium resolution sensors provide daily coverage in cloud free weather and are used for operational snow snow maps by the US NWS (Rango, 1996) and in some applications of SRM (e.g., Baumgartner et al., 1987). Estimates of snow-covered area based on remote sensing data can significantly improve the performance of even simple snowmelt models in alpine terrain (Kite, 1991; Armstrong and Hardman, 1991). For operational purposes, empirical approaches using combination of remote sensing data to estimate snow-covered area, and snow-depth networks to estimate SWE are continuing to improve (Martinec and Rango, 1991; Martinec et al., 1991). If SCA observations can be provided at intervals of a week or two, SRM can be used for forecasting without any historical data on snow cover depletion (Seidel et al., 1994).

2.5 SNOWMELT STUDIES FOR HIMALAYAN BASINS AND SATLUJ BASIN

The snowmelt studies carried out in the Himalayan region may be broadly categorized as studies related with regression analysis, empirical relationships and application of snow melt simulation models.

2.5.1 Development of regression relationships

In the regression analysis category, regression was carried out to co-relate the snow cover area with the runoff. Efforts were also made to co-relate the winter snowfall and snowmelt runoff. Rango et al., (1979), used the satellite imageries for finding the snow covered areas during early April over the Indus river and the Kabul river in Pakistan which was regressed with the flows of April to July for the years 1969-73. The early spring snow

covered area was significantly related to April through July 31 streamflow, in regression analysis for each watershed. Predictions of the seasonal flows for 1974 using the regressed equations obtained were found to be within 7% of the actual flow. The relationship between snow cover area and runoff of the Beas basin has been studied by Gupta et al., (1982). Snow cover area was mapped from Landsat imageries and the snow cover area and the subsequent runoff in different sub-basins was found to be well co-related. It has been interpreted that there have been years of uniformly heavier and lighter snowfall all over the basin and snowmelt discharges have systematically varied.

Jeyram and Bagchi, (1982), estimated the snowline altitude and the snow cover using Landsat imageries for Tons river basin in Himalayas. A relationship was observed between the snowline of Beas, Ravi and Tons. Lean season discharge of Sainj river has been studied by Krishnan, (1983), in reference to winter snowfall and discharge, to establish the relationship between two variables. The studies have revealed that both these parameters have a high co-relation coefficient of 0.91. Based on this study, a simple linear regression model was evolved to forecast (three to four months in advance), the lean season discharge of Sainj river solely on the basis of winter snowfall.

Dey and Goswami, (1983), have presented results of studies involving utilization of satellite snow cover observations for seasonal stream flow estimates in Western Himalayas. A regression model relating seasonal flow from April through July 1974 to early April snow cover, explained 73% and 82% of the variance, respectively, of measured flows in Indus and Kabul rivers. The importance of permanent snow covered area in the study of the snowmelt was brought out by Ferguson, (1985). A study was carried out for the glacierized mountains (Upper Indus in Pakistan) and a model was developed for annual variation of runoff and its forecasting. The approach is based on identification of a number of glaciological and climatological factors other than snow covered area. Roohani,

(1986) related the information about extent of snow cover obtained from the Landsat MSS imageries for the months of March to June with the snowmelt runoff assumed as total flow minus baseflow for different sub-basins of Chenab river. A general linear relationship was obtained. Mohile et al., (1988), carried out a study to develop a regression relationship between temperature of Kaza and snowmelt runoff collected at a proposed dam across Spiti river, about 4 km upstream of Kaza at an elevation of about 3639 m, in the Satluj basin.

A regression model using percentage of snow covered area of Satluj basin up to Bhakra dam and seasonal snowmelt runoff (April – June) for the years 1975-78 was attempted by Ramamoorthi, (1983). The model was used to forecast the seasonal snowmelt runoff in Satluj for 1980. At the end of June 1980 it was found that the difference between the forecast quantity and observed flows was about 9%.

2.5.2 Application of empirical relationships

Several snowmelt studies using empirical relationships between temperature and snowmelt runoff have been made. Such empirical relations are generally a function of degree-day factor and snow cover area. Thapa, (1993), estimated snowmelt by considering the melt due to influence of temperature and rainfall in the snow covered area for Beas basin up to Larji. The relationship between snow covers acquired with the help of satellite imageries and the cumulative discharges of the months of March, April and May for the year 1973,1975,1976 and 1977 was studied. Due to availability of limited meteorological and hydrological data, the estimation of snowmelt runoff has been limited to the sub-basin upstream of Manali.

Bagchi, (1981), carried out a study of snowmelt runoff in Beas basin using satellite images. Temperature index method was employed using a lapse rate of $0.65^{\circ}\text{C}/100\text{m}$. The

value of degree-day factor was considered as $2.1 \text{ mm C}^{-1} \text{ day}^{-1}$. The study was carried for the Beas basin up to Manali. An empirical model for prediction of snowmelt runoff in Satluj basin has been used by Upadhyay et al., (1983). The model for computation of snowmelt runoff has been presented as a function of degree-day factor. Upadhyay et al., (1983), also analyzed the various components of energy input to a snow cover and monthly budget for net energy available for snowmelt have been worked out for a number of stations in Himalayas.

The snowmelt runoff generation for a sub-catchment of Beas basin was made by Agarwal et al., (1983), using point energy and mass balance approach. The contribution of various energy sources in different conditions was also worked out. Snowmelt runoff was estimated using the degree-day method. Snowmelt thus arrived was compared with the observed discharge. The study was based on the data for the year 1981-92 collected from the snow courses located in the sub-catchment. Results indicate that although net radiation balance remains the dominant source of melt energy, yet sensible and latent heat contribute in the range of 40% to 60% of the total energy for the altitudes below 3000 m in the open area during clear and partly cloudy days in the active snowmelt period. The influence of radiation on cloudy days ranges from 20% to 34%. Upadhyay et al., (1985), have shown that for Beas and Satluj basin, the snowmelt caused by the incoming solar radiation is predominant over other physical processes such as long wave energy transfer at the snow-air interface, convective heat exchange and latent heat released by condensation. It was shown that the results obtained by the degree-day approach varied significantly from the results obtained by energy balance approach.

2.5.3 Application of simulation models

Only limited studies have been carried out either to develop or to test the existing models for simulation of snowmelt runoff in the Himalayas. A snow melt runoff model was developed and verified using 1977, 1978 and 1979 data of Beas river basin up to Manali by Seth, (1983). The model uses the information regarding the aerial extent of permanent and temporary snow cover obtained through satellite imageries, observed data of precipitation for November to May and daily temperature for the pre-monsoon season. The model considers the altitudinal effect on temperatures, the orographic effect on precipitation, melt water effect of rain falling on the snow-covered area. Simple routing relation was used for obtaining the daily stream flow at the catchment outlet. It was found that the results generally improved by increasing the number of elevation zones. Singh, (1989), tested the snowmelt runoff model for Beas basin up to Manali for a limited period. The results of the model were found satisfactory with a goodness of fit as 0.83 and 0.61 for the years 1978 and 1979 respectively. Dey et al., (1989) employed the SRM to simulate runoff during the snowmelt season from the Kabul river basin in the Himalayas. Several potential modifications were carried out to account for certain factors that give poor simulation due to location of climate stations being vertically and horizontally at a great distance from the snowmelt contributing area, unrepresentative lapse rates etc. These modifications improved the simulation accuracy, quite significantly.

Shashi Kumar et al. 1992 applied SRM model for two study areas viz. The Beas basin up to Thalot and Parbati River up to Pulga dam site. Landsat MSS data for the runoff seasons of 1986 and 1987 were digitally analysed using sophisticated interpretation techniques. The areal extent of the snow cover was evaluated for each elevation zone. This information along with data regarding temperature, precipitation, degree-day factor, temperature lapse rate and runoff coefficients were input into the model, which runs on a

personal computer. Simulation studies were carried out to obtain a good fit between the simulated discharges at Thalot and Phulga dam site, and the actual discharges as measured by user departments.

2.6 SOIL EROSION /SEDIMENT YIELD AND RESERVOIR SEDIMENTATION STUDIES

2.6.1 Soil erosion and sediment yield

In India, an area of about 1,750, 000 km² out of the total land area of 3,280,000 km², i.e., 53% of total land area is prone to soil erosion (Narayana and Ram Babu, 1983). The accelerated soil erosion has irreversibly converted vast tracts of land into infertile surfaces over the country. Deposition of soil eroded from upland areas in the downstream reaches of rivers has caused aggradation. This has resulted in an increase in the flood plain area of the rivers, reduction of the clearance below bridges and culverts and sedimentation of the reservoirs.

The rivers emerging out from the Himalayan region transport the sediment at a very high rate. The other regions of India with most spectacular erosion is the severely eroded gullied lands along the banks of Yamuna, Chambal, Mahi and other west flowing rivers in Gujarat and the southern rivers, namely, the Cauvery and the Godavari river systems. As a result, agricultural production is greatly affected on the red soils, which cover an area of 720000 km² in the basins of the Chambal and Godavari (Verma et al., 1968). The depth of these soils is limited to 200 mm, in most of these areas. The lateritic soils which are associated with rolling and undulating topography have been found to lose about 4000 tonne km⁻² of valuable top soil annually due to erosion in Peninsular India (Ram Babu et al., 1978). The black soils, occupying nearly 640,000 km², are usually utilized for crop production under rainfed conditions. Surprisingly, these lands are

normally cultivated and kept fallow during the intense rainy season, making them susceptible to serious erosion.

The entire Himalayan region is afflicted with a serious problem of soil erosion and rivers flowing through Himalayan region transport a heavy load of sediment. Himalayan and Tibetan region cover only about 5 percent of the Earth's land surface, but supply about 25 percent of the dissolved load to the world oceans (Raymo and Ruddiman, 1992). A total of 1.8×10^9 tonne yr^{-1} of suspended sediment (about 9% of the total annual load carried from the continents to the oceans world-wide) is transported in three major river systems; the Brahmaputra, Ganga and Indus; in a combined runoff of $1.19 \times 10^3 \text{ km}^3$ (Meybeck, 1976). About 75% of the runoff in these three major rivers occur between June and September, in response to the monsoonal precipitation, snow and glacier melt (Collins and Hasnain, 1995). Current estimates of sediment yield of the Ganga and the Brahmaputra rivers together is about 1.0×10^9 tonnes year^{-1} (Subramanian, 1993), compared with the global annual sediment flux of about 15×10^9 tonnes year^{-1} (Milliman and Meade, 1983). Contemporary rates of denudation in the Himalayas are undoubtedly high in comparison with continental averages, as might be expected in an area of recent and continuing tectonic activity. The Himalayan rivers draining the tectonically active belts show a very high sediment yield. The ongoing interaction of Indian and Eurasian plates maintain uplift, and high elevations ensure large glaciers and steep unstable slopes which maintain sediment supply to the rivers of the subcontinent (Collins and Hasnain, 1994).

In the Himalayan mountains, as a consequence of loss of forest cover coupled with the influence of the monsoon pattern of rainfall, the fragile catchments have become prone to low water retention and high soil loss associated with runoff (Valdiya 1985, Rawat and Rawat 1994, Joshi and Negi 1995). Large-scale deforestation, which occurred in the lower

range, known as Siwalik range of Himalayas during the 1960s, caused the soil on the land surfaces to be directly exposed to the rains. This unprotected soil was readily removed from the land surface in the fragile Siwalik by the combined action of rain and resulting flow (Kothyari, 1996). Most parts of the Himalayas, particularly the Siwalik, which represent the foothills of the Himalayas in the northern and eastern Indian states, are comprised of sandstone, grits and conglomerates with the characteristics of fluvial deposits and with deep soils. These formations are geologically weak, unstable and hence highly prone to erosion. Accelerated erosion has occurred in this region due to intensive deforestation, large-scale road construction, mining and cultivation on steep slopes. Approximately 30,000 km² have been severely eroded in the north-eastern Himalayas due to shifting cultivation (Narayana and Ram Babu, 1983). Increased runoff during the summer monsoon rains has been transferring sediments into the streams and causing floods (Ives and Messerli, 1989). Availability of typical rocks in the particular regions also adds substantially to sediment load. For example, presence of clay-rich rocks, such as the Spiti shales and schist and the widespread existence of limestone deposits, lacustrine muds, and tills contribute to sediment supply to the Spiti River in greater Himalayan range. The combined effects of natural and anthropogenic instability can be visualised in widespread surface erosion processes and local mass movements. Similar erosional features have also been reported by Fort (1987) for dry continental Mustang Himalaya of Nepal.

Deforestation and associated soil erosion has caused desertification of land in the Siwalik Hills in the Hoshiyarpur district of the Punjab state. In 1852, the extent of degraded land in this area was 194 km², which increased to 2000 km² in 1939, and then to 20,000 km² in 1981 (Patnaik, 1981). Similarly, large tracts of cultivable land have been abandoned because of the erosion of topsoil in the Kotabagh area of the Nainital district in

the state of Uttar Pradesh (Valdiya, 1985). In addition about 45% of the perennial hill springs in these areas go dry during the non monsoon season because of the reduction in groundwater storage resulting from the erosion of the pervious soil horizons (Valdiya, 1985).

Inspite of the history of sediment measurements in the River Ganga dating back to the early 19th century when Rev. R. Everest published his report in *Royal Asiatic Society, Bengal*, on (soluble and insoluble) sediment transport (Everest, 1832), measurements of discharges and sediment concentrations near the portals of the glaciers have not been continued and the country lost an early initiative on availability of records for long term time series. The review of the literature shows that most of the studies in our country are carried out for the plain rivers or for some rivers in the lower part of the Himalayas. Sedimentation study for high altitude glacierized basins in the Himalayas are very limited. The same is true for the Himalayan glaciers where systematic studies are lacking. Only few studies based on the limited time period are available only for few specific glaciers. These studies can not be generalized even for the near by glacier because of changes in geology and topography.

2.6.2. Effect of sedimentation on reservoirs

A large number of dams have been constructed in India since independence for irrigation, hydroelectric power generation, domestic water supply, flood mitigation etc. Most of these reservoirs have been designed for a life period of 100 years and more. But excessive siltation from accelerated erosion due to human interference is threatening to reduce the live capacity of these reservoirs. The useful life and capacity of reservoirs are being depleted faster than planned because of increasing soil erosion in their catchments. Annual sediment inflow into many of the reservoirs in India varies from 0.6-122.7 ha

m/100 km² (0.8-172 tonne/ha) of the catchment (Dos et al., 1969), and except for a few well protected catchments, others are producing much higher yields than the 5.7-6.9 ha m indicated by Khosla (1951). Deposition in the reservoirs can be decreased only with implementation of soil conservation measures in their catchments. Narayana and Ram Babu (1983) estimated the magnitude of total soil erosion taking place in India. This was computed on the basis of various soil loss studies from different land units and land uses, reservoir sedimentation data, and river sediment discharges. It was reported that on the country scale approximately $5,334 \times 10^6$ tonnes of soil (1,640 tons/km²) is being annually eroded. The country's rivers carry an approximate quantity of $2,052 \times 10^6$ tons (626 t /km²). Of this, nearly 480×10^6 tonnes is deposited in various reservoirs and $1,572 \times 10^6$ tons are washed into the sea every year. In other words, about 29% of the total eroded soil is permanently lost to the sea, 10% is deposited in reservoirs resulting in loss of storage capacity of 1%-2% per year, and 61% of eroded soil is being transported from one place to other. Although these rates are approximations, soil erosion is a serious matter and integrated measures of soil erosion control are needed.

Analysis of the sedimentation data (Murthi, 1977; Shangle, 1991) indicates a wide range of sedimentation rates in these reservoirs. For example, for some large reservoirs, such as the 2.4×10^9 m³ Ram Ganga reservoir in UP, the data indicate a very small rate of sedimentation, while the 3.1×10^9 m³ Srirama Sagar reservoir in Andhra Pradesh was found to have lost 25% of its capacity during the first 14 years of impounding. The reservoir sedimentation rates estimated by various investigators are given in Table 2.1. Based on a screening analysis of the available data, Morris (1995) concluded that some of the reservoirs in India have lost as much as 50% of their capacity to date. By 2020, it is expected that 27 of the 116 reservoirs will have lost half their original capacity and by the

year 2500, only about 20% of India's existing reservoirs will have lost 50% of their capacity.

From remote sensing application point of view the literature review indicates that multi-temporal remotely sensed data were analysed in the demarcation of water spread area and quantity of water in the reservoir in the studies carried out so far. Extraction of water spread area has been assessed on the basis of reflectance in different wave length regions and density slicing approach have been used for estimation of sedimentation rate in a reservoir. Various studies are carried out using such approaches. The use of remote sensing techniques to estimate suspended sediment has been reported by several investigators (Solomonson, 1973; Bartolucci et al., 1977; Holyer, 1978; Khorram, 1981). Smith et al. (1980) determined siltation in the Aswan high dam reservoir by comparing reflectance values in the green and red portions of the spectrum. The surface area of the entire reservoir was determined by totalling all pixels classified as water. Research findings indicate that siltation during the flood period were largely confined to the main river channel of the reservoir and large embayments. Areas of extensive siltation were identified and the amounts of deposition were determined through ground surveys. This information was used to predict the distribution of silt deposits in the reservoir. Rao et al. (1985) used a visual interpretation technique on large-scale imagery of Landsat – MSS to estimate the water spread area at different levels of Sriramsagar reservoir. They used these water-spread estimates to evaluate the capacity of the reservoir and concluded that these results are comparable with hydrographic survey observations. Water spread of Hirakud reservoir from multirate Landsat- MSS imagery was computed by Mohanty et al. (1986) and reported that the area capacity curves derived using remote sensing data were almost similar to the curves obtained from the conventional methods.

Table 2.1: Reservoir sedimentation rates in India (Morris, 1995).

Reservoir	River Basin	Year of construction	Catchment area (km ²)	Reservoir volume (mm)	Sedimentation rate (mmYr ⁻¹)	50% capacity lost (Yr.)	Life of reservoir (Yrs.)
Srirama Sagar	Godavari	1970	91,750	35	0.62	1998	56
Nizam Sagar	Godavari	1930	21,694	39	0.64	1960	61
Matatila	Betwa	1956	20,720	55	0.44	2018	124
Hirakud	Mahanadi	1956	83,395	97	0.66	2030	147
Tungabhadra	Krishna	1953	28,179	133	1.01	2019	132
Bhakra	Satluj	1958	56,980	172	0.60	2101	287
Maithon	Damodar	1955	6,294	218	1.43	2031	152
Lower Bhavani	Bhavani	1953	4,200	222	0.44	2205	504
Mayurakshi	Ganga	1954	1,860	327	1.63	2054	201
Gandhisagar	Chambal	1960	23,025	336	0.96	2135	350
Koyna Dam	Krishna	1961	776	3851	1.52	3228	2533

Suvit et al. (1988) employed digital techniques in which density slicing of Landsat – MSS near-IR data was performed for extracting the water spread area of Ubolratana reservoir in Thailand. They correlated computed surface areas with the water levels and calculated the reservoir capacity based on the surface area obtained using cone formula. For monitoring the use of water from a reservoir on a fortnightly/monthly basis, Jagadeesha et al. (1991) also used satellite data for determining water spread area at various reservoir stages and an average crop water requirements at different stages of growth was determined. The crop area information was also obtained from satellite data. They adopted Borland and Miller (B&M) method, one of the operational methods, for finding the pattern of distribution of deposited sediments between the various zones of the reservoir. Goel and Jain (1996) carried out a reservoir sedimentation study using density-slicing approach for water spread area extraction. They used IRS-1 A (LISS II) data to evaluate reservoir sedimentation in Dharoi reservoir.

2.6.3 Estimation of soil erosion

Soil erosion/sediment yield is estimated using sediment curve, erosion modelling and related procedures. The regression equations, which relate the sediment yield to basin and hydrometeorological conditions in that basin, are mostly used for prediction of sediment yield from ungauged catchment. The simulation models provide a physically based representation of the process occurring in small segments of the catchment and route the response of these segments to the catchment outlet.

Surveys for determination of soil erosion rates from catchments and deposition rates in reservoirs are frequently conducted by the various governmental agencies in India (ICAR 1984; and CBIP 1981). Measurements of sediment load are made in many rivers across the country by other governmental agencies (CS&WC, 1991; Shangle, 1991). Nevertheless, sediment loads remain ungauged for the majority of the streams, because of

the limitation of funds. However, the other hydrological data, such as rainfall and runoff, are available for the majority of river basins. Estimation procedures can therefore be used to estimate erosion rates for such catchments. In India Joglekar (1965) and Varshney (1975) have suggested a number of enveloping curves for the prediction of sediment yield for different catchment areas. Correlation studies conducted by Jose and Das (1982) revealed that area alone do not have any significant association with sediment production rate (SPR) and hence there is scope for multivariate analysis using climatic and physiographic parameters. Statistical models on a spatially distributed basis have been developed by Mishra and Satyanarayan (1991) and Bundela et al. (1995) for small watersheds in river Damodar in east India.

Several equations are also available to estimate soil erosion. The Universal Soil Loss Equation (USLE), developed by Wischmeier and Smith (1978), is one of the most useful and reflects considerable research data. The USLE, an empirical equation, estimates average annual mass of soil loss per unit area as a function of most major factors affecting sheet and rill erosion. This equation is written as

$$A = RKSLCP \quad (2.10)$$

where A is soil loss per unit area, expressed in units selected for K and for the period selected for R; in practice, the units are usually selected so that A is computed in tons per acre per year, but other units can also be selected. R is the rainfall-runoff factor- the number of rainfall-erosion index units, plus a factor for runoff from snow melt or applied water where such runoff is significant. K is erodibility factor-the soil loss rate per erosion index unit for a specified soil as measured on a unit plot, L is slope length factor- the ratio of soil loss from the field slope length, S is the slope steepness factor, C is crop management factor and P is the support practice factor. The USLE gives estimate of total soil detached and displaced over short distances, but does not indicate the sediment

delivered to the reservoir. Much deposition and reduction in sediment yield occurs between the sediment source and reservoirs. This reduction is estimated with a sediment delivery ratio. Sedimentation in reservoirs defined by trap efficiency depends on factors such as the ratio of runoff inflow to reservoir capacity, sediment size, shape and stage of the reservoir, outlet works, and methods of reservoir operation. In India, reservoir sedimentation is generally estimated from the suspended load of the stream feeding the reservoirs, and by periodic direct measurement of sediment deposition in reservoirs.

An isoerodent map of India has been prepared based on the erosion index values (Ram Babu et al., 1978), which shows the potential erosivity of rainfall (Singh et al., 1990). Methods have also been evolved for determination of the off site deposition of eroded soil and the sediment yield from large catchments (Garde and Kothyari, 1987; Narayana and Ram Babu, 1983; Kothyari et al., 1994). However, a statistical study to date for estimation of sediment yield from large catchments was made by the work of Garde and Kothyari (1987). An analysis of the data from 50 catchments with areas ranging from 43 km² to 83,880 km² produced the following equation for mean annual sediment yield in plain areas:

$$S_{am} = C P^{0.6} F_e^{1.7} S^{0.25} D_d^{0.10} (P_{max}/P)^{0.19} \quad (2.11)$$

Where

$$F_e = (0.8 F_A + 0.6 F_G + 0.3 F_F + 0.1 F_W)/A$$

where S_{am} is the mean annual sediment yield in cm, C is a coefficient depending on the geographical location of the catchment, P is the average annual rainfall in cm, S is the land slope, D_d is the drainage density in km km⁻², P_{max} is the average maximum monthly rainfall in cm and A is the catchment area in km². F_e is defined as the erosion factor and F_A is the area of arable land in the catchment, F_G is the area occupied by grass and shrub

while F_W is the area of wasteland and F_F is the forested area. These factors can be obtained using GIS. No relationship was given for mountain basins.

2.6.4 Relationships between suspended-sediment concentration and discharge

Suspended sediment concentration discharge relationship of the form $S_s = aQ^b$, where S_s is suspended sediment concentration, Q discharge, and a and b best fit estimated parameters. In regions where seasonal variation in erosion processes and source areas are controlled by floods generated by both spring snowmelt and summer storms, seasonal variation in sediment yield may mask any relationship with discharge (Walling, 1998). The relationship between sediment and discharge and the character of suspended sediment transport have been investigated for individual hydrological events (Heidel, 1956; Guy, 1964; Arnborg et al., 1967; Carson et al., 1973; Loughran, 1976; Wood, 1977; Marcus, 1989; Williams, 1989). Variations in sediment concentration have been attributed to exhaustion and replenishment of the sediment supply, differences in travel distance between source areas and the locations of the measuring station, the location of sediment source areas and the existence of a time lag between sediment concentration and discharge peaks. Williams (1989) developed models for sediment rating relationships (linear and curved) for individual hydrological events by comparing sediment concentration and discharge ratios at a given discharge on the rising and falling limbs of discharge hydrographs. Although he summarized the physiographical and hydrological reasons for the existence of each type of relationship associated with sediment rating curves, only partial understanding of the controlling factors exists.

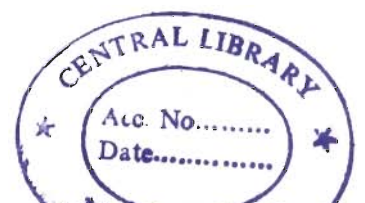
2.7 SEDIMENT YIELD STUDIES FOR HIMALAYAN BASINS AND SATLUJ BASIN

2.7.1 Himalayan basins

For Himalayan basins some typical studies have been carried out. Rao et al. (1995) has worked on sediment yield estimation for Chenab basin. In this study data of 9 sediment stations within Chenab basin varying from 17 to 27 years was utilised to develop a statistically significant spatial model to estimate sediment yield using geomorphological, climatic and landuse, landcover parameters. The sediment yield was estimated for total and fine sediment for monsoon, winter, pre-monsoon and annual seasons. The study revealed the high rates of sedimentation in Chenab basin and its effect on capacity of existing Salal dam reservoir near Jammu.

The sediment yield response of snow and glacier dominated catchments in the Himalayas is different from rainfed catchments in the rest of India. Rao et al. (1997) attempted to relate sediment yield with geomorphological, landuse and climatic parameters for the Chenab (22,200-km²) basin, which is a large Himalayan basin. Sediment yield characteristics in the Chenab basin vary depending on the season. During the winter season (October-March) the sediment yield is minimal and is less than 5-10% of the annual yield. During pre-monsoon season (April-June) the seasonal snow cover melts in the intermediate and upper reaches and lower reaches receive rain. Thus, a significant sediment yield is observed from the catchment in the pre-monsoon season. During the monsoon season (July-Sept.) rainfall contribution to flows is very high in the lower reaches and gradually tapers at elevations of about 4,000 m (Singh et al., 1995). Air temperatures are also at their maximum during the season resulting in snow and glacier melt from permanent snow covered zones. Consequently, a major part of the sediment yield is received during the monsoon season. Average sediment yields for annual and

510627



monsoon season periods in terms of coarse, medium and fine sediment are shown in Table 2.2.

The rates of suspended sediment transport in the Chenab river are high as compared with other river systems in India (with exception of Ganges) (Sundd 1991) and in the world (Holeman 1968; Milliman and Meade 1983). The precipitation and runoff characteristics in the Chenab basin influence sediment yield to a large extent. Snowmelt and glacier melt runoff contribution increase with elevation, while rainfall decreases with elevation in the upper reaches (Rao et al., 1996; Singh and Jain, 1993). To verify, how far rain is responsible for sediment production in various subbasins of Chenab located at different elevations, mean weighted rainfall during the monsoon (Jul. – Sep.) in each sub-basin was correlated (log-linearly) with sediment yield per unit area using 10 years of concurrent data, assuming that catchment characteristics remained unchanged during the period. The correlation coefficients, r , shown in Table 2.3, with exception of Kuriya sub-basin indicate less sediment yield on rainfall in the upper reaches as compared with the lower reaches of Chenab basin. In other words, rainfall may have little to do with the sediment yield in the upper reaches of Chenab catchment. The amounts of mean rainfall during the monsoon season (July-Sep.) and the winter season (Oct.-Mar.) decreases with increase in elevation (Table 2.3). Consequently sediment response characteristics vary markedly between the upper and lower reaches of the catchment and hence the low coefficient of correlation is obtained for Kuriya stations in the transition zone. The transition zones also experience rain-on-snow phenomena. Beside rainfall, some of the reasons besides rainfall may also be attributed to the prevailing geologic and soil conditions and melts runoff from permanent snow cover zones with presence of glaciers in the upper reaches, as compared with the lower reaches.

Table 2.2: Average sediment yields in the Chenab basin at different locations along with their composition during the monsoon period (Rao et al., 1997).

Site	Annual average sediment yield (t/km ² /yr)	Monsoon Season			Total Sediment yield For monsoon Period (Jul.- Sep.) (t/km ² /yr)
		Fine	Medium	Coarse	
Akhnoor	1029	455.9	180.8	85.9	722.7
Benzwar	1597	694.5	360.9	169.6	1225.0
Dhamkund	1900	533.5	386.4	314.3	1234.3
Ghousal	513	221.2	90.3	69.7	381.3
Kuriya	878	300.9	152.4	138.9	592.3
Premnagar	1363	222.9	112.9	102.9	438.7
Sirshi	939	221.4	186.6	146.7	554.8
Tandi	371	164.0	70.6	51.3	286.0
Tillar	373	92.4	62.2	40.7	195.4

Table 2.3: Correlation of mean basin monsoon rainfall with sediment yields (t/km^2) (Rao et al., 1997)

Sediment Station	Basin average winter rainfall up to respective gauging sites (mm)	Elevation of sediment gauging station (m)	Basin average monsoon rainfall up to respective gauging sites (mm)	Correlation coefficient Between mean weighted rainfall and sediment yield
Akhnoor	588	305	740	0.61
Dhamkund	277	600	353	0.70
Premnagar	201	886	252	0.75
Kuriya	226	1,106	229	0.16
Benzwar	408	1,135	197	0.66
Sirshi	103	1,162	170	0.50
Tillar	71	2,066	153	0.50
Tandi	15	2,846	90	0.33
Ghousal	17	2,850	90	0.44

2.7.2. Satluj basin

Satluj basin is one of the major basins in the Western Himalayas. Sharma et al. (1991) have studied suspended sediment load in the Satluj river basin in detail and identified the sediment load at different sites within the basin. About 80% of the annual flow of the Satluj River system originates from basins in the High Himalaya, that is, Tibet, Spiti and Kinnaur, occurs between May and September and is primarily due to snowmelt. Suspended sediment increases exponentially with increase in discharge and occurs in very high concentrations during June, July, and August. The Spiti River experiences a higher volume of water but less sediment relative to the other two basins. The high-suspended

sediment concentrations in the river system during the summer months and reduced water supply during winter will affect the operational efficiency of hydroelectric projects being planned for the Satluj River. Annual sediment deposition in the Bhakra Reservoir is of the order of $35.8 \times 10^6 \text{ m}^3$, giving an average 50 cm thick sediment layer (Anonymous, 1986). At this rate the effective life of the Bhakra reservoir for power generation is calculated to be only about 150 years and it is predicted that the reservoir will be fully silted up in about 400 years. Dredging operations in reservoirs are invariably difficult and expensive. There is considerable evidence, however, that these high rates of sedimentation can be reduced by the application of corrective treatment measures in the upper catchments (Gupta, 1980; Das et al. 1981; Jiang et al., 1981; Narayana, 1987). Before such measures can be seriously contemplated an assessment of the magnitude of sedimentation in different river basins and the identification of the source area will be required.

(a) Suspended sediment concentration

The suspended sediment concentration begins to increase as the discharge increases from April onward. It remains low during April and May and increases dramatically at the beginning of June. It remains at quite high levels until the third week of August when it begins to fall again. By the end of September the concentration is very low and between October and March it is nearly negligible. Sharma et al. (1991) reported that Satluj and Spiti concentrations at Khab during the same year and period, which varied between 2,000 and 4000 mg l^{-1} and between 1000 and 2000 mg l^{-1} , respectively. The concentration levels for a particular year, however, cannot be taken as a general rule as there is considerable annual variation and variation between the same months of different years. The mean monthly concentrations at Wangtu for April, May, June, July, August, and September were 234, 496, 2611, 2819, 2612, and 664 mg l^{-1} , respectively, with CV's from 45 to 58%. The monthly concentrations for the Satluj and the Spiti at Khab from

April to September were even more variable than that for the Satluj at Wangtu, having coefficient of variation ranging from 58 to 169%. However, the concentrations were relatively higher for the Satluj and lower for the Spiti at Khab, compared to the Satluj at Wangtu. The sudden increase of the sediment concentrations in the river system may occur more or less simultaneously. For instance, concentrations varying from 12,000 to 14,000 mg l⁻¹ shot up on 10 August 1982 simultaneously for each of the sub-catchments. Suspended sediment concentration increased exponentially with increase in discharge (Sharma et al., 1991). Although the relationship shows inter-annual variation, it is quite accurate for certain years. Dunne (1977) has reported a similar type of relationship between discharge and suspended sediment with inter-annual variation.

(b) Suspended sediment load

The mean annual suspended sediment load in the Satluj at Wangtu has been estimated to be approximately $18.7 \times 10^6 \text{ m}^3$, or 26.2×10^6 tonnes. The loads calculated for the Spiti and for the Satluj at Khab were $5.6 \times 10^6 \text{ m}^3$ and $5.0 \times 10^6 \text{ m}^3$, respectively. The residual value for Kinnaur, therefore, would be $8.1 \times 10^6 \text{ m}^3$. The annual sediment loads were more variable than the discharges with coefficient of variation being 46.4, 67.1, and 50.7% for the Satluj at Wangtu, for the Spiti at Khab, and for the Satluj at Khab, respectively.

Although the area of the Kinnaur catchment and its relative water yield is less than that of the Spiti, its sediment yields are almost 1.5 times that of the latter. Accordingly, the annual sedimentation rate from the Kinnaur catchment is $1571 \text{ m}^3/\text{km}^2/\text{yr}$ compared to $953 \text{ m}^3/\text{km}^2/\text{yr}$ from the Spiti catchment (Sharma et al., 1991). Sedimentation rate from Tibet is relatively low: only $137 \text{ m}^3/\text{km}^2/\text{yr}$. The Tehri catchment of 7511 km^2 (of which 2328 km^2 are snow clad in the Himalaya) contributes 14.6×10^6 tonnes of silt annually (Singha and Gupta, 1982); it also gives a sedimentation rate of $1390 \text{ m}^3/\text{km}^2/\text{yr}$, similar to that of

the Kinnaur catchment. The actual sedimentation rates of the Kinnaur and Spiti catchments are much higher than the assumed figure ($360 \text{ m}^3/\text{km}^2/\text{yr}$) on which the earlier designs of reservoirs in India are based (Varshney, 1979). Of the annual sediment of $35.8 \times 10^6 \text{ m}^3$ deposited in the Bhakra reservoir (Anonymous, 1986), half (52.2 percent) is being added from the Tibetan, Spiti, and Kinnaur catchments, their individual contributions being 14.0, 15.6 and 22.6%, respectively. Thus, higher than calculated sedimentation from the Kinnaur and Spiti catchments will hamper the operational efficiency of hydroelectric projects to be built on the Satluj River system in Kinnaur and Spiti and this will also lead to a shortening of the original expected life of the projects. Table 2.4 shows annual suspended sediment load and its composition observed at different locations in the Satluj River. A comparison of sediment yield observed for different Himalayan catchments is given in Table 2.5.

Table 2.4: Composition of suspended sediment in the Satluj river system (1977-1985) (Sharma et al., 1991)

River/Site	Annual suspended sediment load (10^6 m^3)	Annual Suspended sediment load (10^6 tonnes)	Fine (%) (<0.075m m)	Medium (%) (0.075-0.20mm)	Coarse (%) (>0.20 mm)
Sutlaj at Khab	5.0	7.0	64.1	22.3	13.6
Spiti at Khab	5.6	7.84	66.4	21.1	12.4
Sutlaj at Wangtu	18.7	26.2	59.9	23.2	16.9

Table 2.5: Comparison of sediment yield observed for different Himalayan catchments

Catchment	Sediment Yield (m ³ /km ² /yr)	Sediment yield (t/km ² /yr)
Kinnaur	1571	2199.4
Spiti	953	1334.2
Tibet	137	191.8
Tehri	1390	1946.0

2.8 CONCLUDING REMARK

The review of literature has provided useful information about status of research in the area of snow hydrology with emphasis on snowmelt runoff modelling.

The status of limited data availability in rugged inaccessible terrain has resulted in very few attempts for systematic modelling of snowmelt runoff process. It is seen that simple modelling approaches using degree-day method are equally effective to energy balance approach with limited data and number of assumptions. The need for division of river basin into elevation bands is well established for the range of elevation differences for mountainous region. It is also seen that, there are typical three parts of the river basin, which require proper representation in a model. These are (i) snow free (ii) seasonal snow covered and (iii) permanent snow covered areas. The variation in temperature with elevation can be well represented by lapse rate approach. Besides surface runoff due to snow and ice melt and rainfall; there is also significant contribution of baseflow. The infiltrated water from snowmelt and rain contributes to baseflow and as well as deep groundwater (which does not contribute to runoff at the basin outlet and may appear

downstream). The storage effect in transformation of effective precipitation into runoff can be represented by one or two linear reservoirs (in series). Any modelling exercise has to provide suitable model structure as well as use appropriate optimisation procedure for calibration of storage parameters.

The processes of soil erosion and sedimentation are equally important for fragile Himalayan region. The available approaches for sediment yield estimation is mostly empirical. Some attempts have been made with application of GIS approaches. However, these methods do not consider orographic effect on rainfall and correspondingly on sediment yield.

In recent years, the remote sensing applications have provided simple and versatile techniques for reservoir sedimentation structure. However, no such application has been made for reservoirs in Himalayan region, which has extensive soil erosion prone areas.

CHAPTER 3

THE STUDY AREA AND DATA USED

The western Himalayas cover the hilly areas of Jammu and Kashmir, Himachal Pradesh and Uttaranchal in India. Two important river systems originated from western Himalayan region are Indus system-Indus, Jhelum, Chenab, Ravi, Beas and Satluj and Ganga system - Yamuna, Ramganga, Sarda and Karnali. These rivers are fed by snowmelt and rainfall during the summer and by groundwater flow during the winter. The Satluj basin has a reasonable good hydro meteorological network. The hydropower potential of this basin is highest among the other basins of Indus system. Therefore, the study area chosen in this research work is Satluj basin up to Bhakra dam (Figure 3.1). For carrying out sedimentation study Bhakra reservoir located in the foothills of the western Himalayan region has been selected. The details of the study area and data availability have been described in the following sections.

3.1 THE STUDY AREA

3.1.1 The Satluj basin

The Satluj river rises in the lakes of Mansarover and Rakastal in the Tibetan Plateau at an elevation of about 4,572 m and forms one of the main tributaries of Indus river. It travels about 322 km in the Tibetan province of Nari-Khorsam forming a plateau by successive deposits of boulders, gravel, clay and mud. The flow of Satluj, obtained mainly from snow and glaciers has cut a valley about 914 m deep through these deposits. After flowing in north-westerly direction, it changes direction towards south-west and



N

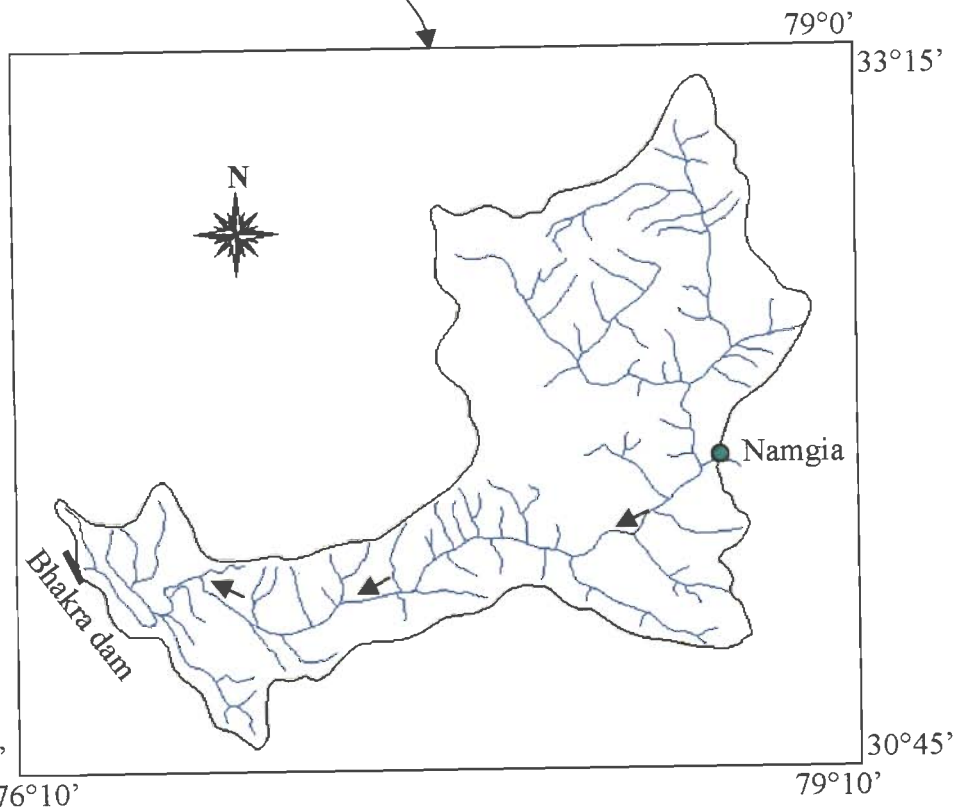


Figure 3.1: Map of the Satluj basin up to Bhakra dam

covers another 322 km up to Bhakra gorge, where the 225.55 meters (740 ft) high straight gravity dam (Bhakra/Govind Sagar) has been constructed.

This large river flows through areas having varying climatic and topographic features. Most of the basin in Tibetan plateau and some areas down stream are without any rainfall and have cold desert climate. At Namgia, near Shipki, its principal Himalayan tributary, the Spiti joins it, just after entering India. Below this dry region, it flows through the Kinnaur district of Himachal Pradesh, where it gets both snow and rain. Numerous glaciers drain directly into Satluj at various points along its course and many Himalayan glaciers drain into its tributaries. In the lower part of the basin only rainfall is experienced. The topographical setting and availability of abundant water provides a huge hydropower generation potential in this river and hence several hydropower schemes are planned/coming up on this river.

The total catchment area of Satluj River up to Bhakra dam is about 56,500 km² of which about 22,305 km² lies in India including whole catchment of the Spiti basin. The elevation of the catchment varies widely from about 500 m to 7000 m, although only a very small area exists above 6000 m. Mean elevation of the basin is about 3600 m. The gradient is very steep at its source and gradually reduces down stream. Owing to large differences in seasonal temperatures and great range of elevation in the catchment, the snowline is highly variable, descending to an elevation of about 2000m during winter. The permanent snowline in this part of Himalayan range is about 5400 m (BBMB, 1988). Upadhyay et al. (1983) reported that about 11% area of the total Satluj catchment lies under glaciers. Kulkarni et al. (1999) made a glacier inventory of the Satluj basin using remote sensing data and found out that total area under glacier and permanent snow fields as 1515 km² and 1182 km² respectively. These two areas are distributed in 169 sub-basins.

Indian part of the Satluj basin is elongated in shape. The shape and location of this basin is such that major part of the basin area lies in the greater Himalayas where heavy snowfall is experienced during winters. In the reservoir area, the catchment starts from Bhakhra dam, where it is flanked on both sides by the foothills of the Shivalik ranges, diverging from a narrow gorge to a very wide width of about 24 km and again narrowing down up to Kasol forming the tip of the reservoir. The lower catchment largely drains directly into the reservoir and the higher slopes drain through tributaries. The important tributaries are the Soel khad, Aseed khad, Ali khad, Gamrola khad, Ghambhar khad, Seer khad, Sukhar khad, Sarhali khad and Lunkar khad.

The salient characteristics of the whole Satluj catchment are summarised in Table 3.1.

Table 3.1: The salient topographical and hydrometeorological features of the Satluj catchment (WAPCOS, 1996)

Reach	Catchment area (km ²)	Elevation range (m)	Average annual Rainfall (mm)	Major source of contributions to the streamflow
Tibetan plateau	37050	4000-6000	Nil	Snow and glacier
Spiti Valley	7084	3300-5300	Scarce	Snow and glacier
Namgia to Rampur	6490	3000-4800	Little	Snow and rainfall
Rampur to Suni	2068	1200-3000	1000-1500	Rainfall
Suni to Kasol	700	900-2000	910-1630	Rainfall
Kasol to Bhakhra	3108	600-2000	1520	Rainfall
Total	56,500			

As shown in Table 3.1, some parts of the catchment receive heavy rainfall during the monsoon season from July to mid September. Sometimes monsoon season extends up to late September and very rarely up to early October. The average rainfall in the

catchment is 1140 mm. The Satluj runoff basically consists of two parts, one part is derived from the melting of the snow and the other results from the rainfall in the catchment. The monsoon is generally marked by high river flows and occasional floods in Satluj. There are significant contributions from snow and glaciers into stream flows of Satluj. The contributions from snow and ice vary with season to season, being maximum in summer months.

3.1.2 Bhakra reservoir

For carrying out the reservoir sedimentation study, Bhakra reservoir, which is also known as Gobindsagar, was chosen for assessment of sedimentation. The Bhakra dam, one of the oldest built in India, was commissioned in 1963. This dam has controlled the devastating floods and benefits to irrigation and power have brought prosperity to the north India. This dam has a designed dead storage of 2431.81 Mm³ and live storage of 7436.03 Mm³; i.e., total storage of capacity 9867.84 Mm³. As a result of the construction of the Bhakra dam on Satluj river at Bhakra, a huge lake has been created on the upstream side of dam called the Gobindsagar reservoir. It has enormous water spread area, extending over 168.35 km² at full reservoir level (515.11 m). Its head touches a point about 12.87 km above Slapper village near Kasol.

The Bhakra reservoir is fed by the flows consisting of contribution from rain and melting of snow. Singh and Kumar (1997) have studied precipitation distribution for several Himalayan basins and found that maximum contribution to annual rainfall is received during monsoon season (42-60%), whereas the minimum (5-10%) is received in post-monsoon season. Consequently, the reservoir attains its maximum water level just after the monsoon season. Water level of the reservoir gradually depletes due to various types of uses and reaches lower levels before onset of the subsequent monsoon. The Satluj river

transports heavy amount of sediment, which is detrimental to the life of the reservoir. The silt contribution in this basin is largely due to deforestation, over-grazing in the pasture lands, unscientific agricultural practices, farming at elevated terraces etc. (BBMB, 1997). This region is also very prone to landslides and slips which may be one of the major sources of sediment in this river. The natural factors that also attribute to high levels of sediment transport from the study region are steep topographic gradient, poor structural characteristics of soils; clay rich rocks such as Spiti shales and schists; and wide spread existence of limestone deposits (Sharma et al., 1991).

3.2 CLIMATIC CONDITIONS AND SEASONAL VARIATIONS IN THE STUDY BASIN

The great contrast in the topographical relief results in variety of climate in the Himalayas. Such regions are characterized by numerous small climatic differences over short horizontal distances. Principal controls producing such differences are those of altitude, local relief and mountain barrier effect. The most important factors controlling the weather and climate in the Himalayas are the altitude and aspect. Largely due to variations in altitude, the climate varies from hot and moist tropical climate in lower valleys, to cool temperate climate at about 2000 m and tends towards polar as the altitude increases beyond 2000 m. Altitude controls not only temperature but rainfall also. The second factor controlling the climate is aspect of slopes. Usually the south facing slopes are sunnier and also get more rain. Further, in each individual range the snowline is higher on southern aspect as these slopes have more sunshine. Also, the snow line in the eastern Himalayas is higher than in the western Himalayas.

Depending upon broad climatic conditions the following four seasons prevail over the basin:

(a) Winter season (December - March)

The precipitation during this season is caused by extratropical weather system of mid-latitude region originating from Caspian sea and moving eastward. This winter weather system is known as western disturbances and approach India from the west through Iran, Afghanistan and Pakistan. With the setting of the winter season these western disturbances have the tendency to move along lower latitudes. Ordinarily these disturbances remain at high latitudes and do not influence the Himalayas. But, as the season advances they come lower and lower and by the end of December these cover more or less whole Himalayas. Such disturbances recede to their original position, which lies beyond the Himalayan Mountains by the end of winter season.

The precipitation during this season is generally in the form of snow in the greater Himalayas, snow and rain in the middle Himalayas, and light to moderate rain over the outer Himalayas and the adjoining north Indian plains. Precipitation occurs at intervals throughout the winter season. It is found that average frequency of occurrences of these disturbances is about 3 to 5 each month, which reduces as the season advances. The higher precipitation in the western Himalayas during these months is the combined effect of the nearly east-west configuration of the Himalayas and eastward movement of the winter weather system. The precipitation associated with this weather system decreases considerably as they move eastward along the Himalaya because of increasing distance from the source of moisture. These weather systems cause snowfall at higher elevations

(b) Premonsoon season (April - June)

Generally, pre-monsoon season lasts for about a period of 3 months from April to June and is considered as transit period between winter and southwest monsoon. Light to moderate rains are essentially caused by air mass convective storms. Convection increases because of increasing trend of temperature in the Himalayan region in this season.

(c) Monsoon season (July - September)

Normally, the moist air currents cause precipitation over the Himalayas from Bay of Bengal in this season. Sometimes, in association with certain weather situations both branches of monsoon (i.e., the Bay of Bengal and Arabian sea) arrive simultaneously in this region heralding the onset of monsoon. These currents, after striking the Burma and the eastern Himalayas are deflected westwards and travel along the Himalayas. Rainfall decreases westward because of increasing distance from the source of moisture i.e. Bay of Bengal or Arabian Sea, which results in less amount of moisture content in the air currents. Consequently, lesser precipitation is observed as one moves further west. This is the season of abundant rain and rivers are generally flooded. Snow and glaciers at very high altitudes continue melting during this season. The monsoon normally starts withdrawing from this region towards the end of September.

It was observed that while the monsoon currents give copious rainfall over the Indian plains and lower Himalayas. At the time of crossing greater Himalayan ranges and approaching trans-Himalayan regions, these currents become practically dry as most of the moisture content they initially carried is precipitated during their passage over the plains and mountain ranges of the Himalayas. It results in insignificant rainfall in the trans-Himalayan region.

(d) Post Monsoon (October- November)

During this season clear autumn weather sets in and there is generally little rainfall. This is the driest season in the entire Himalayas as well as in the plain areas.

The presence of glacier and snowfields over an extensive area in the western Himalayan is not only a dominant feature relevant to the climate alone, but is factor that significantly enters into many hydrological implications. Accumulation of snow during

winter and period of snowmelt coinciding with the gradual rise in temperature, actually regulate the flow and make it available at the time of year when it is needed most.

3.3 PRECIPITATION DISTRIBUTION IN THE SATLUJ BASIN

Examination of rainfall distribution in the Satluj reveals a distinct pattern of rainfall distribution for the outer, middle and greater Himalayan ranges (Table 3.2 and 3.3). Snow distribution with altitude has been studied for the greater Himalayan range of Satluj basin because snowfall data were available only for this range. Snow distribution in the greater Himalayan range of Satluj basin was studied sub-basin wise because snowfall data are recorded at number of stations. The important conclusions drawn from the recent study carried out by Singh and Kumar (1997) are as follows:

1. The rainfall distribution with altitude on the leeward side of outer Himalayas has shown that for all the seasons rainfall increases linearly with elevation in Satluj basin. Based on limited rainfall data on the windward side of the outer Himalayas in the Satluj basin, it was observed that rainfall on the windward side is higher than that of on the leeward side. Both higher number of rainy days and high rainfall intensity are found responsible to increase rainfall with altitude in the outer Himalayan range in the Satluj basin.

2. Rainfall analysis of the greater Himalayan range has revealed that little rain is observed in this range. It is possible because most of the moisture of monsoon currents (which contributes maximum in annual rainfall), is precipitated over outer and middle Himalayan ranges. Rainfall variation with altitude has shown that it exponentially decreases with elevation in the post-monsoon and pre-monsoon seasons. The annual distribution also followed this exponentially decreasing trend with altitude. Rainfall distribution in the monsoon season has shown no specific decreasing trend with altitude in this basin. The winter season rainfall decreases linearly with elevation in this range. Negligible rainfall is

observed above 3000-m elevation. The reduction in rainfall at higher elevation was found to be due to lesser number of rainy days at those elevations in this range.

3. It was observed that orographic effect on rainfall has led to maximum rainfall in the outer Himalayan range in the Satluj basin. Average annual rainfall decreases considerably from outer Himalayan range to middle Himalayan range in the Satluj basin. Annual rainfall is further drastically reduced in the greater Himalayan range in the Satluj basin. Contribution of seasonal rainfall to annual rainfall has shown that over all the ranges of Himalayas in the Satluj basin, monsoon rainfall contributed maximum to the annual rainfall. Which is 45-71% in the Satluj basin. Minimum rainfall is experienced in the post-monsoon season in the outer and middle Himalayas because of less moisture content availability in this season. In the greater Himalayan range minimum rainfall is experienced in the winter season in the Satluj basin because most of the precipitation falls in the form of snow over this range. Contribution of pre-monsoon rainfall in annual rainfall increases from outer Himalayas to greater Himalayas and becomes significant in the greater Himalayan range. Contribution of winter rainfall is also found significant in the middle Himalayan range.

4. Snowfall has shown different trends of increase with elevation in different parts of Satluj basin. For example, snow increases linearly with elevation in the Spiti and Baspa basins, whereas for the upper Satluj sub-basin it first increases and then decreases. Maximum and second to maximum snow is observed in the month of March and February, respectively in all the valleys in the greater Himalayan range of the Satluj basin.

5. Based on the rainfall and snowfall data at four stations located at different elevations in the greater Himalayas, a ratio of total annual snowfall to total annual precipitation has been worked out. It is found that ratio of snowfall to the annual precipitation varies linearly with altitude. All the stations recorded more than 60% snow contribution in the

annual precipitation. An extrapolation of this linear relationship indicates that above 6000 m elevation, whatever precipitation occurs may be falling as snow only.

Table 3.2 Seasonal distribution of average rainfall in different ranges of Himalayas in the Satluj basin. The contribution of respective season in the annual rainfall is also indicated (Singh and Kumar, 1997).

Himalayan range	Side	Rainfall (mm)				
		Winter	Pre-monsoon	Monsoon	Post-monsoon	Annual
Outer	Leeward	155(10.9%)	146 10.3%)	1010(71.3%)	105 (7.4%)	1 416
	Windward	172(14.3%)	201(16.7%)	725 (60.3%)	106 (8.8%)	1203
	Average	164 (12.5%)	174(13.3%)	868 (66.2%)	106 (8.0%)	1312
Middle	Leeward	209 (28.0%)	128(17.2%)	336 (45.0%)	73 (9.8%)	746
Greater	Leeward	6(3.0%)	75 37.5%)	105(52.5%)	14 (7.0%)	200

Table 3.3 Average annual rainydays, rainfall intensities, snowdays and snowfall intensities for different ranges of Himalayas in the Satluj basin (Singh and Kumar, 1997).

Himalayan range	Side	Rainy days	Rainfall intensity (mm/rainy day)	Snow days	Snowfall intensity (mm/snowday)
Outer	Leeward	88	16	-	-
	Windward	84	14	-	-
	Average	86	15	-	-
Middle	Leeward	87	9	-	-
Greater	Leeward	35	9	-	-
Spiti sub-basin	-	-	-	22	16
Baspa sub-basin	-	-	-	31	15
Upper Satluj sub-basin	-	-	-	18	13

3.4 STREAMFLOW CHARACTERISTICS OF SATLUJ RIVER AT BHAKRA DAM

The streamflow of the Satluj River consists of the contribution from rain, snow and glaciers and respective contribution of each component varies with time of the year. Generally, snows melt contribution starts from March and lasts until June/July depending upon the snow pack water equivalent accumulated in the preceding winter season and prevailing temperatures in the summer season. As the summer season progresses, the snowmelt contribution increases continuously and exceeds the rainfall component. Thus in the pre-monsoon season (April-June), a major part of streamflow is generated from seasonal snow. During monsoon season (July-September), monsoon rains producing higher discharges in the river augment flow. Generally, high discharges/floods are observed in the months of July and August and these are essentially due to heavy rain in the lower part of the basin. Usually, the end of May/June ablates seasonal snow accumulated on glaciers during winter season and glaciers start contributing to streamflow thereafter. Glaciers contribute to their maximum in the months of July and August. As such glacier melt runoff contribution lasts till September/October. In the post-monsoon season, streamflow is believed to be partly from the glaciers and some occasional rain events. Streamflow is observed minimum during winters because no melting takes place due to low temperature regime. Baseflow contribution sustains the flow in the river in this period.

3.5 DATA AVAILABILITY

The study chosen for this study falls mainly in the state of Himachal Pradesh. For carrying out this study the data used consists of Survey of India toposheets, hydrometeorological data and remote sensing data.

3.5.1. Topographic data

The Satluj basin up to Bhakra dam in India falls in toposheet nos. 53 A, B, E,I,L and 52 H,L and P at a scale of 1:250,000.

For studying sediment yield in the lower Satluj basin i.e. from Suni to Kasol, following toposheets at a scale of 1:50,000 were used.

Toposheets no. are 53 A/15,16 and 53 E/3,4

3.5.2 Hydrometeorological data

For the safe and judicious operation of Bhakra reservoir a hydrometeorological network has been set up in the Satluj River basin by BBMB, Nangal. In the Satluj basin rainfall is observed at 10 stations maintained by BBMB and they are Bhakra, Berthin, Kahu, Suni, Kasol, Rampur, Kalpa, Rackchham, Namgia and Kaza. The data from all these stations are available from 1983 onwards. Maximum and minimum temperatures, dry and wet bulb temperatures are observed at 6 observatories namely are Bhakra, Rampur, Kalpa, Rackchham, Namgia and Kaza. At four observatories BBMB has installed instruments to record continuous temperature using thermographs. The evaporation data is available only from one station located at Bhakra. The location of these hydrometeorological stations is shown in Figure 3.2.

In order to monitor the river flows there are five number discharge sites on the main Satluj river at Namgia, Rampur, Suni, Kasol and Bhakra. The catchment area from Rampur to Bhakra contributes major rainfall component during the monsoon season. The gauge discharge observations are taken for 24 hours during the monsoon period so that the high floods discharge absorption in the reservoir.

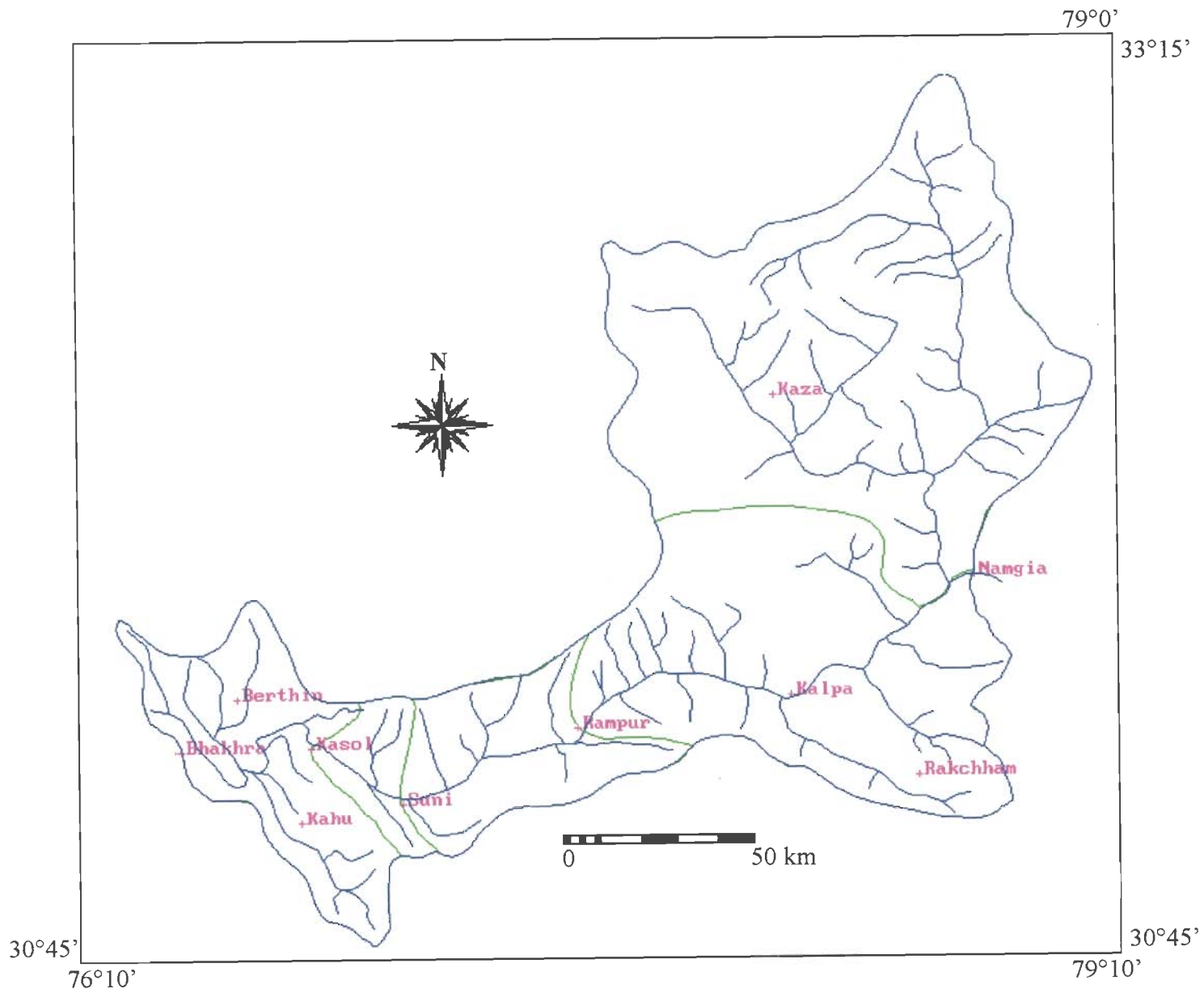


Figure 3.2 : Drainage network map showing hydrometeorological stations

3.5.3 Sediment and reservoir level data

The daily sediment load data of two stations namely Suni and Kasol were collected for the years 1991-1996. For carrying out the reservoir sedimentation study the daily water level data of the reservoir was also collected for a period of 1988-1998.

3.5.3 Remote sensing data

To find out maximum and minimum (permanent) snow covered area and to prepare snow cover depletion curves, remote sensing data for the months of March to October, have been used. The data of all the months was not available due to cloud cover or other reasons. Landsat (MSS) (80m resolution), IRS (LISS-I) (72.5 m resolution) and IRS WiFS (180 m resolution) data were procured from National Remote Sensing Agency (NRSA) for the study period. Landsat data have been used for a period of 2 years (1986-87) whereas IRS LISS-I data was used for the remaining 5 years (1988-93). For the years 1996-1999, IRS WiFS data have been used. The data for IRS-1C/1D was covered in path and row of 96-50. The dates for the years 1996 to 1999 are as follows: 1.12.96, 07.03.97, 24.4.97, 18.5.97, 11.6.97, 5.7.97, 24.10.97, 2.11.97 and 20.12.97. For the year the date are as follows: 13.1.98, 26.2.98, 26.3.98, 19.4.98, 13.5.98, 28.10.98, 21.11.98 and 15.12.98. For the year 1999 the date for which the data was procured include 21.3.99, 14.4.99, 25.6.99, 16.11.99 and 13.11.99.

For reservoir sedimentation study, the data of LISS-II sensor of IRS-1B satellite, which is having good resolution of 36.25 m, was used. This multispectral data was having information of four bands, which were very helpful in the identification of water spread area. The reservoir water spread area was covered in A2 quadrant of Path 30 and Row 45 of the satellite. The National Remote Sensing Agency (NRSA), Hyderabad, was contacted for acquisition of remote sensing data for the period selected above. Due to cloud cover,

some of the dates could not be obtained. The remote sensing data of following dates was procured: 1.10.88, 14.11.88, 28.12.88, 19.1.89, 10.2.89, 4.3.89, 17.4.89, 16.10.96, 7.11.96, 21.12.96, 12.1.97, and 15.6.97.

Table 3.4 : Details of Landsat and IRS LISS I satellite data used in the study

Year	Dates	Satellite/Sensor	Path/row
1986	17 April	LANDSAT (MSS)	146/36
	02 May	LANDSAT (MSS)	146/36
	20 June	LANDSAT (MSS)	146/36
	31 August	LANDSAT (MSS)	146/36
1987	20 March	LANDSAT (MSS)	146/36
	30 April	LANDSAT (MSS)	146/36
	07 June	LANDSAT (MSS)	146/36
	09 July	LANDSAT (MSS)	146/36
	10 August	LANDSAT (MSS)	146/36
1988	11 September	LANDSAT (MSS)	146/36
	07 March	IRS 1 (LISS1)	29/45
	12 June	IRS 1 (LISS1)	29/45
1989	30 September	IRS 1 (LISS1)	29/45
	03 March	IRS 1 (LISS1)	29/45
	08 May	IRS 1 (LISS1)	29/45
1990	09 September	IRS 1 (LISS1)	29/45
	12 March	IRS 1 (LISS1)	29/45
	25 April	IRS 1 (LISS1)	29/45
	08 June	IRS 1 (LISS1)	29/45
	22 July	IRS 1 (LISS1)	29/45
1991	26 September	IRS 1 (LISS1)	29/45
	12 April	IRS 1 (LISS1)	29/45
	04 May	IRS 1 (LISS1)	29/45
1993	27 October	IRS 1 (LISS1)	29/45
	18 April	IRS 1 (LISS1)	29/45

3.6 DATA PROCESSING

Data processing is a broad term covering all activities from receiving records of observed raw data to making them available in usable form. Raw data as observed and recorded may contain many gaps and inconsistencies. These raw data are processed through a series of operations such as making necessary validation checks, in-filling missing values in a data series, processing of raw data to estimate required variables and analysis of data for commonly required statistics etc.

For the data processing of available data and validation, HYMOS software was used. HYMOS is an information system for storage, processing and presentation of hydrological and environmental data (HYMOS, 1999). Data validation is carried out to correct errors in the recorded data where there is possible, to assess the reliability of a record even where it is not possible to correct errors. Data validation is the means by which data are checked to ensure that the database created is the best possible representation of the true value of the variable at the measurement site at a given time or in a given time interval. There are two types of data validation available in HYMOS/SWDES. Primary validation is primarily involved with comparisons within a single data series and concerned with making comparisons between observations and pre-set limits and/or statistical range of a variable or with the expected hydrological behaviour. Secondary data validation consists of comparisons between the same variable at two or more stations and is essentially to test the data against the expected spatial behaviour of the system. Data entry of rainfall, temperature and discharge data have been made according to HYMOS format. Processing and validation of these data have been carried out as explained below.

Daily data of rainfall has been validated against limits within which it is expected. For that purposes the lower limit has been fixed as zero while maximum limit has been fixed on the basis of historical records which is 300 mm. From the annual report, missing days, rainfall in a month, number of rainy days, maximum daily rainfall etc. have been obtained and checked from the available records. From daily plot of all the year, extraordinary high value is marked and confirmed with data collecting agency. In this way, daily rainfall data was scrutinized for each month and checked. After carrying out primary and secondary validation of the values, which were found as incorrect or doubtful, were corrected. For validation of temperature data inspection of data has been made for unrealistic values. In some cases, errors were found due to typing error. These errors were removed and the entry of correct data has been made.

CHAPTER 4

CONTRIBUTION OF SNOW AND ICE MELT AT BHAKRA IN ANNUAL STREAMFLOW AT BHAKRA

Generally, because of rugged terrain and inaccessibility to the higher altitude, a scanty snow- gauge network exists in the Himalayas, where heavy snowfall is experienced. Therefore, assessment of snowfall over the whole basin becomes very difficult under such conditions. Network of rain gauges is reasonably good in the few Himalayan basins including the present study basin and allows for better estimates of rainfall input to the basin. Thus, rainfall input along with the total streamflow and evapotranspiration information can be used for assessing the snow and glacier melt contribution. To assess the contribution of snow and glacier melt runoff into annual flows of the Satluj River, the following water balance approach has been used.

$$SGC = Q - (R - E) \quad (4.1)$$

where SGC is the contribution from snow and glacier melt runoff, Q is the observed flow, R is the rainfall input to basin and E is evapotranspiration losses from the basin. Application of water balance approach for estimating average contribution of snow and glacier melt runoff to annual flows requires a long water budget period for the analysis. In the present study, a period of 10 years has been considered as water budget period. There are two important reasons for considering a long water budget period for such basins. First, a long water budget period like 10 years or so, can cover reasonable number of dry and wet years and the outcome from the analysis would represent a true average value. Secondly, it can be

assumed that all the losses from the rain and snowmelt in the form of infiltration and percolation, except evapotranspiration, would reach at the outlet of the basin within the water budget period. This also allows for no separate consideration for baseflow in the analysis. Further, consideration of 10 years period as water budget period is a highly safe criterion specially for the mountainous basins having significant relief variation from the outlet to upper part of the basin. In such basins time taken by the infiltrated and percolated water will be very less than that in the plain watersheds. Various components needed in the analysis are determined as follows.

4.1 RAINFALL

The total rainfall depth at each station over the water budget period was obtained by making cumulative sum of daily rainfall. Then isohyets were drawn and rainfall input to the study basin was estimated. Cumulative annual isohyetal map of the Satluj basin up to Bhakra Dam for a period of 10 years (Oct., 1986 – Sept., 1996) is shown in Figure 4.1. Isohyetal method is considered more reliable for the mountainous basins where topography influences the precipitation due to high relief and different orientations. Such effects can be observed from the rainfall distribution in the basin shown by the isohyets. The distribution of isohyets exhibits that a good rainfall is observed in the lower and middle parts of the basin, whereas it is less in the upper part. The range of annual isohyets varies from 1000 mm to 1400 mm. Such high variation in the rainfall is a compound effect of several factors such as height of mountain barrier, strength of moisture bearing currents wind, its moisture content and orientation of mountain range with respect to prevailing wind direction. Table 4.1 shows that annual rainfall for the whole study basin varied from 313 mm to 423 mm. Detailed investigations on precipitation distribution in the study basin have been made by Singh and Kumar (1997). Singh and Kumar (1997) reported that

annual rainfall decreases from outer Himalayan range to the greater Himalayan range in this basin. Different patterns of precipitation distribution were found for different Himalayan ranges covered in this basin. Similar patterns of rainfall were found for other basins of Himalayas (Singh et al., 1995; Singh and Kumar, 1997).

4.2 STREAMFLOW

Streamflow characteristics have already been described in Chapter 3. Based on 10 years (Oct., 1986 - Sept., 1996) flow data analysis, monthly distribution of streamflow at Bhakra Dam is shown in Figure 4.2 and quarterly distribution is given in Table 4.2. It can be noticed that maximum flow is observed in the month of July followed by August and minimum in the month of February. About 83% of the total annual flow is observed during pre-monsoon and monsoon seasons because a high contribution from the all sources of runoff is produced in these two seasons. In the other two quarters, flow is only 17% of the total annual flows. It can be observed that annual runoff depth from the study basin varied from 464 mm to 632 mm (Table 4.1).

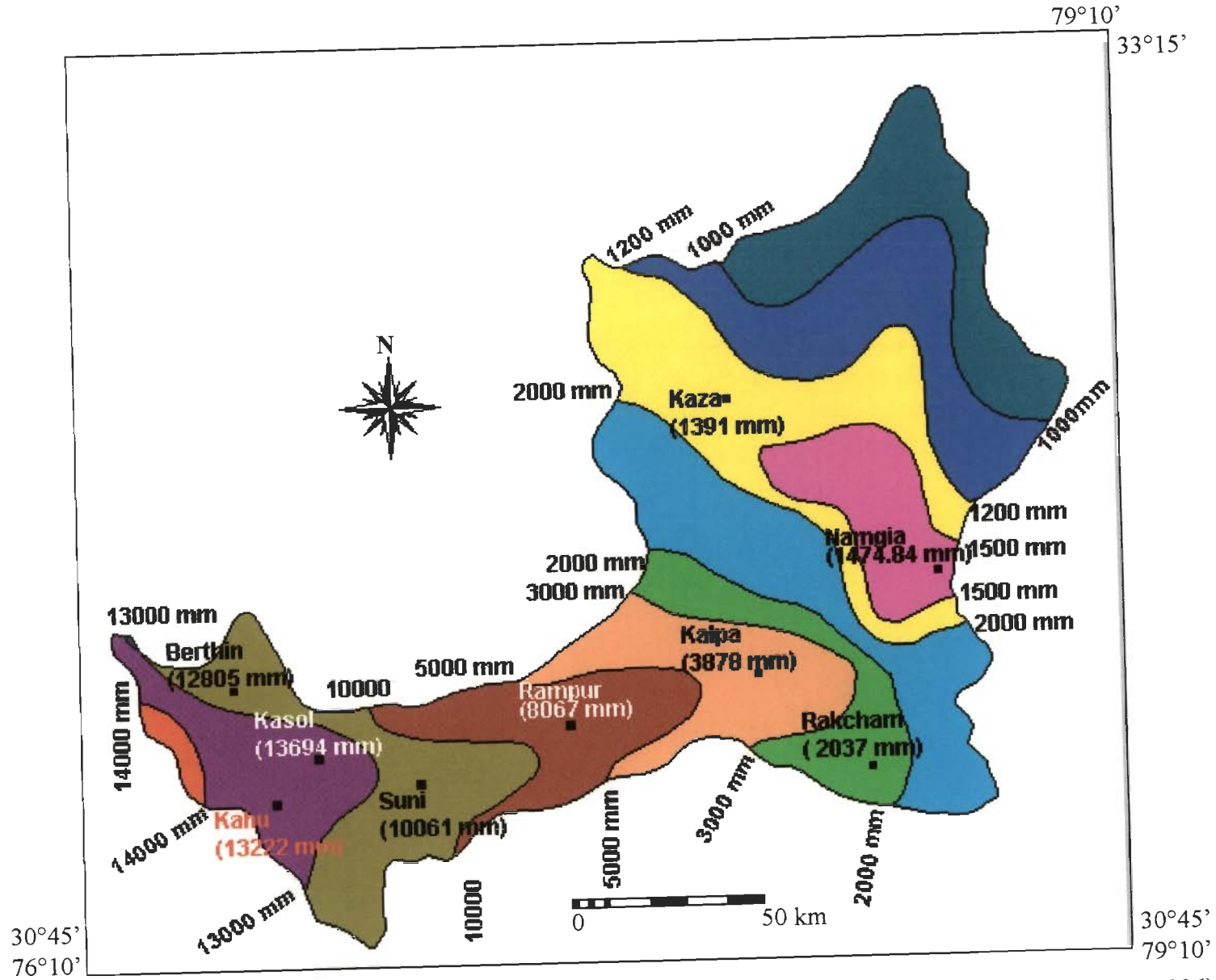


Figure 4.1: Cumulative isohyetal map of the Satluj basin up to Bhakra dam for a period of 10 years (1986-1996)

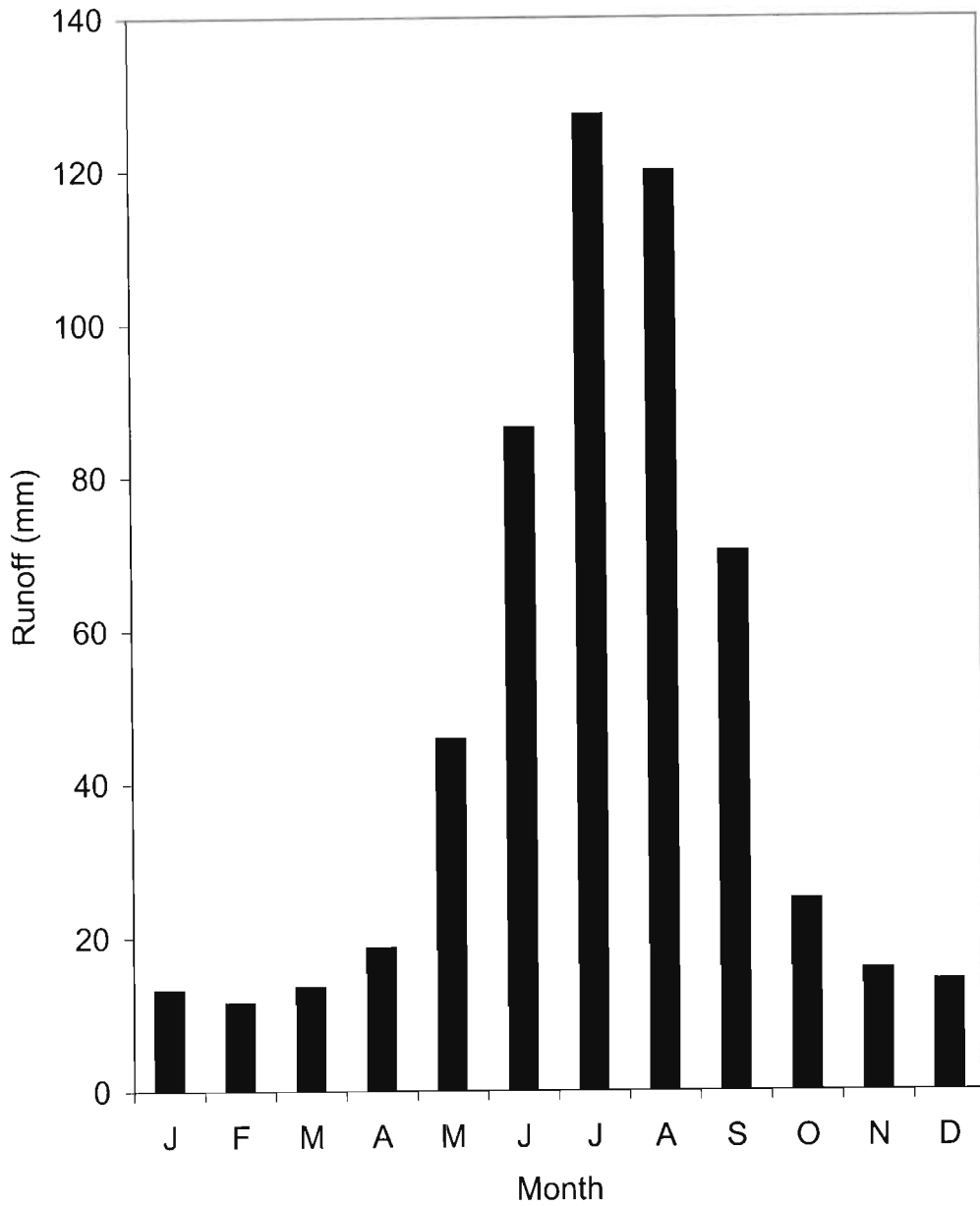


Figure 4.2: Monthly average discharge of Indian part of Satluj river observed at Bhakra

Table 4.1 : Computed rainfall, runoff and evapotranspiration for different years for Satluj

River basin

S. No	Year	Rainfall (mm)	Runoff (mm)	Evapotranspiration losses (mm)
1	1986/87	373.5	519.2	157.2
2	1987/88	464.8	588.8	131.8
3	1988/89	366.2	517.6	137.6
4	1989/90	423.4	631.6	137.8
5	1990/91	313.1	571.8	153.1
6	1991/92	366.2	553.9	143.7
7	1992/93	352.8	464.0	155.8
8	1993/94	360.4	610.4	145.2*
9	1994/95	382.0	560.4	145.2*
10	1995/96	346.0	595.8	145.2*

* Average annual values based on the first seven values were considered

Table 4.2 Quarterly distribution of the annual flows of Satluj River at Bhakra Dam.

S. No.	Period	Average runoff (mm)	Contribution to Annual flow .
1.	October - December	55.0	9.9
2.	January - March	38.1	6.9
3.	April - June	150.9	26.8
4.	July - September	317.4	56.4
5.	Year (October-September)	561.4	100

4.3 SNOW COVERED AREA

The snow cover in the Himalayas occurs and exists depending on the terrain and climatic conditions of the terrain. This snow cover can be categorized into temporary snow cover, seasonal snow cover, permanent snowfields and glaciers in the form of ice. Snow cover that stays for a few days and then melts away is termed as “temporary snow cover”. This usually occurs at lower altitudes during winter and even sometimes at higher altitudes during summer. Snow cover that is formed over weeks or months by consecutive snowfalls and which melts away gradually during the following summer is termed as “seasonal snow cover”. Above a certain altitude and in certain situations, some amount of snow is carried over to the next winter season without melting during summer, and this turns into ‘firn’ and ultimately ice, adding to the permanent snowfields and glaciers. The seasonal snowpack contributes to the water resources during summer months, and therefore is very important in hydrological studies.

Since very little information on snow is collected regularly in the Himalayas, remote sensing remains the only practical way of obtaining at least some information of the snow cover in the large number of basins in the Himalayas. The availability of satellite data provides useful periodic information about extent of snow cover and thus form a base in snow covered mountains. At present the visible, near IR and thermal IR data from various satellite (Landsat, IRS, NOAA) are being used for mapping the areal extent of snow cover in the Himalayan basins. Since 1972 Landsat MSS started acquisition of data at a spatial resolution of 79 m. Later next Landsat satellites (Landsat 2,3,4 &5) were launched, the spatial resolution was improved to 30 m. Whereas IRS satellites (IRS 1A, 1B, 1C and 1D) provide resolution ranging from 72 m (LISS I) to 23.5 m (LISS III). In WiFS sensor launched with IRS-1C and 1D is having a resolution of 180 m.

The duration for which the seasonal snow cover stays in the basin is variable from basin to basin and also from year to year. In the present study, Landsat/IRS data in the form of B/W positive, FCC and digital data were used. The details of all the data used in the present study is already provided in Chapter -3. Visual as well as digital image classification techniques have been applied for snow cover mapping after geo-referencing process. These two techniques are discussed in brief in the following sections:

4.3.1 Visual classification

These base maps were overlaid on the positive prints developed from the film negatives of band 3 & 4 and also on False Colour Composite (FCC). The registration of the maps with images was carried out manually. Because whole area of the basin was not covered in a single image, therefore, the data of the closest date of adjoining imagery was used to find out the snow-covered area in the basin.

When mapping the snow cover, there are several possible features on the image, which were considered in order to prevent misidentification of snow and snow free areas. For example, cloud tops exhibit a very bright reflectance in the visible/infrared bands, which is often indistinguishable from snow. These aspects have been kept in view while delineating snow covered areas. Small portions of the order of less than 1 km² in snow covered area, which are under shadow (either from terrain features or clouds) have been considered as snow bound. The maps depicting snow covered areas for March/April and September/October have been prepared for the period for which data was available. After preparation of final maps, these were digitized using digitizing module of Integrated Land and Water Information System (ILWIS). The database of these snow covered maps was prepared in GIS and snow covered area has been computed.

4.3.2 Digital image classification

4.3.2.1 Geometric Correction and Registration

A base map of the Satluj basin from Survey of India (SOI) topographical maps was prepared and converted to digital form. All the sub scenes were geometrically corrected using the base map and carefully selecting the ground control points (GCPs). Well-distributed GCPs are essential for a successful geometric correction but it is very difficult to select such control points in high mountainous areas, because the roads and other infrastructures used for control points normally follow major valleys and very few run across the uplands. This becomes further complicated in a snow-covered region. A first order polynomial transformation was performed and resampling was done using the nearest neighbour interpolation method. The accuracy of registration was visually verified by overlaying the selected ground features on the geo-referenced images. This procedure was observed to be appropriate because the study area contains features, which can be recognized on images and has boundaries corresponding to rivers, reservoir and roads etc. The final products ensure that all data sets are comparable and areas can be measured. The basin area from each satellite image was extracted using an overlay mask.

After registration work is over the classification was applied to the images. Before classification, the images were studied in detail. Contrast stretching of individual raw bands is one of the initial steps and is effective in improving interpretability of different features through increasing contrast. To have an idea of frequency distribution of the data, image histogram of the bands have been studied. The following ground features were considered for preparing the snow covered area maps.

4.3.2.2 Shadows

The Himalayan Mountains are rugged and have high relief. As the Landsat and IRS data have been acquired in the early forenoon, the prevailing low-angle of illumination leads to shadows. In such cases, snow covered shadowed regions appear similar to snow-free areas in tone. Before classification it is necessary to discriminate between snow-free area and the shadows. Small portions in snow covered area, which are under shadow have been considered as snow bound.

4.3.2.3 Cloud cover

Cloud cover has been seen as the main constraint on the possible operational implementation of the satellite monitoring of snow cover based on satellite data representing visible part of electromagnetic spectrum. Using the estimated snowline altitude and assuming a similar accumulation of snow above the calculated snowline in these obscured regions may approximate the area of snow concealed by cloud. A sequence of satellite images, where different parts of each image are cloud free, can be classified and overlaid to produce fuller areal information for the same snow day or for a snow event. The assumption is that the snow condition for the two images remained the same and only the positions of clouds changed for the successive images. Assuming that the snow conditions did not change significantly between these times, the combined classified image reveals the fuller extent of snow distribution for that day. Extrapolations of snow area beneath clouds for two images have been attempted in this study.

4.3.2.4 Classification

In the present study unsupervised classification using the Iterative Self-Organizing Data Analysis Techniques (ISODATA) has been applied. The ISODATA uses the

minimum spectral distance to assign a cluster for each candidate pixel. It begins with a specified number of arbitrary cluster means which are then processed repetitively, so that these arbitrary means shift to the means of clusters in the data. The required inputs for running the ISODATA process are the number of clusters in the output file, the convergence threshold which is the maximum percentage of unchanged pixels reached between two iterations, and the maximum iteration which is the maximum number of times that ISODATA should recluster the data and prevents ISODATA from running too long or from potentially getting "stuck" in a cycle without reaching the convergence threshold.

The snow covered area obtained from March/April and September/October for different years are given in Table 4.3. The results indicate that a major portion of the basin is covered by snow in the month of March/April (Figures 4.3 to 4.12). Information available on snow cover area for Satluj basin from Paul et al. (1995) was also used in this study. Paul et al. (1995) has estimated snow covered area for Satluj basin from the digital analysis of NOAA-AVHRR data which is supported by Landsat-MSS and TM and IRS-LISS- I data. Snow covered area was determined from February to July for a period 1986 to 1993, using all relatively cloud free images. Paul et al. (1995) used a digital terrain model (DTM) of 1-km resolution to extrapolate snow cover under clouds. The digital basin mask was used along with the classified image to compute the snow-covered area. The snow covered area on different dates was plotted against time and curves were drawn to obtain depletion curves for each year. Interpolation/extrapolation of these curves provided the information on snow covered area for the months for which snow covered area was not available.

Snow covered area in the basin for the months of March/April and September/October, which usually indicates maximum and minimum snow cover area in

the basin, respectively, were determined for different years (Table 4.3). Based on 10 years data analysis, it was found that about 65% (14,498 km²) of the basin is covered by snow by the end of March/April and after melt season it reduces to 20.3% (4,528 km²). Results indicate that about 9,970 km² area becomes snow-free during the melt season. To estimate evapotranspiration losses snow covered area is required on monthly basis. It was computed either using satellite data or linearly interpolated using available snow cover information.

Table 4.3 : Snow covered area (SCA) and permanent snow covered area (PSCA) in the Indian part of Satluj basin up to Bhakra reservoir. Total area of the Indian part of Satluj River up to Bhakra reservoir is 22305 km².

Year	Month	Snow covered area expressed as % of total basin area	Month	Permanent snow covered area expressed as % of total basin area
1986	March	64	September	15
1987	March	59	September	12
1988	March	71	September	35
1989	March	63	September	20
1990	March	70	September	17
1991	March	63	September	30
1992	March	72	September	16
1993	March	58	September	17

4.4 EVAPOTRANSPIRATION

The net rain input to the basin can be obtained by subtracting total evapotranspiration losses from the total rainfall depth over the water budget period.

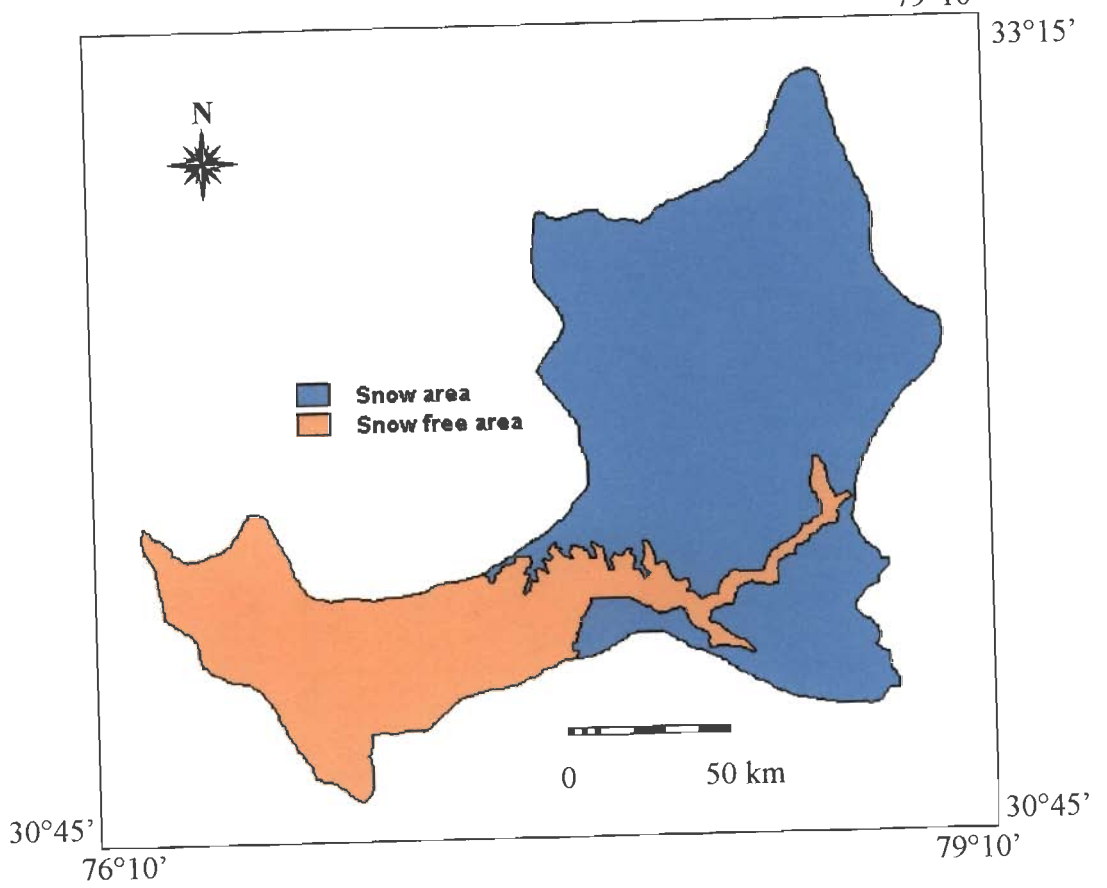


Figure 4.3 : Snow cover distribution in the Satluj basin for 7.3.1988

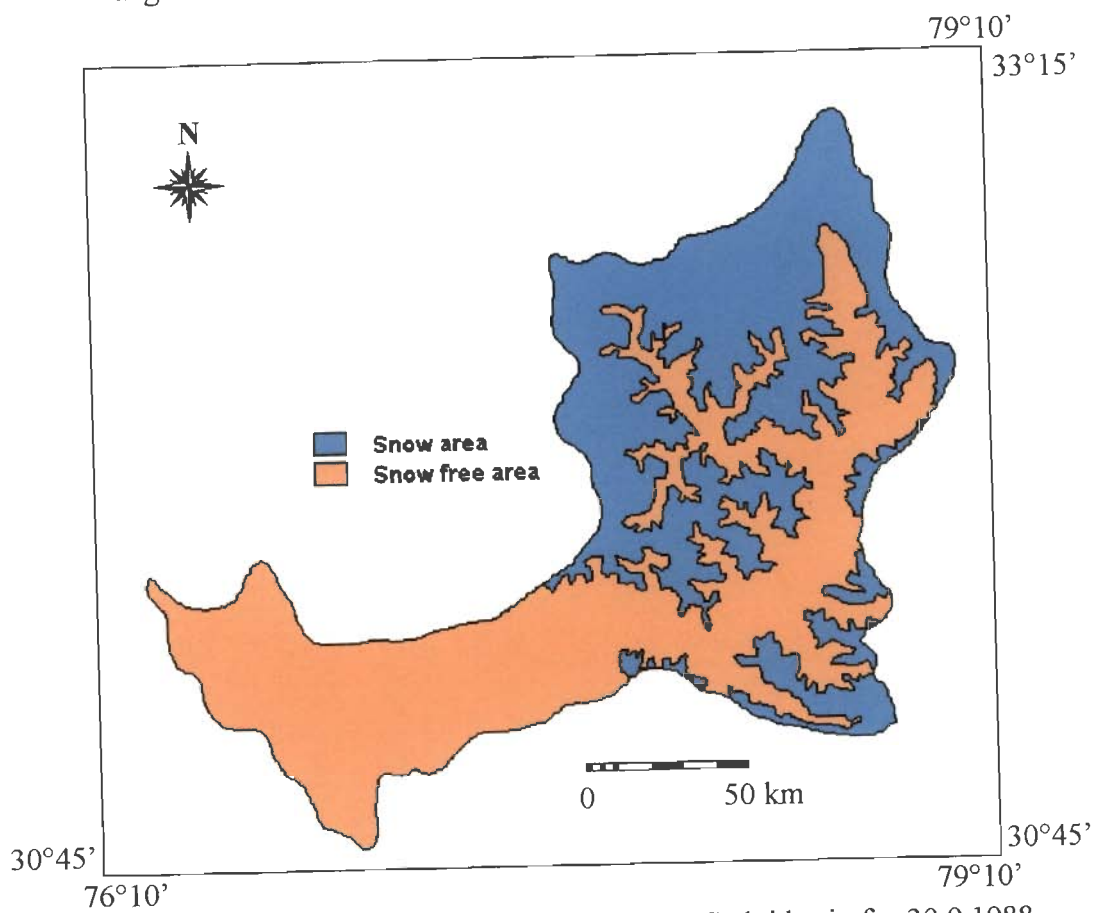


Figure 4.4 : Snow cover distribution in the Satluj basin for 30.9.1988

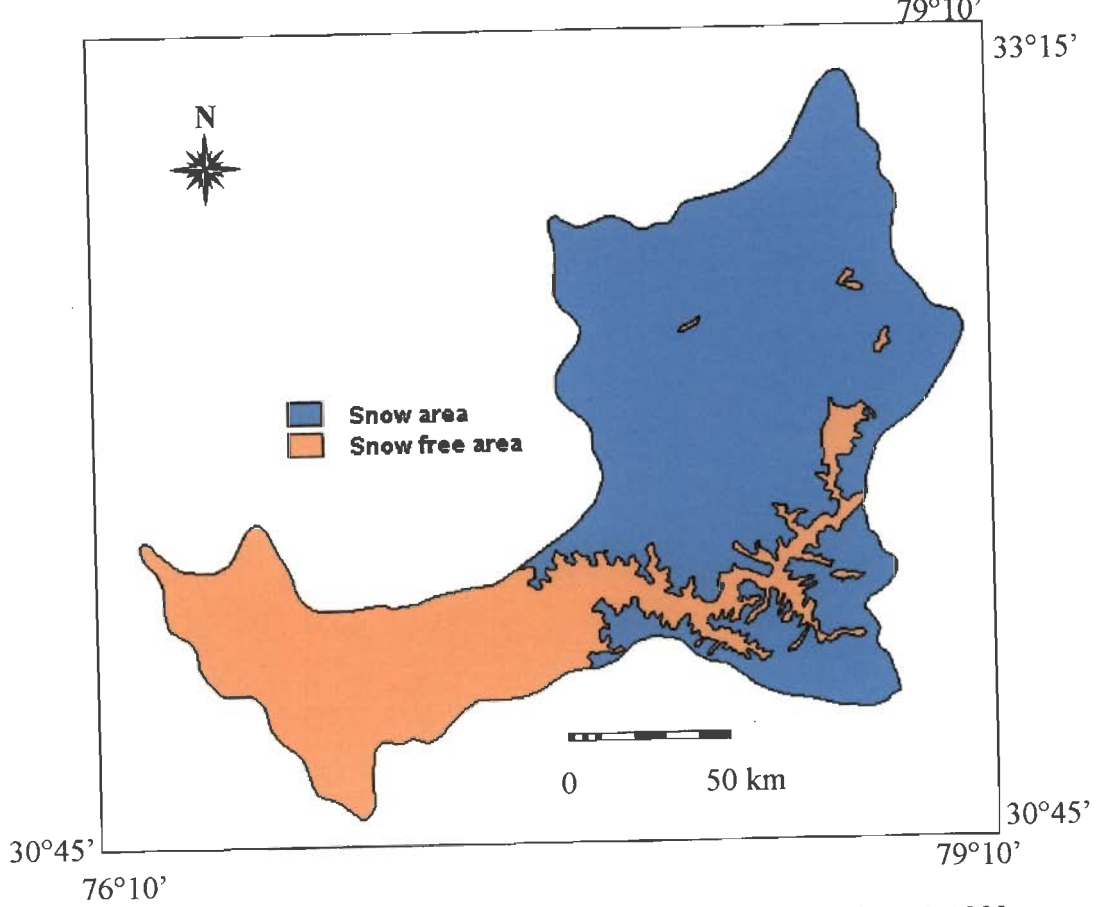


Figure 4.5 : Snow cover distribution in the Satluj basin for 3.3.1989

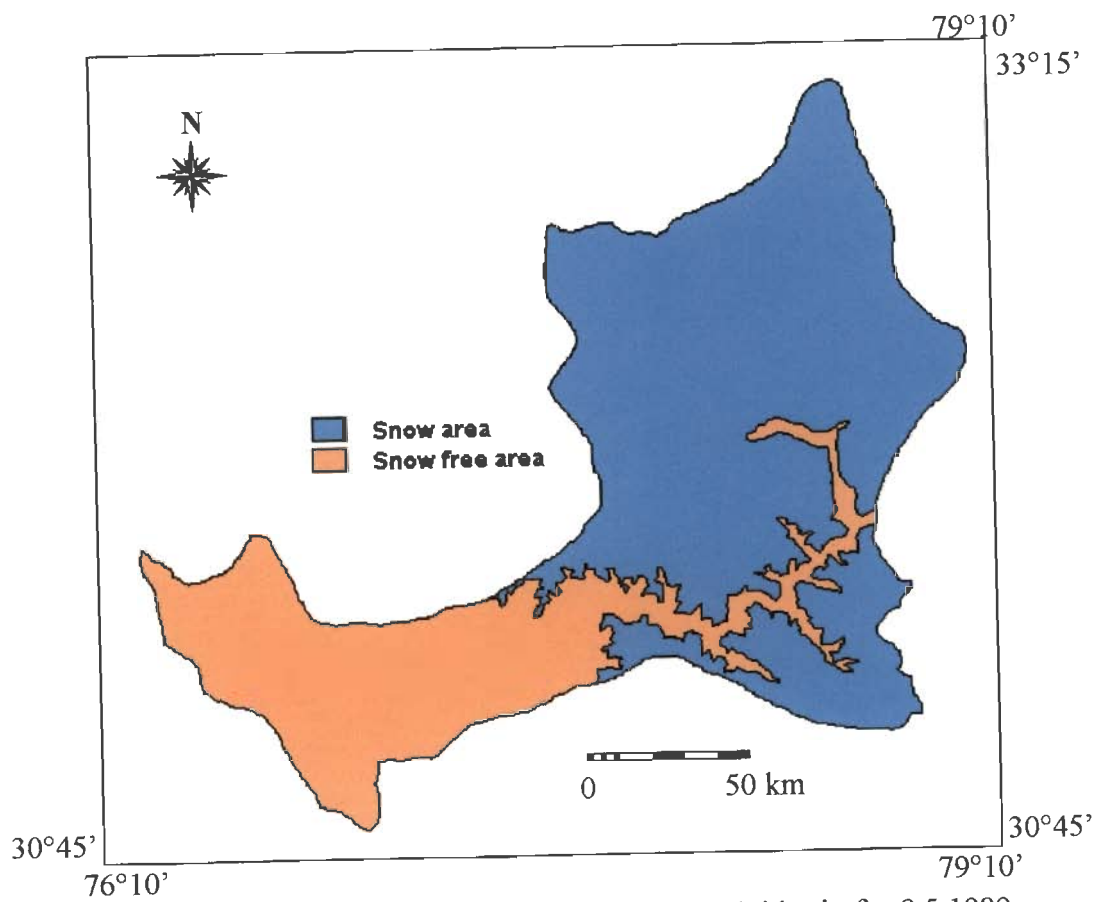


Figure 4.6 : Snow cover distribution in the Satluj basin for 8.5.1989

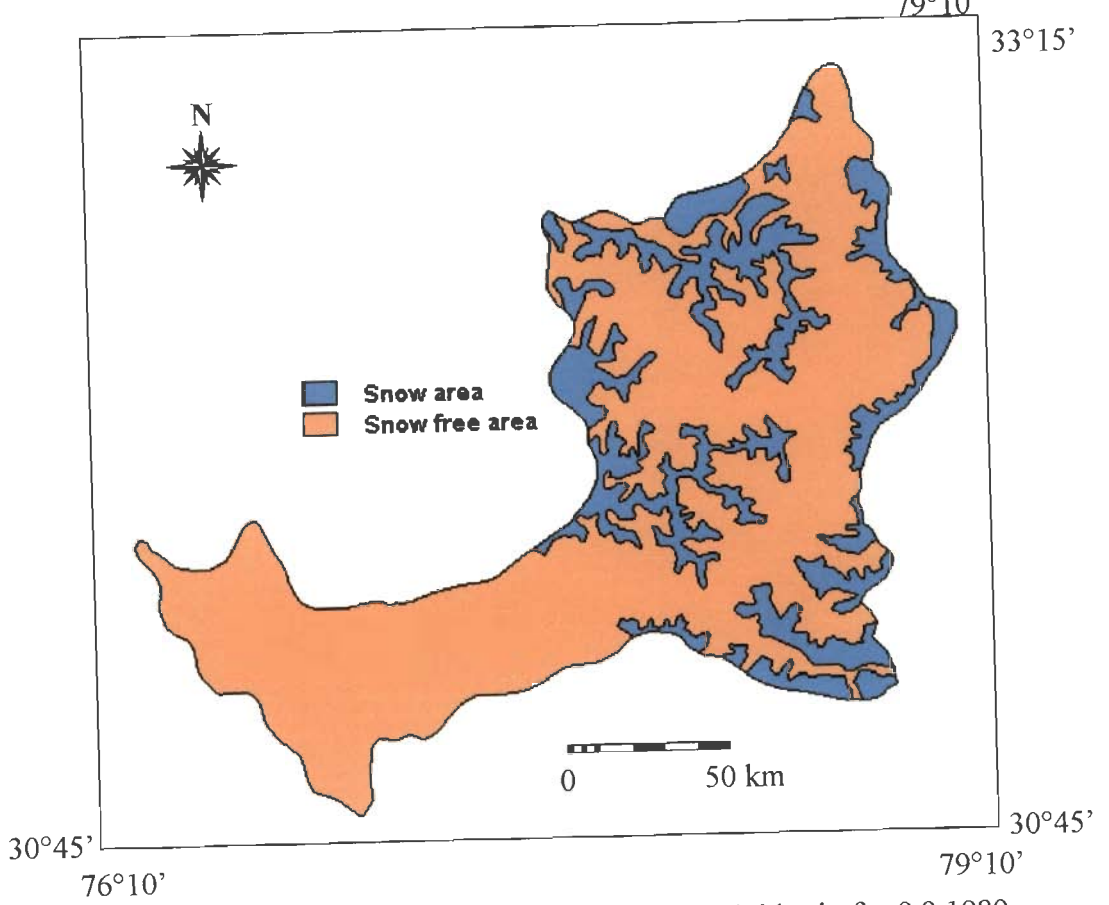


Figure 4.7 : Snow cover distribution in the Satluj basin for 9.9.1989

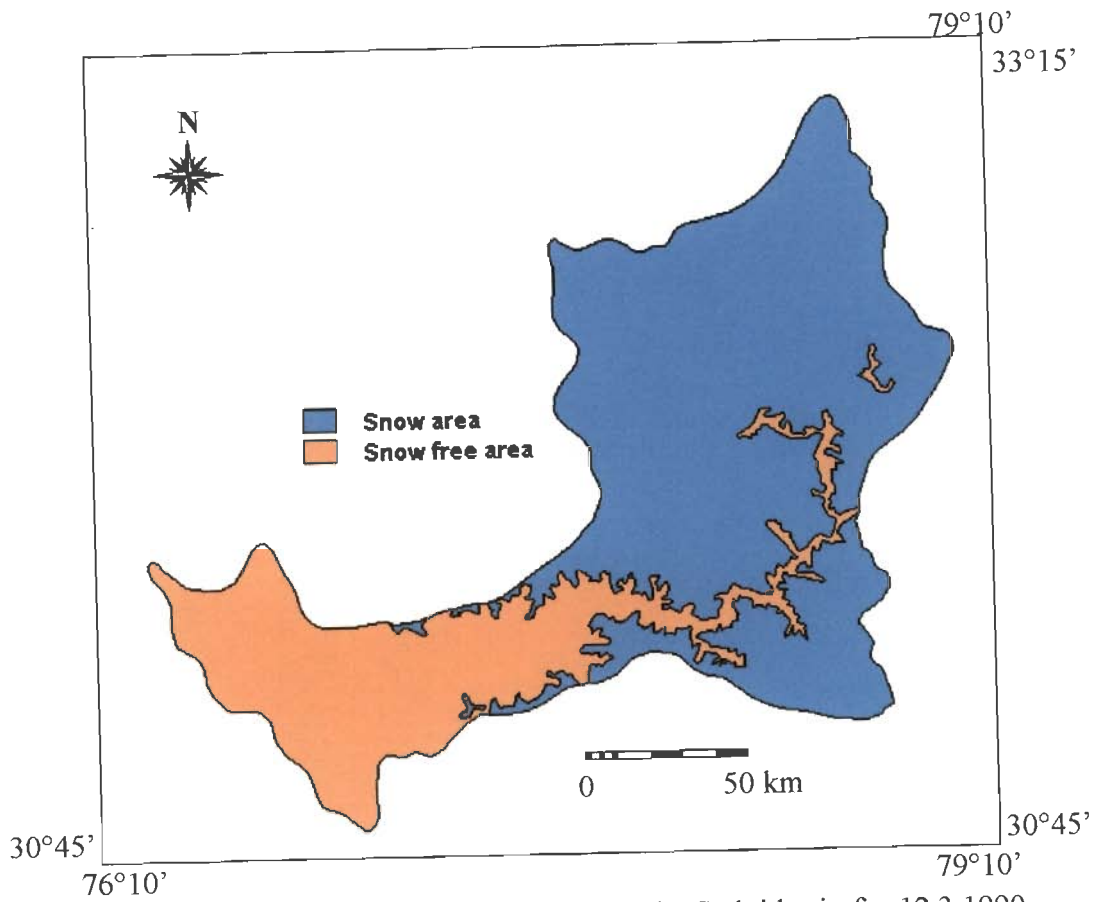


Figure 4.8 : Snow cover distribution in the Satluj basin for 12.3.1990

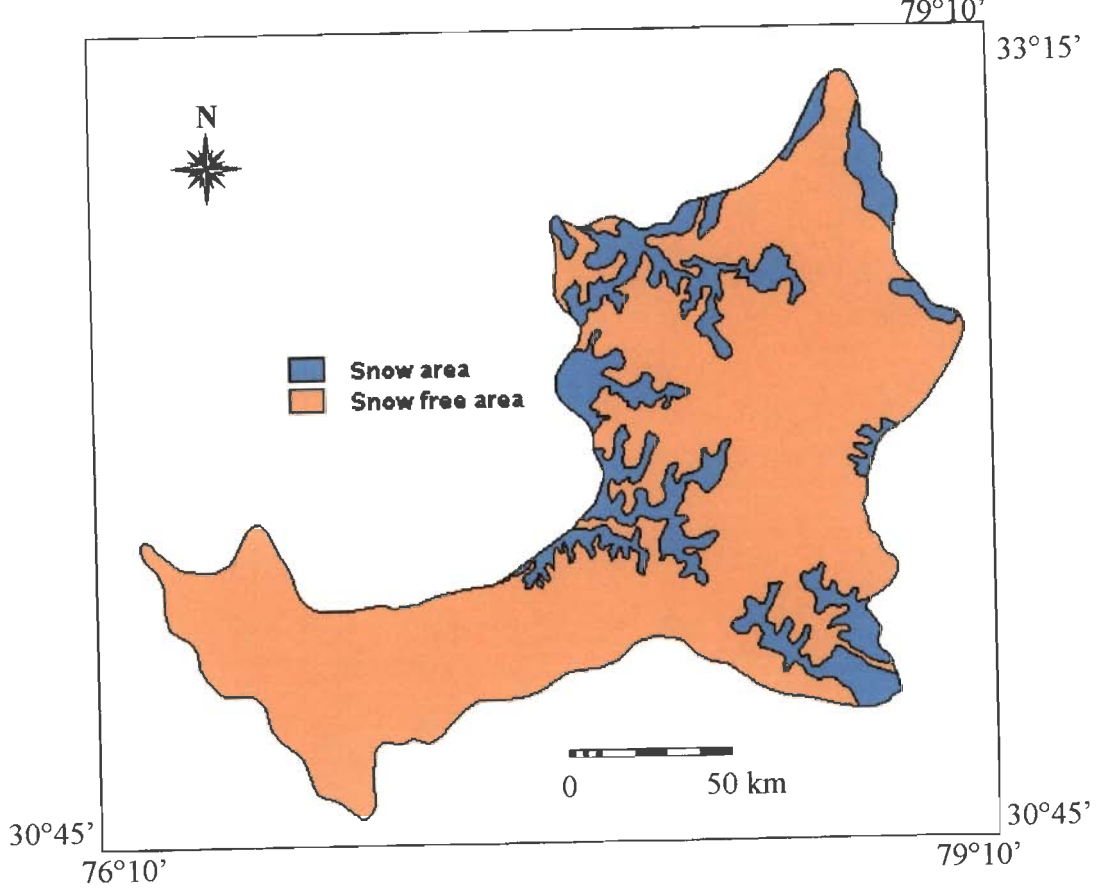


Figure 4.9 : Snow cover distribution in the Satluj basin for 22.7.1990

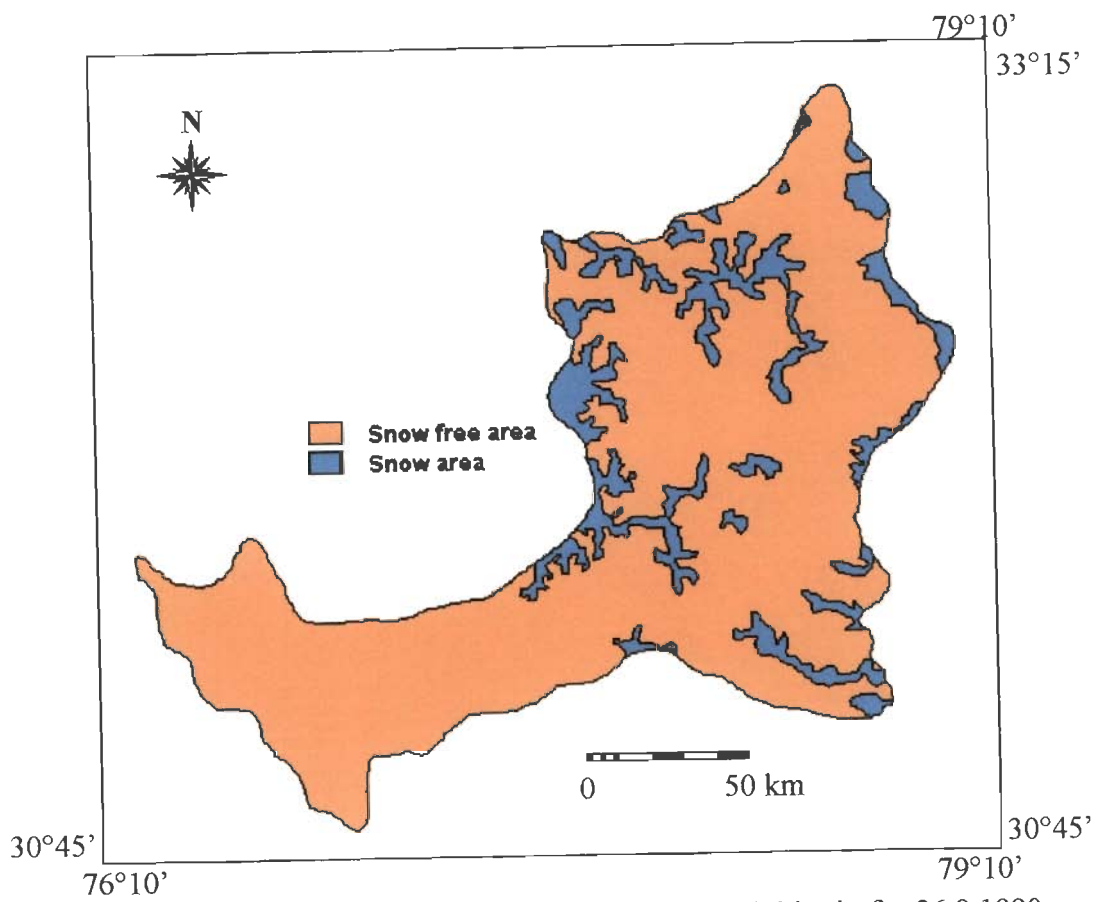


Figure 4.10 : Snow cover distribution in the Satluj basin for 26.9.1990

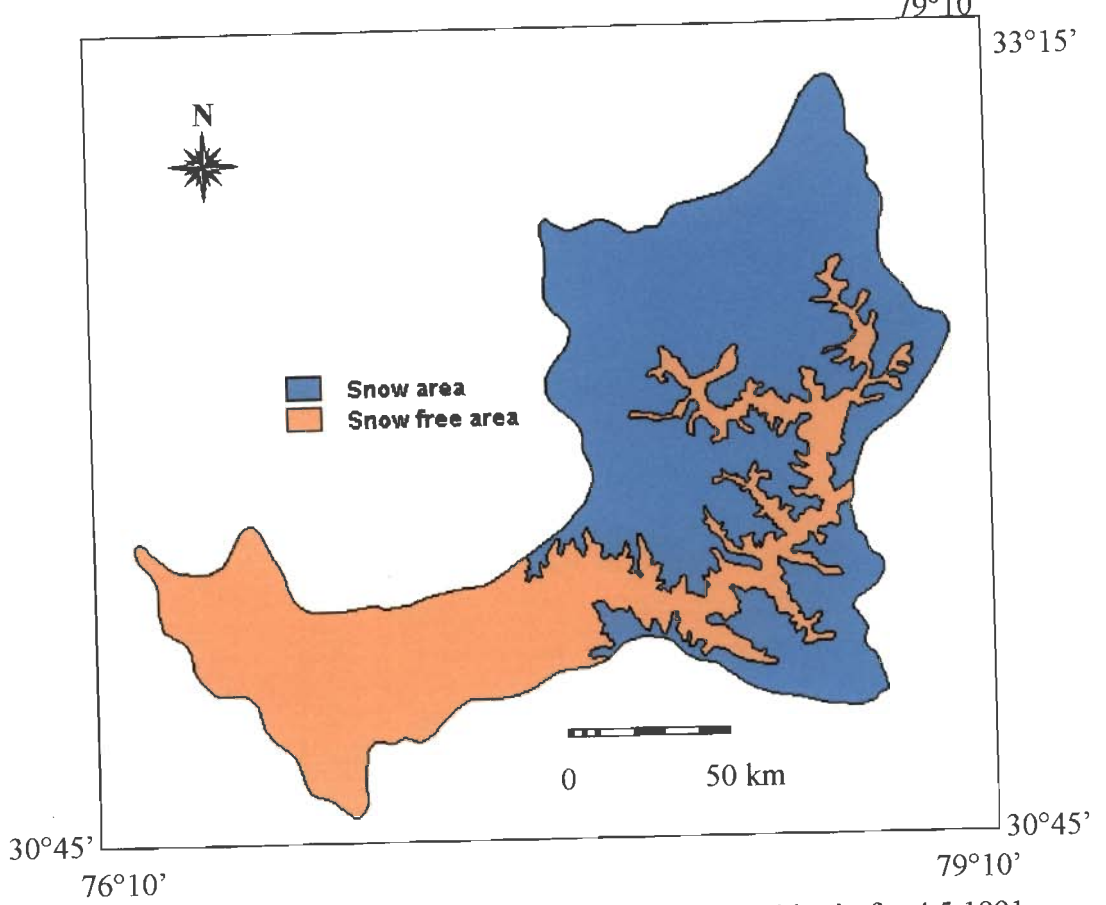


Figure 4.11: Snow cover distribution in the Satluj basin for 4.5.1991

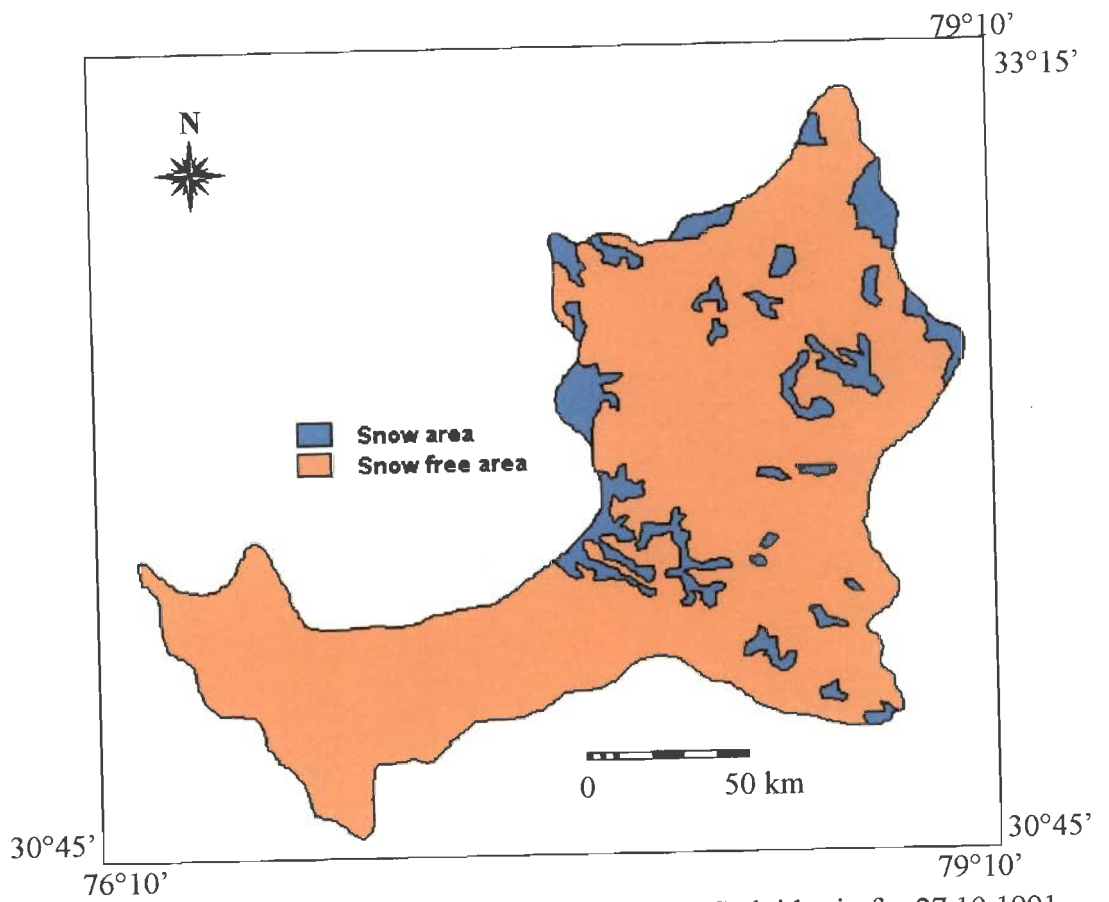


Figure 4.12 : Snow cover distribution in the Satluj basin for 27.10.1991

Evapotranspiration losses from the snow covered area are very small (Bengtsson, 1980) whereas those from the snow-free area may be significant depending upon the soil moisture conditions. Therefore, identification of snow-covered and snow-free area is required for estimating evapotranspiration losses from the whole basin. It is to be pointed out that rainfall occurring over the snow covered area is absorbed or infiltrated through snowpack without significant evaporation losses. Whereas rainfall occurred on the snow-free area is reduced in accordance with the evapotranspiration losses from the snow-free area.

First monthly evapotranspiration losses were estimated and then these monthly values were used to compute total losses from the basin. The information on snow-free area in conjunction with actual evapotranspiration (AET) was used to get total evapotranspiration losses from the whole basin. Due to warmer climate in the lower and middle part of the basin, most of the evapotranspiration takes places from these areas of the basin. The pan evaporation and air temperature data were available at Bhakra (518m), which lies on the lower basin boundary of the basin. Because no other dataset was available for estimating evapotranspiration in the basin, therefore, temperature and pan evaporation data (US Weather Bureau Class A pan evaporimeter) of Bhakra was used for this purpose. Monthly pan evaporation observed at Bhakra was correlated with mean monthly maximum temperature, minimum temperature and mean temperature observed at the same station. It was found that out of these three relationships, mean monthly maximum temperature provided the best correlation with monthly pan evaporation ($r^2 = 0.84$). In an another study, Singh et al. (1995) also studied the relationship between pan evaporation and different meteorological parameters, namely, maximum temperature, minimum temperature, wind speed, relative humidity, duration of sunshine hours. They also found that out of these five meteorological parameters the highest correlation (0.85)

was obtained for maximum air temperature and evaporation relationship. Relationship between mean monthly maximum temperature, T_{\max} and monthly pan evaporation, $Evap$, for the study basin is shown in Figure 4.13 and can be expressed as

$$Evap = 11.63 \times \exp(0.077 \times T_{\max}) \quad (4.2)$$

This relationship was used to compute evapotranspiration from the snow free area. In order to obtain the representative value of evapotranspiration losses from snow-free part of the basin, it was computed at mid elevation of snow-free area. Mid elevation of snow-free area was determined using information on snow-covered area and area-elevation curve of the basin. As the melt season advances, the snow-covered area reduces resulting an increase in snow-free area. Therefore, mid elevation of the snow-free area changes with time. It increases in summer as snow line moves up and reduces during winter period when snow line lowers down. The available mean monthly temperatures of Bhakra were extrapolated to the mid elevation of snow-free area using a temperature lapse rate. The extrapolation of temperature was made using following relationship:

$$T_{\max} = T_{b\max} - \delta \times (h - h_b) \quad (4.3)$$

where, T_{\max} is the mean monthly maximum temperature ($^{\circ}C$) at elevation h (m) in the basin, δ is the temperature lapse rate ($0.6^{\circ}C/100$ m), $T_{b\max}$ is the mean monthly maximum temperature of Bhakra ($^{\circ}C$) and h_b is the elevation of base station (518 m).

Equation (4.2) and (4.3) provided the pan evaporation at mid elevation of snow-free area, which was considered as representative of evapotranspiration for snow free area. Monthly potential evapotranspiration from snow-free area was computed by multiplying

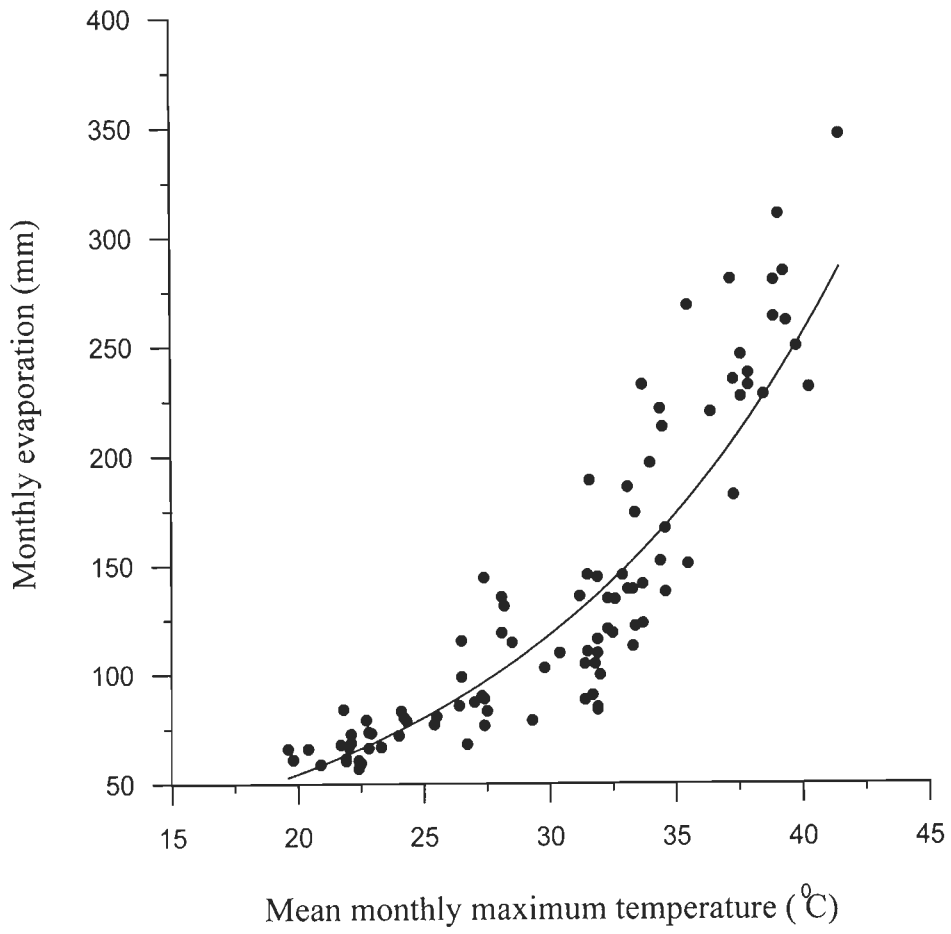


Figure 4.13 : Relationship between mean monthly maximum temperature and monthly pan evaporation at Bhakra

estimated pan evaporation by pan coefficient. However, true values of pan coefficient have been reported between 0.6 to 0.8 for US Weather Bureau Class A pan evaporimeter, but an average value (0.7) is recommended for use (Chow, 1964). In addition to mid elevation approach, evapotranspiration losses from the basin were also estimated using a distributed approach called as GIS based approach. A digital elevation model (DEM) of the basin was prepared and used for computation of elevation of desired point in the basin (Figure 4.14). In GIS based approach, first a temperature distribution map using Equation (4.3) was prepared. For the factor h , the DEM has been considered and maximum temperature at each grid was computed. It is to be noted here that, the temperature distribution was prepared only for snow free area for each month. As given in Equation (4.2) that a relationship between maximum temperature and evaporation has been developed. Using this relationship and with the help of temperature distribution map, a evaporation distribution map was prepared. From this an average value was obtained for every month and multiplied by 0.7 to get potential evaporation.

Monthly or annual AET from the basin can be computed using potential evapotranspiration (PET) provided information on AET/PET is available for the period of interest. No study has been reported for the Himalayan region giving information on AET/ PET for this region, which can be straightway adopted. Therefore for computation of ratio of AET/PET an analysis of rainfall and mean temperature has been carried out for the snow free part of the basin, which controls evapotranspiration losses from the basin. During winter period the basin get less rainfall and temperatures are also low, therefore little AET takes place from the basin during this period. During the premonsoon period (April to June) the temperature are high but again rainfall is less and hence PET is high but the AET is not significant. During monsoon period (July to September) the rainfall provides sufficient moisture for evaporation from soil and temperature is also high,

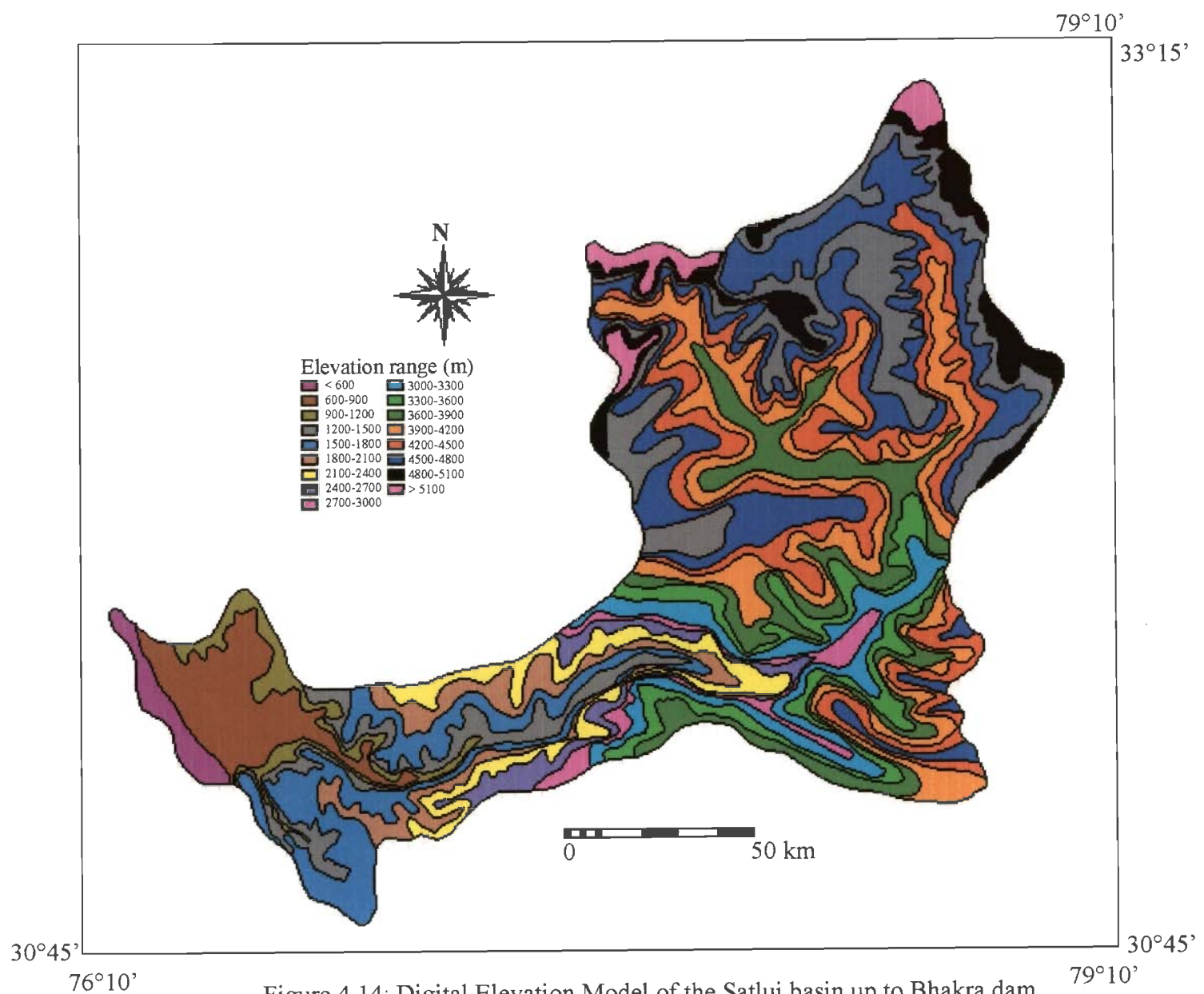


Figure 4.14: Digital Elevation Model of the Satluj basin up to Bhakra dam

therefore AET is comparable to PET. On the basis of trends of rainfall and temperature, the AET/PET was distributed over a period of 12 months. AET and PET were considered closer in the monsoon period because sufficient soil moisture is available to evaporate. Whereas AET was kept minimum in the winter period when temperatures are very low resulting in less evapotranspiration losses. The distribution for each month was obtained on the basis of analysis of monthly rainfall and temperature patterns in the lower part of the basin. The approximate values of AET/PET for different months starting from January was considered as 0.20, 0.20, 0.15, 0.20, 0.15, 0.25, 0.85, 0.90, 0.65, 0.25, 0.25, 0.25. These values provide AET/PET as 0.40 on the yearly basis. For a particular month, estimated monthly AET and extent of snow free area provided actual evapotranspiration losses. Cumulative monthly values over the water budget period give total evapotranspiration losses from the basin.

The monthly evapotranspiration obtained using mid elevation approach and GIS based approach for different years are given in Table 4.4. The distribution of monthly actual evapotranspiration using GIS based approach for a year is shown in Figure 4.15 and 4.16. For different years, variation in the computed annual evapotranspiration from these two different approaches ranged between 2 to 8%. Total cumulative evapotranspiration losses over the water budget period were estimated to be 1486 mm and 1413 mm using Mid elevation approach and GIS based approach, respectively. In Table 4.4 the values of evapotranspiration obtained using both the techniques has been provided. The average of these two values have been taken and given in the Table 4.1. It is noticed that both approaches provided only about 5% difference in the total evapotranspiration losses.

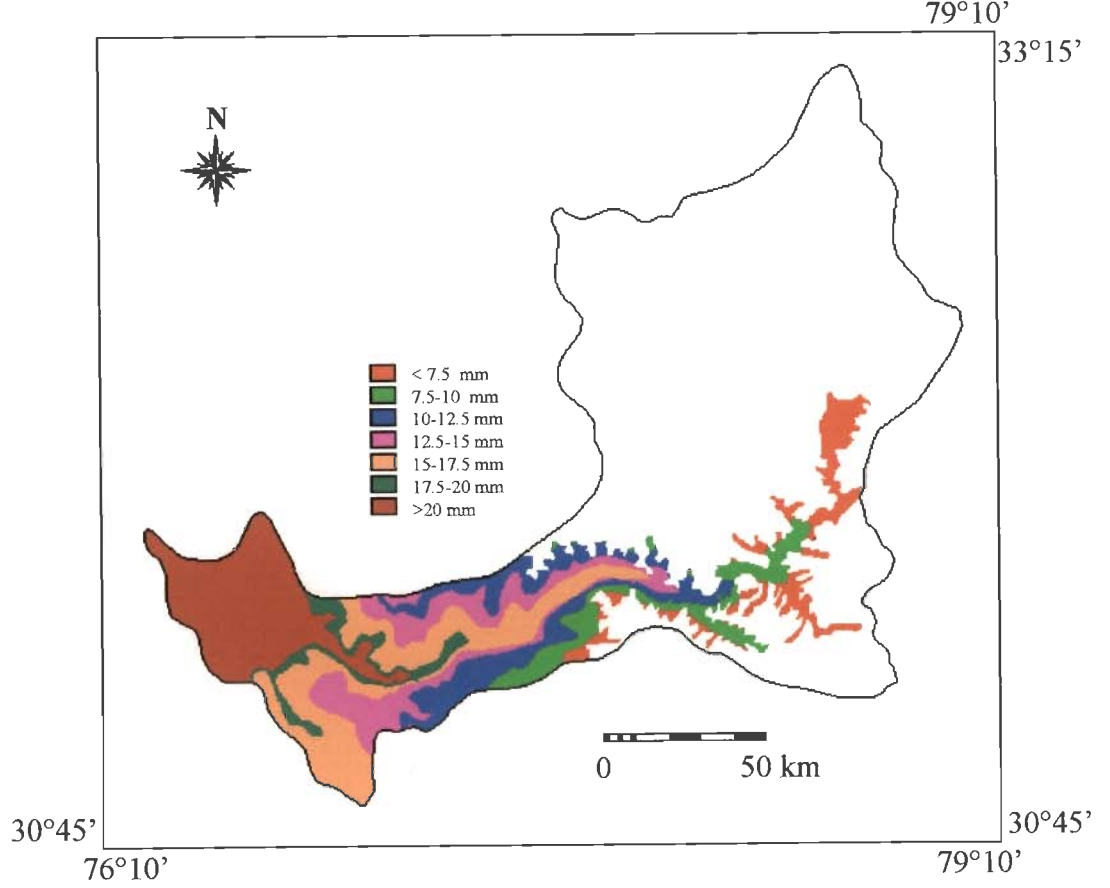


Figure 4.15 Monthly evapotranspiration distribution in the Satluj basin for March, 1989

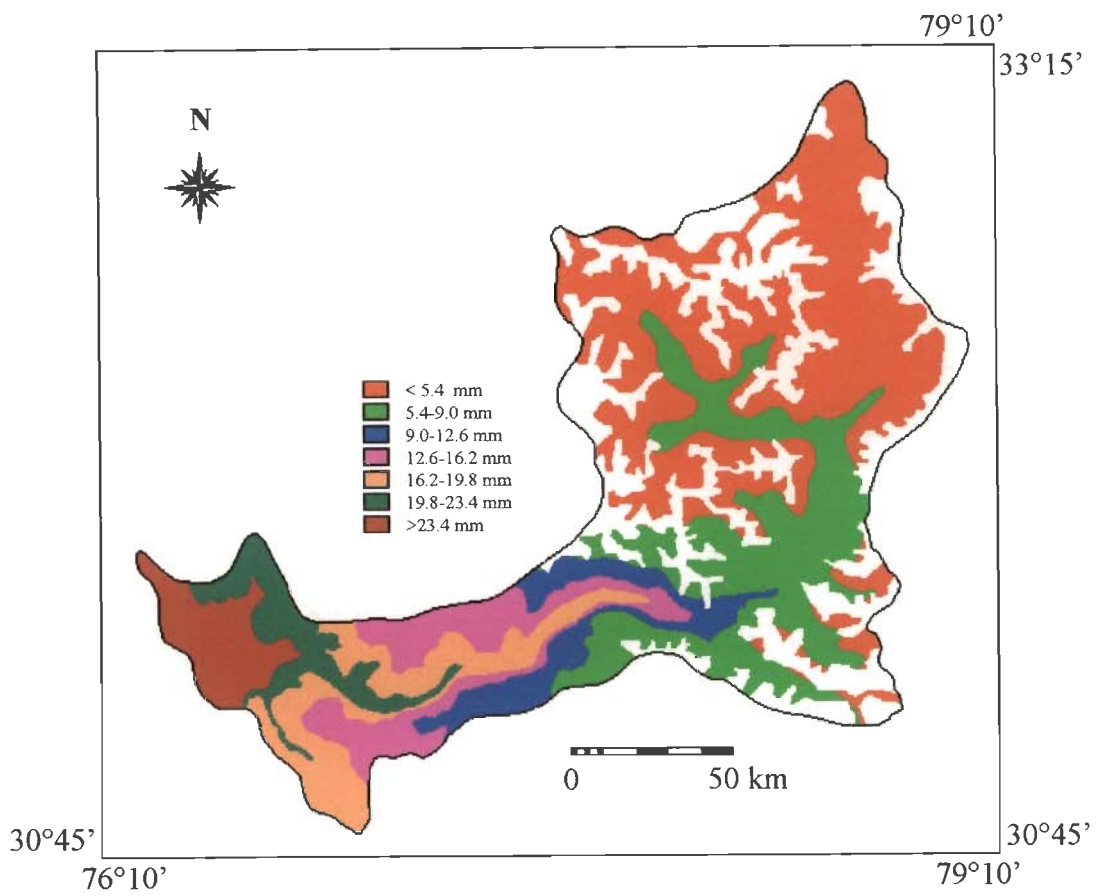


Figure 4.16 Monthly evapotranspiration distribution in the Satluj basin for Oct., 1989

Table 4.4 : Monthly evapotranspiration computed for different years for the Indian part of Satluj basin up to Bhakra. E1 and E2 represent monthly evapotranspiration computed using mid elevation approach and GIS based approach, respectively.

Year/ Mon.	1986/87		1987/88		1988/89		1989/90		1990/91		1991/92		1992/93	
	E1 (mm)	E2 (mm)	E1 (mm)	E2 (mm)	E1 (mm)	E2 (mm)	E1 (mm)	E2 (mm)	E1 (mm)	E2 (mm)	E1 (mm)	E2 (mm)	E1 (mm)	E2 (mm)
Oct.	8.0	7.6	8.6	7.9	7.0	5.6	10.0	8.9	8.7	6.9	8.2	6.8	9.1	8.3
Nov.	6.4	8.5	6.2	8.2	4.8	5.7	5.7	7.3	7.0	9.1	5.5	6.7	5.8	7.2
Dec.	3.5	4.3	4.2	4.7	3.3	3.7	3.5	3.7	3.9	4.4	3.7	3.4	3.6	4.0
Jan	2.6	3.0	2.4	2.6	1.8	1.8	2.6	2.8	2.4	2.7	1.9	2.0	2.0	2.2
Feb	3.2	3.5	3.2	3.4	2.4	2.6	2.4	2.5	2.9	3.2	2.5	2.4	3.2	3.8
Mar	2.9	2.9	2.5	2.0	2.7	2.5	2.0	1.7	2.8	2.7	2.2	1.8	2.6	2.6
Apr.	6.7	7.0	7.0	6.1	5.7	5.7	5.5	5.0	5.5	5.4	6.3	6.4	6.6	6.8
May	4.7	4.5	7.9	6.6	7.5	6.8	7.8	7.6	7.7	7.0	7.5	7.5	9.5	9.5
June	12.9	12.4	14.1	14.5	10.9	8.3	14.5	14.3	13.9	14.8	15.0	16.5	15.8	17.1
July	45.7	40.6	28.3	25.6	35.7	32.6	30.4	27.4	44.8	43.9	34.4	33.2	32.6	30.9
Aug.	36.3	33.5	29.5	25.3	35.2	32.6	33.6	30.8	33.1	29.6	32.8	30.7	44.3	40.7
Sept.	27.6	26.0	23.2	19.5	26.3	24.0	23.4	21.7	23.5	20.3	25.8	24.1	22.5	20.8
Total	160.5	153.8	137.1	126.4	143.3	131.9	141.4	133.7	156.2	150.0	145.8	141.5	157.6	153.9

Following the above mentioned two approaches, evapotranspiration losses were estimated for all the years for which snow-covered/snow-free data was available. Using available information, an average yearly evapotranspiration was obtained and used for the years for which data were not available. Therefore in Table 4.1 for the last three years period the evapotranspiration losses are given as the average value. An average value of the evapotranspiration losses (1450 mm) for the water budget period (or 145 mm/year) was obtained from the above two computed values and used in further calculations.

4.5 SNOW AND GLACIER CONTRIBUTION

Average snow and glacier contribution in the annual flow of Satluj River at Bhakra Dam was computed using water balance Equation (4.1). Runoff depth, rainfall input and evapotranspiration losses for different years are listed in Table 4.1. Cumulative values each component for the water budget period were used for estimation of the contribution of rainfall, and snow and glacier in the total annual runoff from the basin (Table 4.5).

Table 4.5: Snow and glacier melt for Satluj River at Bhakra using 10 years (1986/87-1995/96) data

Period	Runoff (mm)	Rainfall (mm)	Evapotrans- piration losses (mm)	Rain contribution to runoff		Snow and glacier contribution to runoff	
				(mm)	(%)	(mm)	(%)
10 years (1986/87- 1995/96)	5614	3748	1450	2298	41	3314	59

The average snow and glacier melt runoff contribution into annual flows was found to be about 59% and rest, 41% from the rain.

4.6 CONCLUDING REMARK

The application of water balance approach for a snowfed basin has been made to find out the snow and glacier contribution in the basin. The location of gauging site where snow and glacier contribution is being computed is also very important because percentage of snow covered area in the total drainage area changes from site to site. In the present case, for all the sites upstream of Bhakra the snow and glacier contribution in the annual flows will be higher due to increase in the percentage of snow covered area in the total drainage area of the basin. The results indicate that there is a significant contribution from snow (59%) in the study basin. Therefore development of a snowmelt model for a basin having major component from snow is required for such basins. In the present this aspect, i.e., development of snowmelt runoff model has been taken and covered in detail in the next chapter.

CHAPTER 5

MODELLING OF STEAMFLOW FOR A SNOWFED BASIN

Modelling of streamflow from a basin is based on transformation of incoming precipitation to outgoing streamflow by considering losses to the atmosphere, temporary storage, lag and attenuation. Hydrological models use for simulation or forecasting of streamflow are generally categorized as simple regression models, black-box models, conceptual models and physically based models. Black-box models are generally lumped in nature by treating a basin as a single spatial unit. Physically based models use appropriate physical equations contain equations for all the processes involved. These models are invariably distributed and involve desegregation of basin into zones or grid cells. Conceptual models may be either lumped or distributed with one or more storage represented by conceptual units and connected by incoming and outgoing fluxes representing different hydrological pathways.

When precipitation falls as snow it snow accumulates in the basin and snowpack is developed. Conceptually snowmelt runoff models are rainfall-runoff models with additional component or routines added to store and subsequently melt precipitation that falls as snow. Some snowmelt runoff models are purpose built and are not intended for use in non snowy environments, though they have to make some allowance for precipitation which falls as rain during the melt season. In general, the part of the model which deals with snowmelt, has to achieve three operations at each time step (Ferguson, 1999)

- extrapolate available meteorological data to the snowpack at different altitude zones
- calculate rates of snowmelt at different points, and

- integrate snowmelt over the concerned effective area of the basin and estimate the total volume of new melt water.

The melt water and rainfall, if any, is then routed to the basin outlet. In the next time step the model has to take into account of changes in snow-covered area because there is general depletion of snow covered area with time. In the present study a conceptual model for simulation of streamflow for Satluj river basin which is a highly snowfed basin, has been developed. The structure of the model and algorithms used are discussed in detail in the following sections.

5.1 DEVELOPMENT OF SNOWMELT MODEL (SNOWMOD)

The snowmelt model (SNOWMOD) is designed to simulate daily streamflow in mountainous basin where snowmelt is major runoff component. The process of generation of streamflow from snow covered areas involves primarily the determination of the amount of basin input derived from snowmelt alongwith some contribution from glaciermelt and rain. Most of the Himalayan basins experience runoff from the snowmelt as well as rain. The contribution of rain comes from the lower part of the basin having elevation less than 2000m, the middle part between 2000m to 4000m contributes runoff from the combination of rain and snowmelt while in the high altitude region having elevation more than 4000m, runoff computation comes from the glacier melt. The contribution from snow and glacier is controlled by the climatic conditions and therefore, varies from year to year. The importance of snow and glacier contributions in Satluj basin has already been presented and discussed in Chapter 4.

Himalayan basins are complex in nature in terms of input to the basin and have contributions from all the three sources, i.e., rain, snow and glacier. For these types of basins, situation becomes more complex because contribution from each component is not

known or could not be observed separately. The observed flow consists of the contribution from all these three sources in addition to the base flow/ground water contribution. For the Himalayan basins, most important factor influencing the development of model and the approach to be adopted, is the limited availability of data. There is very sparse network of measurement stations in the high altitude region of the Himalayas. Data collected at most of the measurement stations consist of mostly temperature and precipitation data. Most of the meteorological data required for the application of energy balance approach is hardly available. Therefore, development of a conceptual model with an index approach for calculating the snow and glacier melt runoff is the suitable choice for snowmelt runoff in the Himalayan basins. Keeping in view the limited data availability, the structure of the present model has been kept simple so that all suitable/available data is properly utilised.

5.2 MODEL STRUCTURE

The flow chart of the model structure is shown in Figure 5.1. Specific major considerations in the design of the model components are as follows:

- (a) The model computes or simulates the snow melting and runoff processes on a daily basis. The basin is divided into snow covered and snow free part and modelling of runoff is carried out separately from these two parts.
- (b) Use of practical yet theoretically sound methods for subdividing the basin in evaluating the various physical and hydrologic processes relevant to snow melt and its appearance as streamflow at the outlet.
- (c) The model has ability to perform simulation computations over any specified time interval according to the availability of input data

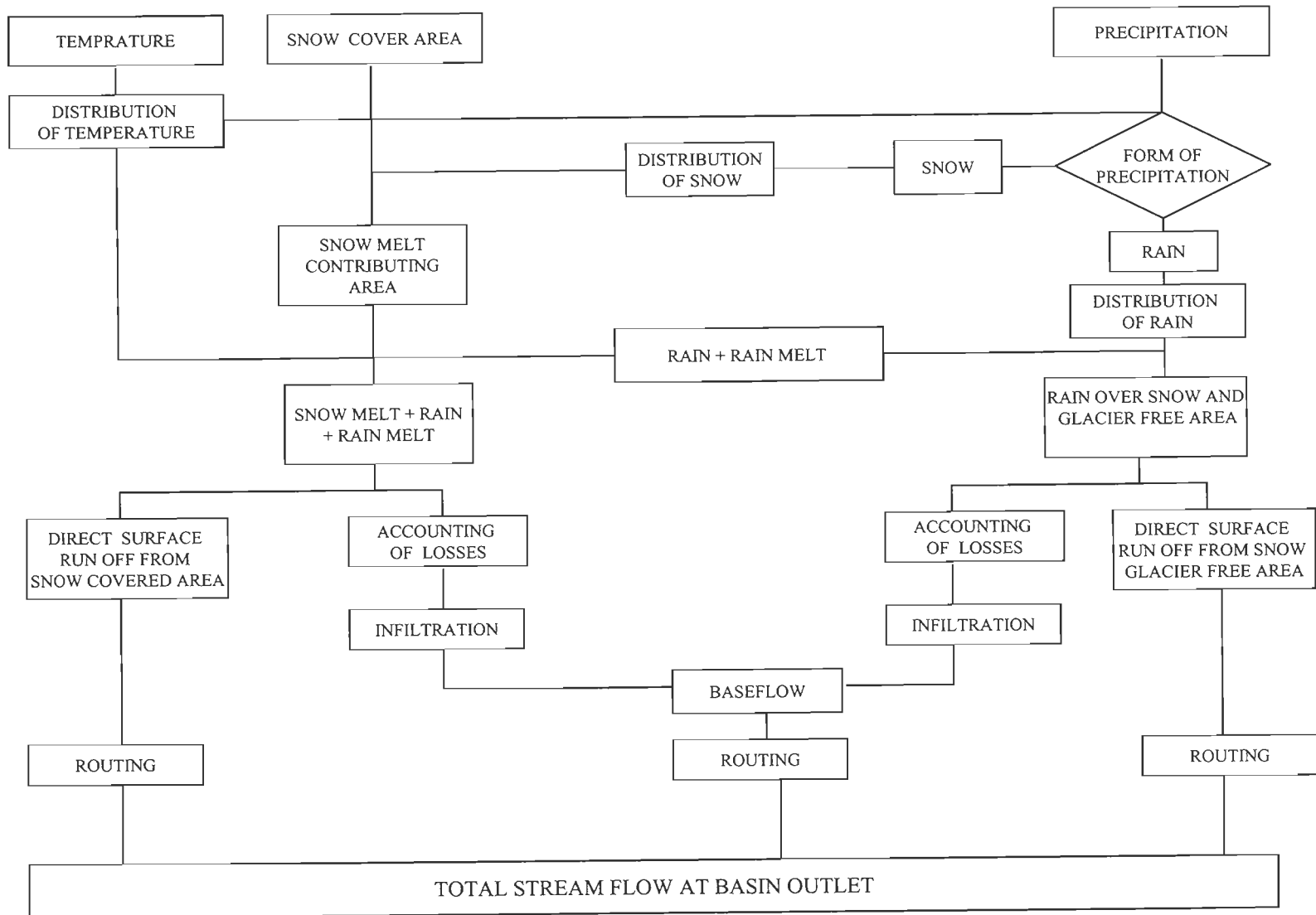


Figure 5. 1: Structure of the snowmelt model (SNOWMOD)

- (d) Capability of the model to adjust itself to specified or observed conditions of streamflow from the previously computed amounts, and maintaining continuity of functions in further processing.
- (e) Optimisation of parameters used in routing of the rainfall-runoff and snowmelt runoff.

In order to execute this SNOWMOD model, the following input data are required:

- 1) Physical features of the basin which include snow covered area, elevation bands and their areas, altitude of meteorological stations, and other watershed characteristics affecting runoff.
- 2) Time variable data include precipitation, air temperatures, snow-covered area, streamflow data, and other parameters determining the distribution of temperature and precipitation.
- 3) Information on the initial soil moisture status of the basin
- 4) Miscellaneous job control and time control data which specify such items as total computation period, routing intervals etc.

5.3 MODEL VARIABLES AND PARAMETERS

5.3.1 Basin Characteristics

5.3.1.1 Division of catchment into elevation bands

In the mountainous catchment where temperature and snow depth vary with elevation, the drainage area is divided into some convenient number of the bands of elevations and each elevation band is treated as a separate watershed with its own characteristics and initial snow cover area. Snowmelt is computed from each elevation band using temperature data. This approach allows a proper quantitative appraisal of the evolution and depletion of snowpack in the mountainous basins. The number of bands in a

basin will depend upon the topographic relief of the basin. However, there is no specified range of altitude for slicing the basin in the bands, but an altitude difference of about 500 m or so is considered appropriate for dividing the basin into elevation bands. Moisture input for each band is the sum of snowmelt and rainfall. Runoff for each band is computed from watershed runoff characteristics developed for that particular band. Streamflow for the whole basin is found by summing the runoff synthesized for all elevation bands. The program stores for every elevation band a value for each component of flow and each routing increment. The program maintains an inventory of snow cover area, soil moisture, snow accumulation, and all other values required for making the computation for the next period.

Digital elevation model (DEM) of the study area has been prepared from SOI contours and already shown in Chapter 4. For the preparation of the area-elevation curves, the basin has to be divided into a 10 number of elevation bands. The area of the catchment falling in each elevation band was measured and the area elevation curve of the basin was prepared. The area covered in each elevation band is given in Table 5.1 and area elevation curve is shown in Figure 5.2. In the beginning and end of the curve, elevation is almost increasing linearly with area. In the elevation bands of 3000-3600 m and 3600-4200 m, the curve is represented by a mild slope and the area covered is more in comparison of area covered in other elevation bands.

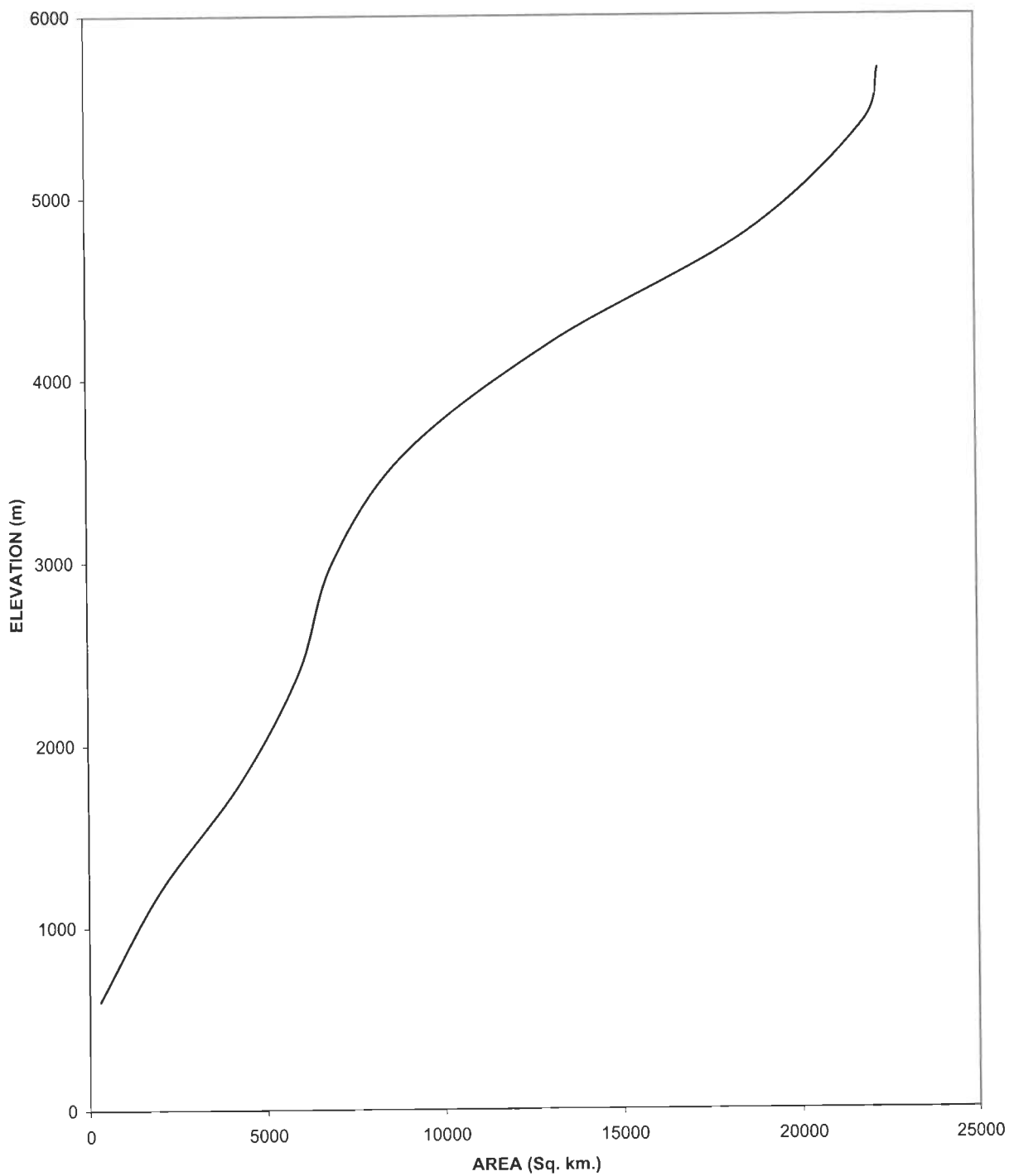


Figure 5.2 : Area elevation curve for Satluj basin upto Bhakra

TABLE 5.1 : Satluj basin area covered in different elevation band

Zones	Elevation range (m)	Area (km ²)
1.	<600	308.8
2.	600-1200	1702.6
3.	1200-1800	2283.2
4.	1800-2400	1660.0
5.	2400-3000	955.6
6.	3000-3600	2073.7
7.	3600-4200	4121.9
8.	4200-4800	5460.3
9.	4800-5400	3275.8
10.	>5400	433.3

5.3.2 Meteorological Characteristics

5.3.2.1 Precipitation data and distribution

Some of the most significant data-related problems in mountainous basins are associated with the measurement of the amount and spatial distribution of precipitation. WMO (1986) made a comparative study of various snowmelt models and it was concluded that precipitation distribution assumptions and the determination of the form of precipitation were the most important factors in producing the accurate estimates of runoff volume. The distinction between rain and snow for each elevation band is very important for all snowmelt models because precipitation falling in the form of rain and snow behaves differently in terms of contribution to the streamflow. The contribution of rain to the streamflow is faster than that of snow because snow is stored in the basin until it melts, whereas rain almost immediately contributes to streamflow. On any elevation band, the precipitation may fall as rain or snow. Rain on a elevation band or a part of the band is

added directly to the moisture input. Snow is added to the previously accumulated snow, if any. The new snow that falls on the previously snow covered area becomes part of the seasonal snowpack and its effect depends on the condition of the snowpack. The rain falling over a cold snowpack in the early melt season, will be frozen in the snowpack and would not be available immediately to the runoff. It would melt when favourable atmospheric and snowpack conditions are available. But if the rain is falling over the ripe snowpack, it is transferred through the snow layer and contributes to runoff.

For the study basin (Satluj basin) daily precipitation data were available at ten raingauge stations within the study area, namely, Bhakra, Berthin, Kahu, Kasol, Suni, Rampur, Kalpa, Rakchham, Namgia and Kaza. The location of raingauge and temperature stations is shown in Figure 3.2 in Chapter 3. Following the trends of hydrographs, the period of November to October has been considered as water year in this study. For different elevation bands, data of different stations have been used as shown in Table 5.2. The locations and altitude of each station is already given in Chapter 3. The raingauge has been assigned to the different bands on the basis of its proximity to the respective band according to altitude of the station. For the second band, the rainfall data was available for the four stations at about same elevations. Therefore for this band, the average value of these four stations viz. Suni, Berthin, kasol and Kahu have been taken. The typical rainfall distribution over the basin for the year 1985-86 is shown in Figure 5.3.

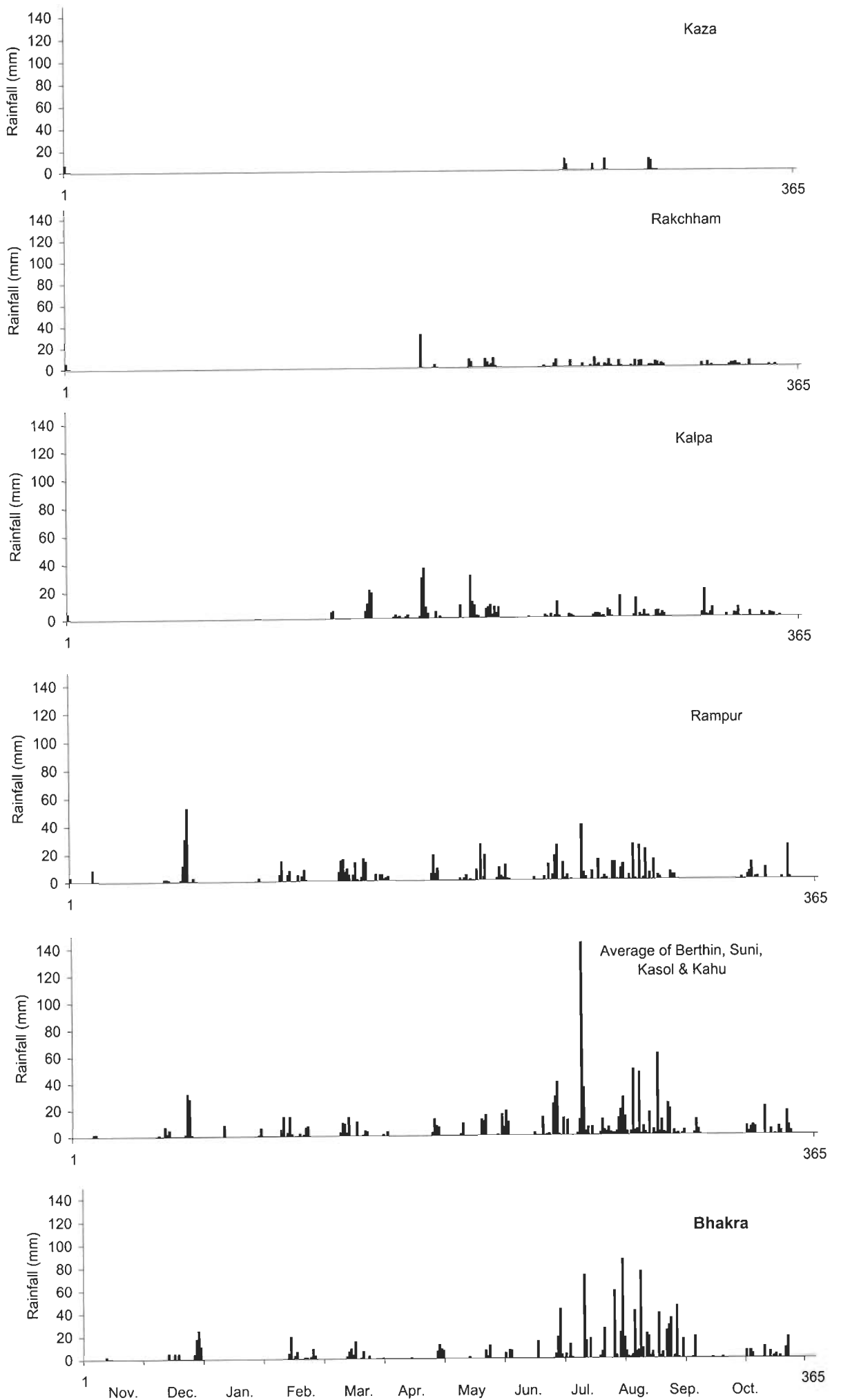


Figure 5.3 : Plot of daily rainfall data for some stations in Satluj basin for the year 1985-86

TABLE 5.2 : Raingauge and temperature stations used for different bands

Band	Elevation range(m)	Raingauge station	Temperature station
1.	<600	Bhakra	Bhakra
2.	600-1200	Average of Berthin, Suni, Kasol and Kahu	Bhakra
3.	1200-1800	Rampur	Rampur
4.	1800-2400	Rampur	Rampur
5.	2400-3000	Kalpa	Kalpa
6.	3000-3600	Rakchham	Rakchham
7.	3600-4200	Rakchham	Rakchham
8.	4200-4800	Kaza	Kaza
9.	4800-5400	Kaza	Kaza
10.	>5400	Kaza	Kaza

5.3.2.2 Temperature data – Space and time distribution

Snowmelt runoff computations in the mountain regions require reliable temperature data for all the elevation bands of the basin. Usually the temperature data are available at few locations in the basin. These point values are extrapolated or interpolated to the mid elevation of each elevation band using a predefined temperature lapse rate in the model. Lapse rates are known to be quite variable, ranging from high values of about the dry adiabatic lapse rate to low values representing inversion conditions. For example, during continuous rainstorm conditions the lapse rate will approximate the saturated adiabatic rate, whereas under clear sky, dry weather conditions, the lapse rate during the warm part of the day will tend to the dry adiabatic rate. During the night, under clear sky conditions, radiation cooling will cause the temperatures to fall to the dew point temperature, and this is particularly true for a moist air mass. As a result, night-time lapse rates under clear skies

will tend to be quite low, and at times even zero lapse rates will occur. The trends of variation of temperature show that a complete and detailed representation of the variability of temperature lapse rate is not possible in a snowmelt runoff model. But in case temperature data are available at least at two stations, one near the outlet of the basin and one near the highest elevation, somewhat realistic temperature lapse rate could be computed and used for extrapolation/interpolation in the various bands. When data of only one station is available, a lapse rate has to be assumed in order to extrapolate temperature from base station to the appropriate mean hypsometric elevation.

The daily temperature in the various elevation bands have been calculated by using the temperature lapse rate approach, by extending data from the base station by the following equation,

$$T_{ij} = T_{i,\text{base}} - \delta (h_j - h_{\text{base}}) \quad (5.1)$$

Where,

T_{ij} = daily mean temperature on i^{th} day in j^{th} zone ($^{\circ}\text{C}$)

$T_{i,\text{base}}$ = daily mean temperature ($^{\circ}\text{C}$) on i^{th} day at the base station

h_j = zonal hypsometric mean elevation (m)

h_{base} = elevation of base station (m)

δ = Temperature lapse rate in $^{\circ}\text{C}$ per 100 m.

The temperature lapse rate must be carefully selected and it should be indicative of the mountainous region where the basin is located, on some kind of prior climatic knowledge. Generally the temperature is lapsed at $6.5^{\circ}\text{C}/\text{km}$ or at a specified rate to the mean hypsometric elevation of each elevation band.

For the study area (Satluj basin) daily maximum and minimum temperature were available for five stations viz. Bhakra, Rampur, Kalpa, Rakchham and Kaza. Mean temperature was computed and used in this study. As mentioned earlier the total basin was divided into ten elevation bands. For each band, a base station was assigned, as given in Table 5.2. For the corresponding bands, temperature was extrapolated/interpolated using the base station data. The temperature distribution is shown in Figure 5.4 for one year i.e. 1985-86. The mean temperature was then extrapolated to the respective elevation bands by a lapse rate of $0.65\text{ }^{\circ}\text{C}/100\text{ m}$ (Singh, 1991).

5.3.2.3 Snow cover

The snow cover area has to be estimated from the satellite imageries / digital data as information is not available on the extent of the snow covered area for different months during the snowmelt period. In the snow melt runoff computations, attention is usually focussed on determining the snowmelt rate. But the continuously changing snow cover in the basin may overshadow the improved accuracy. The changing snow cover may be of little importance in flat areas with uniform snow cover or for forecasting only the total seasonal snowmelt volume. On the other hand, it plays a dominant role in the mountainous catchments where snow cover area gradually decreases from maximum to minimum. In catchments with rugged terrain and sharp mountain ridges, the evaluation by planimetry is impossible as the snow cover consists of numerous dispersed snow patches.

The snow cover area in the study basin for the years 1986-1993 was determined using Landsat and IRS-1A/1B (LISS-I) satellite data. This is given and shown in the form of Figures already in Chapter 4. For modelling of streamflow, data of some recent years have been used and snow covered data was needed for these years. Therefore, the snow cover area for the years 1997-1999 have been taken from IRS-1C/1D WiFS sensor.

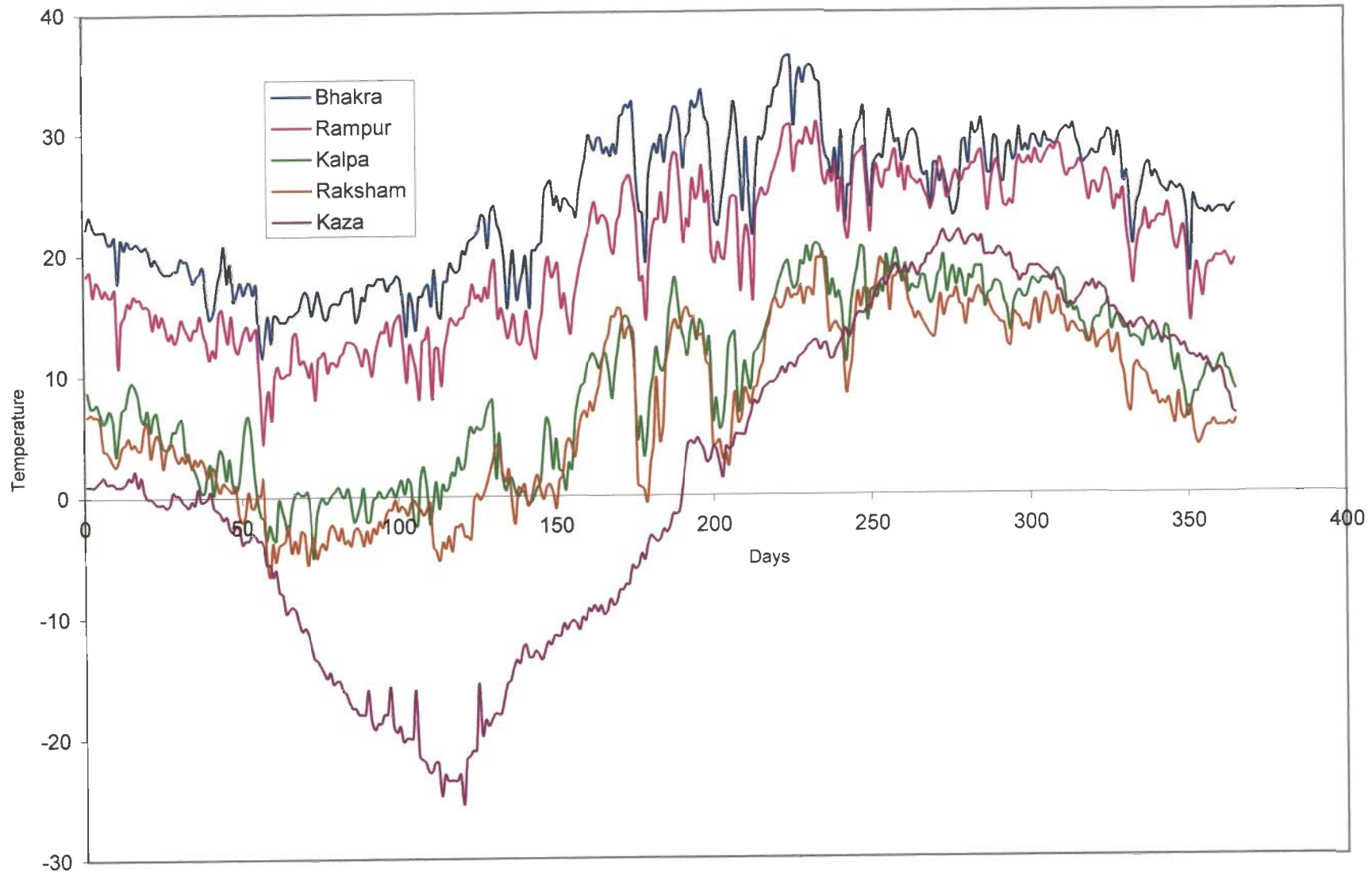


Figure 5.4 : Daily temperature distribution for some stations in Satluj basin for the year 1985-86

However, this sensor is having coarse resolution but for the large catchment this can be successfully applied. In this study, data for these three years have been taken and processed in the similar way as processed for IRS LISS I data. The snow cover area maps have been using ERDAS IMAGINE and the area has been estimated. The snow cover area in each elevation band is plotted against the elapsed time to construct the depletion curves for the various elevation bands in the basin. For the snowmelt runoff computations on a daily basis, the daily snow cover values were taken from these depletion curves. The snow cover depletion curves vary significantly from year to year and, therefore, the snow cover depletion curve has to be made separately for each year under consideration to be used as input to the model. The depletion curves prepared for the study basin have been shown in figure 5.5 and 5.6 for the period 1986-93 and 1997-1999, respectively.

In order to simulate runoff on the daily scale from the basin, daily snow cover area for each band was used as input to the model. For calculating this, snow cover map has been overlaid on elevation band maps. Then for each year snow cover in each elevation band for the available dates was calculated. Using this information alongwith the snow cover depletion curves, snow cover area in each elevation band on daily basis for each year has been calculated. For one-year i.e. 1985-86, the variation of snow covered area in each elevation band, is shown in Figure 5.7. Bands 1,2 and 3 are having no snow cover and therefore not included in this figure.

5.3.2.4 Rain on snow

Rain-on-snow events, in which snowmelt may be limited, are also hydrologically important (Colbeck, 1975; Berg et al.,1991). Most of the largest floods in British Columbia, Washington, Oregon and California have been associated with rain-on-snow (Kattelmann 1987; Brunengo, 1990). Archer et al. (1994) reported that in Britain more frequently

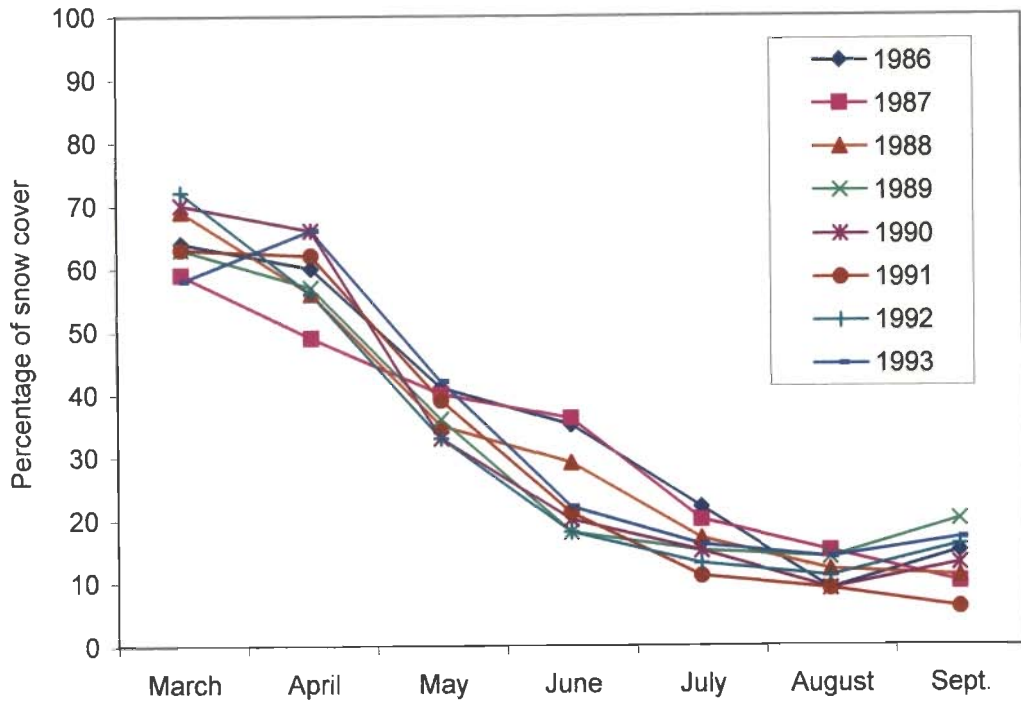


Figure 5.5 : Snow cover depletion curves for Satluj basin for the years (1986-93)

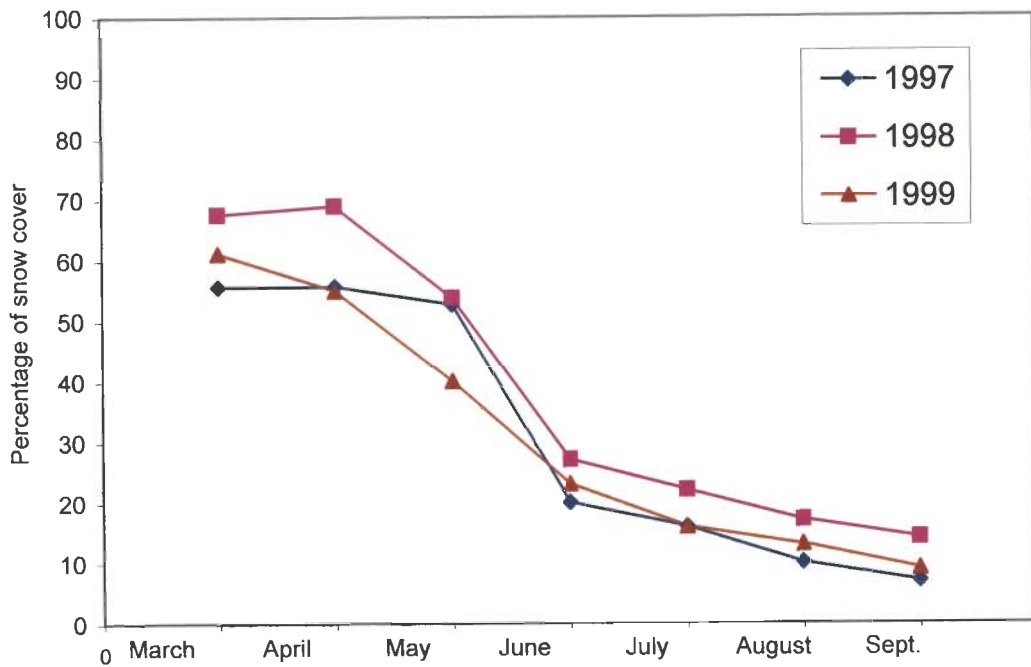


Figure 5.6: Snow cover depletion curves for Satluj basin for the years (1996-99)

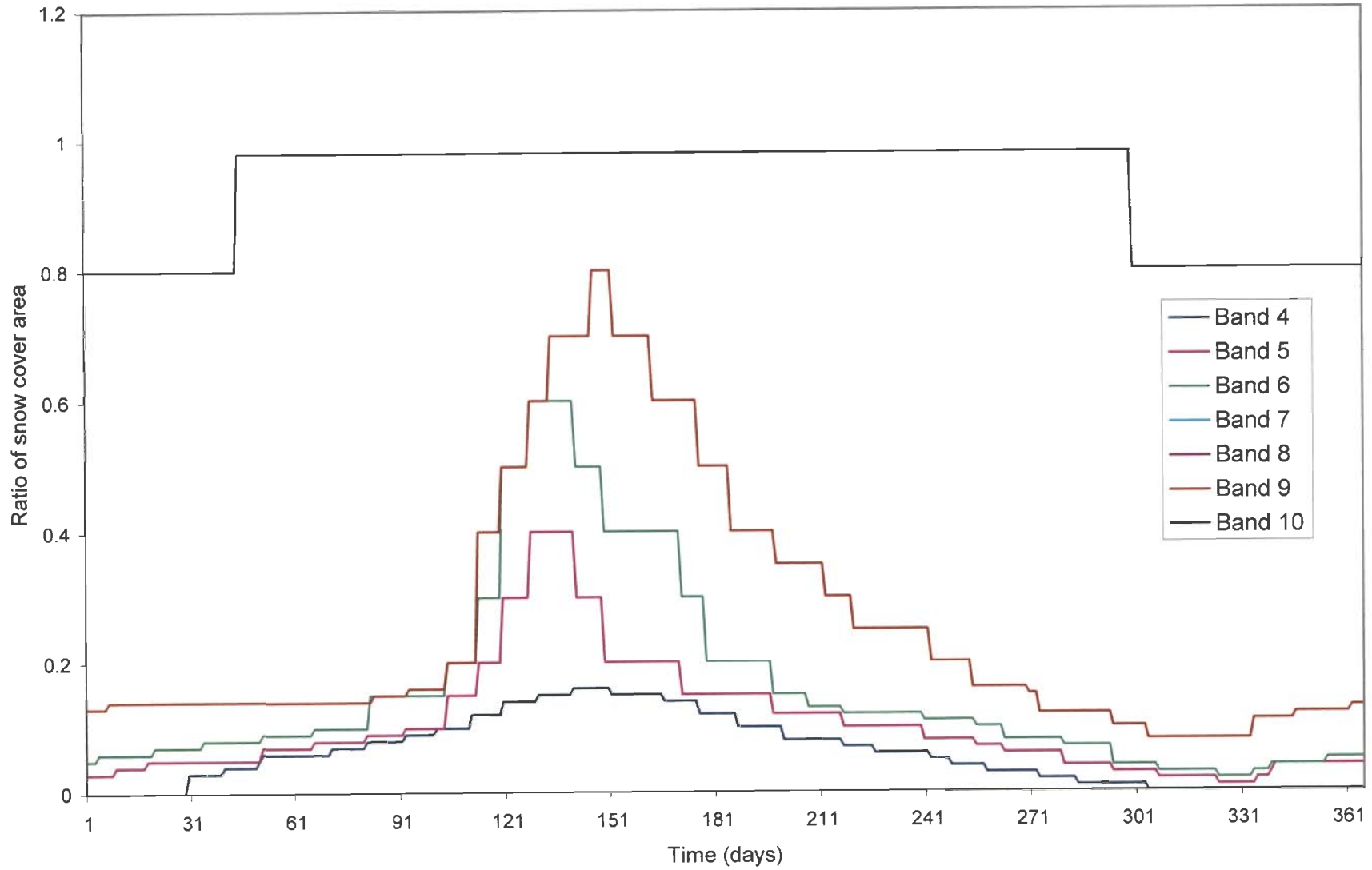


Figure 5.7 : Fraction of snow cover area in different elevation bands of Satluj basin for the water year 1985-86

flooding results from combination of melting snow and rainfall. A good rainfall occurs in the high altitude regions of Himalayas during the active melting period (Singh et al., 1995; Singh and Kumar, 1996). Further, rain-on-snow events are also considered a major cause in the release of avalanches. Introduction of liquid water into snow weakens the bond between grains and alters the snow texture, which results in reduced mechanical strength of the snowpack. Various studies have been carried out to understand the role of rain in triggering avalanches in maritime climates (Conway et. al, 1988, Heywood, 1988; Conway and Raymond, 1993).

When rain falls on the snowpack it is cooled to the temperature of snow. The heat transferred to the snow by rainwater is the difference between its energy content before falling on the snow and its energy content on reaching thermal equilibrium within the snowpack. For snowpacks isothermal at 0°C, the release of heat results in snowmelt, while for the colder snowpack this heat tends to raise the snowpack temperature to 0 °C. In case the snowpack is isothermal at 0°C, the melt occurring due to rain is computed by

$$Q_p = \rho_w C_p (T_r - T_s) P_r / 1000 \quad (5.2)$$

where,

Q_p = energy supplied to the pack by rain ($\text{kJ m}^{-2} \text{d}^{-1}$)

ρ_w = density of water (1000 kg m^{-3})

C_p = specific heat of water ($4.20 \text{ kJ kg}^{-1} \text{ } ^\circ\text{C}^{-1}$)

T_r = temperature of rain ($^\circ\text{C}$)

T_s = temperature of snowpack ($^\circ\text{C}$)

P_r = depth of rain (mm d^{-1})

Substituting the values of various parameters in the above equation, it reduces to

$$Q_p = 4.2 T_r P_r \quad (5.3)$$

Usually, rain temperature is considered equal to the air temperature on that day.

The melt caused by this energy is computed as

$$M_r = Q_p / (\rho h_f B) \quad (5.4)$$

where,

m_r = melt caused by the energy supplied by rain (mm d^{-1})

h_f = latent heat of fusion of water (335 kJ kg^{-1})

B = thermal quality of snow (0.95-0.97)

5.3.2.5 Degree days

Air temperature expressed as degree-days are used in snow melt computations as an index of complex energy balance tending to snow melt. A degree-day, in its broad sense, is a unit expressing the amount of heat in terms of the persistence of temperature for 24-hour period of $^{\circ}\text{C}$ departure from a reference temperature. The simplest and most common expression relating snowmelt to temperature index is,

$$M = D(T_i - T_b) \quad (5.5)$$

where,

M = depth of melt water (mm) produced in a unit time

D = degree-day factor ($\text{mm } ^{\circ}\text{C}^{-1} \text{ d}^{-1}$)

T_i = index air temperature ($^{\circ}\text{C}$)

T_b = base temperature (usually, 0°C)

Although temperature and other hydrologic conditions vary continuously throughout the day, daily mean temperature is the most commonly used index of temperature for snowmelt. Where only maximum (T_{\max}) and minimum temperatures (T_{\min}) are available, the number of degree-days is computed as

$$T_i = T_{\text{mean}} = (T_{\max} + T_{\min})/2 \quad (5.6)$$

At stations where hourly readings are made, the number of degree-days for each 24 hour period is determined by summing the hourly temperatures and dividing by 24. Further 0°C base temperature is generally used in computation of degree-days. This follows from the idea that most snowmelt results directly from the transfer of heat from the air in excess of 0°C . Some investigators have also used only T_{\max} for computing the degree-days. In that case a lower value of D_f is used along with a lower value of base temperature.

5.3.3 Model Parameters

5.3.3.1 Degree-day factor

The degree-day factor, D , is an important parameter for snowmelt computation and converts the degree-days to snow melt expressed in depth of water. D is influenced by the physical properties of snowpack and because these properties change with time, therefore, this factor also changes with time. The seasonal variation in melt factor is well illustrated by the results obtained from the study reported by Anderson (1973). The lower value being in the beginning of melt season and higher towards the end melt season. A wide range of a values has been reported in the literature with a generally increase as the snowpack ripens. For example, Garstaka (1964) reported extreme values of D_f as low as $0.7 \text{ mm } ^{\circ}\text{C}^{-1} \text{ d}^{-1}$ and as high as $9.2 \text{ mm } ^{\circ}\text{C}^{-1} \text{ d}^{-1}$. Yoshida (1962) reported the values of D to be between 4.0-8.0

$\text{mm}^{\circ}\text{C}^{-1}\text{ day}^{-1}$, depending on the location, time of year and meteorological conditions. Singh and Kumar (1996) determined the D factor by monitoring a known snow surface area of the snow block within the snowpack at an altitude of about 4000m in the western Himalayan region in the summer. The mean daily value of the D was computed to be $5.94\text{ mm }^{\circ}\text{C}^{-1}\text{ day}^{-1}$, while for a dusted block it increased to $6.62\text{ mm }^{\circ}\text{C}^{-1}\text{ day}^{-1}$. In glacierized basins, the degree-day factor usually exceeds $6\text{ mm }^{\circ}\text{C}^{-1}\text{ d}^{-1}$ towards the end of summer when ice becomes exposed (Kotlyakov and Krenke, 1992). As discussed above that D changes with season, therefore, when using degree-day approach, changes in D with season should be taken into account. In the present study in the starting of melt season for every month low value of degree-day factor has been taken and it go on increasing till the end of melt season i.e. the month of September. The range of the values of degree-day factors used in this study is given Table 5.3.

5.3.3.2 Form of precipitation

The distinction between rain and snow for each elevation band of the basin is very important for all the snow melt models because precipitation falling in the form of rain or snow behaves differently in terms of contribution to the streamflow. The contribution of rain to the streamflow is faster than that of snow because snow is stored in the basin until it melts whereas rain contributes almost immediately. Precipitation in each period is assumed to fall as snow above the freezing elevation and rain below that elevation. On any one of the bands, precipitation might fall as rain, as snow, or a combination of the two. Rain on a band or part of a band is added directly to moisture input. Snow is added to the previous accumulation, if any. Accumulated snow is assumed to cover the entire band. Each band must be either snow free or fully snow covered. Further, the response of snows fallen over the accumulated snow or snows free area, is different. The new snow that falls over the

previously snow covered area becomes the part of the previous seasonal snowpack and its effect on runoff depends on the condition of the snowpack. For example, rain falling over the cold snowpack, like in the early melts season, will be frozen in the snowpack and it is not immediately available for runoff. It melts when favourable atmospheric and snowpack conditions are available. But rain falling over the ripe snowpack is transferred through the snow layer and becomes available to contribute to runoff. The new snow falling over the snow free area is considered as precipitation to be added to snowmelt, with delayed effect until the next warm day.

For this purpose a critical temperature is specified in the model to determine whether measured precipitation is rain or snow. This is of particular importance for models, which simulate the build-up of snow cover from precipitation data. From direct observations, T_{crit} is generally higher than 0°C as found by Charbonneau et al. (1981). Therefore, value of T_{crit} is usually selected slightly above the freezing point and may vary from basin to basin. The value of $T_{crit} = 2^{\circ}\text{C}$ is considered in this model. It indicates that

if $T_m \geq 2^{\circ}\text{C}$, all precipitation is rain,

if $T_m \leq 0^{\circ}\text{C}$, all precipitation is snow,

if $T_m \geq 0^{\circ}\text{C}$ and $T_m \leq 2^{\circ}\text{C}$, precipitation will be considered as a mixture of rain and snow and their proportion will be worked out in the following way:

$$\text{Rain} = (T_m / T_{crit}) * P \quad (5.7)$$

$$\text{Snow} = P - \text{Rain} \quad (5.8)$$

where P is the total observed precipitation.

5.3.3.3 Runoff Coefficients

The runoff coefficient takes care of the losses, i.e., the difference between the available water input and outflow from the basin. The average value of runoff coefficient

for a basin is represented by the ratio of annual runoff to annual precipitation. The runoff coefficient is likely to vary throughout year as a result of changing vegetation and soil moisture, which can be varied accordingly in the model. At the start of the snowmelt season, losses are usually very small because these are limited to the evaporation from the snow surfaces at higher elevations. But as the snowmelt season progresses, when some of the soil becomes exposed due to the melted snow and when some vegetation grows, more losses must be expected due to evapotranspiration and interception. The model uses different runoff coefficients for rain and snow, i.e., C_r for rain and C_s for snow respectively. The runoff coefficient for snowmelt is usually higher than that for rainfall. The runoff coefficient varies from month to month, throughout the season in a basin. The selection of the value of runoff coefficients requires first hand knowledge of the basin and its hydrologic behavior under different hydro-meteorological conditions.

Table 5.3: Parameter values used in calibration of model

S.No.	Parameter	Symbol	Value
1.	Degree-day factor	D	1.0 – 4.0 mm.°C ⁻¹ .day ⁻¹
2.	Runoff coefficient for rain	C_r	0.40 - 0.70
3.	Runoff coefficient for snow	C_s	0.50 – 0.80
4.	Temperature lapse rate	δ	0.65°C/100 m
5.	Critical temperature	T_c	2°C
6.	Number of linear reservoirs for snow free area	N_r	2
7.	Number of linear reservoirs for snow covered area	N_s	1
8.	Number of linear reservoirs for subsurface flow	N_b	1

The above description gives detail on the various input data/parameters used to compute the depth of snowmelt and rainfall runoff in the basin. The losses to the runoff

depth as computed using runoff coefficients, were the input to the subsurface flow regime. The computation of surface runoff as well as subsurface runoff is given in the following sections.

5.4 COMPUTATION OF DIFFERENT RUNOFF COMPONENTS

The streamflow from a snowfed river has three components namely, runoff from the snow covered area, snow free area and baseflow. The computation of runoff for each component was made for each elevation band separately and then output from all the bands was integrated to provide the total runoff from the study basin.

5.4.1. Surface runoff from snow covered area

The runoff from snow covered area consists mainly of (i) snowmelt caused due to temperature, (ii) melt water due to heat transfer to the snow under rainy condition and (iii) runoff from rain itself falling over snow covered area. These three sources of runoff from snow covered area are described below.

(a) Snowmelt for each band of the basin due to temperature was computed using degree-day approach. In this approach degree-day factor is used to convert degree-days to snowmelt expressed in depth of water.

$$M_{s,i,j} = C_{s,i,j} D_{f,i,j} T_{i,j} S_{c,i,j} \quad (5.9)$$

where,

$M_{s,i,j}$ = snowmelt in terms of depth of water on i^{th} day for j^{th} band (mm)

$C_{s,i,j}$ = coefficient of runoff for snow on i^{th} day for j^{th} band (value less than one)

$D_{f,i,j}$ = degree-day factor on i^{th} day for j^{th} band ($\text{mm} \cdot ^\circ\text{C}^{-1} \text{d}^{-1}$)

$T_{i,j}$ = temperature on i^{th} day for j^{th} band ($^\circ\text{C}$)

$S_{c,i,j}$ = Ratio of snow covered area to the total area of j^{th} band on i^{th} day

(b) Runoff depth due to snowmelt from the heat transferred to snow by the rain falling on the snowpack. The depth of snowmelt caused by rain in a band is given by,

$$M_{r,ij} = 4.2 T_{ij} P_{ij} S_{c,ij} / 3335 \quad (5.10)$$

where,

$M_{r,ij}$ = snowmelt in terms of depth of water due to rain on snow on i^{th} day for j^{th} band (mm)

P_{ij} = rainfall on snow on i^{th} day for j^{th} band (mm)

(c) Runoff depth from rain falling over snow covered area is given by,

$$R_{s,ij} = C_{s,ij} P_{ij} S_{c,ij} \quad (5.11)$$

In the above calculations for computation of runoff from rain, the coefficient C_s is considered (not C_r), because the runoff from rainfall falling on snow behaves like the runoff from melting of snow.

The total discharge from the snow covered area is computed by summation of the runoff from each elevation band on a daily basis. Thus, discharge from the snow covered area for all the bands is given by

$$Q_{sca} = \sum_{j=1}^n (M_{s,ij} + M_{m,ij} + R_{s,ij}) A_{sca,ij} \alpha \quad (5.12)$$

where, n = the total number of bands

α = a factor used to convert the runoff depth into discharge or in other words conversion of the depth units to $\text{m}^3 \cdot \text{s}^{-1}$. This conversion factor comes out to be $1000/86400$ or 0.0116.

$A_{sca,ij}$ = Snow covered area in the j^{th} band on the i^{th} day

5.4.2 Surface runoff from snow free area

The source of surface runoff from the snow free area is rainfall. Like snowmelt runoff computations, runoff from snow free area was also computed for each band. The runoff depth from the rainfall occurring over snow free area is given by,

$$R_{f,ij} = C_{r,ij} P_{ij} S_{f,ij} \quad (5.13)$$

where,

$C_{r,ij}$ = coefficient of runoff for rain on i^{th} day for j^{th} band (value less than one)

P_{ij} = rainfall on snow on i^{th} day for j^{th} band (mm)

$S_{f,ij}$ = Ratio of snow free area to the total area of j^{th} band on i^{th} day. The ratio $S_{f,ij}$ is calculated by subtracting the ratio $S_{c,ij}$ from 1, i.e., $S_{f,ij} = (1 - S_{c,ij})$

The runoff depth from the snowfree area is converted to discharge in cumecs in the same way as for the snow covered area as given above (equation 5.12). The runoff from snow free area for all the bands is thus given by

$$Q_{sfa} = \sum_{j=1}^n R_{f,ij} A_{sfa,ij} \alpha \quad (5.14)$$

where, $A_{sfa,ij}$ = Snow free area in the j^{th} band on the i^{th} day

5.4.3 Estimation of subsurface runoff

The balance from the total snowmelt and rainfall after accounting for surface runoff, contributes to the groundwater through infiltration and appears at the outlet of the basin with a delayed effect through a groundwater reservoir. The depletion of this groundwater storage also takes place due to evapotranspiration and percolation of water to deep groundwater zone or inactive zone. It is assumed that 50% of the water, which percolates down to shallow groundwater contribute to base flow. The remaining 50 % is assumed to

account for loss from the basin due to evapotranspiration and percolation to deep groundwater.

The depth of runoff contributing to baseflow from each band is therefore, given by

$$R_{b,ij} = 0.5 * [(1-C_{r,ij}) * R_{r,ij} + (1-C_{s,ij}) * M_{t,ij}] \quad (5.15)$$

where, $M_{t,ij} = M_{s,ij} + M_{r,ij} + R_{s,ij}$

The sub surface runoff was computed by multiplying this depth with conversion factor α area, and given as follows:

$$Q_b = \sum_{j=1}^n R_{b,ij} A_{ij} \alpha \quad (5.16)$$

where, A_{ij} is the total area and it is sum of $A_{sca,ij}$ and $A_{sfa,ij}$

5.4.4. Total runoff

The total runoff from the basin is calculated by adding the different components of runoff for each day, expressed as follows:

$$Q = Q_{sca} + Q_{sfa} + Q_b \quad (5.17)$$

As discussed above, the direct runoff is considered to result from overland or near surface flow, while baseflow is regarded as being a result of groundwater contribution into the stream. Infact, the contribution to baseflow starts only after the topsoil is saturated. For this purpose a soil moisture index (SMI) has been considered in the present study. The routing of surface and subsurface runoff has been carried out separately and described in the following sections.

5.5 ROUTING OF DIFFERENT COMPONENTS OF RUNOFF

5.5.1 Routing of surface runoff

The catchment routing refers to the transformation of input to the basin either in the form of rainfall or snowmelt to the outflow from the basin. The flows emerging out from the snow covered area and the snow free area are routed through a cascade of linear reservoirs. The linear reservoir cascade routing method is one of the most popular and frequently used method for catchment routing (Singh and Singh, 2001). Because of the difference in response from snow covered area and snow free area, the routing of these two components were done separately. When inflow is passed through a linear reservoir, the peak and time base characteristics of the outflow are influenced according to the storage characteristics of the reservoir. In case, the inflow is passed through a series of linear reservoirs with equal storage coefficient, an integrated effect of all the reservoirs will be observed in the outflow from the last reservoir. The outflow of the upper reservoir is routed through the next reservoir. Considering n reservoirs in series, the outflow from the second reservoir is the inflow to the third reservoir and so on. The outflow from the n^{th} reservoir represents the response of catchment in terms of outflow. Thus, each reservoir plays its role in affecting attenuation and lag characteristics of the outflow. The analytical version of the cascade of equal linear reservoirs is known as the 'Nash Model'. In order to derive the general routing equation for a series of n reservoirs, the first outflow from the first reservoir is obtained as follows.

A spatially lumped form of the continuity equation is expressed as

$$\frac{dS}{dt} = I - Q \quad (5.18)$$

where S is the storage or volume of water within the reach, I is the inflow rate, Q is the outflow rate, dS/dt is the volume of storage, k and x are routing parameters. It is assumed that at $t=0$, $I=Q$. Another relation between storage and discharge is hypothesized. This

relation is called the storage equation, which may be linear or non-linear. A commonly used linear form of storage-discharge relationship may be written as

$$S=kQ \quad (5.19)$$

where storage S is proportional to Q with proportionality constant k (linear storage coefficient). The discretised form of Equation (5.17) can be written as

$$\frac{(S_2 - S_1)}{\Delta t} = \frac{(I_1 + I_2)}{2} - \frac{Q_1 + Q_2}{2} \quad (5.20)$$

wherein subscript 1 and 2 refer to the conditions at the start and end of time interval Δt , respectively and Δt is the routing period or discretization time interval. For the linear reservoir case:

$$S_1 = k Q_1 \quad (5.21)$$

$$S_2 = k Q_2 \quad (5.22)$$

Substituting Equations (5.21) and (5.22) in (5.20) and solving for Q_2 gives the following equation:

$$Q_2 = C_0 I_2 + C_1 I_1 + C_2 Q_1 \quad (5.23)$$

$$\text{where, } C_0 = \frac{\Delta t / k}{2 + \Delta t / k} \quad (5.24)$$

$$C_1 = C_0 \quad (5.25)$$

$$C_2 = \frac{2 - \Delta t / k}{2 + \Delta t / k} \quad (5.26)$$

C_0, C_1, C_2 are the routing coefficients and the sum of these coefficients equals unity, i.e.

$$C_0 + C_1 + C_2 = 1$$

In the case of a cascade of reservoirs, the output of one reservoir becomes input to the next reservoir. Thus, outflow from the n^{th} reservoir can be expressed as

$$Q_{n+1,j+1} = C_0 Q_{n,j+1} + C_1 Q_{n,j} + C_2 Q_{n+1,j} \quad (5.27)$$

where n and j represent the reservoir number and time index, respectively. Because for a linear reservoir, $C_0 = C_1$, the equation representing the outflow from the n^{th} reservoir can be written as

$$Q_{n+1,j+1} = 2C_1 \bar{Q}_{n,j+1} + C_2 Q_{n+1,j} \quad (5.28)$$

where

$$\bar{Q}_{n,j+1} = \frac{Q_{n,j+1} + Q_{n,j}}{2} \quad (5.29)$$

Equation (5.29) was used for the catchment routing in the model. This method was applied to the routing of different components of streamflow separately and then the total outflow from the basin was computed by summing the different routed components of runoff.

For a rainfed river basin, hydrological behaviour of the basin depends upon the extent of snow covered area (SCA) of the basin. In the beginning of the melt, a higher extent of SCA provides a delayed response of the runoff, which improves with the advancement of the melt season. The basic reason for this is that the melt water first infiltrates through snowpack and flows as overland flow under the snowpack before emerging as outflow from the basin. Thus, in the beginning the depth and extent of the snow covered area is higher therefore it provides much delayed effect. At the same time in the beginning of the melt, snow free area (SFA) is less therefore time of concentration for rainfall from the basin is lower, representing a fast response due to lower extent of SFA. As

melt season progresses, the SCA of the basin reduces and SFA increases and therefore they are complementary to each other. Finally with the increase in snowmelt, time of concentration for SCA reduces whereas for SFA it increases. Keeping in view the different response of snow melt and rain from SCA and SFA and their variations with time, it is considered appropriate to split the basin into two parts namely SCA and SFA and handle each part separately for computation of runoff from these parts. Therefore for routing the surface runoff, the catchment is considered as divided into two parts, i.e., snow covered area and the snow free area. Each part is then conceptualized as a cascade of linear reservoirs. The storage coefficients for the SFA and for the SCA are assumed to be functions of snow free area and effective snow covered area respectively. In case of k_s the effective snow cover area was considered instead of total snow covered area. The effective snow cover is only area of total snow cover area, which is contributing to snowmelt. Effective snow covered area would be less than or equal to the total snow cover area. The total snow cover area, snow free area and effective snow cover area are shown in Figure 5.8. As discussed above, the snow cover and snow free area vary throughout the period. In order to cater for the variable area, the variable storage coefficients were considered. It is achieved by relating the storage coefficients for the snow cover as well as snow free area in the nonlinear form as follows.

$$k_r = a_r (A_{sf})^{br} \quad (5.30)$$

$$k_s = a_s (A_{sc})^{bs} \quad (5.31)$$

where,

k_r = storage coefficient for the snow free area

k_s = storage coefficient for the snow covered area

A_{sf} = total snow free area in the basin

A_{sc} = total effective snow covered area in the basin

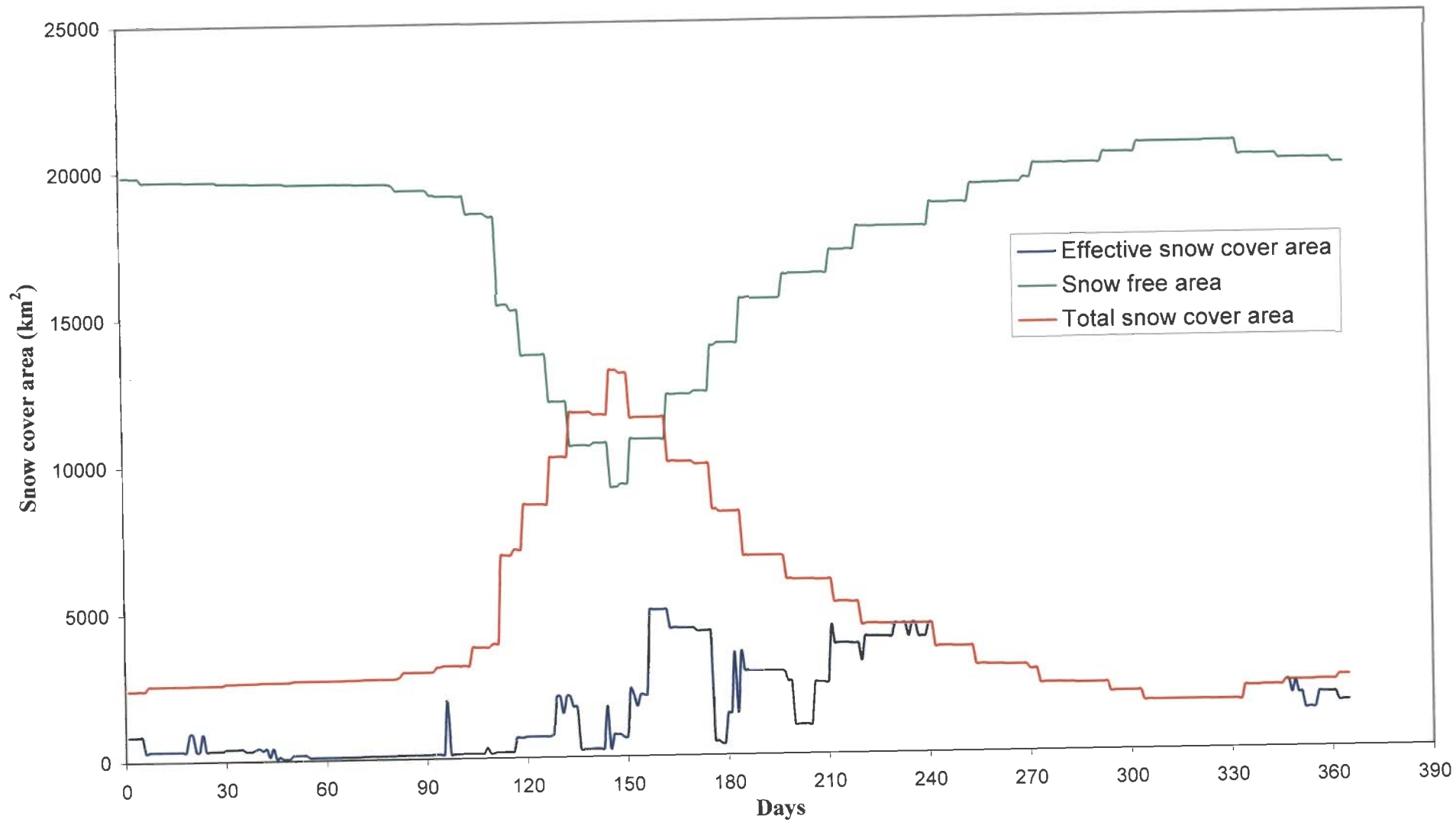


Figure 5.8: Time distribution of snow cover and snow free area for the water year 1985-86

a_r and b_r = model parameters for snow free area

a_s and b_s = model parameters for effective snow covered area

Such relationships are possible because of the trend of removal of snow from the basin. Total deletion of snow at a particular location is controlled by snow depth and climatic conditions. The depth of snow is less at the lower altitudes, while it is more at the higher altitudes. In the initial stage of melt season, as the temperature increases, snow from the lower part depletes at faster rate because of lower snow depth in the area. In other words snow covered area becomes snow free area at a faster rate. In the later part of the melt season snow line moves up in the basin where the depth of snow is more and therefore the depletion is slow as compared to lower part.

Model parameters (a_r , b_r , a_s and b_s) were optimised using given datasets as described in the section 5.6 on calibration of model.

5.5.2. Routing of subsurface runoff

When all the surface runoff discharges out from the drainage basin at its outlet, baseflow or subsurface flow sustains the flow in the stream. Subsurface flow is considered to be the relatively slow movement of the water comprising of surface runoff from the unsaturated zone to a stream channel. The source of subsurface flow is infiltrated water in excess of field capacity of soil. This excess water percolates to shallow groundwater zones or moves down slope at shallow depths from point of infiltration to some point of discharge above the water table. Deep percolation of groundwater represents the process whereby water enters deep groundwater reservoir, which does not contribute discharge at the catchment outlet and which may appear further downstream/may become part of deep inactive groundwater storage.

The subsurface runoff is routed in the same way as surface runoff, which is explained in the previous section. In case of subsurface routing, the storage coefficient (k_b) was determined using recession of streamflow data. Normally, baseflow is simulated considering routing through a single reservoir. Therefore, in the present study only one reservoir is considered for the routing of the subsurface flow. For determination of storage coefficient in case of subsurface flow, baseflow recession analysis has been carried out. There are many methods available for representation of recession of baseflow, but the exponential type is most widely used. If a basin is considered as a linear reservoir, the outflow discharge Q from the reservoir at time t will be a linear function of the volume of water stored in the reservoir, S that is already given in Equation (5.18). Again the same can be reproduced as follows:

$$S = kQ \quad (5.32)$$

where k is a recession coefficient for the drainage from the glacier reservoir. The continuity equation for the reservoir can be written as:

$$I - Q = \frac{dS}{dt} \quad (5.33)$$

where I is the input in the form of melt or liquid precipitation or both. From Equations (5.35) and (5.33) one contains:

$$I = Q + \frac{k \cdot dQ}{dt} \quad (5.34)$$

During a recession $I=0$, and therefore integration yields:

$$Q(t) = Q_0 e^{-t/k} \quad (5.35)$$

where, Q_0 is the discharge at time $t = 0$.

The parameter k is known as recession constant, or the depletion factor. By taking logarithm of this equation,

$$\ln Q = \ln Q_0 - \frac{t}{k} \quad (5.36)$$

Baseflow discharge Q can be plotted against time on semilog paper using the above equation. The coefficient k is considered as storage constant k_b . This value of k_b was determined by fitting a straight line to the plotted data. A part of rainfall/ snowmelt is accumulated in the subsurface reservoir, which is released slowly as baseflow.

In the present study, for determination of k_b , the long-term streamflow records were available. In order to compute the k_b , the trend of streamflow from the available record was examined for a number of years. It was noticed that minimum flow in the river was during winter period (November to March). The trend of streamflow shows a continuous recession of flow from the basin during this period, except for some anomalous change in the flow due to local thunder storms. The data so selected were apparently linear on the semi-log paper. Each baseflow period was then fitted to Equation (5.36) for computing the storage coefficient for subsurface flow.

The plots for three-year data are shown in Figure 5.9 alongwith the equation derived for each case. The storage coefficient obtained from these graphs is given in Table 5.4. The average value for all these years comes out to be approx. 110 and therefore in the present study a value of 110 days has been taken as storage coefficient for subsurface routing.

Table 5.4: Storage coefficient for subsurface flow for different years

S.No.	Year	k_b (days)
1.	1986	105
2.	1987	111
3.	1988	113

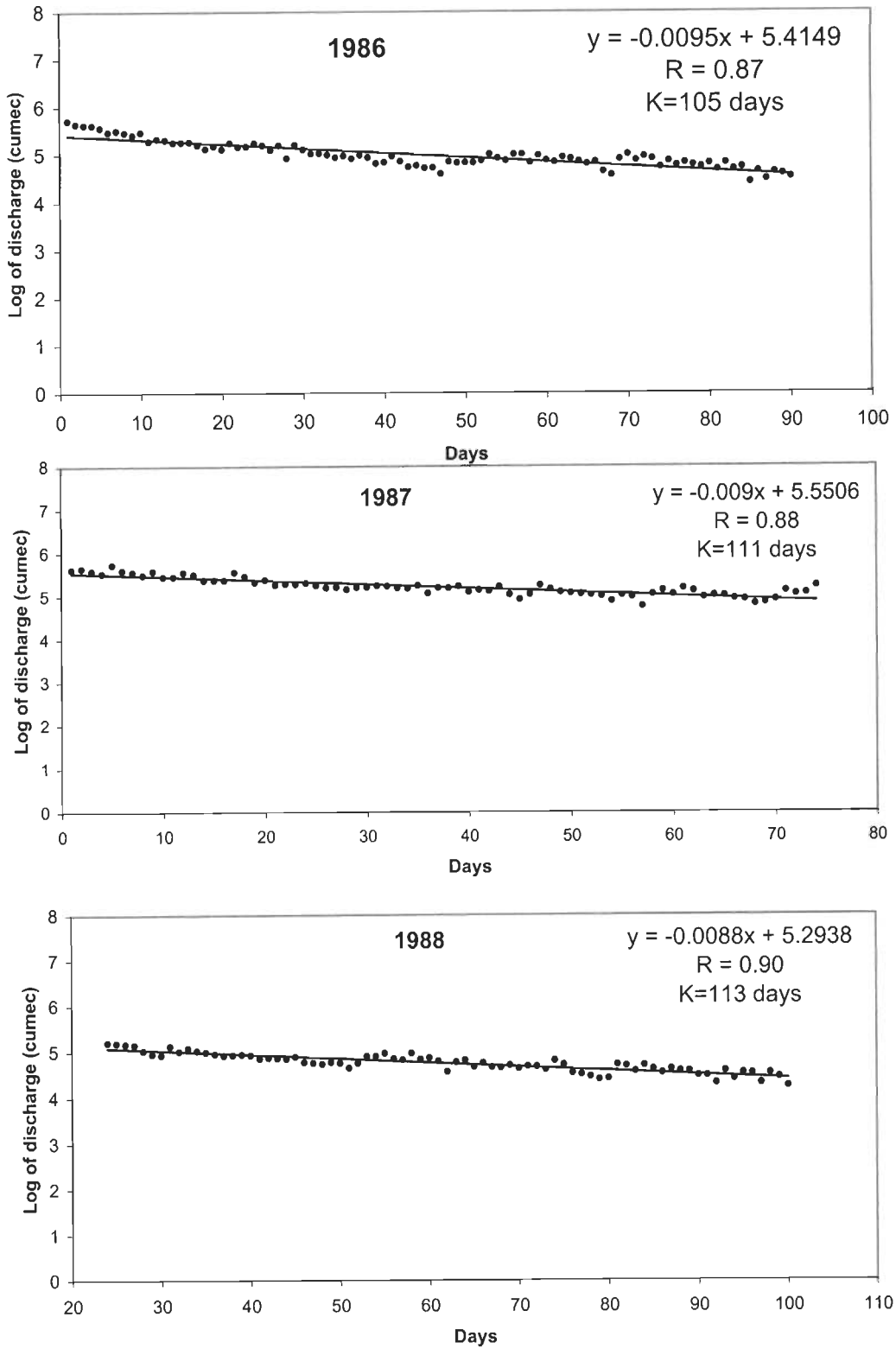


Figure 5.9 : Storage coefficient (K_b) for subsurface flow for different years

5.6 EFFICIENCY CRITERIA OF THE MODEL

Numerous statistical criteria are available for numerical evaluations of model accuracy in each single year, in a particular season of the year, or a sequence of years or seasons. In a study of snowmelt models, the World Meteorological Organisation (WMO, 1986) suggest several efficiency criteria that are particularly useful for snowmelt modelling. The most important criteria for model evaluation identified in the WMO study is the visual inspection of linear scale plots of simulated and observed hydrographs. Several numerical criteria are also identified as useful for model evaluation.

The model performance on a daily basis is commonly evaluated using the non-dimensional Nash-Sutcliffe 'R²' value (Nash and Sutcliffe, 1970) as given by the equation,

$$R^2 = 1 - \frac{\left\{ \sum_{t=1}^n (Q_0 - Q_e)^2 \right\}}{\left\{ \sum_{t=1}^n (Q_0 - \bar{Q}_0)^2 \right\}} \quad (5.37)$$

where,

R^2 = Nash-Sutcliffe coefficient of goodness of fit

Q_0 = daily observed discharge from the basin

Q_e = daily estimated discharge from the basin

\bar{Q}_0 = mean of observed discharge

n = number of days of discharge simulation

The value of Nash-Sutcliffe coefficient is analogous to the coefficient of determination and is a direct measure of the proportion of the variance of the recorded flows explained by the model.

The model performance on a seasonal basis can also be determined by computing the percentage volume difference between the measured and computed seasonal runoff as,

$$D_v = \frac{\left\{ \sum_{t=1}^n Q_o - \sum_{t=1}^n Q_e \right\} 100}{\left\{ \sum_{t=1}^n Q_o \right\}} \quad (5.38)$$

where, D_v is the percentage volume difference between the measured and computed seasonal runoff.

5.7 CALIBRATION OF MODEL

The model was calibrated using a daily data set of a period of 3 years (1985-86 to 1987-88). Various points involved in the calibration process of the model are discussed as follows.

5.7.1 Optimization

It is necessary to fit and test the model on observed data from the catchment to be simulated. Hydrologic models are generally calibrated using observed streamflow records at the outlet of a basin. Regardless of the technique used in fitting, the available data set is split into two parts: using one part to fit or calibrate the model and the second part as independent data set to test how the model performs in simulation mode (Blackie et al., 1985). In both fitting and testing the results suitable objective function is to be employed to assess when the degree of agreement between the observed, Q_o , and estimated flows Q_e , is acceptable. The most commonly used objective function F , is a simple summation of squares of residuals and for acceptable fit minimisation of F is used as criterion.

$$F = \sum (Q_e - Q_o)^2 \quad (5.39)$$

If any change in the parameter values can effect no further reduction in the value of F , then the optimum fit of the model-generated flow values on the observed data set has been achieved. It means, the optimization attempts to adjust the parameters to minimise the value of the objective function. The following three calibration procedures are generally adopted to arrive at a satisfactory set of process parameters: (Fleming, 1972).

1. Trial and error adjustments to parameters based on pattern recognition techniques.
2. Automatic parameter adjustments using computer programming internal to the model which check the criterion of accuracy and adjust the parameters based on some defined procedures.
3. A combination of the trial and error adjustment to reach a near-optimal set of parameters and automatic adjustments to refine and finalise the selection.

In the present study, third approach has been applied, in which, the combination of both trial and error optimization using on-line computer processing and interactive graphics to assess the starting values of parameters. These starting values can then be used with a deterministic optimization procedure to arrive at the refined optimum set of parameter levels.

The present study uses the Rosenbrock optimization technique (Kuester et al., 1973) for optimization of parameter values. The parameter adjustment proceeds by stages. To start the fitting process, the model is assigned an initial set of parameter values and upper and lower bounds for each parameter. The model is run, and the objective function is calculated and stored as a reference value. A step of user specified length is attempted in the first search direction, and the model is run again with the adjusted parameter value. If the resulting value of the objective function of less than or equal to the reference value, the trial

is registered as a success, and the appropriate step size for each parameter is multiplied by 3 for the next adjustment along the axis. If a failure results, the step is not allowed and the step size is multiplied by $-1/2$. That is, the next adjustment along this search axis will be in opposite direction and only one-half the magnitude of the current adjustment. An attempt is made in the next search direction and the process continues until the end-of-stage criteria are met. At this point, a new orthogonal search pattern is determined and another stage of optimization undertaken. Rosenbrock technique has the provision for putting constraint i.e. lower and upper limits on the parameter values, so that after calibration, the parameter values obtained lie within the realistic limits.

In this study, parameter optimization has been carried out in the routing part. When the flows are routed through the cascade of linear reservoirs as conceptualized in the model, the values of storage coefficients were optimized. The runoff emanating from the snow-free area and the snow covered area is routed separately through cascade of linear reservoirs. The flow from snow free area is fast and therefore two reservoirs have been considered for the snow free area whereas in case of snow covered area, the flow is relatively slow and therefore only one reservoir was considered. This means that the basin is represented by unequal linear reservoirs having storage coefficient k_r and k_s respectively for the snow free area and the snow covered area. The storage coefficients k_r and k_s are considered to be function of the respective areas, which is changing on a daily basis, and are represented as given in Equations (5.30) and (5.31).

There were four parameters a_r , b_r , a_s and b_s which were to be optimised using available data. To estimate these parameters, model was fitted for the observed and estimated data using snow-covered area, daily rainfall and daily temperature as input and calculating the daily streamflow as output. The four parameters listed above were evaluated by the optimisation technique, so that the observed and calculated values of daily stream

agree for the period of record used in calibration and the value of objective function stands minimum. Although it is difficult to find a true 'global optimum', many optimisations run with different initial values and different parameter perturbations can increase the likelihood of obtaining parameter values close to the global optimum. As discussed earlier, in this study Rosenbrock optimization procedure has been applied. Many optimization runs were performed for each calibration using different initial parameter values.

The model was calibrated for 1985-1988 by varying the initial parameters and optimization was carried out. A combined period of three water years has been considered to consider the varying climate from year to year. The calibrated parameter values have been computed considering the overall performance of the model and reproduction of the flow hydrograph for the three years period. A sensitivity analysis has been carried out for all the parameters. The parameter b_r and b_s are more sensitive. The values of these parameters were kept low within lower range of 0 to 0.15 in comparison to other two parameters having range of 0 to 1. On the basis of different values of these parameters, the objective function was calculated. For calibration run, the optimised values of a_r , b_r , a_s and b_s were found as 0.65, 0.14, 0.8, 0.13 respectively. The result of calibration for this period is shown in Figure 5.10. In this figure all the three components of streamflow namely runoff from snowmelt, runoff due to rainfall and baseflow are shown separately. The contribution of baseflow starts only after the topsoil storage is filled. For this purpose a soil moisture index (SMI) has been considered in the present study. The value of SMI used in this study was 150 mm. This value was determined on the basis of an appropriate match between observed and computed streamflow for the initial period.

From this figure, it can be seen that the estimated hydrograph match very well for all the years. The peaks in the inflow hydrograph are reproduced within reasonable limit. It can be seen that the highest peak of Sept. 1988 was well estimated by the model. The results of

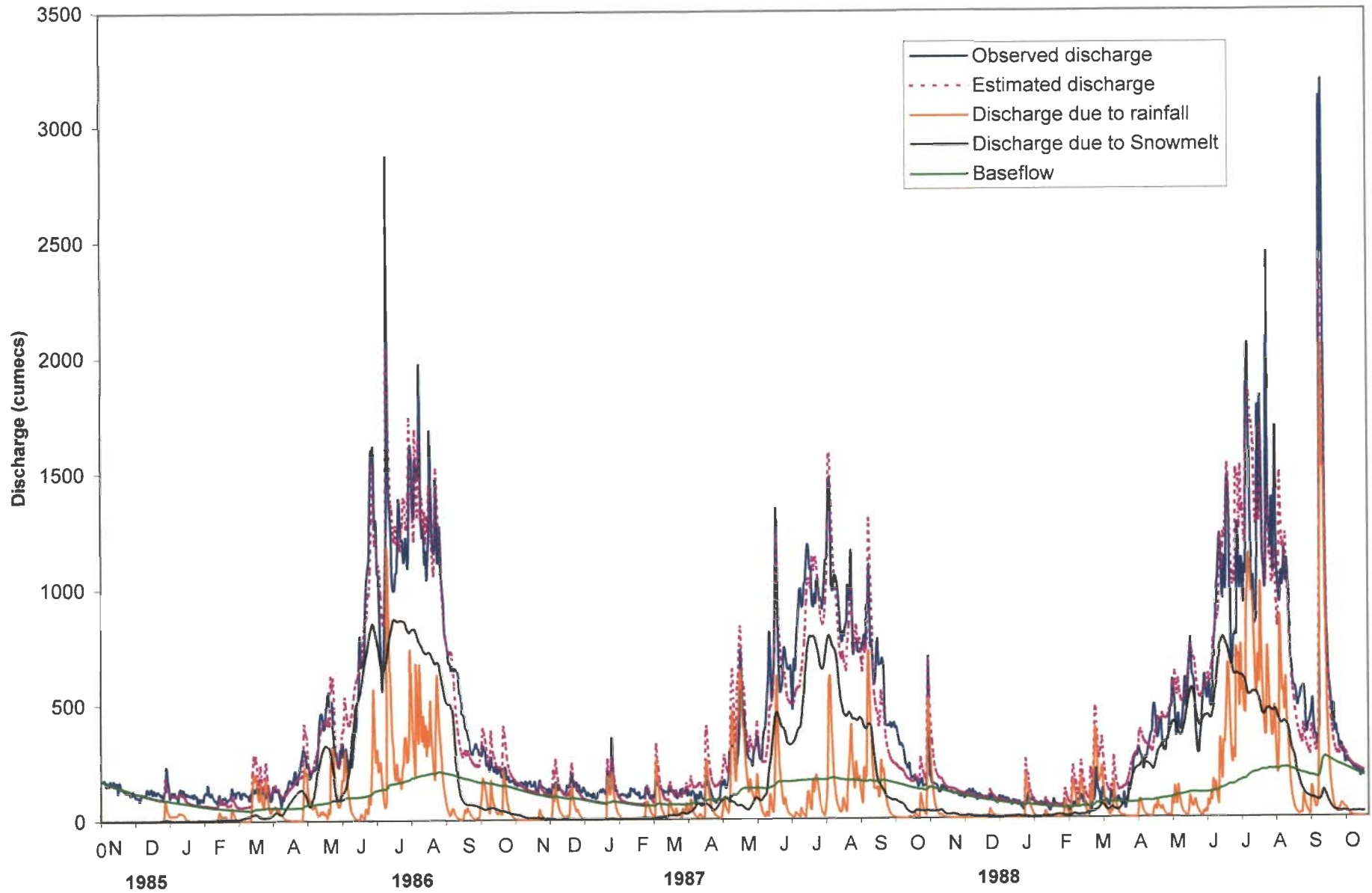


Figure 5.10 Comparison of observed and simulated runoff hydrographs for calibration period of 3 water years (1985-86 to 1987-88) for Satluj basin upto Bhakra

calibration were evaluated against the efficiency criteria already described in section on EFFICIENCY CRITERIA. The efficiency of the model for the calibration period is given in Table 5.5.

TABLE 5.5 : Model efficiency during calibration period of three years

Period considered	R ²	Volume difference (%)	Root mean square error (rmse)
1985-1986	0.93	1.57	0.28
1986-1987	0.89	2.88	0.30
1987-1988	0.81	7.26	0.50
1985-86 to 1987-88	0.90	2.23	0.34

It is noticed that for all the three years the daily discharge simulated with efficiency ranging from 0.81 to 0.93 and difference in volume ranging from 1.57% to 7.26%, which indicates good performance of the model for all the years. The value of R² for the years was low in comparison to other two years. The reason for this is that this year was comparatively wet year and there was also heavy rainfall in the month of September in 1988. Due to this, there was a high runoff peak in this year, which could not be reproduced well. Therefore, the R² was low and the difference in volume was somewhat high.

5.7.2 Sensitivity analysis of optimised parameters

Alongwith optimization analysis, sensitivity analysis has frequently been used as a means of ranking the variables in order of relative importance. Sensitivity is in fact, a measure of the effect of change in one factor on other factor. Sensitivity analysis usually shows that model performance is much more sensitive to some parameters than others. In this study, a sensitivity analysis was performed on the optimized parameters for the study

basin. The estimation of parametric or component sensitivity requires a measure of the change in objective function. A sensitivity plot is a graphical comparison of the percent change in objective function and the percentage change in a parameter value. In sensitivity plot the percentage change in the value of the objective function is computed for different percentage change in a parameter value (McCuen, 1973). The percentage changes in the parameters considered here are ($\pm 10\%$, $\pm 20\%$, $\pm 30\%$, $\pm 40\%$, $\pm 50\%$) of optimized value (while other parameters were not changed). The sensitivity results are reported as the percentage change in the value of objective function accompanying the percentage changes in the model parameters (Table 5.6). It is also shown in the form of sensitivity plots (Figure 5.11). All the plots shown in the figure shows that the trend of the curve is unimodal indicating one minima only. Unimodal function is monotonic on either side of the minimum point. In the above table, the change in objective function is from 5.4% to 24.5% in case of change of parameter a_r from -50% to $+50\%$. While in case of other parameter b_r the change in objective function is from 14.0% to 15%. The change in objective functions due to change in other parameters is very low, i.e., of the order of about 2 to 3%. It is seen that parameter a_r and b_r are more sensitive in comparison to parameters a_s and b_s with respect to the effects of change in their values on the objective function. The effect of reduction in value of parameter a_r from its optimised value is comparatively much more than increase in its value. It thus shows that in the simulation of runoff, the two parameters (a_r and b_r) related with storage effect for snow free area having contributions of rain have much more influence than corresponding to two parameters a_s and b_s for snow covered area. The optimisation procedure therefore, more likely to provide comparatively better estimates of optimised values for parameters a_r and b_r .

Table 5.6: Percentage change in objective function due to percentage change in parameter values

Change in parameter a_r (other parameter unchanged)	Change in objective function (%)	Change in parameter a_r (other parameter unchanged)	Change in objective function (%)	Change in parameter a_r (other parameter unchanged)	Change in objective function (%)	Change in parameter a_r (other parameter unchanged)	Change in objective function (%)
-50%	24.5	-50%	15.0	-50%	3.3	-50%	2.2
-40%	13.1	-40%	11.2	-40%	2.1	-40%	1.4
-30%	7.3	-30%	7.4	-30%	1.1	-30%	0.6
-20%	2.5	-20%	3.8	-20%	0.4	-20%	0.4
-10%	0.4	-10%	0.3	-10%	0.2	-10%	0.3
+10%	0.5	+10%	1.1	+10%	0.2	+10%	0.6
+20%	1.4	+20%	4.0	+20%	0.6	+20%	1.6
+30%	3.0	+30%	6.6	+30%	0.9	+30%	2.1
+40%	4.3	+40%	10.2	+40%	1.1	+40%	2.6
+50%	5.4	+50%	14.0	+50%	1.4	+50%	3.2

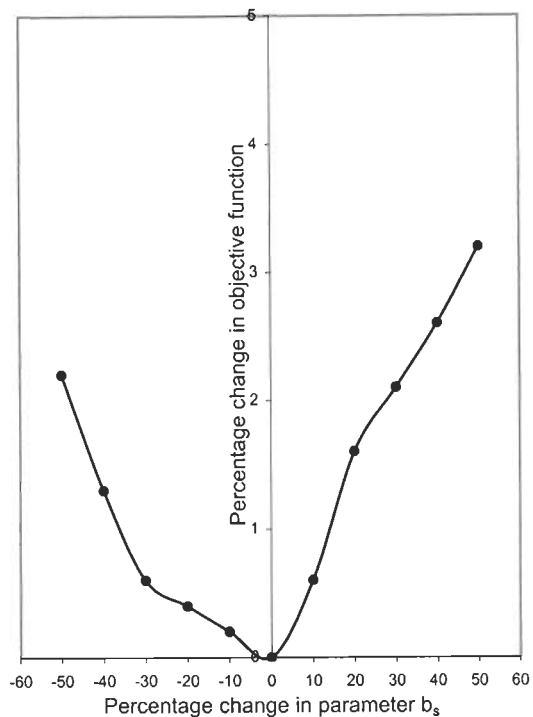
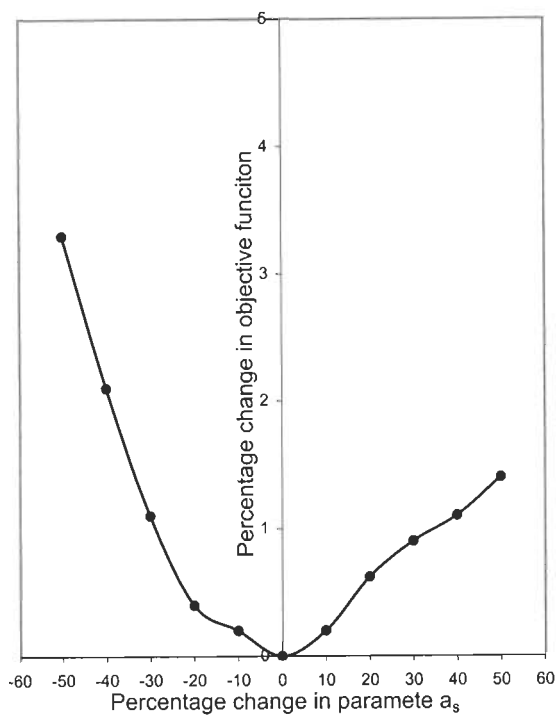
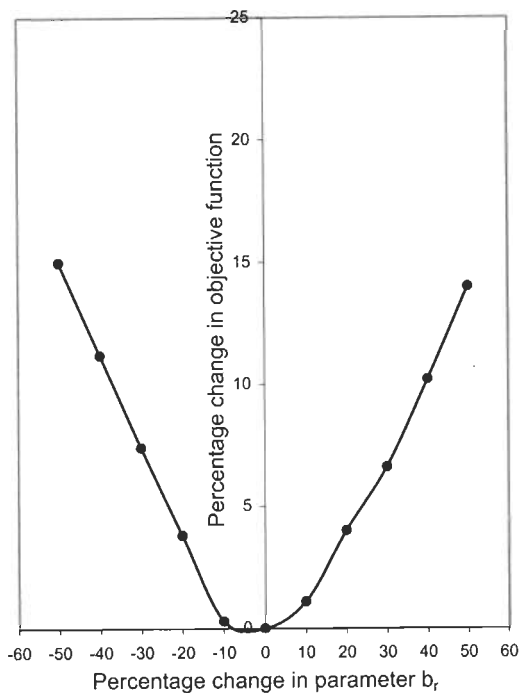
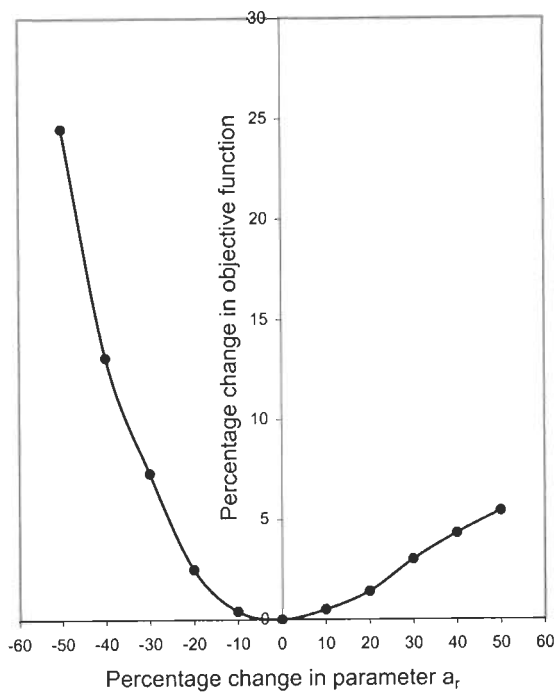


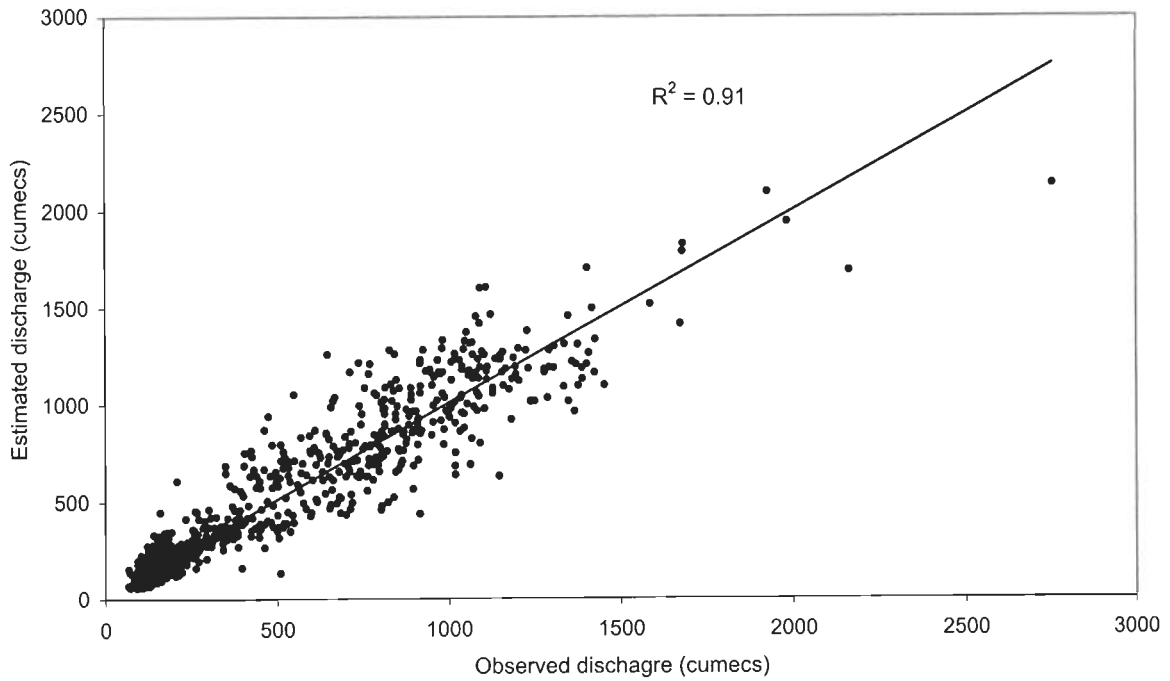
Figure 5.11: Variation in objective function with variation in the different model parameters

5.8 SIMULATION OF STREAMFLOW

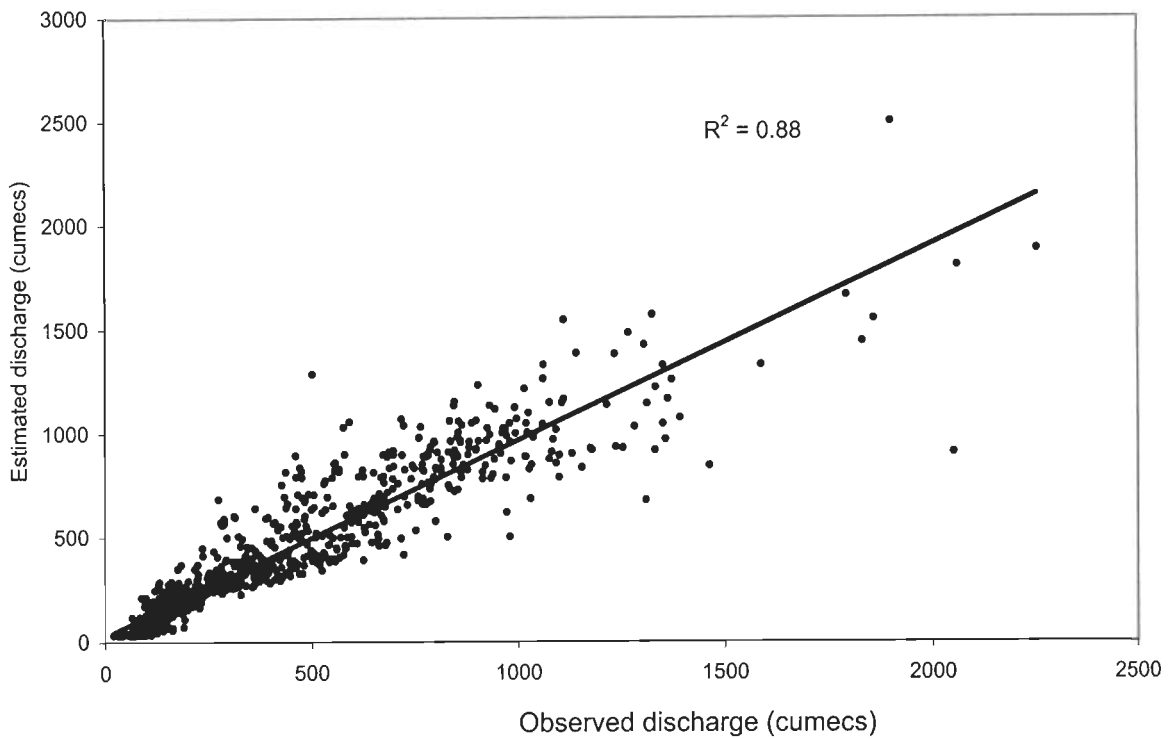
After successful calibration of the model, it was used for simulation for two independent sets of the data consisting of three years, i.e., for the year 1988-91 and 1996-99. In the simulation mode for testing the performance, the three years have been combined to apply the model as carried out during calibration. The parameter estimates obtained in the calibration stage were used to simulate the runoff hydrograph for the period as mentioned above.

The simulation accuracy is determined by checking how well the model simulates the actual flow conditions. For this observed and estimated values of runoff were plotted as shown in Figures 5.12. From this figure it can be seen that the observed and estimated flow is correlated well and R^2 is high for both the data sets. The comparison of the estimated and observed discharges for the years 1988-91 and 1996-99 by the model is given in Figures 5.13 and 5.14.

The efficiency criteria used for comparison of model performance during simulations are given in Table 5.7 depicting difference in volume between the observed and computed flows, efficiency or coefficient of determination and root mean square errors (rmse) the model. For the two sets of period for which the simulation was performed the value of efficiency is in between 0.89-0.94 and 0.88 – 0.93 for the period 1988-89 to 1990-91 and 1996-97 to 1998-99 respectively. The difference in volume is less for all the years indicating a good match between the observed and estimated values for two independent data sets.



(a)



(b)

Figure 5.12 : Comparison between observed and simulated daily runoff for two sets of validation period (a) Three water years(1996-97 to 1998-99)(b) Three water years (1988-89 to 1990-91)

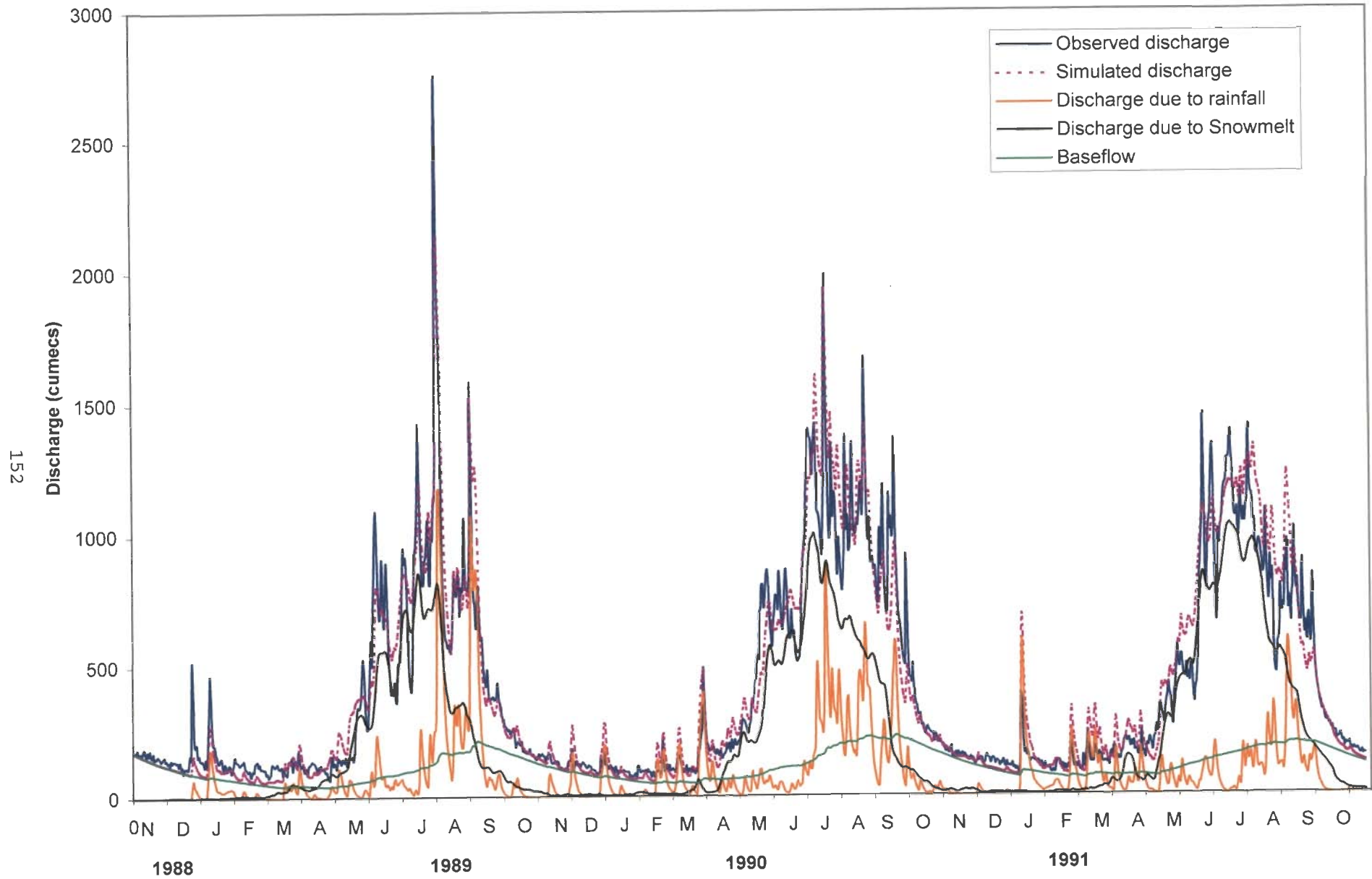


Figure 5.13 Comparison of observed and simulated runoff hydrographs for validation period of 3 water years (1988-89 to 1990-91) for Satluj basin upto Bhakra

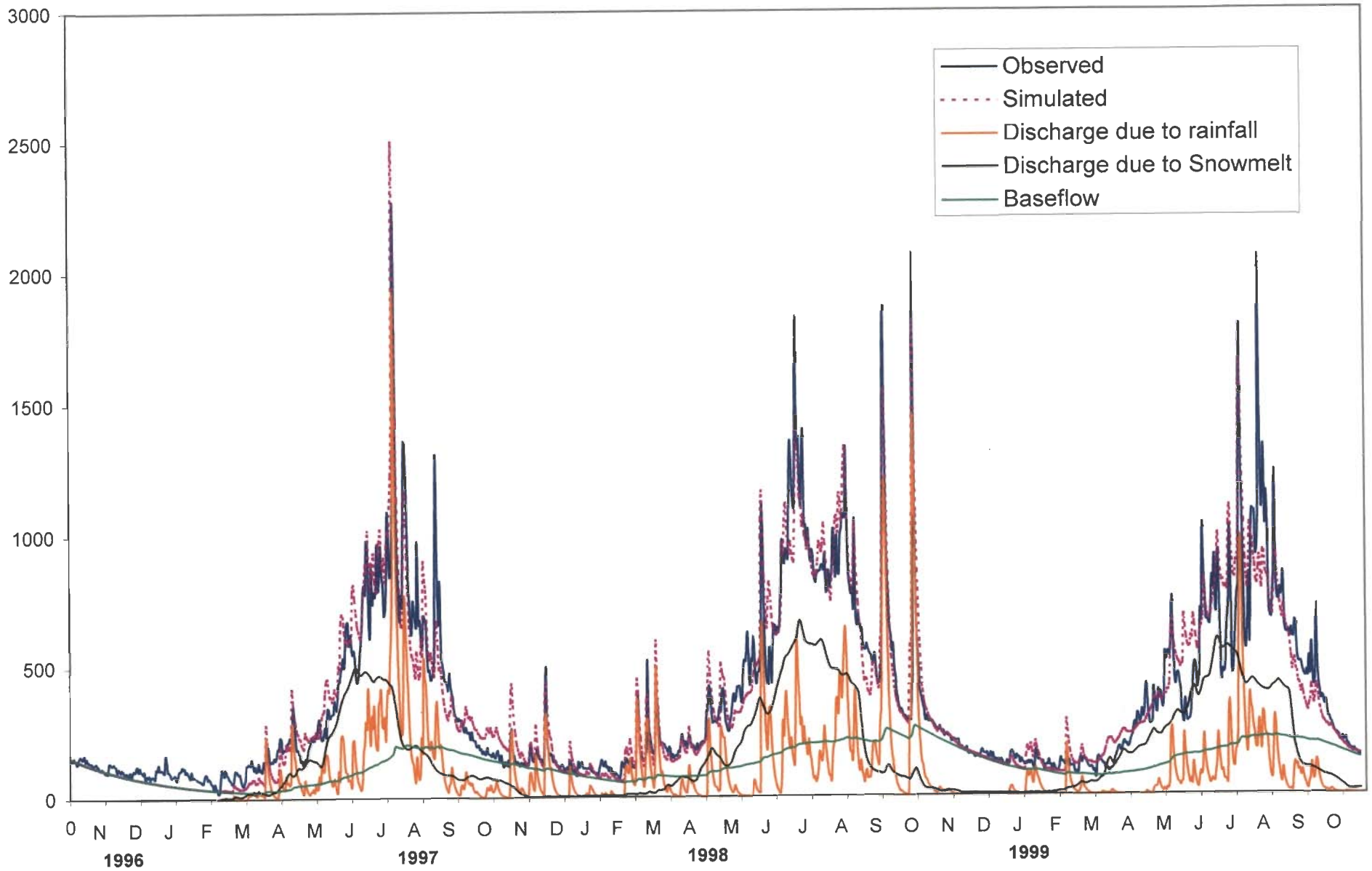


Figure 5.14 : Comparison of observed and simulated runoff hydrographs for validation period of 3 water years (1996-97 to 1998-99) for Satluj basin upto Bhakra

TABLE 5.7 : Model efficiency for the two sets of simulation period of 3 years each

Period considered	R ²	Volume difference (%)	Root mean square error (rmse)
1988-1989	0.89	0.57	0.33
1989-1990	0.93	0.55	0.46
1990-1991	0.94	0.53	0.57
1988-89 to 1990-91	0.90	3.46	0.30
1996-1997	0.88	1.72	0.35
1997-1998	0.92	1.65	0.49
1998-1999	0.93	1.58	0.60
1996-97 to 1998-99	0.90	1.26	0.30

In all the figures, different components of total streamflow, i.e., runoff due to snowmelt, runoff due to rainfall and baseflow are shown separately. The observed and estimated hydrograph for all the years indicate very good reproduction of the flows. From the figures, it is clear that all the peaks in the outflow hydrographs are due to rainfall. In general, the volumes and peaks are reproduced well by the model for all the years. The hydrograph recessions also fitted well but in some cases the peaks were underestimated. The contribution of snowmelt is higher especially during the pre monsoon period when there is no contribution from rainfall. Even during monsoon period the contribution from snowmelt is significant. It is well known that the baseflow sustains the flow in the stream during winter period when there is no discharge either from snowmelt or from the rainfall. The baseflow is also plotted in the figures and the reproduction of baseflow is also quite satisfactory. It can be seen that during monsoon period when there is increase in recharge due to rainfall, the trend of baseflow is also increasing.

CHAPTER 6

ASSESSMENT OF SEDIMENT YIELD AND RESERVOIR SEDIMENTATION

Assessment of soil erosion, sediment transport and deposition of sediment in the reservoirs is considered essential for the land and water management. The magnitude of sediment transported by the rivers has become a serious concern for the water resources projects. The soil erosion and sediment yield is one of the major problems in Himalayan region. In the present study assessment of sediment yield has been made for the Satluj river, which flows through the western Himalayan region. Two approaches have been used for the assessment of sediment yield (i) relationship between suspended sediment load and discharge and (ii) empirical relationship, have been used. The first approach was used for Satluj basin up to Suni (52,983 km²), Kasol (53,768 km²) and also for the intermediate basin between Kasol and Suni (785 km²). In this approach, the sediment discharge relationship was developed using daily data for a period of three years (1991-1993) and was applied for the two years 1994 and 1996 for estimation of sediment yield. The second approach, which gives annual sediment yield, could be used for a small intermediate basin only because of data availability constraints. There were two reasons for selecting a small basin to use the second approach. First, this part is highly soil erosion prone area in the whole basin and secondly the data required for empirical relationships were available or could be derived for this basin. For estimation of the sediment yield using the empirical relationship, various geographical parameters such as land use, topographical etc. were generated using Geographic Information System (GIS) technique.

A part of the sediment generated in the upstream area is deposited in the reservoir located downstream. The assessment of sedimentation in the reservoir has also been made using remote sensing techniques. The location of intermediate basin and Bhakra reservoir is shown in Figure 6.1. The above two aspects have been discussed in the following sections:

6.1 SOIL EROSION AND SEDIMENT YIELD

The present study involves estimation of sediment yield using following two methods for sediment yield assessment for separate study areas in the Satluj basin.

6.1.1 Relationship between sediment yield and discharge

The sediment yield and discharge data were available for Suni and Kasol in the Satluj basin. The availability of these data sets has been given already in Chapter 3. BBMB is collecting sediment yield data in the field and the procedure followed by this organisation is given as follows. For determining the suspended sediment concentration, the sample were drawn from three transects across the river with the help of buckets thrown from a bridge. After stirring well, representative samples of 3 liters each were drawn from the three buckets. The samples were then passed separately through a 100-mesh sieve and the fraction retained was dried and weighted. It represented the coarse fraction (> 0.20 mm). The sieved samples were again stirred and allowed to stand for the time required for settling of the medium fraction (0.075-0.20 mm) depending upon the temperature of water. A settling time of 27-14 seconds was allowed for water temperature between 0 and 30°C. The medium fraction was also dried and weighted. A 25-ml sample of the remaining material was dried and weighted to represent the fine fraction (< 0.075 mm) and dissolved salts. Another 25 ml was filtered out, dried and weighted, to represent dissolved salts. The weight of the fine fraction was

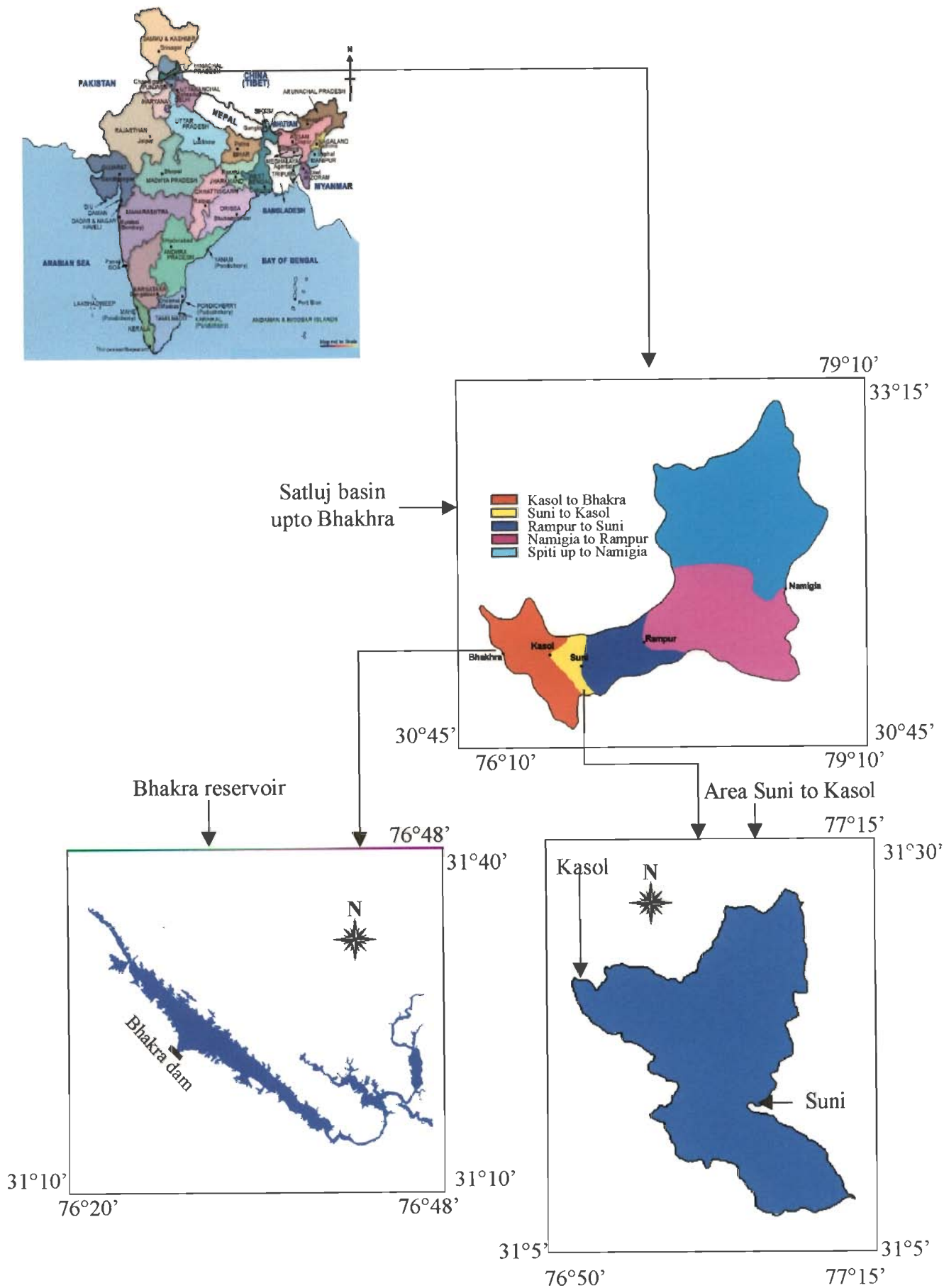


Figure 6.1: Location of intermediate basin and Bhakra reservoir

determined by subtracting the weight of the dissolved salts from that of the fine fraction plus dissolved salts. Calculation was then made to determine the average sediment concentration in one liter of water. The sediment load in the river was calculated by multiplying to the sediment concentration with corresponding discharge. This was converted to m^3 by dividing the load in tonne by 1.4, assuming that the sediment density was 1.4 t/m^3 . Sediment yield and discharge for the intermediate catchment between Kasol and Suni were obtained by subtracting the contributions at Suni and Kasol. The distribution of suspended sediment load suggests that it start increasing from April onward as the discharge increases. However, it remains low during April and May and then increases drastically in the beginning of June and remains high until August. Since discharge in the river is high in the monsoon period, therefore, silt load is also maximum in the river in these months. By the end of October, the load reduces significantly and becomes negligible during winter season (November to March). The concentration levels in the river cannot be generalised because it varies considerably from year to year and from month to month (Sharma et al., 1991).

General statistics of daily discharge and sediment yield for a period of five years (1991-96) for different sites is given in Table 6.1 and 6.2. From this analysis it is found that the daily maximum values of sediment yield varies from 12.60 to 31.47, 14.23 to 40.32 t/km^2 and 210.30 to 420.63 t/km^2 for Suni, Kasol and intermediate basins respectively. While for the corresponding basins, the maximum discharge values vary from 1480.0 to 1898.7 cumecs, 1648.7 to 2050.6 cumecs and 184.5 to 223.7 cumecs, respectively. The analysis of discharge and sediment yield at both Suni and Kasol indicates that maximum discharge and sediment yield were in the year 1994. The reason for the high values of discharge and sediment yield in this year, is the high rainfall occurring in this part of the basin. The standard deviation is a standard measure of the spread in data values and the sediment yield value is higher for intermediate basin because this part is rainfed only and is more soil erosion prone.

The value of C_v for discharge at Kasol and Suni is almost because of the proximity of these two sites. The value for intermediate basin is relatively higher which indicates the large variation in the discharge from this part. The coefficient of variation for the intermediate basin is higher in comparison to other two sites because the soil erosion from this part is high.

Table 6.1 : Statistics of daily discharge (cumec) at Suni, Kasol and intermediate basin

Statistics	Site	1991	1992	1993	1994	1996
Maximum	Suni	1636.8	1480.0	1701.7	1898.7	1710.2
	Kasol	1804.3	1648.7	1873.2	2050.6	1861.3
	Intermediate basin	186.1	221.1	223.7	210.3	184.5
Minimum	Suni	94.9	104.9	102.7	99.2	102.6
	Kasol	99.2	106.3	104.9	100.0	104.9
	Intermediate basin	0.6	0.4	0.1	0.7	0.3
Mean	Suni	450.9	383.5	327.2	458.1	432.2
	Kasol	485.1	413.2	344.9	489.2	465.6
	Intermediate basin	34.2	29.7	17.8	31.1	33.3
Stand. Dev.	Suni	438.1	353.2	271.6	478.4	412.9
	Kasol	477.6	386.8	291.6	515.7	438.8
	Intermediate basin	43.3	38.8	25.2	42.4	35.1
C_v	Suni	0.97	0.92	0.83	1.04	0.95
	Kasol	0.98	0.93	0.84	1.05	0.94
	Intermediate basin	1.26	1.31	1.42	1.36	1.10

Table 6.2: Statistics of daily sediment yield (t/km^2) at Suni, Kasol and intermediate basin

Statistics	Site	1991	1992	1993	1994	1996
Maximum	Suni	12.6	13.3	13.9	31.5	24.2
	Kasol	14.2	19.2	23.2	40.3	27.5
	Intermediate basin	282.9	420.6	323.0	375.9	321.8
Minimum	Suni	0.004	0.004	0.005	0.005	0.005
	Kasol	0.006	0.005	0.007	0.007	0.008
	Intermediate basin	0.010	0.011	0.010	0.700	0.130
Mean	Suni	1.57	1.08	0.73	1.96	1.79
	Kasol	1.88	1.41	0.92	2.39	2.07
	Intermediate basin	22.88	23.56	17.76	31.05	20.67
Stand. Dev.	Suni	2.58	1.87	1.41	4.01	3.27
	Kasol	3.07	2.45	1.92	4.97	3.71
	Intermediate basin	38.72	45.42	25.21	42.40	36.91
C_v	Suni	1.65	1.73	1.94	2.04	1.83
	Kasol	1.63	1.74	2.09	2.07	1.79
	Intermediate basin	1.69	1.93	1.42	1.37	1.79

To estimate sediment yield from the study basin, relationships between sediment yield and discharge were developed for Suni, Kasol and intermediate basin using three years of (1991-1993) daily data. Because of the scatterdness in the data in mountain region, the data have to first transform to linearize the trend and reduce the heteroscedasticity. For developing these relationships, a \log_{10} transformation was identified as most suitable. The common logarithmic transformation will yield the most normally distributed data, with minimised skewness, kurtosis and variance (Fenn, 1985,

Willis et al., 1996 and Hodgkins, 1999). In the present study, therefore, logarithmic transformation was applied to the values of discharge and sediment yield. A relationship between S and Q was obtained using best fit linear regression approach for log transformed data. Such relationships for three different sites are shown in Figures 6.2 for different basins. These relationships are given as follows:

$$\text{For Suni} \quad \log_{10}(S) = 2.89 * \log_{10}(Q) - 7.96 \quad (6.1)$$

$$\text{For Kasol} \quad \log_{10}(S) = 2.79 * \log_{10}(Q) - 7.66 \quad (6.2)$$

$$\text{For the intermediate basin} \quad \log_{10}(S) = 1.53 * \log_{10}(Q) - 1.26 \quad (6.3)$$

where S is the daily sediment yield (t/km^2), Q is the daily discharge (cumec). The value of R^2 for the above three relationships was computed to be 0.96, 0.96 and 0.77 for Suni, Kasol and for intermediate basin, respectively, showing that for all the sites S was well correlated with Q.

In order to test the developed relationship, these equations were used for an independent set of data for 2 years (1994 and 1996). However, data of the year 1995 was also collected but some of the values of daily sediment yield were missing in this data and therefore this year was not considered in this study. A comparison of estimated and observed values of daily sediment yields for these two years is shown in Figures 6.3 and 6.4. The correlation coefficient (R^2) between observed and estimated values of sediment yield for the year 1994 were computed to be 0.83, 0.81 and 0.60 for the site Suni, Kasol and for intermediate basin respectively. While the corresponding values of R^2 for the year 1996 were 0.81, 0.82 and 0.43. The value of R^2 for the intermediate basin for these two years is lower than other two sites, which may be, because the soil erosion from this part is relatively high

and the discharge is highly variable. The observed and estimated values of sediment yield for the three cases are given in Table 6.3. These figures indicate that for both the years, the sediment yield for the pre monsoon period was over estimated using developed relationship, but it is matching well for the remaining period. The reason for overestimation during premonsoon period may be low discharge and therefore the sediment yield could not be reproduced very accurately using this relationship. The peaks in case of sediment yield at two sites, i.e., at Kasol and Suni are simulated close to observed values, while for intermediate basin the peaks could not be reproduced very well.

Table 6.3 : Observed and estimated annual total of sediment yield for different years

Year	Sediment yield for Suni (t/km ²)			Sediment yield for Kasol (t/km ²)			Sediment yield for intermediate basin (t/km ²)		
	Obs.	Est.	Diff. in Obs. & est. sedi. yield (%)	Obs.	Est.	Diff. in Obs. & est. sedi. yield (%)	Obs.	Est.	Diff. in Obs. & est. sedi. yield (%)
1994	716.2	975.2	36.2	874.7	1149.8	31.4	10261.0	6370.7	34.9
1996	656.1	715.7	8.9	756.8	834.6	10.3	7565.5	6092.8	19.3

The results show that the estimated values at Suni and Kasol are close to the observed values in the year 1996. The results of the year 1994 were not so good because of the high rainfall and high discharge in this particular year. The statistics of the discharge and sediment yield data given in Table 6.1 and 6.2 also indicate that the maximum values of discharge and sediment yield occur in this year. Due to these reasons the estimated values of sediment yield could not be reproduced very accurately for the year 1994.

For calculation of annual sediment yield from the intermediate basin, another approach was also used, which is given in the following section.

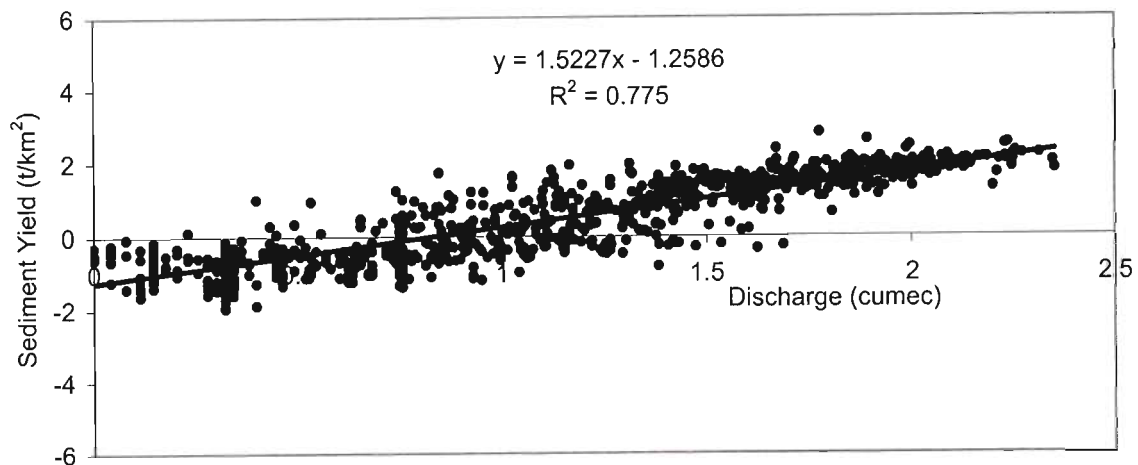
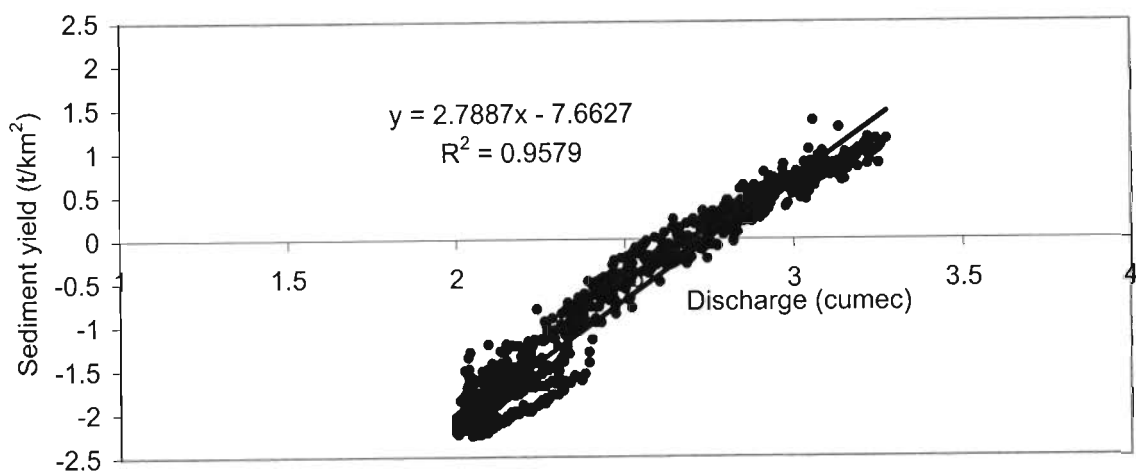
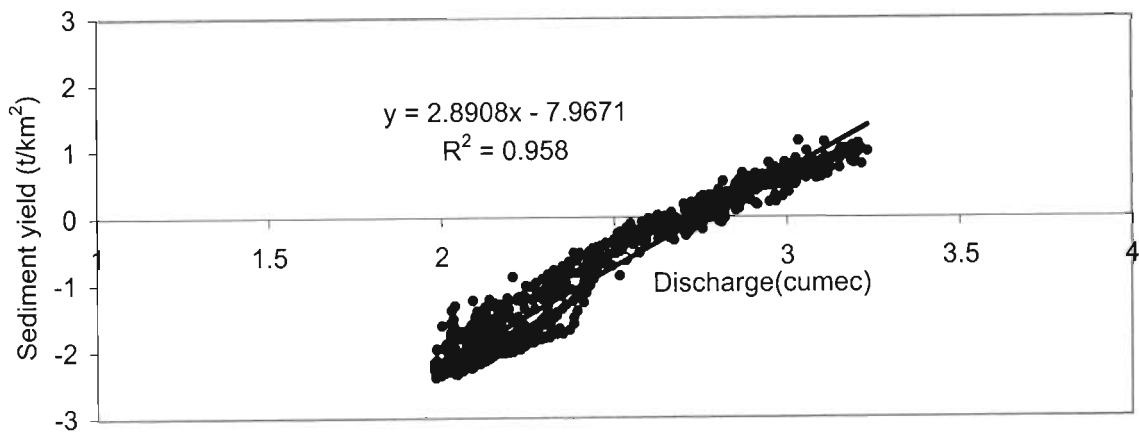


Fig. 6.2 : Relationship between log values of discharge and sediment yield at Suni, Kasol and for intermediate basin

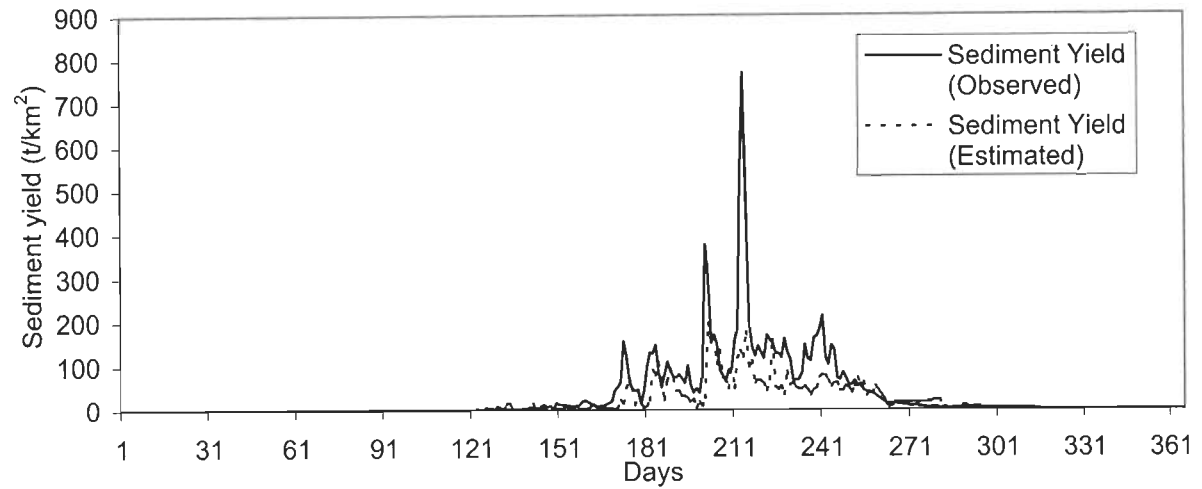
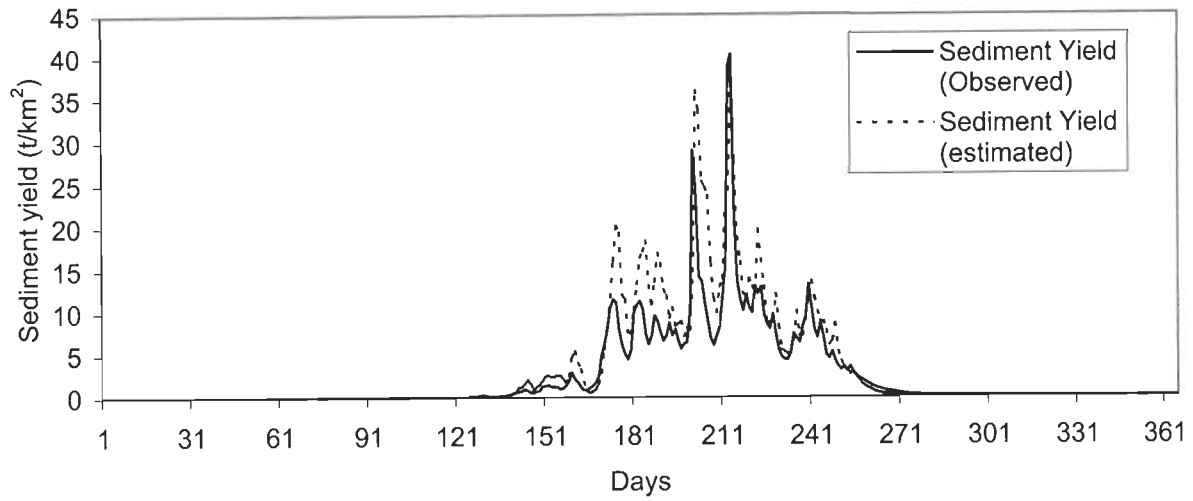
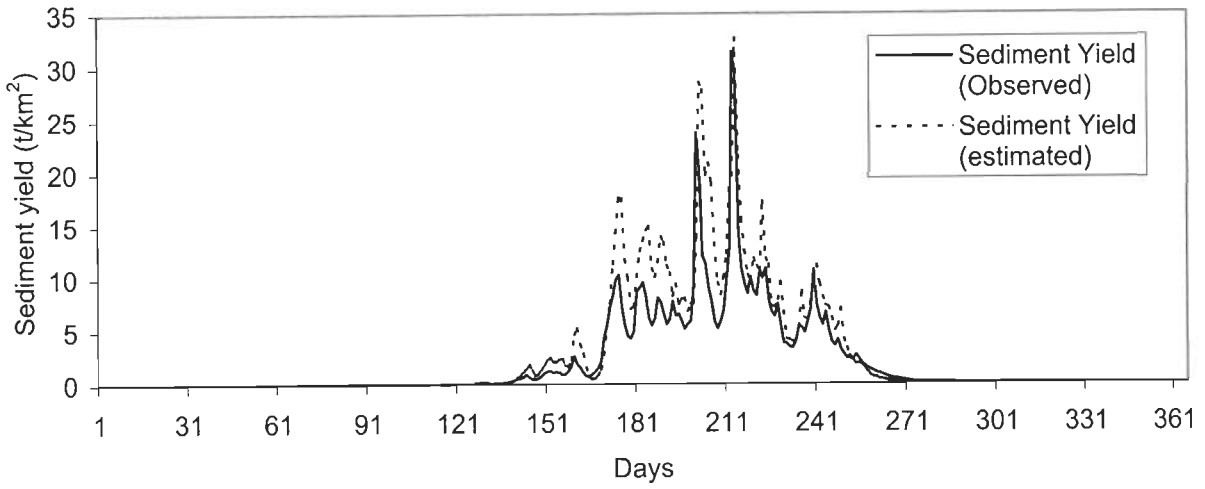


Fig. 6.3 :Comparison between observed and estimated sediment yield at Suni, Kasol and intermediate basin (1994)

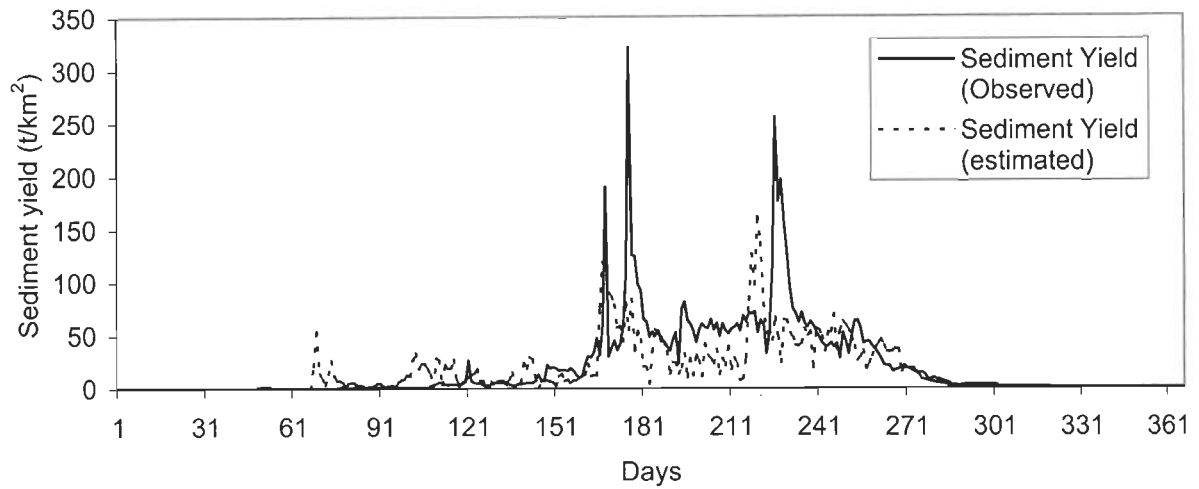
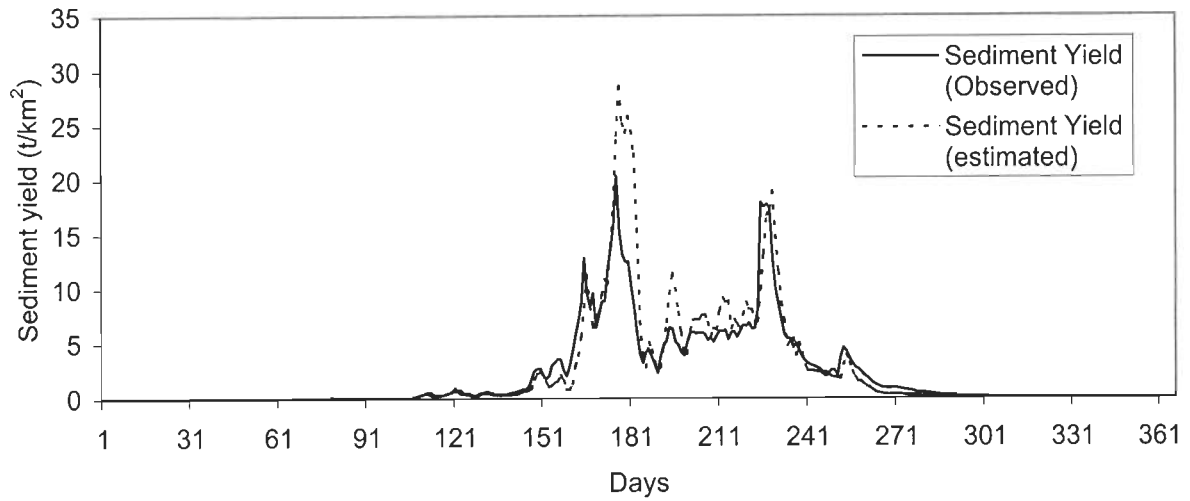
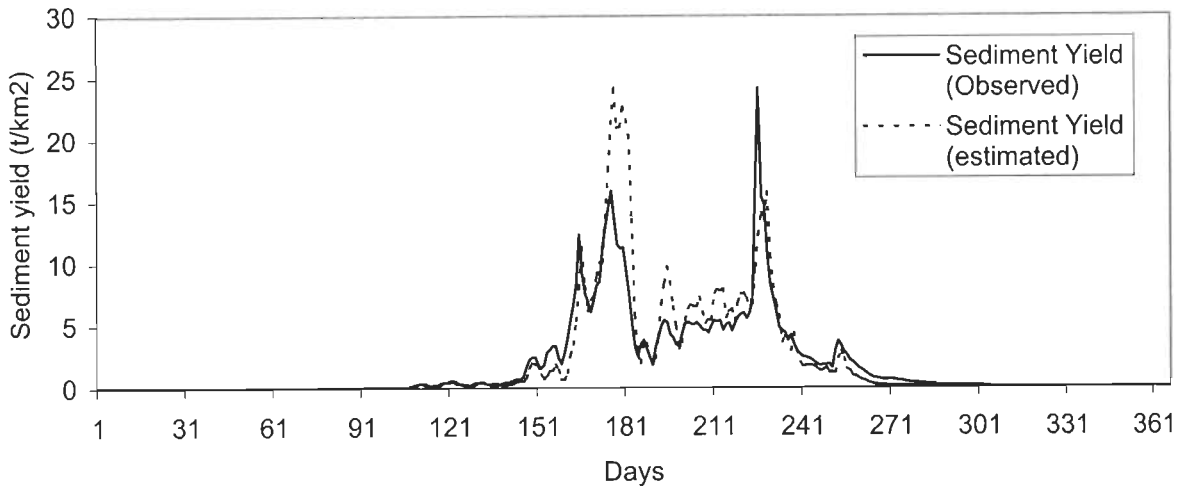


Figure 6.4 :Comparison between observed and estimated sediment yield at Suni, Kasol and intermediate basin (1996)

6.1.2 Estimation of annual sediment yield for intermediate basin using sediment yield equation (Second approach)

For estimation of sediment yield there are various techniques from sediment rating curve to erosion modelling. Depending upon the methodologies adopted for modelling of the sediment yield for a basin, there are numerous models available. These models vary from a simple regression relationships to complex simulation models. The simulation models provide a physically based representation of the process as occurring in small segments of the catchment and route the response of these segments to the catchment outlet. The regression equations link the spatial variation in annual sediment yield to climatic and physiographic variables of the basin. These regression equations which relate the sediment yield to hydrometeorological conditions in that basin, are mostly used for prediction of sediment yield from the ungauged catchment.

In the present study, the following empirical relationship was used for estimation of annual sediment yield for the intermediate basin as given below.

$$S_a = 1.182 * 10^{-6} P^{1.29} A^{1.03} D_d^{.40} H^{0.08} F_c^{2.42} \quad (6.4)$$

where A is catchment area (km²), L is length of stream (km), H is catchment slope, D_d is drainage density, F_c is vegetation cover factor, P is annual mean precipitation (mm) and S_a is annual sediment yield (Mm³). The above Equation (6.4) was developed by Garde et al. (1983) for average annual sediment yield estimation using data of 50 catchments located in plain region of India. The range of the area used in developing this equation varies from 43 to 83,880 km².

Various topographical and morphological parameters used in the Equation (1) were derived for the study basin in GIS mode using Survey of India (SOI) toposheets. Computation of these parameters using manual methods like area measurement using dot grid method or using planimeter and length measurement using curvimeter are very tedious and time consuming. The boundary of drainage catchment, its area, contours and all streams were extracted from SOI toposheet at a scale of 1:50,000. The drainage map of the study area is shown in Figure 6.5. In the present work calculations of various inputs viz stream ordering, numbers, length etc., which are required for calculating drainage parameters, was estimated using GIS technique. The analog data was converted into digital form and a database was created in GIS environment using ILWIS. The process of database creation for the basin in ILWIS involves collection of relevant available data, converting these data into digital format, digitization error checking and correction and finally conversion of data acquired in vector structure to raster format. Digitization, which is the most time consuming part of the analysis, was carried into parts to minimise the digitization errors. Then the digitized map was corrected for many types of errors such as proper joining of the streams, proper overlaying of the segments etc. The system then auto edits the coverage and splits the stream of the higher order at the point where they meet. Individual stream (segment) lengths are computed by default and stored in a table alongwith the order of each stream. The area and perimeter of the basin were computed after converting segment (boundary) map to polygon map. After converting the contour map into digital form, it was rasterised and then interpolation using krigging from isolines (interval 20 m) was carried out. This interpolated map gives the elevation at each point (pixel) in the basin and known as digital elevation model (DEM). This map was reclassified into a interval of 200 m and shown in Figure 6.6.

For determination of stream order, Strahler's system, which is slightly modified Horton's method, was followed (Strahler, 1964). Application of this order system through

ILWIS over the entire drainage network shows that study basin is a six-order basin. In ILWIS the length of each stream is stored in a tabular form. Total length of each order is obtained by adding length of each stream of the same order. The numbers of different order streams and their lengths are given in Table 6.4 and shown in Figure 6.7. For the intermediate basin drainage density, which is defined as the ratio of the total channel length and catchment area is computed to be 3.58. A slope map was prepared using the DEM and the average slope of the intermediate basin was calculated to be 0.48. The land use factor, which represents the ratio of forest area and non-forest area in the basin, was computed using the land use map of the study basin (Jain et al., 1998). Since the forest area and agriculture area in the intermediate basin is almost same, therefore the land use factor is taken as 0.5.

Table 6.4: Number of different of different order streams and their lengths

Order	Number of streams	Total length (km)
1	3323	1658
2	1444	442
3	691	198
4	28	103
5	6	56.2
6	1	36.5

The rainfall data of the two stations, namely, Suni and Kasol, which are falling in the intermediate basin, were used. Thiessen polygons of these two stations were drawn from the point interpolation in ILIWS and the weight of each station was determined. From this the annual mean precipitation was determined. As the intermediate basin comprises the area between Suni to Kasol, therefore discharge and suspended sediment

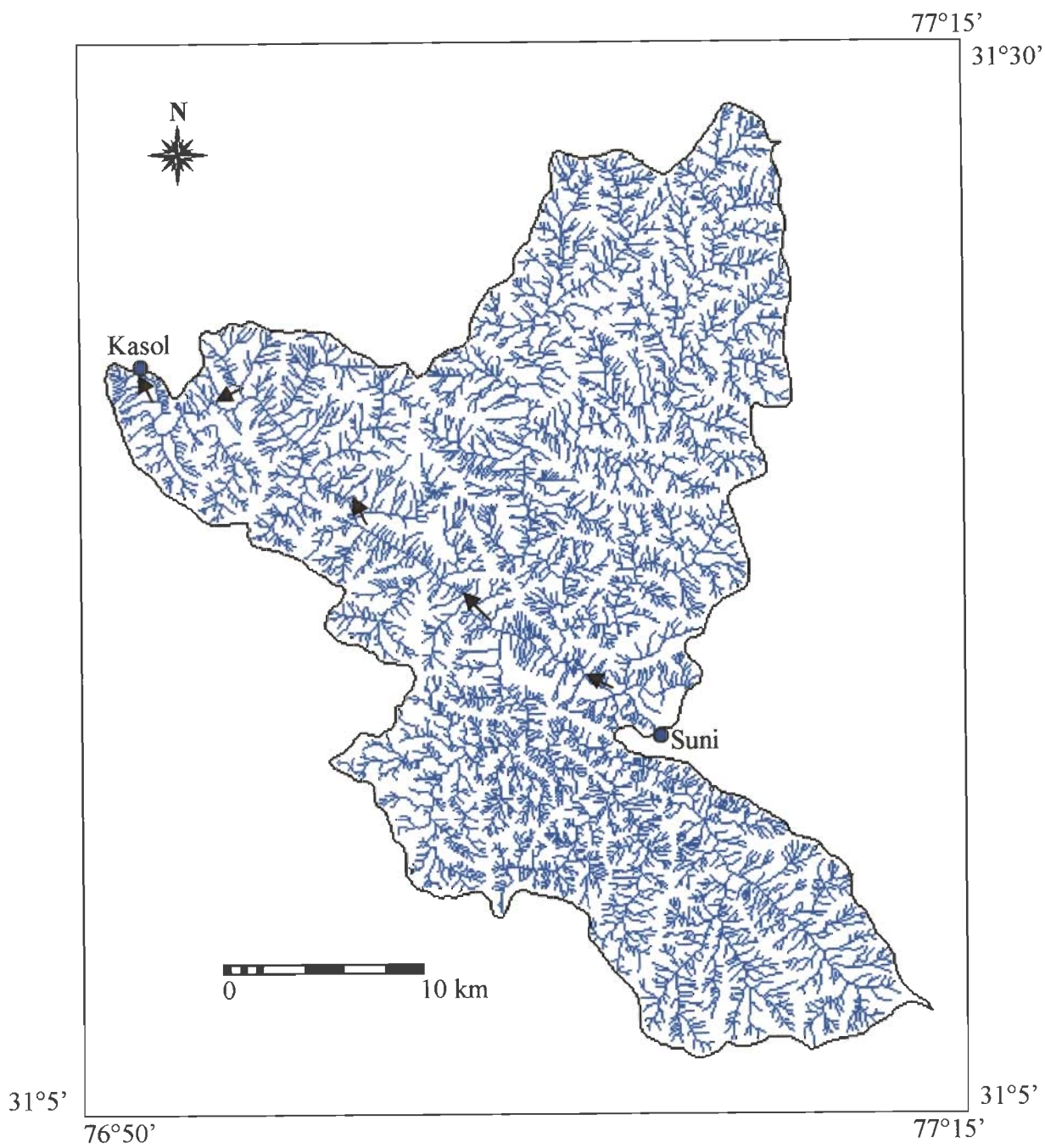


Figure 6.5 : Drainage network map of intermediate basin

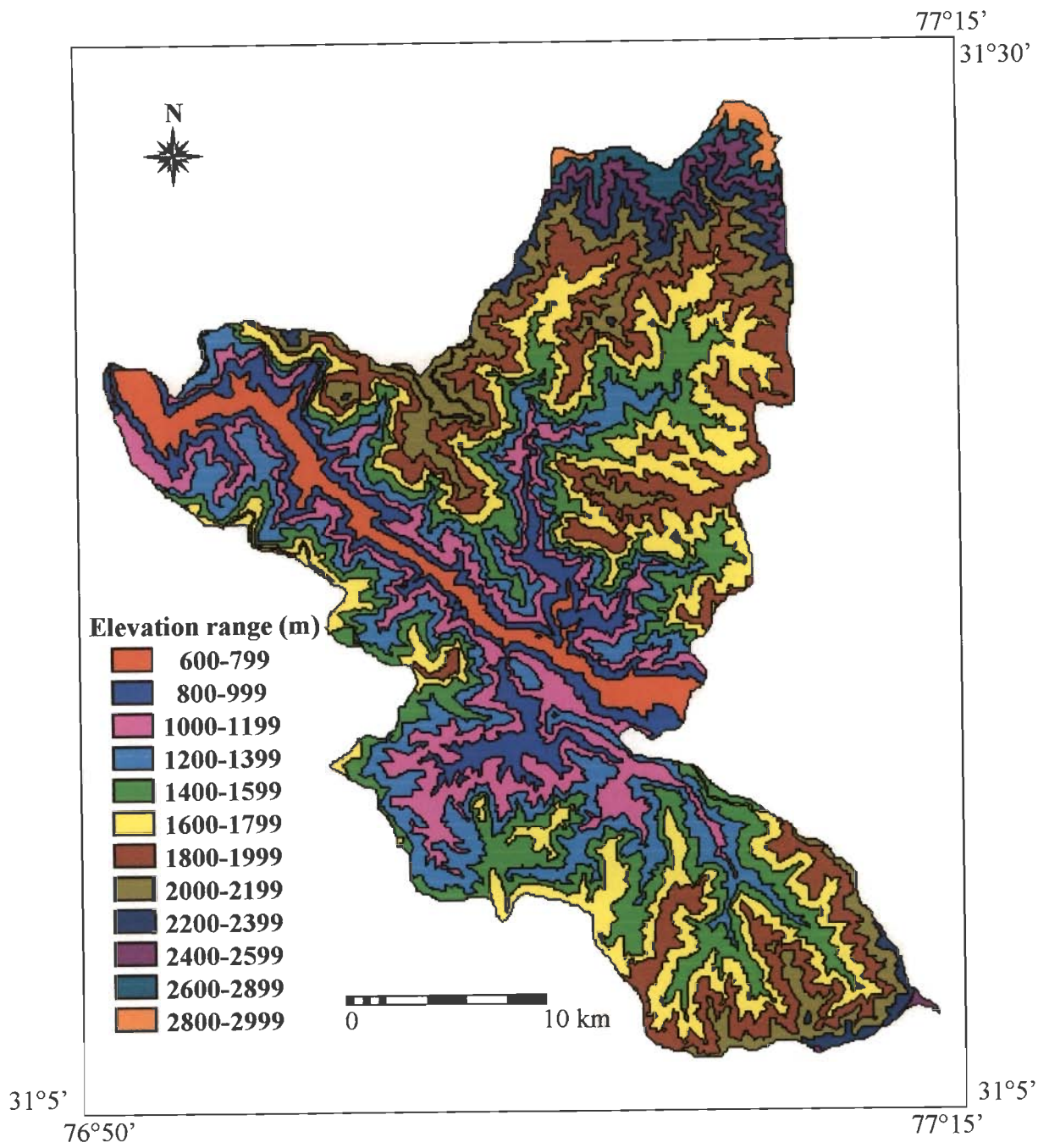


Fig. 6.6 Digital Elevation Model of the intermediate basin

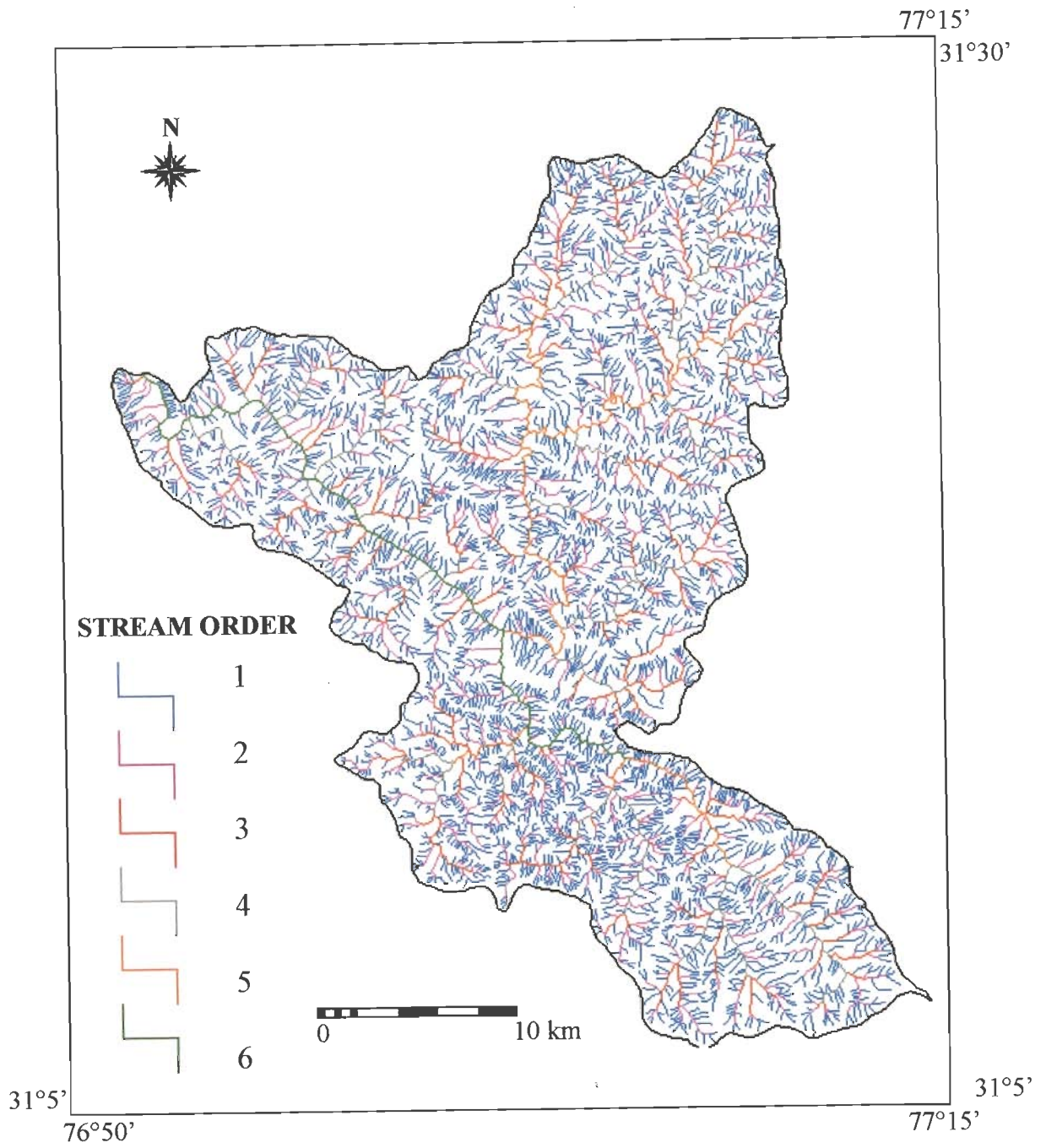


Figure 6.7 : Drainage network map showing different order streams of the intermediate basin

data for this sub-basin have been computed from the daily records available at Suni and Kasol.

Using the above determined parameters, the annual sediment yield for 3 years (1991-1993) was calculated from the empirical relationship given in the Equation (6.4). The annual sediment yield values obtained for 3 years using this relationship are given in Table 6.5.

Table 6.5: Annual values of sediment yield for different years

Year	Observed values (t/km ²)	Estimated values using original equation (t/km ²)	Ratio between observed and estimated value
1991	8143.18	1187.77	6.85
1992	8391.08	2134.77	3.93
1993	4688.66	1523.06	3.07

It is noted from the above table that the estimated values of annual sediment yield are less than the observed the sediment yield for all the year. Moreover, the results show that magnitude of underestimation of sediment yield was similar for all the years. It is understood that the basic reason for underestimation of sediment yield may be that this equation was developed for the plain regions, not for mountain basins. Because precipitation distribution is different in mountainous areas, therefore, the possible reason for underestimation of sediment yield may be orographic behaviour of precipitation due to mountainous terrain of the basin. The behaviour of precipitation in the mountainous basins is very much different than that of plain basins and varies with altitude (Singh et al., 1995, 1997). In the present analysis, only weighted average of two rainfall stations located at the bottom of valley was used in calculation. In fact average rainfall of these two stations does not represent the actual rainfall in the basin. Therefore, an orographic factor, which takes into account the rainfall distribution in the mountainous areas, should also be included in

the above relationship. A study on the effect of orography on precipitation distribution in the Satluj basin has been carried out by Singh et al. (1997). In this study, variation in rainfall with altitude in the Satluj basin has been carried out for three different parts of the Himalayas, i.e., outer, middle and greater Himalayas. For this purpose the stations falling in windward side and leeward side have been studied separately. This study basin falls in the outer Himalayas on leeward side and for this part the annual rainfall increases linearly with altitude. Keeping in view high relief of basin, elevation varies from 600 m to 3000 m, the rainfall increases linearly with elevation. It is expected very high rainfall in the middle and upper parts of the basin. Hence for this basin the P factor has to be multiplied with a constant factor on the basis of orography. To derive this factor, a ratio between observed and estimated annual values of sediment yield was determined for all the three years as given in Table 6.5. It was assumed that an average of these three values will be representative of this factor called as orographic factor. Based on 3-year results, the orographic factor was determined to be 4.60. The Equation (6.4) was revised based on this factor and revised equation is obtained as follows.

$$S_a = 1.118 * 4.60 * 10^{-6} P^{1.29} A^{1.03} D_d^{.40} H^{0.08} F_c^{2.42}$$

or

$$S_a = 5.46 * 10^{-6} P^{1.29} A^{1.03} D_d^{.40} H^{0.08} F_c^{2.42} \quad (6.5)$$

The computation of annual sediment yield for intermediate basin was made using the revised equation for the two independent years, i.e., for 1994 and 1996. The revised value of sediment yield were estimated and given in Table 6.6. From these values it is found that for two years, the estimated value of annual sediment yield is close to observed

value. A comparison of these results was made with the results obtained using developed regression relationship given in last section and presented in Table 6.7.

Table 6.6: Observed and estimated values of sediment yield for different years.

Year	Observed (t/km ²)	Estimated value using original equation (t/km ²)	Estimated value using revised equation (t/km ²)	Difference in obs. and est. values (%)
1994	10261.0	1927.89	8917.19	13.1
1996	565.48	1851.21	8542.67	8.7

Table 6.7: Sediment yields using developed regression equation and using revised equation

Year	Observed value (t/km ²)	Estimated value using developed regression equation (t/km ²)	Difference in obs. and est. values (%)	Estimated value using revised equation (t/km ²)	Difference in obs. and est. values (%)
1994	10261.00	6370.7	37.9	8917.19	13.1
1996	7565.48	6092.8	19.4	8542.67	8.7

From the table it is clear that the percentage error using the above revised relationship is less in comparison to the method based on regression relationship (first approach). In other words the second approach, which considered physical characteristics of the basin, produced better results.

The sediment yield from the Satluj basin enters the Bhakra reservoir located at the downstream limit of the basin. In the above study sediment yield has been estimated at Kasol, which is at the tip of the Bhakra reservoir. Therefore the total sediment yield at the site Kasol represents the sediments which is coming to the reservoir. The total sediment entering into the reservoir will reduce the capacity of the reservoir. From this reduction in the capacity the sedimentation rate can be determined. The sedimentation of reservoir due to higher magnitude of sediment yield is estimated using remote sensing and the same is described in

the next section.

6.2 ASSESSMENT OF RESERVOIR SEDIMENTATION USING REMOTE SENSING

For the present study, Bhakra reservoir located on Satluj River has been selected for the assessment of sedimentation. This reservoir has an enormous spread of water extending over 168.35 km² at full reservoir level of 515.11 m. In the present study application of remote sensing technique has been made for the estimation of sedimentation in the reservoir and the methodology is described in the following sections.

6.2.1. Availability of satellite data

Selection of appropriate period for analysis is very important for the study of reservoir sedimentation assessment using remote sensing technique. The only useful information extracted from the remote sensing data is the water spread area of the reservoir at different dates of pass of the satellite. Though in the wavelength region 0.45 - 0.52 μm , the information within 1 - 2 m depth below the water surface (like sediment concentration, shallow water depth etc.) can be obtained, however it can not be used to quantify the amount of sediment deposition in the reservoir. Therefore, it is imperative to use the remote sensing data of such a period when there is maximum variation in the elevation of the reservoir water surface and consequently, the water spread area.

In India, the reservoirs generally attain the highest level near the end of the monsoon period (October - November) and then deplete gradually before the onset of next monsoon (June - July). Thus, temporal remote sensing data for any water year (October - June) can be selected and analysed. In case, the historical records of maximum and minimum water level for every year are available, the water year of maximum variation is considered the best year

for sedimentation analysis. It is also desirable to select the remote sensing data series of the same water year in sequence to the extent possible, and preferably, the satellite images at the monthly intervals be used.

In the present case, the historical record of annual maximum and minimum observed levels was available with the dam authorities, Bhakra Beas Management Board (BBMB), Nangal. In the present study, the analysis was carried out for two years (1988-89 and 1996-97). In the year 1988-89, maximum level at 514.499 m was observed on 13th. September 1988. The reservoir level fell gradually till the minimum level of 464.286 m was observed on 17th. May 1989. In the year 1996-97, maximum level at 511.771 m was observed on 22nd. September 1996 and the reservoir level fell gradually to the minimum level of 448.75 m on 5th. June 1997. The availability of satellite data is already given in Chapter 3.

It is important to mention here that for the year 1988-89, the sedimentation assessment was restricted to 513.904 m (1.10.88) to 472.232 m (17.4.89) zone of the reservoir. While for the year 1996-97, the sedimentation assessment was restricted to 510.46 (16.10.96) to 450.436 (15.06.97) zone of the reservoir. Further under normal circumstances, the reservoir level varies within or around this range and our main concern was to quantify the sedimentation rate and assess the sediment deposition pattern in the zone of operation (live storage).

6.2.2 Processing of remote sensing data

In this study, digital analysis of several IRS 1B-LISS II scenes were carried out for identifying the water pixels and for determining the water spread area. The following steps were used in the analysis:

6.2.2.1 Import and Visualisation

The data of IRS-1A and IRS-1B satellite and LISS-II sensor for two years 1988-89 and 1996-97 were received from NRSA on the CD-ROM media. The data were processed and analysed using the ERDAS/IMAGINE 8.3.1 software. The data were loaded on the computer from the CD-ROM and was imported in the ERDAS system. Each scene was having 2500 rows, 2520 columns and the information of four bands (three visible and one near-IR). Initially, a false colour composite (FCC) of 4, 3 and 2 Bands combination was prepared and visualised. Then, each individual band was visualised one by one. The pixels representing water spread area (except at the periphery) of the reservoir were quite distinct and clear in the FCC.

6.2.2. Geometric registration

While using the temporal satellite data of the same area, it is required to register the images of different time periods. Using the registered imageries, it was possible to overlay the remote sensing data of different dates, to compare the change in the water spread area and to observe the shrinkage in the water spread with time, particularly the tail end of the reservoir.

The images of October, 1988 was considered as the base image since it was very sharp and clear and was completely cloud and noise-free. The images of other dates were registered with this image. For carrying out the registration, some clearly identifiable Ground Control Points (GCPs) like crossing of rivers, canals, sharp turns in the rivers, dam, bridges etc. were located on both the images. Ten GCPs were selected for geo-referencing in all the cases. A polynomial transformation of first order was performed and resampling was done using the nearest neighbour interpolation method. Now looking at the statistics, some points, which generated big errors, were deleted and replaced by other points so as to obtain

the satisfactory registration. In this manner, all the available images were registration with respect to base map. After completing this process, different images were displayed one over the other and the superimposition was compared. The registration of the images was found to be satisfactory.

6.2.2.3 Identification of Water Pixels

The identification of the water pixels was the basic information, which was extracted from the remote sensing data. Though spectral signatures of water are quite distinct from other land uses like vegetation, built-up area and soil surface, yet identification of water pixels at the water/soil interface is very difficult and depends on the interpretative ability of the analyst. Deep-water bodies have quite distinct and clear representation in the imagery. However, very shallow water can be mistaken for soil while saturated soil can be mistaken for water pixels, especially along the periphery of the spread area. Secondly, it is also possible that a pixel, only at the soil/water interface, may represent mixed conditions (some part as water and other part as soil).

Different techniques were tried to distinguish and separate out the water pixels. Density slicing of the near-IR band was carried out and compared with the standard FCC. Though most of the water pixels could be accounted for by this technique, it was not considered to give exclusive water pixels in a satisfactory way. The sliced pixels may include some saturated soil pixels also, as the reflectance value of saturated soil is very low in the near-IR band. Supervised classification is another way of identification. Though clearly distinguishable water pixels could be easily separated out by this technique, accurate training sets for peripheral pixels could not be given. In the present study, a generalised algorithm, based on the information of different bands, was used for differentiation of water pixels.

Using the spectral information, the algorithm matches the signatures of the pixel with the standard signatures of water and then identifies whether a pixel represents water or not. The algorithm checks for one condition for each pixel and if a pixel satisfies the conditions, then it is recorded as a water pixel, otherwise not. The condition states that "If the DN value of near-IR band of the pixel is less than the DN value of the band 2 and Band 3, then it must be classified as water otherwise not". Since the absorptance of electromagnetic radiation by water is maximum in the near-IR spectral region, the DN value of water pixels is appreciably less than those of other land uses. Even if the water depth is very shallow, the increased absorptance in the band 4 will cause the DN value to be less than band 3 and band 2. If the soil is exposed (may be it is saturated) at the surface, the reflectance will be as per the signatures of the soil which increases with wavelength in this spectral range. So, this condition differentiates the water pixels exclusively from other pixels.

This condition was employed to differentiate the water pixels in all the imageries. The resulting image of water pixels from this method was compared with the near-IR image and the standard FCC. The results were found to be satisfactory in all the cases. The biggest advantage of using this method was that it avoided the necessity of selecting different limits as is required in NDVI or density slicing. Selection of different limits in different images can cause some non-water pixels to be selected or some water pixels to be rejected.

6.2.4 ANALYSIS AND RESULTS

6.2.4.1 Calculation of sediment deposition

To estimate the actual silt deposits in the Bhakra reservoir vis-à-vis the project assumptions, hydrographic surveys have been carried out in the reservoir every year from 1963 to 1977 and thereafter these surveys were carried out every alternate year. The last hydrographic survey for this reservoir was carried out between October, 1996 to March,

1997. Hydrographic survey was carried out by sounding observations using echo sounder at the cross sections which are 610 m apart. For working out the quantity of silt deposited at each cross section and in the whole reservoir, these results were superimposed over the previous observations (WAPCOS, 1996, BBMB, 1997). Original elevation-area-capacity data of Bhakra is presented in tabular form in Table 6.8 below.

Table 6.8: Original elevation-area-capacity table for Bhakra Reservoir

Reservoir Elevation (m)	Area (Mm ²)	Capacity (Mm ³)
515.11	168.67	9867.86
513.58	165.92	9621.15
512.07	162.48	9346.62
505.97	149.93	8363.01
499.87	137.83	7462.56
493.78	125.04	6673.13
487.68	113.91	5957.71
481.59	103.19	5248.46
475.49	94.49	4687.23
469.39	85.99	4144.49
463.30	78.30	3642.24
457.20	71.46	3120.70
451.11	60.70	2781.50
445.01	59.00	2392.95
438.92	54.02	2053.75
432.32	49.29	1736.74
426.72	45.52	1443.17

The information on the levels of the Bhakra reservoir was obtained from Bhakra Beas Management Board (BBMB), the agency responsible for collection of required data and operation of the reservoir. The reservoir level data is collected from the gauge installed on the

dam. The hourly levels are recorded between 6 A.M. to 6 A.M. and mean daily value of the reservoir level is obtained taking the average of 24 hourly values. Using the original elevation-area as shown in Table 6.8 areas at the intermediate elevations (reservoir elevations on the dates of satellite pass) were obtained by linear interpolation. The revised areas and the corresponding elevations are presented in Table 6.9 for both the years i.e. 1988-89 and 1996-97. The FCC of maximum and minimum water spread area alongwith final water spread area are presented in Figures 6.8 and 6.9 for the year 1988-89 and in Figures 6.10 and 6.11 for the year 1996-97.

Table 6.9 : Reservoir elevation and estimated area on the date of satellite pass

Date of pass	Number of water pixels	Reservoir elevation (m)	Water spread area using remote sensing data (M m ²)
1/10/88	110736	513.90	145.51
14/11/88	108537	511.82	142.62
28/12/88	105000	504.96	137.98
19/1/89	104079	501.99	136.77
10/2/89	93692	496.28	123.12
4/3/89	78935	487.68	103.72
17/4/89	55982	472.23	73.56
16/10/96	106303	510.46	139.69
7/11/96	105120	506.21	138.13
21/12/96	90411	494.62	127.47
12/1/97	76005	487.73	108.99
15/6/97	37147	450.44	48.81

For computation of reservoir capacity between two consecutive reservoir elevations, usually three formulae, prismoidal formula, Simpson formula and trapezoidal formula are used (Patra, 2001). Out of these Trapezoidal formula has been most widely used for

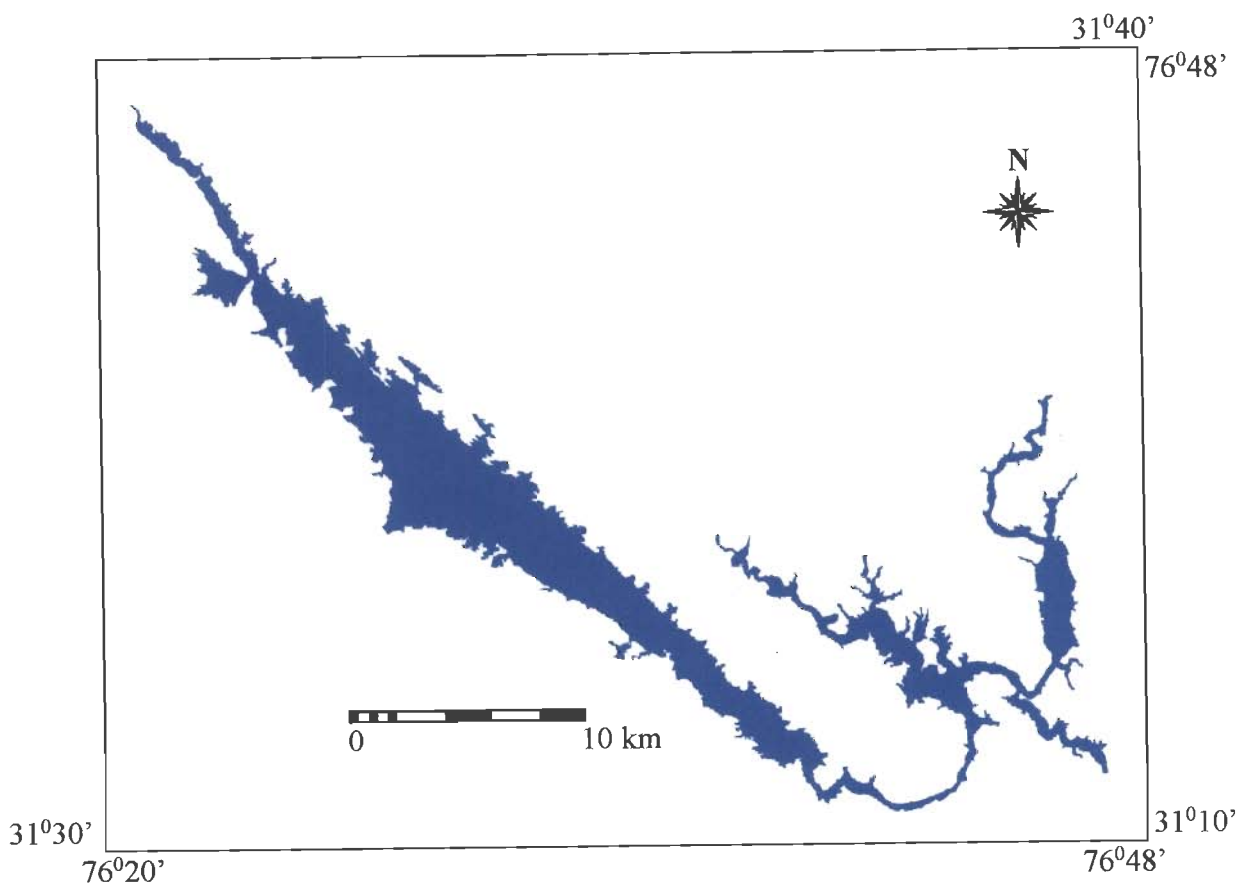
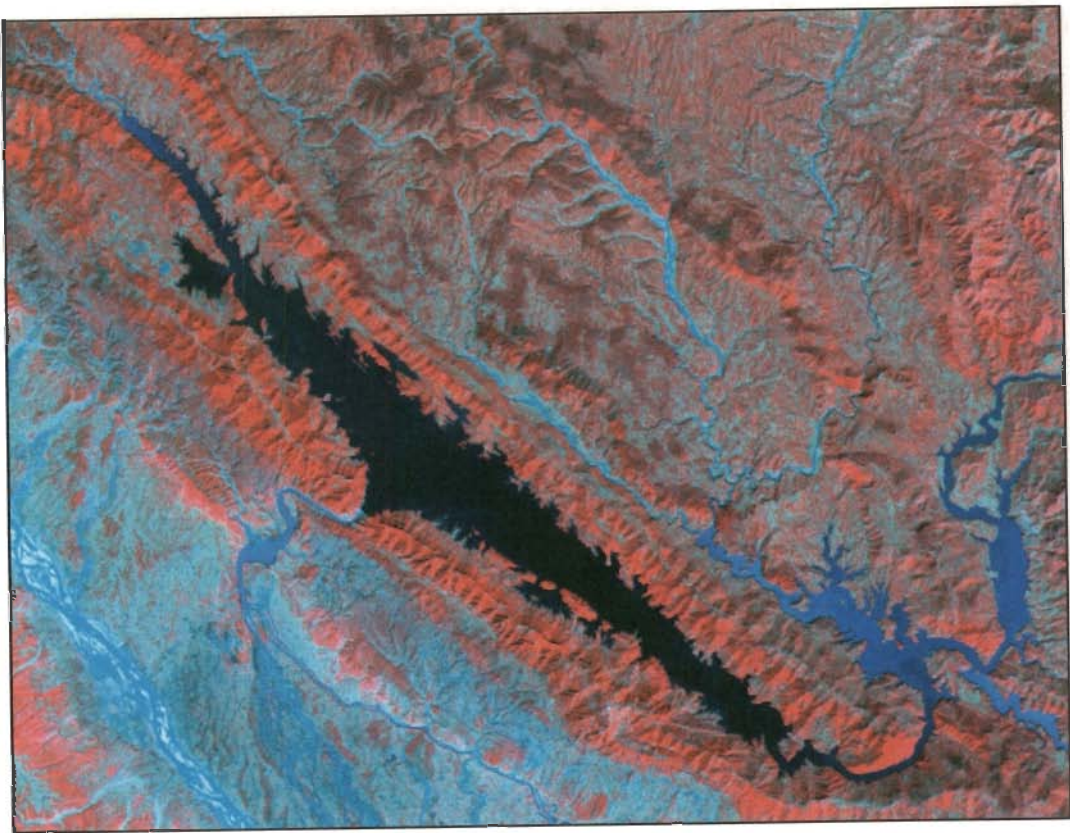


Figure 6.8 : FCC of IRS 1 A LISS II data of 1st. October, 1988 and water spread area of the Bhakra reservoir

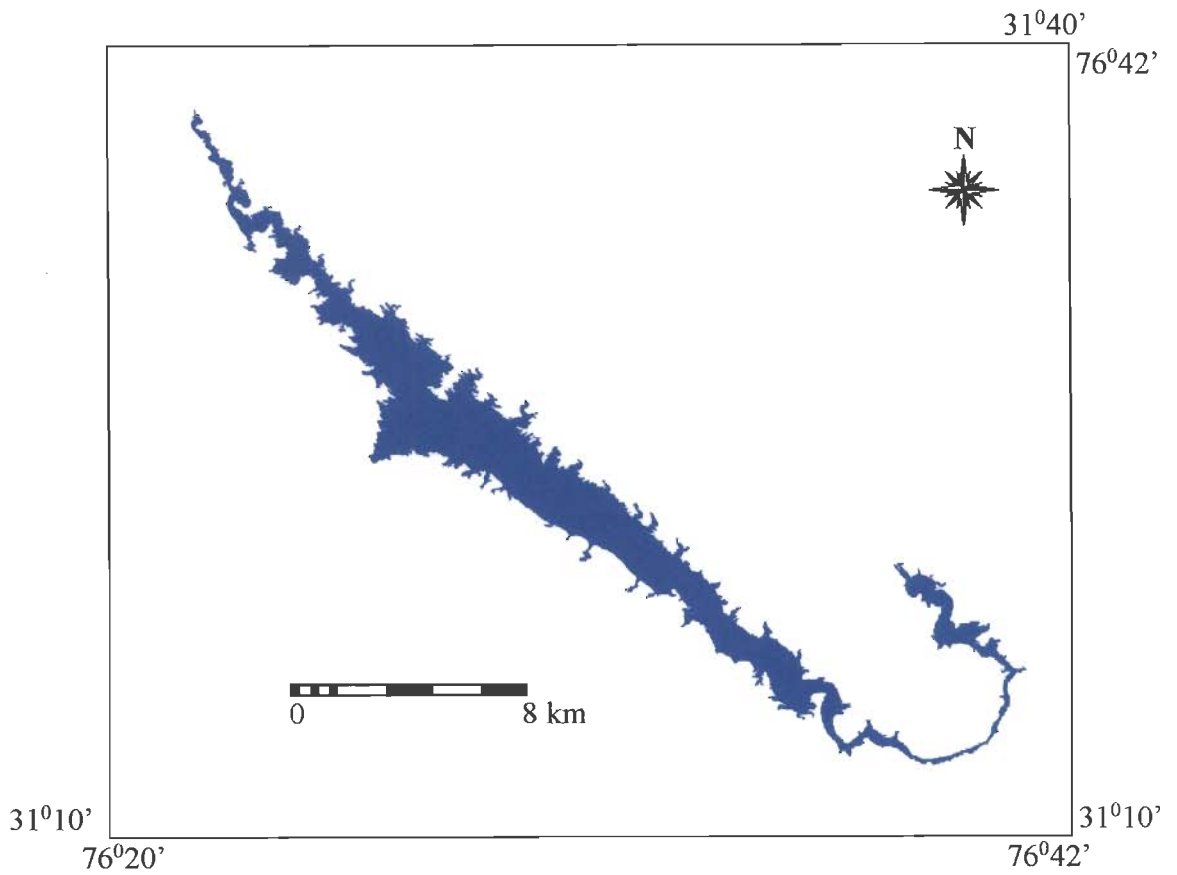
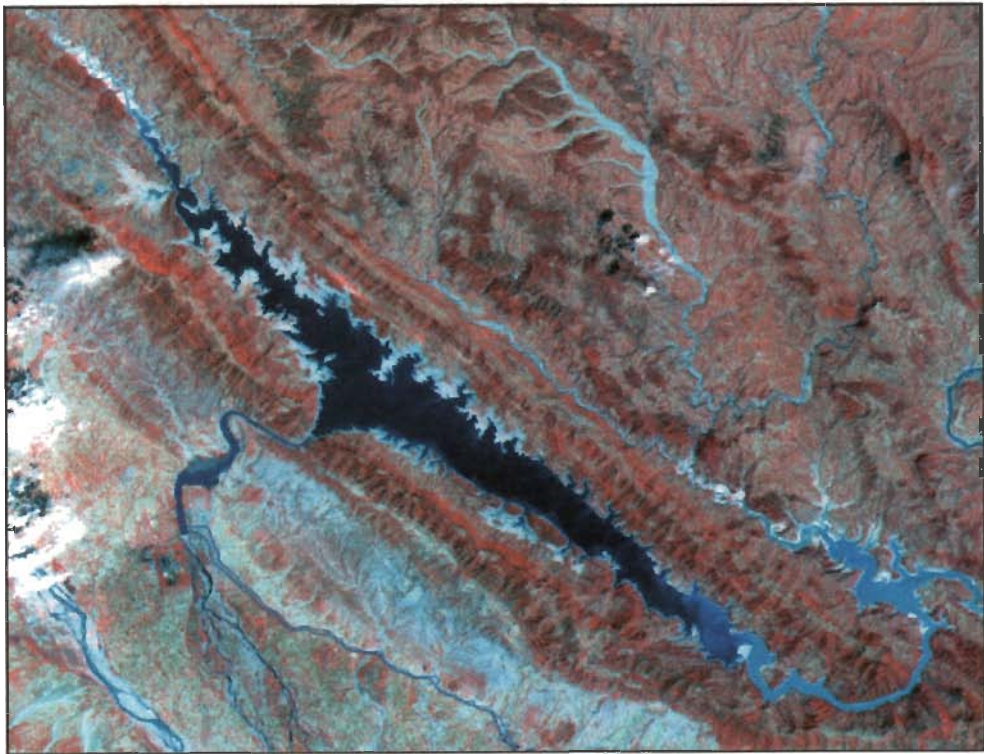


Figure 6.9 : FCC of IRS 1 B LISS II data of 17 April, 1989 and water spread area of the Bhakra reservoir

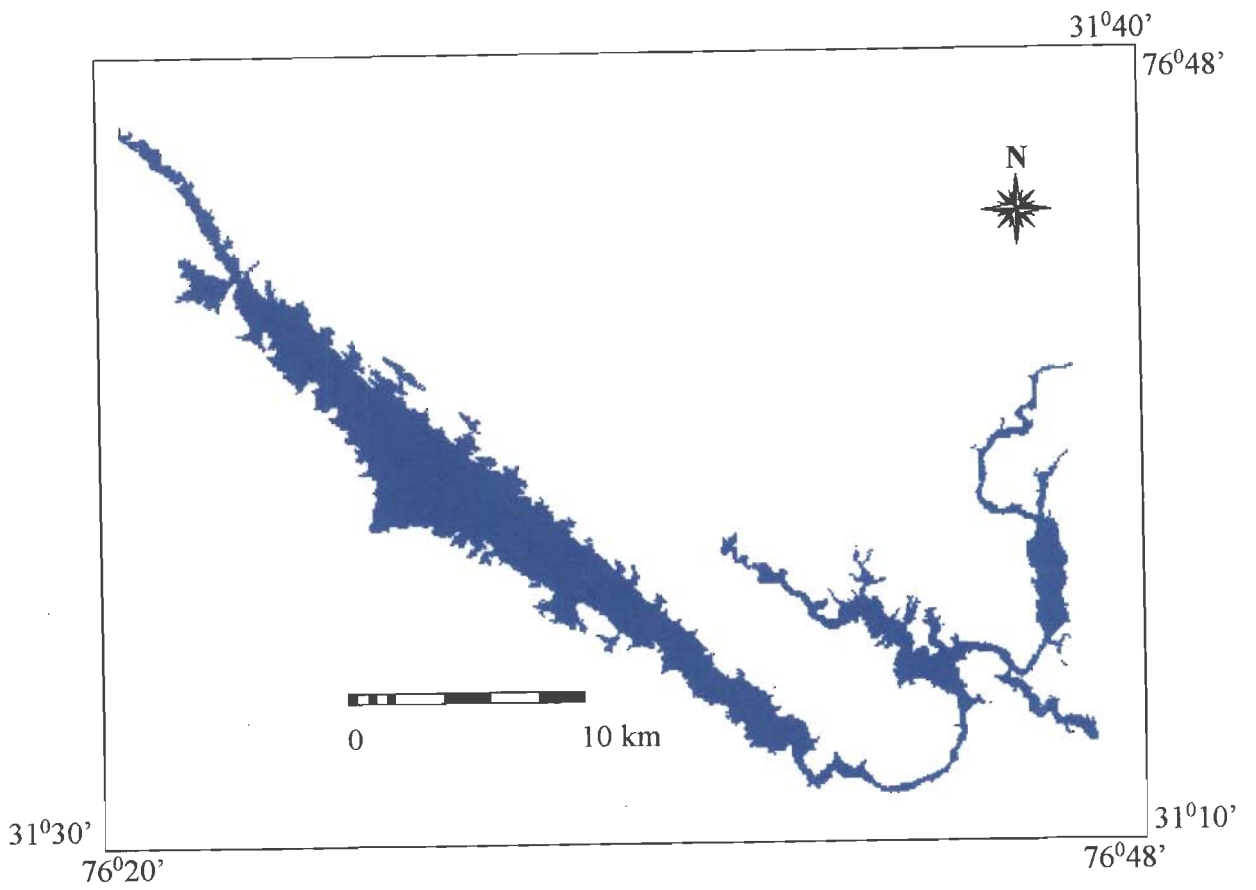
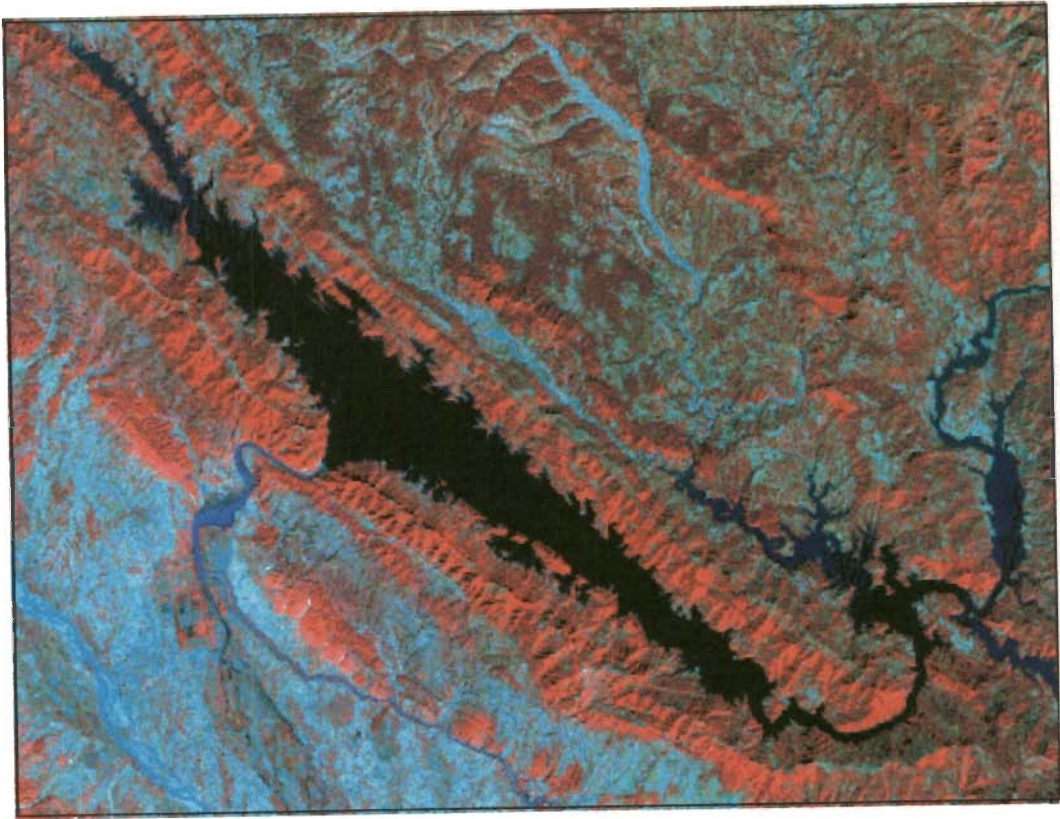


Figure 6.10 : FCC of IRS 1 B LISS II data of 16 October, 1996 and water spread area of the Bhakra reservoir

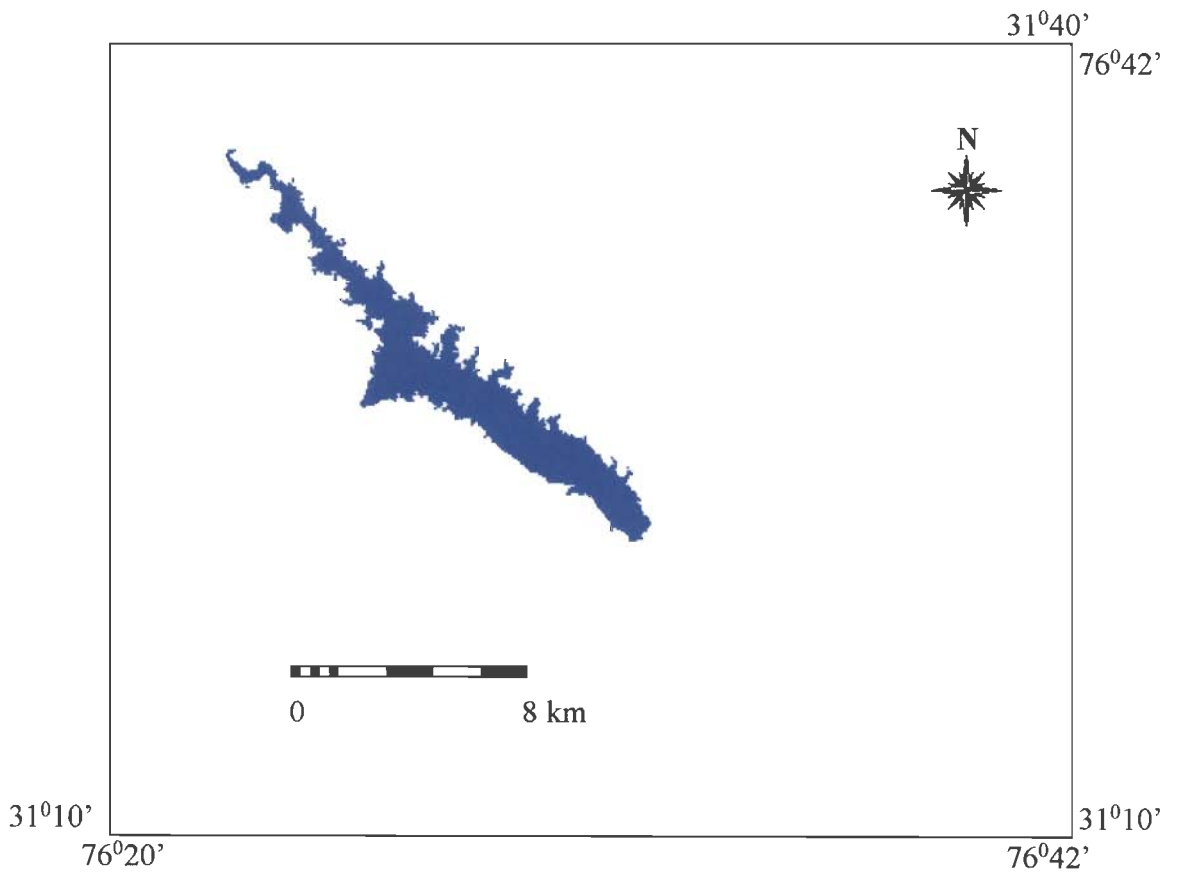
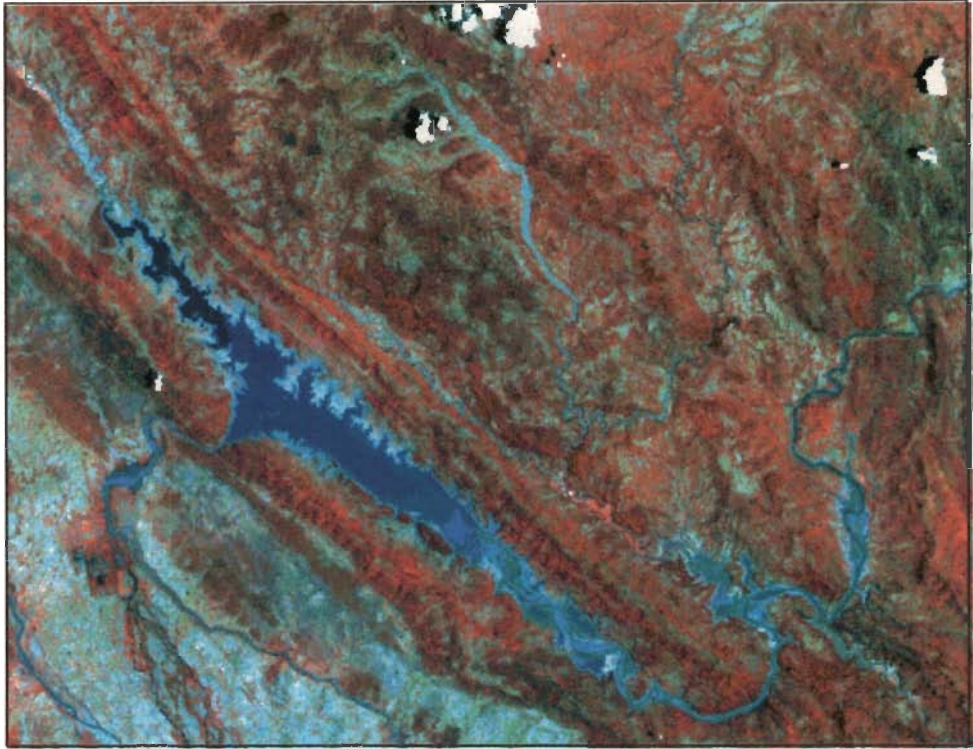


Figure 6.11 : FCC of IRS 1 B LISS II data of 15 June, 1997 and water spread area of the Bhakra reservoir

computation of capacity (Jayapragasam et al. 1980; Manavalan et al.; 1990, Goel et al. 1997). In this method, the cross sectional areas of range lines are planimetered and these data, together with surface areas at full reservoir level between adjacent ranges, are used to compute the sediment volumes, as follows:

$$V = \frac{H}{3} (A_1 + A_2 + \sqrt{(A_1 * A_2)}) \quad (6.6)$$

where V is the volume between two consecutive levels, A₁ is the contour area at elevation 1, A₂ is the contour area at elevation 2 and H is the difference between elevation 1 and 2. The volume of sedimentation deposit between two reservoir levels is computed from the difference between previous capacity survey and satellite derived information.

From the known values of original and estimated areas at different elevations, the corresponding original and estimated capacities were worked out as mentioned above. The cumulative estimated capacity of the reservoir at the lowest observed level (472.232 m) was assumed to be the same as the original cumulative capacity (4415.86 Mm³) at this elevation before the construction of the dam. Above the lowest observed level, the cumulative capacities between the consecutive levels were added up so as to reach at the cumulative original and estimated capacities at the maximum observed level. The difference between the original and estimated cumulative capacity represents the loss of capacity due to sedimentation in the zone under study. The calculations of sediment deposition for the year 1988-89 and 1996-97 are presented in Table 6.10 and 6.11 respectively. The results show that the volume of sediment deposition during 1965 to 1988-89 (24 years) in-between the maximum and minimum observed levels (513.904 m and 472.232 m) is 491.315 Mm³.

Table 6.10 : Calculation of sediment deposition in Bhakra Reservoir using remote sensing for the year 1988-89

Date of satellite pass	Reservoir elevation (m)	Original area (Mm ²)	Estimated area using remote sensing (Mm ²)	Original volume (Mm ³)	Estimated volume using remote sensing (Mm ³)	Original cumulative volume (Mm ³)	Estimated cumulative volume using remote sensing (Mm ³)
1/10/88	513.904	166.62	145.52	342.563	300.552	9656.178	9164.864
14/11/88	511.818	161.80	142.63			91313.616	8864.31
				1064.119	961.484		
28/12/88	504.964	148.83	137.98				7902.827
				432.658	408.507	8249.497	
19/1/89	501.990	142.18	136.77			7816.839	7494.32
				780.062	741.574		
10/2/89	496.281	131.14	123.12			7036.770	6752.706
				1057.294	974.317		
4/3/89	487.679	113.53	103.72			5985.483	5778.429
				1569.623	1312.942		
17/4/89	472.232	90.13	73.56			4415.86	4415.86

For the period up to 1996-97 i.e. for 32 years period the volume of deposition in-between the maximum and minimum observed levels (510.463 m and 450.436 m) works out to be 807.354 Mm³. If the uniform rate of sedimentation is assumed, then as per the 1988-89 analysis, the sedimentation rate in the zone (513..904 m to 472.232 m) is 20.47 M m³ per year. As per the 1996-97 analysis, the rate of sedimentation in the zone (510.463 m to 450.436 m) comes out to be 25.23 M m³ per year.

Table 6.11 : Calculation of sediment deposition in Bhakra Reservoir using remote sensing for the Year (1996-97)

Date of satellite pass	Reservoir elevation (m)	Original area (Mm ²)	Estimated area using remote sensing (Mm ²)	Original volume (Mm ³)	Estimated volume using remote sensing (Mm ³)	Original cumulative volume (Mm ³)	Estimated cumulative volume using remote sensing (Mm ³)
16/10/96	510.463	158.364	139.688	657.322	590.807	8745.836	7938.482
7/11/96	506.212	150.406	138.134	1603.107	1487.525	8088.575	7347.675
21/12/96	494.622	126.572	118.80	828.016	752.157	6485.408	5860.15
12/1/97	487.734	113.998	99.87	3264.892	2716.47	5657.392	5108.0
15/6/97	450.436	63.538	48.813			2392.950	2392.95

6.2.4.2 Comparison of remote sensing results with hydrographic survey

The results of the hydrographic survey carried out in the year 1988-89 are given in the report prepared by WAPCOS (1996). For this survey EAR method was applied to 1965 E-A-C curve to compute the sediment deposition pattern for 1988. The results of this hydrographic survey are given in Table 6.12.

The cumulative capacity at the lowest observed level was assumed to be equal to that of hydrographic survey and the cumulative capacity at the highest observed level was obtained. This was compared with results of hydrographic survey carried out in 1988-89. The calculations are presented in Table 6.13.

Table 6.12: Revised elevation capacity information for Bhakra Reservoir using the results of Hydrographic Survey of 1988-89 (WAPCOS, 1996)

Reservoir elevation (m)	Area (Mm ²)	Capacity (Mm ³)
515.11	168.67	8815.09
513.58	163.55	8570.18
512.07	159.38	8299.78
505.97	145.21	7340.00
499.87	132.16	6471.26
493.78	118.68	5718.48
487.68	107.03	5043.44
481.59	95.90	4377.33
475.49	86.88	3861.53
469.39	78.13	3365.97
463.30	70.26	2912.37
457.20	63.28	2440.10
451.11	52.43	2150.99
445.01	50.69	1813.01
438.92	45.71	1524.43
432.32	41.02	1258.00
426.72	37.33	1014.63

Table 6.13 : Comparison of Results of hydrographic survey with the results obtained using remote sensing

Date of satellite pass	Reservoir elevation (m)	Original volume (Mm ³)	Estimated volume using remote sensing (Mm ³)	Original cumulative volume (Mm ³)	Estimated cumulative volume using remote sensing (Mm ³)
1/10/88	513.90	336.45	300.55	8562.99	8362.75
14/11/88	511.82			8226.74	8062.20
		1031.56	961.48		
28/12/88	504.96			7195.18	7100.72
		416.70	408.51		
19/1/89	501.99			6778.48	6692.21
		742.79	741.57		
10/2/89	496.28			6035.68	5950.64
		978.04	974.32		
4/3/89	487.68			5057.64	4976.32
		1443.89	1312.94		
17/4/89	472.23			3613.75	3613.75

The plot of original and estimated cumulative capacity as derived using remote sensing technique is shown in Figures 6.12 and 6.13 for the year 1988-89 and 1996-97 respectively. The plots of the estimated cumulative capacity as per the hydrographic study and as per the remote sensing analysis for the year 1988-89 is presented in Figure 6.14.

As given above the rate of sedimentation in the reservoir using remote sensing was found to be 20.47 M m³ per year. The average rate of sedimentation for this reservoir using hydrographic survey was 21.93 M m³ per year (WAPCOS, 1996). The result obtained using remote sensing technique compares very well with the result obtained using hydrographic survey.

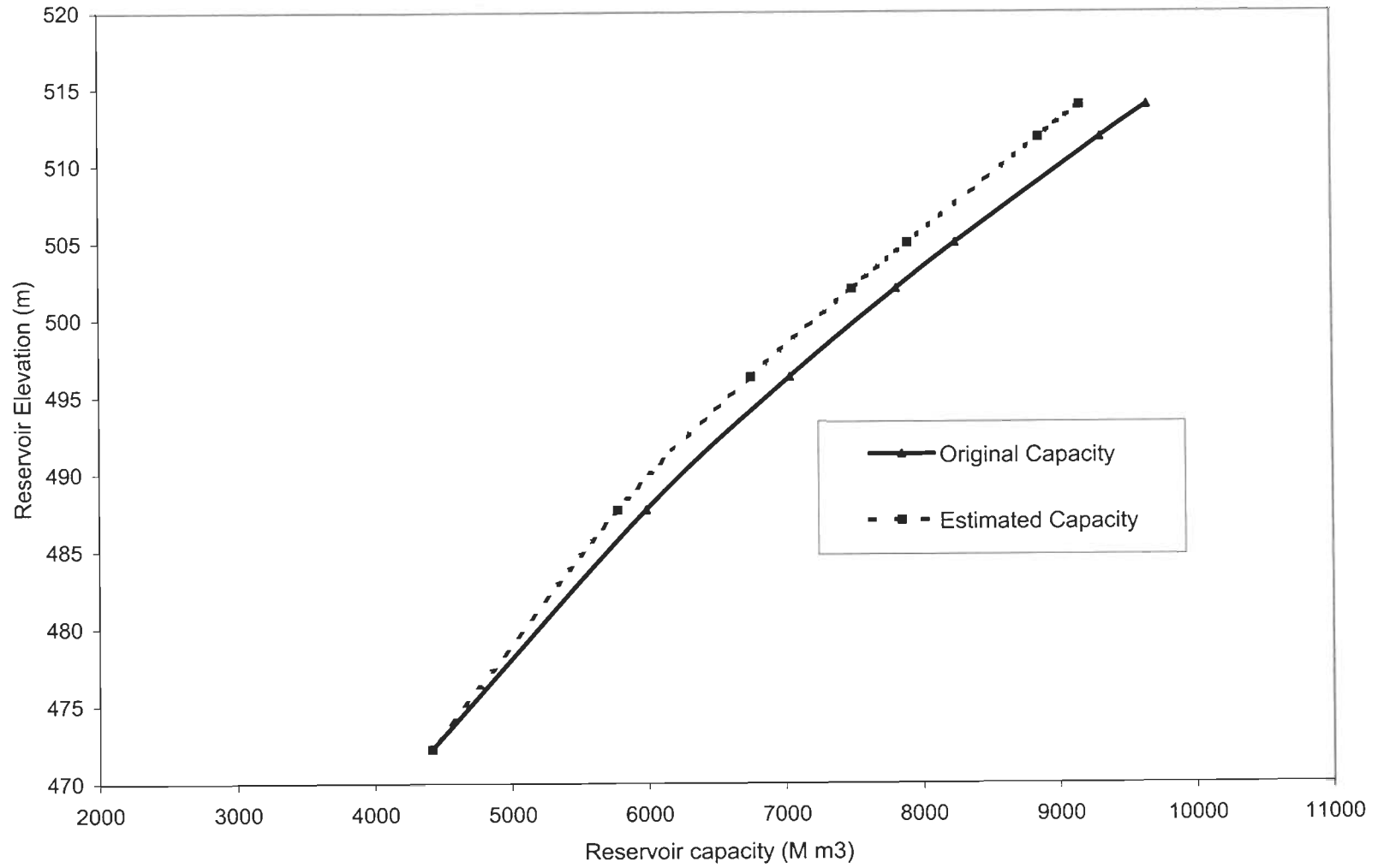


Figure 6.12: Elevation- capacity curves for Bhakra reservoir, India (1988-89)

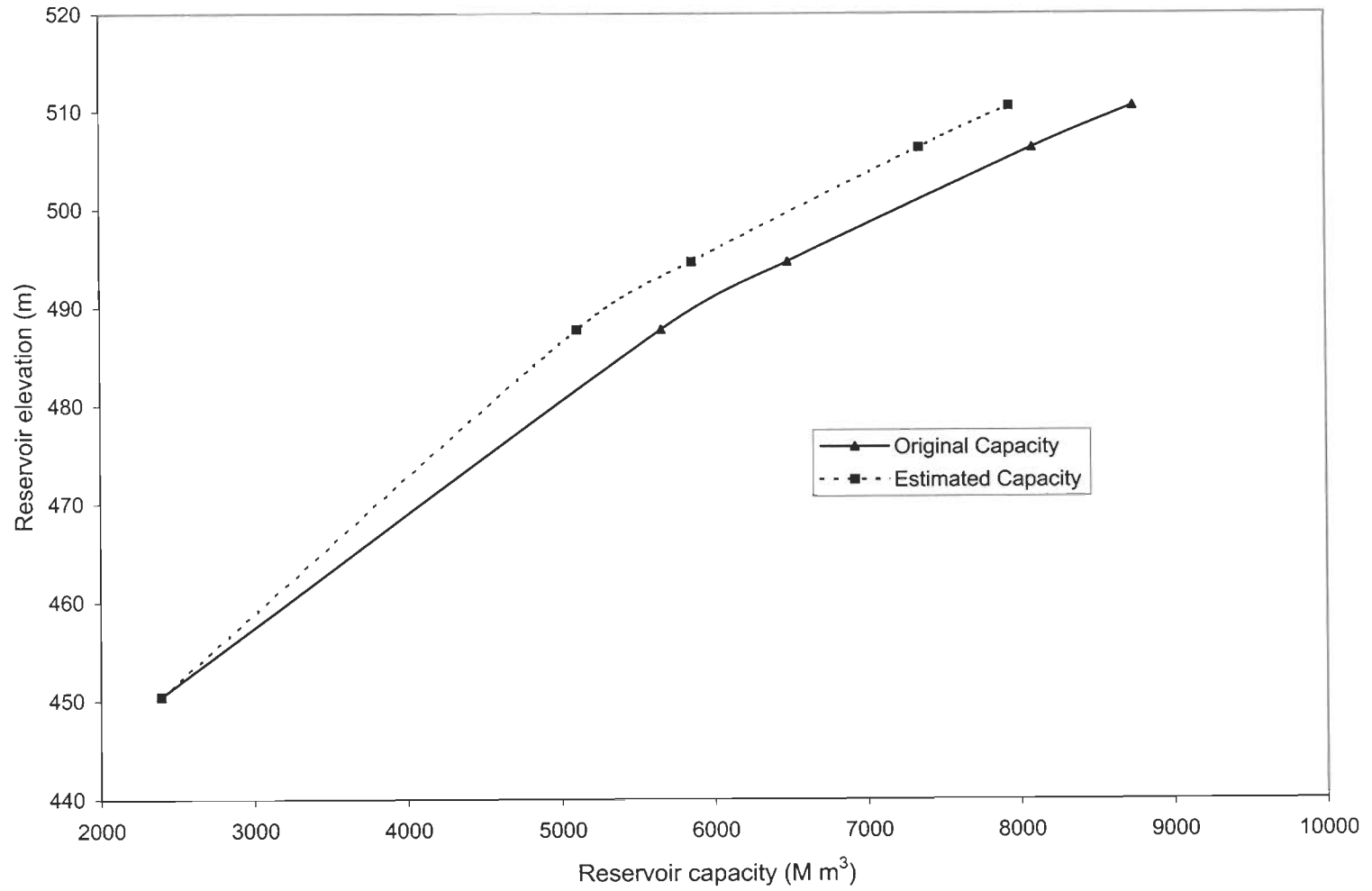


Figure 6.13: Elevation-Capacity curves for Bhakra reservoir, India (1996-97)

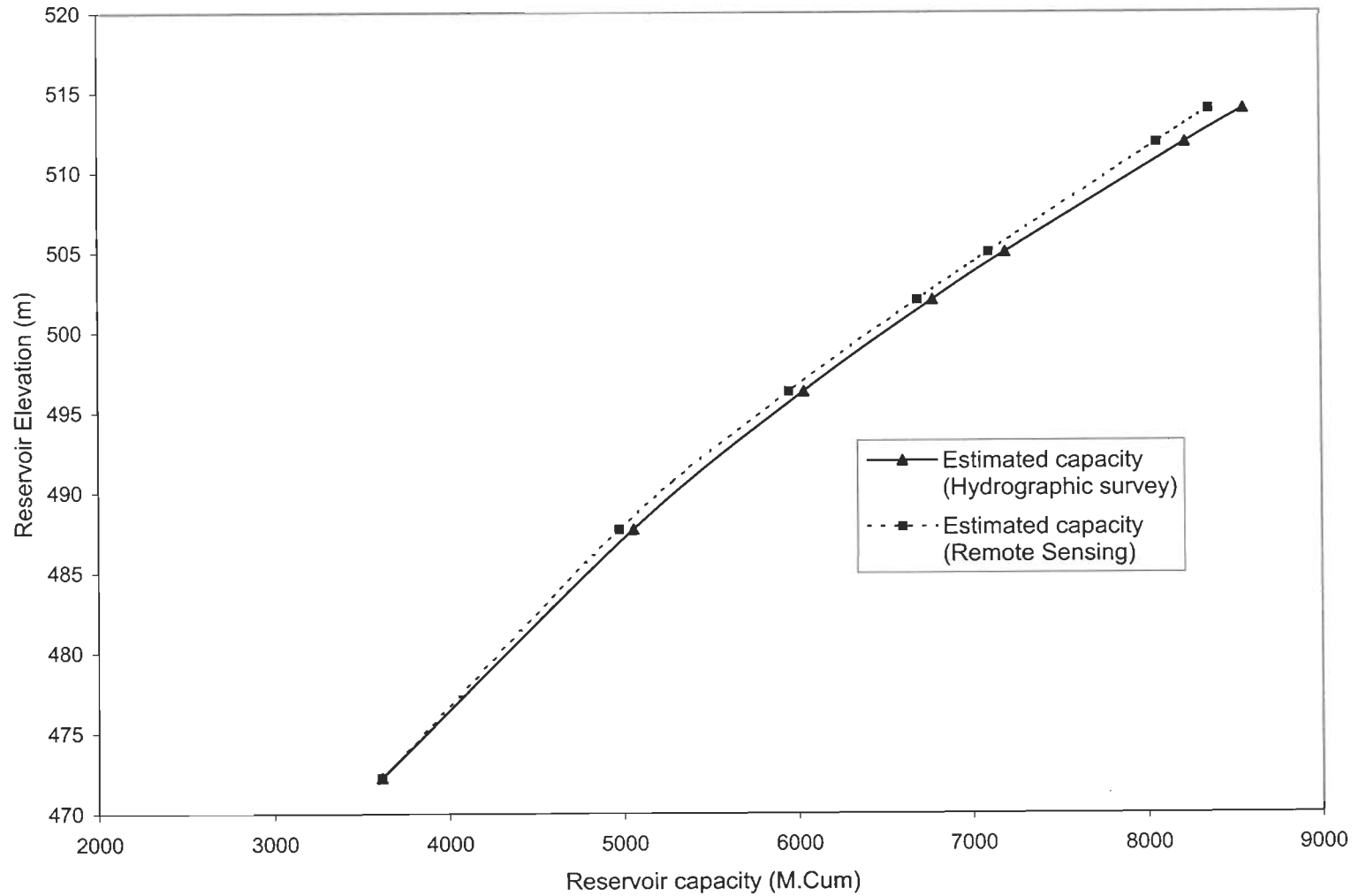


Figure 6.14: A comparison of the results obtained through remote sensing technique and hydrographic survey

The last sedimentation survey was carried out during 1996-and the sedimentation for dead and live load are given separately 97 (sedimentation survey report, 197). The results of the survey for the year 1996-97 are given in table 6.14.

Table: 6.14 Results of Hydrographic survey of 1996-97

Original designed capacity of reservoir in 1965			Capacity of the reservoir in 1996-97		
Dead stoarge (Mm ³)	Live storage (Mm ³)	Total (Mm ³)	Dead storage (Mm ³)	Live storage (Mm ³)	Total (Mm ³)
2431.81	7436.03	9867.84	1763.53	6769.96	8590.57

It is clear from the table that the loss in dead storage and live storage is almost same. In the present study, the analysis has been made only for live storage of Bhakra reservoir, therefore, the results of hydrographic survey for sedimentation in live storage were considered. Table 6.14 shows that as per the hydrographic survey, the loss of live storage from 1965 to 1997, i.e., for a period of 32 years is 666.07 Mm³, thus average sedimentation rate in this zone is 20.81 Mm³ per year.

For the year 1996-97, the estimated capacity, using remote sensing technique, (7938.48 Mm³) was subtracted from the original capacity (8745.84 Mm³) at the same level. The loss in capacity (807.35 Mm³) was attributed to the sediment deposition in the zone of study (510.46 m to 450.44 m) of the reservoir. Thus, the average rate of loss of capacity in the study is computed to be 25.23 Mm³ per year. It is clear from the results obtained using remote sensing based approach reasonably agrees with the results obtained from hydrographic survey.

It is seen that the estimation of sedimentation by remote sensing is highly sensitive to the accurate determination of water spread area. In the present case, an error of 1% in the

estimation of water spread area would result in the sedimentation difference of 48 M m^3 . Though every effort has been made to estimate the water spread area as precisely as possible and uniform method of analysis has been adopted for all the image data sets, yet the difference is equivalent to approximately 4% error in the area estimation. Some of the reasons for the difference between the two results can be either or a combination of the following:

- a) Different criteria of demarcating the tail end of the reservoir. In the present study, the tail has been truncated at the termination point of water spread. In almost all the dates of atleast upto December, when water spread area is more, some part at the tail end is not covered in the path/row obtained from NRSA. Extension of the tail end can result in the increase in spread area and the subsequent lesser volume of sediment deposition.
- b) Mixed pixels having larger proportion of land and smaller proportion of water around the periphery of the reservoir.
- c) In the image of December, 1988, the small storage upstream of the main reservoir was missing and therefore the area in this particular image represented the area of the main reservoir only.
- d) This is a peculiar reservoir consisting of two parts main reservoir and a small storage upstream of main reservoir. Both these storages are connected through a small stream. Since the main inflow in the Bhakra reservoir enters only after passing the small storage, most of the sediment deposition takes place in the small storage only without causing appreciable reduction in the area of main reservoir. Therefore, it is desirable to quantify the sedimentation rate in the small storage only. However, separate hydrographic survey results were not exclusively available for a small storage. Hence, this study was carried out for the full extent of water spread area. It is however, felt that frequent hydrographic survey may be carried out for the small storage while for the main reservoir the frequency of survey could be reduced.

CHAPTER 7

CONCLUSIONS

The Himalayan region is bestowed with tremendous potential of natural resources. Several projects are under operation and some more are coming up in this region to harness these resources. The success of these projects depends to a great extent upon availability of required streamflow having sediment load within permissible limits. The proper assessment of streamflow and sediment requires simple and systematic approaches keeping in view limitations of data availability. In this context, present study has been carried out for a Himalayan basin, i.e., Satluj basin up to Bhakra dam for (i) estimation of contribution snow and glacier (ii) development of a snowmelt runoff model (SNOWMOD) for estimation of streamflow from snowmelt and rainfall (iii) estimation of sediment yield and (iv) assessment of reservoir sedimentation using remote sensing approach. The available field data in the form of daily rainfall, temperature, evaporation, discharge and sediment yield data and Survey of India toposheets and satellite data (IRS-LISS-I, II, IRS-WiFS, Landsat) have been used. The following important findings and conclusions are drawn from the study:

1. A water balance approach has been developed for estimation of snow and ice melt contribution for snowfed basin, which uses rainfall data, and snow cover area information. Using this methodology, the average contribution of snow and glacier melt in the annual flow of Satluj River at Bhakra has been determined which is found to be about 59%. The remaining 41% contribution occurs from the rain. It shows that snow and glaciers provide a substantial contribution to the flows of Satluj River. The study shows that a major portion is covered by seasonal snow during winter. Using satellite data of various years, it

is found that on average about 14, 498 km² (65% of the total drainage area) of the Indian part of Satluj River up to Bhakra Dam, is covered by snow in the month of March. As such seasonal snow cover area is 9970 km² and this area becomes snow free during the melt season. After snow melt season about 4,528 km² (20% of the total drainage area) remains covered by perpetual snow and glaciers in the month of September. For all the sites upstream of Bhakra dam, the contribution of snow melt runoff in total runoff would be higher than 59% due to higher percentage of snow covered area in the upper basins. These findings of the present study are thus relevant for all the projects planned/under execution in the upstream of Bhakra dam.

2. In order to simulate the streamflow for a snowfed basin, which has significant contribution from snow and glacier melt, like Satluj basin, a hydrological model is required. There is no simple systematic model developed for Himalayan region for estimation of snowmelt runoff. Earlier attempts have been made mostly using simple regression type of approach, for this region. Therefore in this study, emphasis has been given for the development of snowmelt model keeping in view the limitations of data availability. The structure of the model has been kept simple and snowmelt has been computed by temperature index or degree-day method. Keeping in new the elevation range and data availability, the basin was divided into 10 elevation bands. During rainfall events in the basin, the effect of rain on melting of snow has also been incorporated in the model. For estimation of snow cover area in the basin and its variation with time, remote sensing data have been used. GIS was used for the preparation of the digital elevation map and computation of the aerial extent of snow cover in different elevation bands. The daily snow cover data was extracted from the depletion curves, which were prepared from the snow cover information obtained from the satellite data. The characteristics of snow cover

in the basin shows that the accumulation of snow at higher altitude zones starts from the month of October. By the end of March, the snowmelt season begins and the snowline recedes up to an elevation of about 2500 m by the month of September at the end of the melt season. It is seen that a large part of the study basin (nearly 50%) contributes actively to streamflow in the form of snowmelt runoff.

For computation of total streamflow at the outlet of the basin, the net inflows (after accounting for base flow and deep groundwater) emanating from the snow cover area and the snow free area have been computed separately. The net inflow from each part is also routed separately through cascades of linear reservoirs. Due to change in the snowline with the melting of snow during the melt period, the snow covered area and snow free area of the basin change with time. The variation in the snow cover area also changes the hydrological response of the basin. In the present study, the storage coefficients of the snow covered area and snow free area have been considered as four model parameters as a function of the respective areas and optimised in the calibration runs. The calibration was performed using the data of the three years 1985-86 to 1987-88 and values of the four optimised parameters were obtained. The sensitivity analysis of the optimized parameters was also carried out to find out the influence of change in each of the parameters on objective function. Using the values of optimized parameters, simulation runs were carried out for two data sets of three years independent years 1988-91 and 1996-1999. The results of calibration and simulation period show a very good performance in daily runoff as indicated by values of efficiency of model (R^2) of the order of 81% and above. The reproduction of the daily flows and hydrograph shape is quite satisfactory. The difference in observed and simulated volume is less than 7.5%. Overall the performance of the model is quite satisfactory. Although the model has been developed and applied for one of the

basins in the Himalayan region, it should be equally applicable to other basins as well. There is much scope to apply this model over other Himalayan basins.

3. The distribution of sediment yield in the study basin shows that the major contribution of sediment into the streamflow occurs in the summer season (April to October) while in winter season (November to March) it is insignificant. A relationship between sediment yield and discharge was established for 3 sites namely Suni, Kasol and for the intermediate basin between Suni and Kasol using 3 years (1991-1993) daily data. This relationship was used to estimate the value of sediment yield for the data of two independent years of 1994 and 1996. There is reasonably good agreement between estimated and observed daily data for these two years for the basin up to Suni and Kasol sites and also for intermediate basin.

For the intermediate basin, an alternative approach was also used and annual sediment yield from two methods was computed. Annual sediment yield using empirical relationship was estimated for intermediate basin from Suni to Kasol. In this approach physiographical characteristics of the basin were considered and required parameters were derived using GIS. The sediment yield computed using three years data by this relationship was underestimated. The reason for this may be attributed to the fact that this equation was developed using the data of Indian catchments located in plain regions while the study area lies in the Himalayan region, where good rainfall occurs due to orographic effect on precipitation. Therefore, the equation was revised by including the orographic factor and sediment yield was re-estimated for 2 years, 1994 and 1996. After incorporating orographic factor, the estimated value of sediment yield with the revised equation is in close agreement with the observed value. A comparison of estimated values of sediment yield for two approaches viz. developed regression relationship and revised equation was also made for intermediate basin. It is found that the results obtained using the second

approach, i.e., revised equation, which considered the physiographical characteristics and orographic factor of the basin, provides better results.

4. The sediment yield generated in the higher reaches cause sedimentation of Bhakra reservoir located downstream on the Satluj River. The conventional methods such as hydrographic and inflow-outflow approaches are in use for estimation of sedimentation in reservoirs. These methods are cumbersome, time consuming and expensive. Therefore in the present study, a new approach based on remote sensing data has been developed and applied. The present analysis using remote sensing data shows that the average sedimentation rate for 24 years (1965-1989) is 20.47 Mm^3 per year, whereas ground observations through hydrographic survey provided sedimentation rate 21.93 Mm^3 for the same period. While the analysis carried out for 32 years (1965-97) gives the sedimentation rate of 25.23 Mm^3 against the hydrographic survey result of 20.84 Mm^3 . The results obtained using remote sensing based approach reasonably agree with the results obtained from hydrographic survey. However, the discrepancy in the rate obtained using remote sensing data can be explained on the basis of accuracy in the determination of water spread area and mixing of water pixels with the land around the periphery of the reservoir.

Satellite remote sensing provided the information on the capacities in the water level fluctuation zone only, which generally lies in live zone of the reservoir. Below this zone i.e., in dead load zone the information on the capacity could be taken from the most recently conducted hydrographic survey. Application of satellite remote sensing technique has enabled a fast and economical estimation of live storage capacity loss due to sedimentation. Keeping in view the cost and time involved in hydrographic surveys it is recommended that hydrographic surveys may be conducted at longer intervals and the

remote sensing based sedimentation studies may be carried out at shorter intervals to make both surveys complementary to each other.

7.1 LIMITATIONS AND SCOPE FOR FUTURE WORKS

From the present study, it was found that the contribution from snowmelt is very significant in the Satluj basin. The similar studies for basins at different sites located in the Himalayan region could be carried out using the methodology developed in this study.

The snowmelt model developed for the present study estimates the runoff of a mountainous snow fed basin based on the temperature index approach. The frequent observation of snowline or snow cover area in the basin in conjunction with the satellite data is likely to improve the accuracy of the snowmelt simulation. The consideration of orographic effect on the precipitation in the high altitude basins would provide an accurate representation of the precipitation distribution with elevation in the basin. The lack of hydrometeorological stations at the higher altitudes restricts the accurate assessment of meltwater. In the present study, the temperature data was extrapolated using the lapse rate of $0.6^{\circ}\text{C}/100\text{ m}$. However, it is always better to establish the actual lapse rate for the catchment. The actual lapse rate study would help in appropriate temperature distribution of the temperature in all the elevation zones. The incorporation of the above mentioned points in the model may improve the performance of the model. The seasonal variation in degree-day factor and runoff coefficients needs to be studied systematically for small experimental basins.

Provision of snowpack simulation using the snowfall data can also be considered for future studies. Further, it is noteworthy that the catchments located at higher altitudes have considerable contribution to the runoff due to the glacier melt also. The glacier melt component can also be incorporated in the model separately. SNOWMOD may be applied

for streamflow forecasting in the Himalayan rivers, which would require an additional information on the meteorological parameters in advance.

The sediment yield and sedimentation studies in other parts of the Himalayan region can also be conducted with the approach developed in this study. In estimation of sediment yield using physiographic data the availability of field data in the upper reaches of Himalayan basin is a limitation. The use of better resolution (spatial and temporal) satellite data can be a remedy for the problems of exact water spread area estimation up to some extent. There is also much scope for application of the remote sensing based approach for assessment of sedimentation in reservoirs located in Himalayan region and elsewhere. Considering the time and cost involved the hydrographic surveys may be conducted at longer interval and the remote sensing based sedimentation surveys may be carried out at shorter intervals. Such practice will be very economical and quicker without any loss in the accuracy of results.

BIBLIOGRAPHY

1. Agrawal, K.C., Kumar, V. and Das, T., 1983, Snowmelt runoff for a catchment of Beas basin. Proceedings of the First National Symposium on Seasonal Snowcover, 28-30, April, SASE, Manali, Vol.-II, 43-63.
2. Agarwal, S., 1991, Effect of Sedimentation - Reservoir Planning. Proceedings for Regional Training Course on Reservoir Sedimentation & Flood Control organised by CWC, December 9-22, 1991.
3. Ageta, Y., 1976, Characteristics of the precipitation during the monsoon season in Khumbu Himal. (In: Higuchi, K., Hakajima, C. and Kusunoki, K., eds. Glaciers and Climates of Nepal Himalayas. Report of the Glaciological Expedition to Nepal. Seppyo, Special Issue, no. 38: 84-88.)
4. Alford D., 1992, Hydrological Aspects of the Himalayan Region. ICIMOD Occasional paper no. 18, Kathmandu, Nepal.
5. Anderson, E.A., 1972, Techniques for forecasting snowcover runoff'. Proceedings of the Symposium on the Role of Snow and Ice in Hydrology', Vol.-II, 840-863.
6. Anderson, E.A., 1973, The National Weather Service River Forecast System – snow accumulation and ablation model. NOAA Technical Memorandum NWSHydro-17, Washington D.C.
7. Anderson, E.A., 1976, A point energy and mass balance model for a snowcover. NOAA Technical Report, NWS19, U.S. Department of Commerce, Washington, D.C., pp. 150.
8. Anderson, E.A., 1978, Streamflow simulation models for use on snow covered watersheds. Proceedings of the U.S. Army Cold Research and Engineering Laboratory, Hanover, New Hampshire, 336-349.
9. Anonymous, 1986, Annual soil and water and conservation report for Satluj catchment under centrally sponsored scheme of soil conservation in the catchment of river valley projects, 1984-85 & 1985-86, department of Forest and Conservation, Government of Himachel Pradesh, Shimla, pp. 41.
10. Archer, D.R., Bailey, J.O., Barret, E.C., and Greenhill, D. 1994. The potential of satellite remote sensing of snow cover Great Britain in relation to snow cover. Nordic Hydrology, 25, 39-52.
11. Armstrong, R., and Hardman M., 1991, Monitoring global snow cover. In Proc. IGRASS'91, IEEE No. 91CH2971-0.
12. Arnborg, L., Walker, H.J. and J. Peippo, 1967, Suspended load in the Colville River. Alaska. Geograf. Annals, Vol. 49, 131-144.

13. Arora, V.P. and Sharma, B.K., 1991, Hydropower development- Role of Himachal Pradesh, India. International conference on hydropower development in Himalayas, April 20-22, Shimla, India.
14. Bagchi, A.K., 1981, Snowmelt runoff in Beas catchment using satellite imageries. Ph.D. Thesis, Department of Civil Engineering, University of Roorkee, Roorkee.
15. Bagchi, A.K., 1982, Orographic variation of precipitation in a high-rise Himalaya basin. (In: Glen, J.W., ed. Hydrological Aspects of Alpine and High-Mountain Areas. International Commission on Snow and Ice (ICSI) Symposium, Exeter, UK, 19-30 July 1982. Proceedings. International Association of Hydrological Sciences. IAHS/AISH Publication, no. 138: 3-9.)
16. Bagchi, A.K., Salomonson, V.V. and Shavsar, P.D., 1979, Studies of snow accumulation characteristics on Himalayan slopes. (In: Contribution of Space Observations to Water Resources Studies and the Management of These Resources, Advances in Space Exploration: COSPAR Symposium Series, no. 9. Oxford, Pergamon Press, 153-156.)
17. Bales, R. C., Galarraga-Sanchez, R. and K. Elder, 1992 Distributed approach to modeling snowmelt runoff in alpine catchments. Proc. of the Workshop on the Effects of Global Climate Change on Hydrology and Water Resources at the Catchment Scale, 207--217, Public Works Research Institute, Tsukuba, Japan, February 1992.
18. Bales, R.C. and Harrington, R.F., 1995, Recent progress in snow hydrology. Reviews of Geophysics, Vol. 33, 1011-1020.
19. Bahadur, J., 1992, Snow and glaciers and their contribution to India's water resources. Roorkee, India. NIH Water Science Educational Series, no. 1.
20. Bahadur, J., 1999 a, Himalayan ecohydrology: An emerging topic. The Himalayan environment edited by S.K.Dash and J. Bahadur, New Age international (P) Limited, Publishers, New Delhi.
21. Bahadur, J., 1999 b, Water resources management in the Himalayan region. The Himalayan environment edited by S.K.Dash and J. Bahadur, New Age international (P) Limited, Publishers, New Delhi.
22. Bahadur, J., Murty, A.S., Lal, V.B. and Das, M.S., 1980, Snow and glacier contributions in a Western Himalayan catchment. Akademia Nauk SSSR. Institut Geografii. Materialy Gliatsiologicheskikh Issledovani. Khronika, Obsuzhdeniia, no. 38: 121-125, English text, 206-207.

23. Bahadur, J. and Dutta, R.K., 1989, Himalayan Glaciology - An emerging Science. Proc. National meet on Himalayan Glaciology, New Delhi - 5-6th June 1989, Department of Science & Technology Govt. of India.
24. Bandhopadhyay, J. and Gyanwali, D., 1994, Himalayan water resources: ecological and political aspect of management. *Mountain Research and Development*, 14(1): 1-24.
25. Banerji, S.K., 1951, Determination of snow-melt in Himalaya. *Weather*, 6(11): 334-338.
26. Barnes, J.C. and Smallwood, M.D., 1975, Synopsis of current satellite snow mapping techniques with the emphasis on the application of near-infrared data. Operational application of snow cover observation. Ed. A. rango, Workshop held at South lake Tahoe, California, 18-20 August, NASA Sp-391, 199-213.
27. Barry, R.G., Fallot, J.M., and Armstrong, R.L., 1995, Twentieth-century variability in snow cover conditions and approaches to detecting and monitoring changes: status and prospects. *Progress in Physical Geography*, 19(4), 520-532.
28. Bartarya, S.K. and Valdiya, K.S., 1989, Landslides and erosion in the catchment of the Gaula River, Kumaun Lesser Himalayas, India. *Mountain Research and Development*, 9(4): 405-419.
29. Bartoluci L.A., Robinson B.F., and Silva, E.F., 1977, Field measurement of spectral response of natural waters. *Photogrammetric Engineering and Remote sensing*, Vol. 43, No.5.
30. Baumgartner, M.F., Martinec, J. and Seidel, K., 1986, Large-area deterministic simulation of natural runoff from snowmelt based on Landsat MSS data. *IEEE Trans. On Geos. And RS*, GE-24, No. 6, 1013-1016
31. Baumgartner, M.F., Seidel, K. and Martinec J., 1987, Toward snowmelt runoff forecasts based on multi sensor remote sensing information. *IEEE Transactions in Geosciences and Remote Sensing* 25, 746-50., *Hydrology*, Vol. 22, 193-210
32. Baumgartner, M.F. and Rango, A., 1991, Snow cover mapping using microcomputer image processing systems. *Nordic Hydrology*, Vol. 22, 193-210
33. Baumgartner, M.F., and Apfl, G., 1994, Monitoring snow cover variations in the alps using the Alpine Snow Cover Analysis System (ASCAS). *Mountain Environments in Changing Climates*, Beniston, M., ed. London: Routledge, 108-120.
34. Bengtsson, L. , 1980. Evaporation from a snow cover. *Nordic Hydrology*, 11,221-234.
35. Berg, N., Osterhuber, R. and Bergman, J. 1991. Rain-induced outflow from deep snowpacks in the central Sierra Nevada, California. *Hydrologic Sciences Journal*, 36, 611-629.

36. Bergstorm, S., 1976, Development and application of a conceptual runoff model for Scandinavain catchments. Dept. Water Resources Engineering, Lund Inst. Technology, Bull. Sr. A 52, Swedish Meterological and Hydrological Institute, Norrkoping, Sweden.
37. Bernier, P.Y., 1987, Microwave remote sensing of snowpack properties: potential and limitations. *Nordic Hydrology*, 18, 1-20
38. Bhakra Beas Management Board (BBMB), 1988, Snow hydrology study in India with particular reference to the Satluj and Beas catchment. (In: Workshop on Snow Hydrology, Manali, India, 23-26 November 1988:Manali, India. Manali. Bhakra Beas Management Board.)
39. Bhakra Beas Management Board (BBMB), 1997, Sedimentation survey report, 1997, BBMB, Bhakra dam circle, Nangal, India.
40. Bhandari, R. and Gupta, C., 1986, Problems of landslides in the Himalaya and future directions. (In: J. Singh, ed., *Environmental Regeneration in Himalaya*, Central Himalaya Environment Association and Gyanodaya Prakashan: India. 17-37.)
41. Bhanu Kumar, O.S.R.U., 1987, Seasonal variation of Eurasian snow cover and its impact on the Indian summer season. (In: Goodison, B.E., Barry, R.G. and Dozier, J., eds. *Large Scale Effects of Seasonal Snow Cover*. International Symposium, Vancouver, British Columbia, Canada, 9-22 August 1987. Proceedings. IAHS/AISH Publication, no. 166, 51-60.)
42. Bhanu Kumar, O.S.R.U., 1988, Eurasian snow cover and seasonal forecast of Indian summer monsoon rainfall. *Hydrological Sciences Journal*, 33(5): 515-525.
43. Blackie, J.R. and Eles C.W.O., 1985, Lumped catchment models, Chapter 11, In: *Hydrological Forecasting*,. Edited by M.G.Anderson and T.P.Burt, John Wiley & Sons.
44. Blöschl, G., and Kirnbauer, R., 1991, Point snowmelt models with different degrees of complexity: Internal processes. *Journal of Hydrology*, 129, (1/4), 127--147.
45. Blöschl, G., Gutknecht, D. and Kirnbauer, R., 1991a, Distributed snowmelt simulations in an alpine catchment 1. Model evaluation on the basis of snow cover patterns. *Water Resources Research*, 27, (12), 3171--3179.
46. Blöschl, G., Gutknecht, D. and Kirnbauer, R., 1991b, Distributed snowmelt simulations in an alpine catchment 2. Parameter study and model predictions. *Water Resour. Res.*, 27, (12), 3181--3188.
47. Braun, L.N., Grabs, W. and Rana, B., 1993, Application of a conceptual precipitation-runoff model in the Langtang Khola basin, Nepal Himalayas. (In: Young, G.J., ed. *Snow and Glacier Hydrology*. International Symposium, Kathmandu, Nepal, 16-21 November

1992. Proceedings. International Association of Hydrological Sciences. IAHS/AISH Publication, no. 218: 221-237.)
48. Bruijnzeel, L.A. and Bremmer, C.N., 1989, Highland-Lowland Interactions in the Ganges Brahmaputra Basin: A review of published literature. International Centre for Integrated Mountain Development, ICIMOD Occasional Paper, no. 11. Kathmandu, Nepal.
 49. Brunengo, M.J. 1990. A method of modelling the frequency characteristics of daily snow amount for stochastic simulation of rain-on-snowmelt events. Proc. Western Snow Conf. 58, 110-121.
 50. Bundela, D. S., Singh, R. and Mishra, K., 1995, Sediment yield modeling for small watersheds in Barker river valley. Institution of Engineers (1) Jr., Vol. 76, 22-25.
 51. Burrard, S.G. and Hayden, H., 1907, Rivers of the Himalaya and Tibet. Calcutta, India. Government Printing.
 52. Byers, A., 1986, A geomorphic study of man-induced soil erosion in the sagarmatha (Mount Everest) National Park, Khumbu, Nepal. Mountain Research and Development, 6(1): 83-87.
 53. Byers, A., 1987, Landscape change and man accelerated soil loss, the case of the Sagarmatha (Mt. Everest) National Park, Khumbu, Nepal. Mountain Research and Development, 7(3): 209-216.
 54. Carrol, T.R., 1990, Operational airborne and satellite snow cover products of the National Operational Hydrologic Remote sensing centre, 47th. Eastern Snow Conference, 87-98.
 55. Carson, B., 1985, Erosion and Sedimentation Process in the Nepalese Himalaya, ICIMOD Occasional Paper no. 1. ICIMOD, Nepal: Kathmandu.
 56. Carsey, F., 1992, Remote sensing of ice and snow: review and status, Intl. J. Remote Sens., 13, (1), 5-11.
 57. Cazorzi, F., and Fontana G.D., 1996, Snowmelt modelling by combining air temperature and a distributed radiation index. Journal of Hydrology, 181(1-4), p. 169-187.
 58. Central Board of Irrigation and Power (CBIP), 1981, Sedimentation studies in reservoirs. Vol. II, CBIP Tech. Report No. 20, New Delhi, India.
 59. Central Soil and Water Conservation Research and Training Institute (CS&WC), 1991, Evaluation of hydrological data. Indo-German bilateral Project on watershed management, Soil and Water Conservation Division (CS&WI), Ministry of Agriculture, New Delhi, India.
 60. Chalise, S.R., 1993, Regional cooperation in hydrological research and training in the Hindu Kush-Himalayas. (In: Young, G.J., ed. Snow and Glacier Hydrology. International

- Symposium, Kathmandu, Nepal, 16-21 November 1992. Proceedings. International Association of Hydrological Sciences. IAHS/AISH Publication, no. 218: 37-47.)
61. Chandra, S., 1993, Recent trends in Himalayan hydrology. Proceedings of SNOWSYMP, 26-28 Sept., 1993, Snow Avalanche Study Establishment (SASE), Manali.
 62. Chang, A.T.C. Foster, J.L. and Hall, D.K., 1990, Effect of vegetation cover on microwave snow water equivalent estimates. International Symposium on Remote Sensing and Water Resources, Enchede, Netherlands, 137-145.
 63. Chang, A.T.C., Foster J.L., Rango, A. and Josberger, E.G., 1991, Use of microwave radiometry for characterizing snow storage in large river basins. In Snow, Hydrology and Forest in high Alpine areas, Number 205, International Assoc. Hydrologic Sciences, Wallingford, England, 73-80.
 64. Charbonneau, R., Fortin, J.P., Morin, G., 1977, The CEQUEAU model: description and examples of its use in problems related to water resources management. Hydrological Science Bull., 22(1), 193-203.
 65. Chiew, F.H.S., Stewardson, M.J., and McMohan, T.A., 1993, Comparison of six rainfall-runoff modelling approaches. Journal of Hydrology, 147, 1-36.
 66. Choubey V.D., 1998, Potential of rock mass classification for design of tunnel support of hydroelectric projects in Himalayas. International conference on hydropower development in Himalayas, April 20-22, Shimla, India.
 67. Church, J.E. Himalaya co-operative snow surveys. Science and Culture, 13(5): 174-177.
 68. Church, J.E. Snow seeking in the Himalaya (Home of snow). Science and Culture, 13(3): 82-86.
 69. Cline, D. W., 1992, Modeling the redistribution of snow in alpine areas using geographic information processing techniques. Proc. of the 1992 Eastern Snow Conf., edited by M. Ferrick, 13--24, 1992.
 70. Cline, D.W., Bales, R.C. and Dozier, J., 1998, Estimating the spatial distribution of snow in mountain basins using remote sensing and energy balance modelling. Water Resources Research, 34, 1275-1285.
 71. Colbeck, S.C. 1975, A theory of water flow through a layered snowpack. Water Resources Research, 11, 261-266.
 72. Collie, J.N., 1911, Journeys in the Himalayas and some factors of erosion. Geographical Journal, 38: 3-31.

73. Collins, D. N., Hasnain, S.I., 1994, Runoff and sediment transport from the glacierized basins at the Himalayan scale Alpine glacier project working paper 15, University of Manchester, U. K., pp. 14.
74. Conway, H. and Raymond, C.F. 1993. Snow stability during rain, *J. of Glaciology*, 39, 635-642.
75. Conway, H., Breyfogle, S., and Wilbour, C.R. 1988. Observations relating to wet snow stability. International Snow Science Workshop, ISSW'88 Comm. Whittler, B.C., Canada.
76. Cracknell, A.P., 1997, *The Advanced Very High Resolution Radiometer* (London: Taylor and Francis).
77. Davies, L.M., 1940, Note on three Himalayan rivers. *Geological Magazine*, 77: 410-412, 175-183.
78. Dey, B. and Bhanu Kumar, O.S.R.U., 1983, An apparent relationship between Eurasian spring snow cover and the advance of the Indian summer season. *Journal of Applied Meteorology*, 21(12): 1,929-1,932.
79. Dey, B. and Bhanu Kumar, O.S.R.U., 1983, Himalayan winter snow cover area and summer season rainfall over India. *Journal of Geophysical Research*, 88(C9): 5,471-5,474.
80. Dey, B., Goswami, D.C. and Rango, A., 1983, Utilization of satellite snow-cover observations for seasonal streamflow estimates in the Western Himalayas. *Nordic Hydrology*, no. 14, 257-266.
81. Dey, B., Sharma, V.K., Goswami, D.C. and Subba Rao, P., 1988, Snow cover, snowmelt and runoff in the Himalayan river basins: final technical report. National Aeronautics and Space Administration, NASA-CR-182434, 37p.
82. Dhanju, M.S., 1992, Snow and Ice Monitoring by Remote Sensing. (In: International Workshop on Snow and Ice. Proceedings. New Delhi, 39p.)
83. Dhar, O.N., Kulkarni, A.K. and Mandal, B.N., 1985, Initiation of first snow surveys in the Himalaya - a brief appraisal. (In: Joshi, S.C., ed. National Symposium on Seasonal Snow Cover, New Delhi, India, 28-30 April 1983. Proceedings, vol. 1. Manali, India. Snow and Avalanche Study Establishment, 164-171.)
84. Dhar, O.N., Kulkarni, A.K. and Mandal, B.N., 1986, Snow survey experiments in the upper Tamur basin (Eastern Nepal). (In: Joshi, S C, ed. Nepal Himalaya Geoecological Perspectives. Nainital, India. Himalayan Research Group 422-431.)
85. Dhar, T.N., 2000, Water resources and water management in north-western Indian Himalayas (NWIH). ICIWRM-2000, Proceedings of International conference on

- integrated water resources management for sustainable development, 19-21 December 2000, New Delhi.
86. Dhir, R.D., 1951, Feasibility of snow survey in the Himalayas. International Association of Hydrological Sciences. IAHS Publication, no. 32, 305-314.
 87. Dhurva Narayan, V.V., Ram Babu, 1983, Estimation of soil erosion in India, Journal of Irrigation and Drainage Engineering, Vol. 109, No.4.
 88. Dhruva Narayan, V.V., 1987, Downstream impacts of soil conservation in the Himalayan region. Mountain Research and Development, 7(3), 287-298.
 89. Dhruva Narayana, V.V. and Shastry, G., 1983, Runoff characteristics of small watersheds in the outer Himalayas of Doon valley. Annual Report of CSWERTI, Dehra Dun, India, Deharadun. 201pp.
 90. Dobhal, D.P. and Kumar, S. 1996. Inventory of Glacier basins in Himachal Himalaya. Journal Glaciology Society of India, Vol. 48, 671-681.
 91. Domroes, M., 1987, Temporal and spatial variations of rainfall in the Himalayan with particular reference to mountain ecosystem. Journal of Nepal Research Centre, 2(3): 41-48.
 92. Donald, J.R. Seglenieks, R., Soulis, E.D., Kouwen, N. and Mullins, D., 1993, Mapping partial snowcover during the melt season using C-band SAR imagery, Can. J. Remote Sensing, 19 (1), 68-76.
 93. Dos, I. C., Pais-Cuddou, M. and Rawal, N.C., 1969, Sedimentation of reservoirs. Journal of the irrigation and drainage division, ASCE, Vol. 95, No. IR3, 415-429.
 94. Dozier, J., 1987, Recent research in snow hydrology. Review of Geophysics, 25, No. 2, 153-161.
 95. Duchon, C. E., Salisbury, J.M., Williams, T. H.L. and Nicks, A.D., 1992, An example of using Landsat and Goes data in a water budget model. Water Resources Research, 28(2), 527-538.
 96. Fayez Abdulla and Laith Al-Badranih, 2000, Application of a rainfall-runoff model to three catchments in Iraq. Hydrological Sciences Journal, 45(1).
 97. Fenn, C.R., Gurnell, A.M. and Beecroft, I. 1985, An evaluation of the use of suspended sediment rating curves for the prediction of suspended sediment concentration in a proglacial stream, Geogr. Ann., 67 A, 71-82.
 98. Ferguson, R.I., 1985, Runoff from glacierised mountains – a model for annual variation and forecasting. Water Resources Research, Vol.21, No.5, 702-705.

99. Ferguson, R.I., 1999, Snowmelt runoff models. *Progress in Physical Geography* 23, 2, 205-227.
100. Fleming, G. 1975. *Computer simulation techniques in Hydrology*, New York, Elsevier, Environmental Science Series.
101. Flerchinger, G.N. and Cooley, K.R., 2000, A ten year water balance of a mountainous semi-arid watershed. *Journal of Hydrology*, 237, 86-99.
102. Fort, M., 1987, Geomorphic and hazards mapping in the dry continental Himalaya: 1:50,000 maps of Mustang District, Nepal. *Mountain Research and Development*, Vol. 7(3), 222-238.
103. Galay, V., 1987, Erosion and sedimentation in the Nepal Himalaya - an assessment of river processes. Kathmandu, Nepal. Water and Energy Commission Secretariat, Report.
104. Garde, R. J. and Kothiyari, U.C., 1987, Sediment yield estimation , *J. Irrig. and Power (India)* Vol. 44(3), 97-123.
105. Garg, S., 1987, Soil erosion in the Sub-Himalayan region - A case study. *Deccan Geographer*, 9(1): 7-14.
106. Garstka, W.U., Love, L.D., Goodell, B.C., and Bertle, F.A., 1958, Factors affecting snowmelt and streamflow. U.S. Bureau of Reclamation and U.S. Forest Service.
107. Goodison, B.E., Walker, A.E. and Thirkettle, F.W. , 1990, Determination of snow water equivalent on the Canadian Prairies using real time passive microwave data. *Proc. of the workshop on applications of remote sensing in Hydrology*, Saskatoon, Saskatchewan, 297-314.
108. Goodison, B.E. and Walker, A.E., 1993, Use of snow cover derived from satellite passive microwave data as an indicator of climate change, *Ann. Glaciol.*, 17,137-142.
109. Goel M.K. and Jain, S.K., 1996, Evaluation of reservoir sedimentation using multi-temporal IRS-1A LISS II data. *Asian-Pacific Remote Sensing and GIS Journal*, Vol. 8, No. 2.
110. Goel, M.K. and Jain, S.K., 1998, Reservoir sedimentation study for Ukai dam using satellite data. UM-1/97-98, National Institute of Hydrology, Roorkee.
111. Gulati, T.D., 1973, Role of snow and ice hydrology in India. (In: *Role of Snow and Ice in Hydrology*, Symposium, Banff, British Columbia, Canada, September 1972. Proceedings, vol. 1. International Association of Hydrological Sciences. IAHS/AISH Publication, no. 107:610-623.)
112. Gupta, R.K., 1993, In : *The Living Himalayas : Aspects of Environmental and Resources Ecology of Garhwal*. Today and Tomorrow Printers & Publishers, 1983.

113. Gupta, M.P., 1985, Necessity for creating network for the gauging of snow in the Himalayas. (In: Joshi, S.C., ed. Symposium on Seasonal Snow Cover, 1st, New Delhi, India, 28-30 April 1983 Proceedings. Snow and Avalanche Study Establishment, Manali, 79-82.)
114. Gupta, R.P., Duggal, A.J., Rao, S.N. Shankar, G., and Singhal, B.B.S, 1982, Snowcover area in snowmelt runoff relation and its dependence on geomorphology – A study from Beas catchment (Himalaya, India). *Journal of Hydrology*, Vol. 58, 325-339.
115. Guy, H. P., 1964, A analysis of some storm-period variables affecting stream sediments transport. *Geological Survey Prof. Paper*, Vol. 462-E, 1-46.
116. Hafner, T., 1993, Himalayan deforestation, changing river discharge, and increasing floods: Myth or reality. *Mountain Research and Development*, Vol. 13, No. 3, 213-233.
117. Hall, D.K. and Martinec, J., 1985, *Remote sensing of Ice and Snow*, Chapman and Hall, Newyork.
118. Haigh, M.J., 1989, Water erosion and its control: Case studies from South Asia. (In: K. Ivanov and D. Pechinov, eds., *Water erosion: Abridged Proceedings of the International IHP/MAB symposium, International IHP/MAB Symposium on Water Erosion, Varna, Sept. 19 - 24, 1988. 1-38. Varna.*)
119. Hanumantha Rao G., Rameshwar Rao and Viswanatham, R., 1985, Project report on capacity evaluation of Sriramsagar reservoir using remote sensing techniques. *Andhra Pradesh Engineering Research Lab., Hyderabad, India.*
120. Harding, R.J., Johnson, R.C., and Soegaard, H., 1995, Energy balance of snow and partially snow covered areas in western Greenland. *International Journal of Climatology*, 15(9), 1043-1058.
121. Hardy, J.P., Albert, M.R. and Marsh, P., 1999, *Snow Hydrology, The integration of physical, chemical and biological systems*, Hydrological Process, 13.
122. Hasnain, S.I., 1989, Himalayan glaciers as a sustainable water resource. *Water Resources Development*, 5(2), 106-112.
123. Heidel, S. G., 1956, The progressive lag of sediment concentration with flood wave. *Trans. Am. Geophysics Union*, Vol. 37, 56-66.
124. Hewitt, K., 1984, *Snow and ice conditions in the Upper Indus Basin: a review and bibliography*. Internal Report. Waterloo, Ontario, Canada, Wilfrid Laurier University, Snow and Ice Hydrology Project.

125. Hewitt, K., 1985, Snow and ice hydrology in remote, high mountain basins: The Himalayan sources of the River Indus. Wilfrid Laurier University, Snow and Ice Hydrology Project Working Paper, no. 1.
126. Hewitt, K., 1986, Upper Indus snow belts: Snowfall and sources of water yield. (In: Hewitt, K., ed. Snow and Ice Hydrology Project Annual Report 1985. Waterloo, Ontario, Canada, Wilfrid Laurier University, 58-63.
127. Heywood, L. 1988. Rain on snow avalanche events-some observations. Proc. International Snow Science Workshop, ISSW'88 Comm. Whistler, B.C. Canada.
128. Hodgkins, R., 1999, Controls on suspended-sediment transfer at high arctic glacier, determined from statistical modelling. *Earth surface processes and landforms*, 24, 1-21.
129. Holeyer, R.J., 1978, Suspended sediment algorithms- Remote sensing of Environment, 323-338.
130. Holzer, T., and Baumgartner, M.F., 1995, Monitoring Swiss alpine snow cover variations using digital NOAA-AVHRR Data. IGARSS'95, Quantitative Remote Sensing for Science and Applications, International Geoscience and Remote Sensing Symposium, Firenze, Italy, 10-14 July 1995, Vol. III, 1765-1767.
131. Hord, R.M., 1986, Remote Sensing-Methods and Application. John Wiley and Sons, Toronto, 362
132. HMGN/UNESCO/ICIMOD, 1992, Mountain hydrology in the Hindu Kush - Himalayan region. (In: Report of the Second Consultative meeting of the Regional Working Group on Mountain Hydrology, 16-18 March 1992. International Centre for Integrated Mountain Development Kathmandu, Nepal.)
133. Hurst, A. and Chao, C., 1975, Sediment deposition model for Tarbela Reservoir. (In: Symposium on modeling technique. vol. 1, American Society of Civil Engineers, 501-520. New York, N.Y.)
134. HYMOS (Version 4.01) Manual. (1999) Delft Hydraulics, P.O.Box 177, 2600 M.H.Delft
135. Illangasekare, T.H., Walter, R.J., Meier, M.F. and Pfeffer, W.T., 1990, Modelling of meltwater infiltration in subfreezing snow, *Water Resources Research*, 26, 1001-1012.
136. Indian Council for Agricultural research (ICAR), 1984, Guidelines and Status of Hydraulic and Sediment Management of Watersheds in selected River Valley Catchments. Water and Soil Conservation division, Ministry of Agriculture, New Delhi, India.
137. Ives, J. D. and Messerli, B., 1989, The Himalayan Dilemma: Reconciling Development and Conservation. United Nations University and Routledge, London.
138. Jagadeesha C.J., Palnitkar, V.G., 1991, Satellite data aids in monitoring reservoir water and

- irrigated agriculture. *Journal Water International*, 16 (1991) 27-37, IWRA.
139. Jain S.K., and Saraf A.K., 1995, GIS for the estimation of soil erosion potential. *Journal GIS INDIA*, Vol. 4, No.1, 3-6.
140. Jain S.K., Kite G.W., Kumar N., Ahmad T., 1998, SLURP Model and GIS for estimation of runoff in a part of Satluj catchment, India. *Hydrological Sciences Journal*, 43(6), December 1998.
141. Jayapragasam, R., and Muthuswamy, K., 1980, Sedimentation Studies in Vaigai Reservoir Using Grid System. *Journal of Irrigation & Power, CBIP*, Vol. 37, No.1, 337-350.
142. Jeyram, A., and Bagchi, A.K., 1982, Snow covered area estimation in Tons' basin using LANDSAT imageries. *Proceedings of the International Symposium on Hydrological Aspects of Mountainous Watersheds*, University of Roorkee, Nov. 4 – 6, 19-23.
143. Jha, V.K., 1982, Hydrological aspects of mountainous terrain: case example from Okhaldhunga area, Nepal Himalayas. (In: *Symposium on Resources Survey for Land Use Planning and Environmental Conservation*, 20-22 October 1982. *Proceedings*. Dehra Dun, India. *Indian Society of Photo-Interpretation and Remote Sensing*: 95-99.)
144. Joglekar, D. V., 1965, *Irrigation research in India*. Centrl board of Irrigation and Power Publ. India, No. 78.
145. Jonch-Clausen, T., 1979, *Systeme Hydrologique European: a short description*. SHE Report I, Danish Hydraulics Institute, Horsholm, Denmark.
146. Jose, C. S. and Das, D.C., 1982, Geomorphic prediction models for sediment production rate and Inters priorities of watersheds in Mayurakshi catchment. *Proc. of the Internaltion Symposium on hydrological aspects of mountainous watersheds*, School of Hydrology, Uni. of Roorkee, India, Nov. 4-6, Vol. 1, pp. 15.
147. Joshi, V. and Negi G.C., 1995, Garwhal Himalaya mein vibhinn bhumi upyog wale do Jalagamo mein jal utpadan udhyayan, Jalvigyan evam Jal Sansadhan par Rasthriya Sangosthi, 303-307, National Institute of Hydrology, Roorkee.
148. Kanwar, S., 1948, Role of glaciers and snow on hydrology of Punjab rivers. India. Panjab Irragation Branch. Central Board of Irrigation Publication, no. 36: 1-30.
149. Kattelmann, R., 1987, Uncertainty in Assessing Himalayan Water Resources. *Mountain Research and Development*, 7(3): 279-286.
150. Kattlemann, R., 1993, Role of snowmelt in generating streamflow during spring in East Nepal. (In: Young, G.J., ed. *Snow and Glacier Hydrology*. International Symposium, Kathmandu, Nepal, 16-21 November 1992. *Proceedings*. International Association of Hydrological Sciences. IAHS/AISH Publication, no. 218: 103-111.)

151. Kawosa, M.A., 1988, Remote Sensing of the Himalayas. Natraj Publisher, Dehradun.
152. Khoram, S., 1981, Use of Ocean colour scanner data in water quality mapping, Photogrammetric Engineering and Remote sensing, Vol. 47, No.5, 667-676.
153. Khosla, A.N., 1953, Silting of Reservoirs. Annual Report: International Association Hydrological Sciences. International Association of Hydrological Sciences. IAHS Publication no. 51, Central Board of Irrigation: India.
154. Kick, W., 1986, Glacier mapping for an inventory of the Indus drainage basin: current state and future possibilities. (In: Richardson, E.L. ed. Symposium on Glacier Mapping and Surveying, University of Iceland, Reykjavik, 26-29 August 1985. Proceedings. Annals of Glaciology, 8: 102-105.)
155. Kite, G.W., 1991, Watershed model using satellite data applied to a mountain basin in Canada, Journal of Hydrology, 128, 1-4, 157-169.
156. Kite, G. W. and Kouwen, N., 1992, A semi-distributed model for a mountain watershed. Water Resources Research, 28(12), 3193-3200.
157. Kothiyari, U. C., 1996, Erosion and sedimentation problems in India. In: Proceedings of International Symposium on Erosion and Sediment Yield. Exeter, U. K. IAHS Publication No. 236, 531-539.
158. Kothiyari, U. C., Tewari, A.K. and Singh, R., 1994, Prediction of sediment yield. J. Irrig. Drain Eng., ASCE Vol. 20(6), 1122-1131.
159. Kotlyakov, N.M. and Krenke, A.N., 1982, Investigations of the hydrological conditions of alpine regions by glaciological methods. In : Hydrological aspects of Alpine and high mountain areas, IAHS publication No. 138, pp 31-42.
160. Kouwen, N. N., Soulis, E. D., Pietroniro, A., Donald, J.R. and Harrington, R. A., 1993, Grouped response units for distributed hydrologic modeling. A.S.C.E. Journal of the Water Resources Planning and Management Division.
161. Krishnan, V., 1983, Relationship between snowfall and lean seasonal discharge of river Sainj at Larji, H.P. Proceedings of the First National Symposium on Seasonal Snow-cover', 28-30, April, SASE, Manali, Vol.-II, 163-173.
162. Krishna, A.P., 1996. Satellite remote sensing applications for snow cover characterization in the morphogenetic regions of upper Tista river basin Sikkim Himalaya. International Journal of Remote Sensing, 17(4), 651-656.
163. Kuchment, L.S., and Gelfan, A.N., 1996, Determination of the snowmelt rate and the meltwater outflow from a snowpack for modelling river runoff generation. Journal of Hydrology, 179(1-4), p. 23-36.

164. Kuester, J.L., Mize, J.H. 1973. Optimization techniques with Fortran. McGraw-Hill Book Company, New York.
165. Kulkarni, A.V., Philip, G., Thakur, V.C., Sood, R.K., Randhawa, S.S. and Chandra, R., Glacial inventory of the Satluj basin using remote sensing technique, Himalayan Geology, Vol. 20 (2), 1999, 45-52.
166. Kunzi, K.F., Patil, S., and Rott., H., Snow cover parameters retrieved from NIMBUS-7 Scanning Multi-channel Microwave radiometer (SMMR) data. IEEE Trans. Geosc. Rem. Sens., GE-20 (4), 453-467.
167. Lamba, S.S. and Prem, K.S., 1975, Integrated development for rivers Sutlej Beas and Ravi for optimum utility of water in Northwestern areas of India. (In: World congress on Water Resources, 2nd Proceedings, New Delhi, 12 - 16 December 1975. 79-87. WCWR: India.)
168. Leaf, D.F. and Brink, G.E., 1973, Hydrologic simulation model of Colorado subalpine forest. Forest services Res. Pap RM 107, US dept. of Agriculture, Fort Collins, Colorado, USA.
169. Leavesley, G.H., Lichty, R.W., Troutman, B.M. and Saindon, L.G., 1983, Precipitation Runoff Modelling System, Users manual. USGS Wat. Resource. Invest. Rep. 83-4238. Geological Survey, reston, Virginia, USA.
170. Leconte, R. and Pultz. T.J. , 1990, Utilization of SAR data in the monitoring of snowpacks and wetlands, Proc. of the Workshop on applications of Remote Sensing in Hydrology, Saskatoon, Saskatchewan, 233-257.
171. Loughran, R. I., 1976, The calculation of suspended sediment transport from concentration versus discharge curves. Catena, Vol. 3, 45-61.
172. Malhotra, R.V., McKim, H.L. and Rangachari, R., 1988, Snow hydrology in the upper Yamuna basin, India. (In: Eastern Snow Conference, 45th, Lake Placid, New York, 8th and 9th, June 1988. Proceedings, 84-93.)
173. Manavalan, P., Sathyanath, P., Sathyanarayn, M., and Raje Gowda, G.L., 1990, Capacity evaluation of the Malaprabha reservoir using digital analysis of satellite data, Tech. Rep. No. RC: BG: WR: 001:90, Regional Remote Sensing Service Centre, Bangalore and Karnataka Engineering Research Station, Krishnarajsagar, India.
174. Marcus, W. A., 1989, Lag-time routing of suspended sediment concentrations during unsteady flow, Geological Society of Am. Bul. Vol. 101, 644-651.
175. Marston, R. A., 1989, Sediment production in a small subalpine watershed of the Manaslu Himal. (In: R.A. Marston, ed. Environment and Society in the Manaslu-ganesh Region of

- the Central Nepal Himalaya: a Final Report of the 1987 Manaslu-Ganesh Expedition, 58-64.)
176. Martinec, J., 1975, Snowmelt runoff model for streamflow forecasts', *Nordic Hydrology*, Vol. 6, No. 3, 145-154.
 177. Martinec, J., and Rango, A., 1983, *The Snowmelt Runoff Model (SRM) Users Manual*. NASA Reference Publication, April 1983.
 178. Martinec, J., Rango, A., and Roberts, R., 1994, *Snowmelt Runoff Model (SRM). User's Manual*. (Updated Edition 1994, Version 3.2). M.R. Baumgartner, ed.. University of Bern. Department of "Geography. *Geographica Bernensia*. 65.
 179. Mayewski, P.A., Pregent, G.P., Jeschke, P.A. and Ahmad, N., 1980, Himalayan and Trans- Himalayan glacier fluctuations and the south Asian monsoon record. *Arctic and Alpine Research*, 12(2): 171-182.
 180. McCuen, R.H., 1973, The role of sensitivity analysis in hydrologic modelling, *Journal of Hydrology*, 18(1973), 37-53.
 181. Mehrotra, R., and Singh, R.D., 1998, The influence of model structure on the efficiency of rainfall-runoff models: A comparative study for some catchments of Central India. *Water Resources Management*, 12, 325-341.
 182. Meybeck, M., 1976, Total mineral dissolved transport by world major rivers, *Hydrological Science Bulletin*, Vol. 21, 265-284.
 183. Milliman, J. D. and Meade, R.H., 1993, Worldwide delivery of river sediments to the Oceans, *Journal of Geology*, Vol. 91, 1-19.
 184. Mishra, N. and Satyanarayan, T., 1991, A new approach to predict sediment yield from small ungauged watersheds, *Journal of Institution of Engineers (India) Agriculture Engg. Div.*, Vol. 73, 30-36.
 185. Mohanty, R.B., Mahapatra, G., Mishra, D. and Mahapatra, S.S. 1986, Report on application of remote sensing to sedimentation studies in Hirakud reservoir, Orissa remote sensing application centre, Bhubaneswar and Hirakud research station, Hirakud, India.
 186. Mohile, A.D., Rao, P.R., Sood, S.C., and Dhillon, M.S., 1988, Snowmelt, its estimation and forecasting. Proceedings of the 54th R&D Session of CBIP, 30th April-3rd May, Ranchi, Bihar, India.
 187. Morris, E.M., 1980, Forecasting flood flows in the Plynlimon catchments using a deterministic distributed mathematical model. In: *Hydrological forecasting IAHS Publ. No. 129*, (Proc. Oxford Symp., April 1980) 247-255.

188. Morris, G. L., 1995, Reservoir sedimentation and sustainable development in India. In. Proc. Sixth International Symposium on river Sedimentation, New Delhi, India, 57-61.
189. Mountains of the World, 1998, Water towers for the 21st. century, A contribution to global fresh water management, Switzerland.
190. Mountain Forum, Bulletin No. 4, September 1999, Mountains of South Asia, Kathmandu, Nepal.
191. Murthy, L.T., 1978, Environmental problems of water resource development in the Himalayan region. (In: Proceedings of water resource development and environment in the Himalayan region, New Delhi: Department of Science and Technology.)
192. Murthy, Y.K., 1978, Environmental Problems of Water Resources Development in the Himalayan Region' Proc. National Seminar on Resources Development and Environment in the Himalayan Region, New Delhi, April 10-13, 1978, Development of Science and Technology, Govt. of India, 58-69
193. Murthy, Y.K., 1981, Water resource potentials of the Himalaya. (In: Lall, J.S. and Moddie, A.D., eds., The Himalaya aspects of change, 152-171. Oxford University Press, India International Center, New Delhi.
194. Murthi, B. N. (ed.), 1977, Sedimentation studies in reservoirs Vol. 1, Central Board of Irrigation and Power Tech. report No. 20, New Delhi, India.
195. Naidu, B.S.K., 1995, Environmental Aspects of Hydropower Development. Proc. Seminar on Environmental Management of Water Resources and Power Projects, Central Board of Irrigation & Power, 6-8 Sept., Indore.
196. Nash, J.E. and Sutcliffe, J.V. 1970. River flow forecasting through conceptual model. Part 1 a discussion of principles. J. Hydrology, 10, 282-290.
197. Negi, S.S., 1982, Environmental problems in the Himalayas. Bishun Singh, Mahendra Prasad Singh, Dehradun: Deharadun.
198. Neve, A., 1911, Journeys in the Himalayas and some factors of Himalayan erosion. Geographical Journal, 38.
199. NOAA, 1992, Airborne Gamma Radiation Snow Survey Program and Satellite Hydrology Program. Users Guide Version 4.0. National Operational Hydrologic Remote Sensing Center, National Weather Service, NOAA, Minneapolis, Minnesota.
200. Pandey, A.N., Pathak, C. and Singh, J.S., 1983, Water sediment and nutrient movement in forested and non-forested catchments in Kumaun Himalaya. Forest Ecology and Management, 7: 19-29.

201. Pathak, C., Pandey, A.N. and Singh, J.S., 1984, Overland flow, sediment output and nutrient loss from certain forested sites in the central Himalaya. *Journal of Hydrology*, 71(3-4): 239-251.
202. Patra, K.C., 2001, *Hydrology and water resources engineering*. Narosa Publishing House, New Delhi.
203. Prasad, Y. 1999. Challenges in the hydropower development of the country. Proceedings of the National workshop on Challenges in the management of water resources and environment in the next millennium: need for inter-institute collaboration, Oct. 8 & 9, 1999. Dept. of Civil Engg., Delhi College of Engineering, Delhi.
204. Puri, S. R., Upadhyay, D.S. and Kaur, S., 1988, Computation of water budget of a snow bound river basin. *Mausam*, 39(1): 103-106.
205. Quick, M.C. and Pipes, A., 1977, UBC watershed model. *Hydrological Sciences Bull*, 22(1), 153-161.
206. Ramsay, W.J.H., 1987, Deforestation and erosion in the Nepalese Himalaya: is the link myth or reality?. *International Association Hydrological Sciences. International Association of Hydrological Sciences. IAHS Publication no. 167: 239-250.*
207. Ramamoorthi, A.S., 1983, Snowmelt runoff assessment and forecasting using satellite data. Proceedings of the First National Symposium on Seasonal Snowcover, SASE, Manali, 28-30, April, Vol-II, 117-120.
208. Ramamoorthi, A.S., 1986, Forecasting snowmelt runoff of Himalayan river using NOAA AVHRR imageries since 1980. (In: Johnson, A.I., ed. *International Workshop on Hydrologic Applications of Space Technology*, Cocoa Beach, Fl., 19-23 August 1985. Proceedings. International Association of Hydrological Sciences. IAHS/AISH Publication, no. 160, 341-348.)
209. Ramashastri, K.S. 1999. Snowmelt modelling studies in India. *The Himalayan environment* edited by S.K.Dash and J. Bahadur, New Age international (P) Limited, Publishers, New Delhi.
210. Ram babu, Tejwani, K.G., Agrawal, M.C. and Bhushan, L.S., 1978, Distribution of erosion index and Iso-erodent map of India. *Indian Journal of Soil Conservation*, Vol. 6, No. 1, 1-14.
211. Rango, A., and Martinec, J., 1979, Application of snowmelt runoff model using LANDSAT data. *Nordic Hydrology*, Vol.10, 225-238.
212. Rango, A., 1992, Worldwide testing of the snowmelt runoff model with applications for predicting the effects of climate change. *Nordic Hydrology*, 23(3): 155-171.

213. Rango, A., Salomonson, V.V. and Foster, J.L., 1977, Seasonal stream flow estimation in the Himalayan region employing meteorological satellite snow cover observations. *Water Resources Research*, 13(1): 109-112.
214. Rango, A., Walker, A.E. and Goodison, B.E., 2000, Snow and Ice. Chapter 11, Remote Sensing in Hydrology and Water Management. Gert A. Schultz and Edwin T. Engman, Springer.
215. Ranzi, R. and Rosso, R., 1991, Physically based approach to modelling distributed snowmelt in a small alpine catchment. in *Snow, Hydrology, and Forest in high Alpine areas*, Intl. Assoc. Hydrol. Sci., Wallingford, England, No. 205, 141-150.
216. Rao, S. V. N., Ramasastri K.S. and Singh R.N.P., 1996, A simple monthly model for snow dominated catchments in Western Himalayas. *Nordic Hydrology*, Vol. 27(4), 255-274.
217. Rao, S. V. N., M. V. Rao, Ramasastri K.S. and Singh R.N.P., 1997, A study of Sedimentation in Chenab Basin in Western Himalayas. *Nordic Hydrology*, Vol. 28, 201-206.
218. Rao, N.M., 1983, Some observations on seasonal snowcover. (In: Joshi, S.C., ed. National Symposium on Seasonal Snow Cover, New Delhi, India, 28-30 April 1983. Proceedings, vol. 1. Manali, India. Snow and Avalanche Study Establishment.)
219. Rao, N.M., Bandyopadhyay, B.K. and Verdhien, A., 1991, Snow hydrology studies in Beas basin for developing snow-melt runoff model. *Journal of Institution of Engineers (India)*, vol. 72, 92-102.
220. Rawat, J. S. and Rawat, M.S., 1994, Accelerated erosion and denudation in the Nana kosi watershed, Central Himalaya, India, Part I: sediment load. *Journal of Mountain Research and Development*, Vol. 14(1), 25-38.
221. Raymo, M. E. and Ruddiman, W.F., 1992, Tectonic forcing of Late Cenozoic climate. *Nature*, Vol. 359, 117-122.
222. Roohani, M.S., 1986, Studies on Hydromorphometry and snowmelt runoff using data of Chenab catchment. Ph.D. Thesis, University of Roorkee, Roorkee, India.
223. Salomonson, V.V., 1971, NIMBUS 3 and 4 observations of snow cover and other hydrological features in Western Himalayas. (In: International Workshop on Earth Resources Survey System, 3-14 May 1971. Proceedings, Vol. 2. Washington, D.C., U.S. National Aeronautics and Space Administration, 444-448.)
224. Saraf, A.K., Foster, J.L., Singh, P. and Tarafdar, S., 1999, Passive microwave data for snow depth and snow extent estimation in the Himalayan mountains, *International Journal of Remote Sensing*, Vol. 20, No. 1.

225. Schanda, E., Matzler, C., and Kunzi, K., 1983, Microwave remote sensing of snow cover. *International Journal of remote sensing*, 4, 149-158.
226. Schroeter, H.O., 1988, An Operational snow Accumulation Ablation Model for Areal Distribution of Shallow Ephemeral Snowpacks. Ph D thesis, University of Guelph, Ontario.
227. Sedimentation studies in reservoirs, 1991, Vol. 1, Technical report No. 20, Research scheme applied to river valley projects, Central Board of Irrigation and Power (CBIP), New Delhi.
228. Seidel, K., Bruschi, W. and Steinmeier, C., 1994, Experiences from real time runoff forecasts by snow cover remote sensing. In proceedings of IGRASS'94, 2090-93.
229. Seth, S.M., 1983, Modelling of daily snowmelt runoff during pre-monsoon month for Beas basin upto Manali. Proceedings of the First National Symposium on Seasonal Snowcover, 28-30 April, SASE, Manali, Vol.-II, 104-115.
230. Shankar, K., 1991, Status and Role of Mountain Hydrology in the Hindu Kush-Himalayan Region. Discussion Paper Series no. 10: MEM Division, ICIMOD: Kathmandu.
231. Sharma, C.K., 1986, The problem of sediment load in the development of water resources in Nepal. *Mountain Research and Development*, 7(3): 316-318.
232. Sharma, P.D., Goel A.K. and Minhas R.S., 1991, Water and sediment yields into the Sutlej River from the high Himalaya. *Mountain Research and Development*, 11(2): 87-100.
233. Shashi Kumar, V., Paul, P.R., Ramana Rao, Ch.L.V., Haefner, H. and Seidel, K., 1993, Snowmelt runoff forecasting studies in Himalayan basins. (In: Young, G.J., ed. *Snow and Glacier Hydrology*. International Symposium, Kathmandu, Nepal, 16-21 November 1992. Proceedings. International Association of Hydrological Sciences. IAHS/AISH Publication, no. 218: 85-94.)
234. Shangale, A.K., 1991, Sedimentation in Indian reservoirs, Paper presented at the International symposium on special problems of Alluvial rivers including those of international rivers, held at Seoul, Korea, Sept., 1991.
235. Shi, J. and Dozier, 1993, Measurements of snow and glacier covered area with single polarization SAR, *Ann. Glaciol.*, 17, 72-76.
236. Sian, K., 1946, Role of Glaciers and Snow on Hydrology of Punjab Rivers. Simla, India. Central Board of Irrigation.
237. Singh, P., 1989, Snowmelt runoff simulation using snowmelt runoff model (SRM) in Beas basin. Proceedings of the 55th R&D Session of CBIP, 26 July, Srinagar, (J&K).

238. Singh, P., 1991, A temperature lapse rate study in western Himalayas. *Hydrology Journal of IAH* Vol. XIV, No. 3, 1991
239. Singh, P., 1991, Status report on snowmelt modelling studies. Roorkee, India. National Institute of Hydrology, SR-19.
240. Singh P., and Quick, M.C., 1993, Streamflow simulation of Satluj River in the Western Himalayas. (In: Young, G.J., ed. *Snow and Glacier Hydrology*. International Symposium, Kathmandu, Nepal, 16-21 November 1992. Proceedings. International Association of Hydrological Sciences. IAHS/AISH Publication, no. 218: 261-271.)
241. Singh, P., Ramashastri, K.S. and Kumar, N. 1995. Topographical influence on precipitation distribution in different ranges of western Himalayas. *Nordic Hydrology*, 26, 259-284.
242. Singh, P. and Kumar, N. 1996, Determination of snowmelt factor in the Himalayan region, *Hydrological Sciences Journal*, 41, 301-310.
243. Singh, P., Spitzbart, G., Huebl, H., and Weinmeister, H.W., 1997, Hydrological response of a snowpack under rain-on-snow events: a field study. *Journal of Hydrology*, 202, 1997, 1-20.
244. Singh P. and Kumar N., 1997. Effect of orography on precipitation in the western Himalayan region. *Journal of Hydrology*, 199 (1997) 183-206
245. Singh, P., Jain, S. K. & Kumar, N., 1997, Snow and glacier melt runoff contribution in the Chenab river at Akhnoor. *Mountain Research Development*, 17, 49-56.
246. Singh, P. and Singh, V.P., 2001, *Snow and Glacier Hydrology*, Water science and technology library, Vol. 37, Kluwer Academic publishers, Dordrecht, The Netherlands.
247. Singh, R. and Mathur, B.S., 1976, Snowmelt estimation of the Beas catchment using meteorological parameters. (In: *Symposium on Tropical Monsoons*. Proceedings. Pune. Indian Institute of Tropical Meteorology.
248. Singh, R., 1978, Remote sensing for meteorological data and short-term snow melt prediction. (In: *Symposium on Remote Sensing of Snow in the Himalayas for Effective Water Control Management for Irrigation and Power*. Nangal, India. Beas and Bhakhra Management Board.)
249. Singh, R., Prakash, O. & Khicher, M. L., 1995, Estimation of evaporation from different meteorological parameters. *Annals of Arid Zones*, 34, 263-265.
250. Singh, V.P. 1988. *Hydrologic Systems: Rainfall-runoff modelling*. New Jersey, Prentice Hall.
251. Singh, V.P. 1992. *Elementary Hydrology*. New Jersey, Prentice Hall.

252. Smith S.E., Mancy, K.H. and Latif, A.F.A., 1980, The application of remote sensing techniques towards the management of the Aswan high dam reservoir, 14th. International symposium on remote sensing environment, San Jose, Costa Rica, 23-30 April.
253. Solomonson, V.V., 1973, Remote sensing applications in water resources- 3rd. Earth Resources Technology Symposium, Washington D.C., Dec. 10-14.
254. Solomonson, V.V. and Bhavsar, P.D., 1979, Symposium on the Contribution of Space Observation to Water Resources Studies and the Management of these Resources, Bangalore, 29 May-9 June 1979. Advances in Space Exploration: COSPAR Symposium Series, no. 9. India. Pergamon Press, 139-142.
255. Steinegger, U., Braun, L.N., Kappenberger, G. and Tartari, G., 1993, Assessment of annual snow accumulation over the past 10 years at high elevations in the Langtang region. (In: Young, G.J., ed. Snow and Glacier Hydrology. International Symposium, Kathmandu, Nepal, 16-21 November 1992. Proceedings. International Association of Hydrological Sciences. IAHS/AISH Publication, no. 218: 155-165.
256. Strahler AN., 1964. Quantitative geomorphology of drainage basins and channel networks, Section 4-II. In handbook of applied hydrology, edited by V.T.Cow, 4: 39-76, New York: McGraw-Hill.
257. Subrahmanyam, V., 1956, The water balance of India according to Thronwaite's concept of Potential Evapotranspiration. Annals of Association of the American Geographers. 46: 300-311.
258. Subramanian, V. and Dalavi, R.A., 1978, Some aspects of stream erosion in the Himalaya. Himalayan Geology, 8: Part 2: 822-834.
259. Suvit Vibulsresth, Darasari Srisangthong, Kanya Thisayakorn, Rasamae Suwanwerakamtorn, Supak Wongparn, Chikchai Rodpram, Sanuk Leelitham and Wanachai Jittanaon , 1988, The reservoir capacity of Ubolratana dam between 173 and 180 meters above means sea level, Asian-Pacific Remote Sensing , Journal No. 1.
260. Swamy, A.N., and Brivio, P.A., 1996, Hydrological modelling of snowmelt in Italian alps using visible and infrared remote sensing. International Journal of Remote Sensing, Vol. 17, No. 16, 3169-3188.
261. Swamy, A.N., and Brivio, P.A., 1997, Modelling runoff using optical satellite remote sensing data in a high mountainous alpine catchment of Italy. Hydrological Process, Vol. 11, 1475-1491.
262. Tarble, R.D., 1963, Areal distributions of snow as determined from satellite photographs, Publ. 65, IAHS, 372-375.

263. Tao, T. and Kouwen, N., 1989, Remote sensing and fully distributed modelling for flood forecasting. *Journal of Water Resources Planning and Management*, ASCE, 115(6), 809-823.
264. Tarafdar, M. R., 1970, Water balance and flow study in the Brahmaputra-Ganges basin of East Pakistan. *International Association Hydrological Sciences. International Association of Hydrological Sciences. IAHS Publication, no. 94: 103-112.*
265. Tejwani, K.G. , 1984, Biophysical and socio-economic causes of land degradation and strategy to foster watershed degradation in the Himalaya. (In: IUFRO symposium of effects of forest land use on erosion and slope stability, East-west Centre: Honolulu, 55-60.)
266. Tejwani, K.G., 1987, Sedimentation of reservoirs in the Himalayan region, India. *Mountain Research and Development*, 7(3): 323-327.
267. Thapa, G.B., Paudyal, G.N. and Weber, K.E., 1989, Soil erosion and lake sedimentation in two small watersheds of Pokhara Valley, Nepal: the need for integrated area development planning exemplified. (In: D. Lianzhen, ed., *Proceedings of the Fourth International Symposium on River Sedimentation*, Beijing, June 5 - 9, 1989, Beijing. Science Press, 4: 390-397.)
268. Thapa, K.B., 1980, Analysis for Snowmelt Runoff During Premonsoon Months in Beas Using Satellite Imageries. Roorkee, India. University of Roorkee, Unpublished M-Tech Thesis.
269. Thapa, K.B., 1993, Estimation of snowmelt runoff in Himalayan catchments incorporating remote sensing data. (In: Young, G.J., ed. *Snow and Glacier Hydrology. International Symposium, Kathmandu, Nepal, 16-21 November 1992. Proceedings. International Association of Hydrological Sciences. IAHS/AISH Publication, no. 218: 69-74.*)
270. Thapliyal, V., 1986, Role of Himalayan Snow Cover. (In: *Basic Physics of Monsoons. Internal Report DST, India, 1-6.*)
271. Thompson, M. and Warburton, M., 1985, Uncertainty on a Himalayan Scale. *Mountain Research and Development*, 5(2): 115-135.
272. Turpin, O., Ferguson, R. and Johansson, B., 1999, Use of remote sensing to test and update simulated snow cover in hydrological models. *Hydrological Process*, 13, 2067-2077.
273. Upadhyay, D.S., 1991, Use of satellite based information in snowmelt run-off studies. *Mausam*, 42(2): 187-194.

274. Upadhyay, D.S., Chaudhary, J.N. and Katyal, K.N., 1983, An empirical model for prediction of snowmelt runoff in Satluj. (In: Joshi, S.C., ed. National Symposium on Seasonal Snow Cover, New Delhi, India, 28-30 April 1983. Proceedings, vol. 1. Manali, India. Snow and Avalanche Study Establishment.
275. U.S. Army Corps of Engineers, 1956, Snow Hydrology, Summary report of snow investigations. U.S. Army Corps of Engineers, North Pacific Division, Portland, Oregon, 1956.
276. Valdiya, K.S., 1985, Accelerated erosion and landslide-prone zones in the central Himalayan region. (In: Singh, J H, ed., Environmental Regeneration in the Himalaya: Concepts and Strategies, Proceedings of the Kathmandu Symposium, November 1992. 12-38. The Central Himalayan Environmental Association: Nainital, India.)
277. Varsheney, R. S., 1975, Text of Engineering hydrology. Nemchand brothers publication, Roorkee, India, pp. 24.
278. Verma, B., Tejwani K.G., Kale M.V. and Patel A.P., 1968, Evaluation of different cropping patterns for runoff and soil loss in Ravine lands. Journal of the Indian Society of Agronomy, Vol. 13, 262-270.
279. Verdhen, A., 1987, Snowmelt runoff prediction model on degree-day method for Beas catchment. Unclassified Studies Report. Manali, India. Snow and Avalanche Study Establishment.
280. Verdhen, A., 1989, Modelling of snowmelt and runoff forecasting. (In: Snow Hydrology Proceedings of the Roorkee First National Workshop, February 1989. India. National Institute of Hydrology.
281. Verdhen, A. and Prasad, T., 1993, Snowmelt runoff simulation models and their suitability in Himalayan conditions. (In: Young, G.J., ed. Snow and Glacier Hydrology. International Symposium, Kathmandu, Nepal, 16-21 November 1992. Proceedings. International Association of Hydrological Sciences. IAHS/AISH Publication, no. 218: 239-248.
282. Viessman, W., Knapp, J.W., Lewis, G.L. and Harbaugh, T.E., 1977, Introduction to Hydrology. Harper and Row, Publishers, New York, 704 pgs.
283. Vohra, C.P. and Srivastava, G.S., 1980, Problems of snow cover assessment: an approach using remote sensing techniques in a pilot project in the Beas River basin, Himachal Pradesh, India. (In: Salomonson, V.V., Bhavasar, P.D., eds. Symposium on the contribution of Space observation to water resources studies and the management of these resources, Bangalore, 29 May-9 June, 1979, Advances in Space Exploration: COSPAR Symposium Series, 9. Pergamon Press, 139-142)

284. Water and Energy Commission Secretariat, 1989, Erosion and sedimentation in the Nepal Himalaya: an assessment of river processes. 181pp. WECS: Nepal.
285. Way, J., Rignot, E., McDonald, K., Viereck, L., Williams, C., Adams, P., Payne, C. and Wood. W., 1993, Monitoring seasonal change in Tiaga forests using ERS-1 SAR data. In Proc. IGRASS' 93, IEEE No. 93CH3294-6.
286. Whetton, P.H., Haylock, M.R., and Galloway, R., 1996, Climate change and snow-cover duration in the Australian Alps. *Climatic Change*, 32(4), 447-479.
287. Williams, G. P., 1989, Sediment concentration versus water discharge during single hydrological events in rivers. *Journal of Hydrology*, Vol. 111, 89-106.
288. Williams, K.S. and Tarboton, D.G., 1999, The ABC's of snowmelt: a topographically factorized energy component snowmelt model. *Hydrological Processes*, 13, 1905-1920.
289. Willis, I.C., Richards, K.S. and Sharp, M.J., 1996, Links between proglacial stream suspended sediment dynamics, glacier hydrology and glacier motion at midtdalsbreen, Norway. *Hydrological process*, Vol. 10, 629-648.
290. Wischmeier, W. H., Smith, D.D., 1978, Predicting rainfall erosion losses. A guide of conservation planning US Dep. Agric. Handb., pp. 537.
291. Wiscombe, W.J. and Warren, S.G., 1980, A model for the spectral albedo of snow. I: Pure snow, *Journal of Atmospheric Sciences*, Vol. 37, 2712-2733.
292. Wood, P. A., 1997, Controls of variation in suspended sediment concentration in the river Rother, West Sussex , England. *Sedimentology*, Vol. 24, 437-445.
293. World Meteorological Organisation (WMO), 1986, Intercomparison of models of snowmelt runoff. Operation Hydrological Rep. 23, WMO 646, Geneva.
294. Yoshida, S. 1962. Hydrometeorological study on snowmelt, *J. Met. Res.*, Vol. 14, 879-899.